Technical Report No. 213

036040-7-T

UNDERWATER SOUND PROPAGATION IN THE STRAITS OF FLORIDA: THE PRELIMINARY ANALYSIS OF THE MIMI EXPERIMENT OF 1970

by

R. M. Heitmeyer

Approved by: Theodore G. Birdsall

Theodore G. Birdsall

COOLEY ELECTRONICS LABORATORY

Department of Electrical and Computer Engineering
The University of Michigan
Ann Arbor, Michigan

for

Contract No. N00014-67-A-0181-0032
Office of Naval Research
Department of the Navy
Arlington, Va. 22217

February 1972

Approved for public release; distribution unlimited.

ABSTRACT

An underwater acoustic propagation experiment was conducted (during the month of November 1970) as part of the Project MIMI propagation and signal processing research program. A periodic broadband signal modulating a 420 Hz carrier was transmitted continuously across the Straits of Florida for 19 days. At the receiving site, the power and phase angle of the carrier, the power in the signal sidebands and the noise power in the signal band were measured. In addition, the total power and the power spectrum in a narrow band about the carrier line were determined as a measure of the modulation due to the forward scattered surface reverberation. Finally, the correlation of the received signal with a stored reference was computed to measure the multipath structure and its stability. This report presents a brief description of the acoustical range, the experiment and the preliminary analysis of the data.

ACKNOWLEDGEMENTS

The experiment described in this report was conducted as part of project MIMI propagation and signal processing research sponsored by Code 468 of the Office of Naval Research. The experiment was jointly conducted by the Acoustics Group of the Rosenstiel School of Marine and Atmospheric Sciences (RSMAS), University of Miami, under the direction of Dr. John Steinberg, and by the Signal Processing Group of Cooley Electronics Laboratory (CEL), University of Michigan, under the direction of Dr. Theodore Birdsall.

The Acoustics Group at RSMAS as a whole deserves special credit for not only maintaining the Miami-Bimini range but also for providing invaluable background information of the propagation conditions in the Straits of Florida. Special thanks go to Mr. Roger Dann who did an excellent job of both collecting the 7-mile hydrophone data and maintaining the equipment at RSMAS.

The signal processing techniques used in the experiment were developed by Dr. Birdsall while the bulk of the credit for the computer implementation of those techniques goes to Mr. Kurt Metzger of CEL. Mr. Gerald Cederquist, Mr. Peter Wood and Mr. Brian Barton also made major contributions to the signal processing effort.

TABLE OF CONTENTS

LIST OF ILLUSTRATIONS (Cont.)

Chapter 1

THE MIMI EXPERIMENT OF NOVEMBER 1970

The underwater acoustic propagation experiment of November 1970 was conducted jointly by the Acoustics Group of the Rosenstiel School of Marine and Atmospheric Sciences at the University of Miami and by the Signal Processing Group of the Cooley Electronics Laboratory at The University of Michigan. A periodic, broadband signal, modulating a 420 Hz carrier was transmitted continuously across the Straits of Florida for 19 days. At the receiving site, the power and phase angle of the carrier, the power in the signal sidebands, and the noise power in the signal band were measured. In addition, the total power and the power spectrum in a narrow band about the carrier frequency were determined as a measure of the modulation due to the forward-scattered surface reverberation. Finally, the correlation of the received signal with a stored reference was computed to measure the multipath structure of the channel and its stability.

During the course of the experiment approximately 9 million digital words of the reception were recorded for later processing. This report, however, contains only the description of the experiment and the preliminary analysis of the on-line results. A more complete report on the results of additional processing of the data is planned.

1.1 The Miami-Bimini Range

Location and Facilities. The Miami-Bimini range, illustrated in Fig. 1, is part of the facilities of the Acoustics Group of the Rosenstiel School of Marine and Atmospheric Sciences (RSMAS) of The University of Miami.[1] It extends across the Straits of Florida from Miami to Bimini, Bahamas.

The transmitting site is located at Fowey Rocks [point 2, Fig. 1(a)] approximately 12 miles from the RSMAS laboratory. At the transmitting site, which is connected to the RSMAS laboratory by telephone lines (point 1, Fig. 1), a bottom mounted projector is located in 72 feet of water at the focal point of a 24 ft. compliant tube, parabolic reflector. It has a maximum output level of 120 dB/ μbar at one meter with a nominal bandwidth of 100 Hz. The 30^{o} beamwidth is directed toward Bimini, a distance of 43 nautical miles

Two receiving sites were used in the experiment. At the first of these, a bottom mounted hydrophone is located in 1000 feet of water at point 4 in Fig. 1(a) approximately 7 miles from the source. The reception from this hydrophone was transmitted to the RSMAS laboratory by marine cable. This site is hereafter referred to as the 7-mile hydrophone. The second receiving site is located off Bimini at point 3 (Fig. 1). There, two bottom mounted hydrophones

[1] J. C. Steinberg, and T. G. Birdsall, "Underwater Sound Propagation in the Straits of Florida," J. Acoust. Soc. Am., 39, 301-315 (1966).

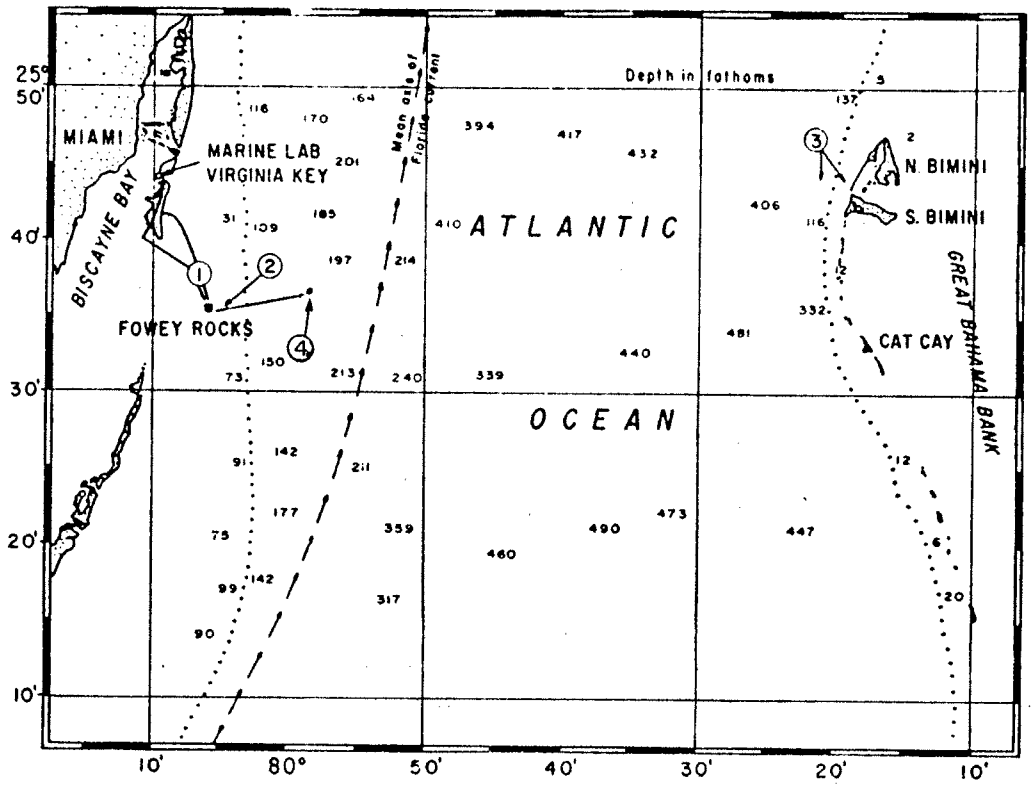

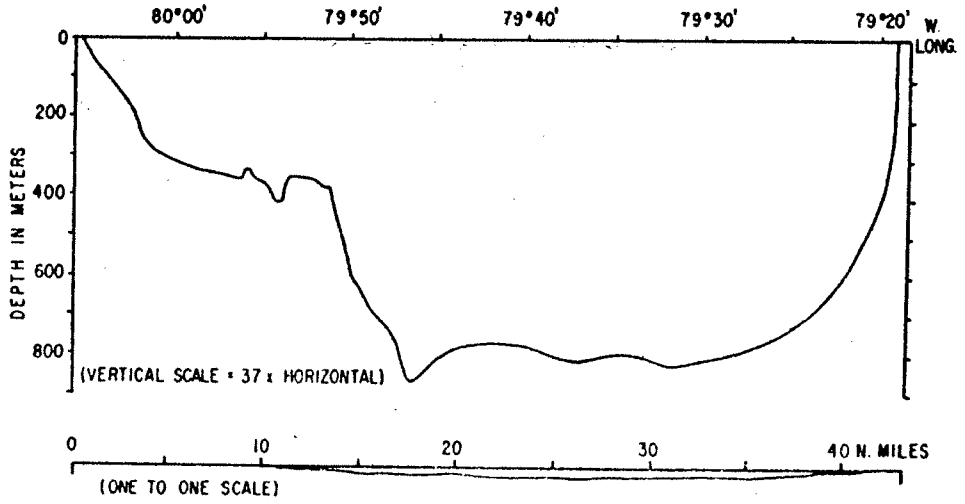

Fig. 1. The Miami-Bimini range: (a) The Straits of Florida, (b) bottom profile

are cable-connected to a laboratory on Bimini. These hydrophones are located at 100 and 1200 feet, 1 and 2 miles off shore and are referred to as the shallow and deep hydrophones, respectively.

Oceanographic and Acoustical Characteristics. The bottom profile of the Miami-Bimini range is illustrated in Fig. 1(b). A shelf extends out from Miami about 15 miles to a depth of 400 meters followed by a sharp drop-off to a depth of 800 meters. Thirty miles beyond, the Grand Bahamas bank rises abruptly from this depth.

A velocity profile, obtained during November 1961, appears in Fig. 2. This profile is characterized by a mixed layer which extends to the relatively constant depth of 100 meters followed by a region of negative velocity gradient. It is noted that the velocity gradient becomes increasingly negative as the Florida shore is approached.

The ray diagram corresponding to the velocity profile of Fig. 2 is shown in Fig. 3. This diagram shows sound being propagated by reflections from surface and bottom, by refraction and reflection from the bottom and by refraction and reflection from the surface. This latter mode of propagation does not appear in ray diagrams calculated from velocity profiles obtained in the spring and summer.

1.2 The Transmitted Signal

The transmitted signal consisted of a linear-maximal, pseudo-random sequence used to complement-phase modulate (CPM) a carrier.

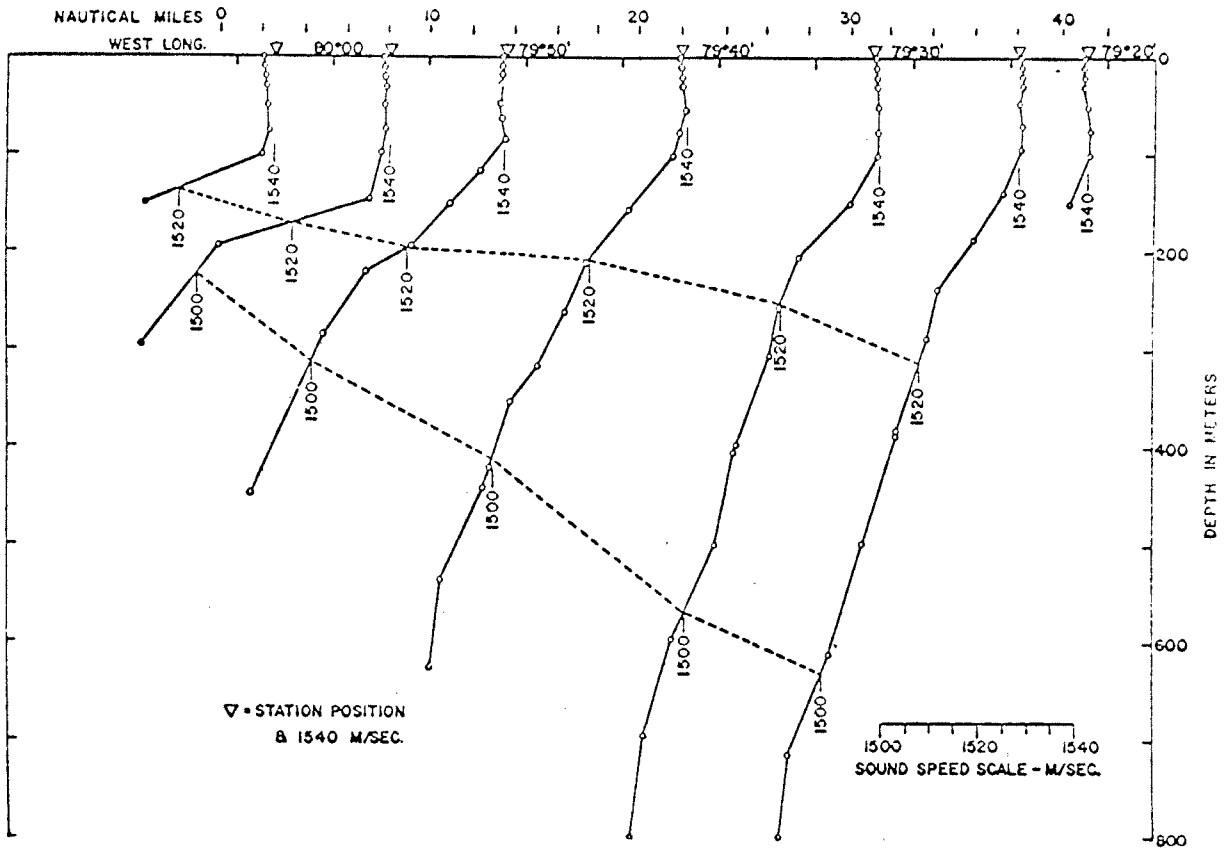

Fig. 2. Sound speed vs depth, Miami to Cat Cay, 28-29 Nov. 1961

The phase of the carrier is shifted to either $+45^{o}$ or -45^{o} depending on the value of the binary digit in the modulating sequence. A portion of a CPM signal is shown in Fig. 4 where:

f_c = carrier

d = duration of the sequence digit

D = number of cycles of carrier per sequence digit

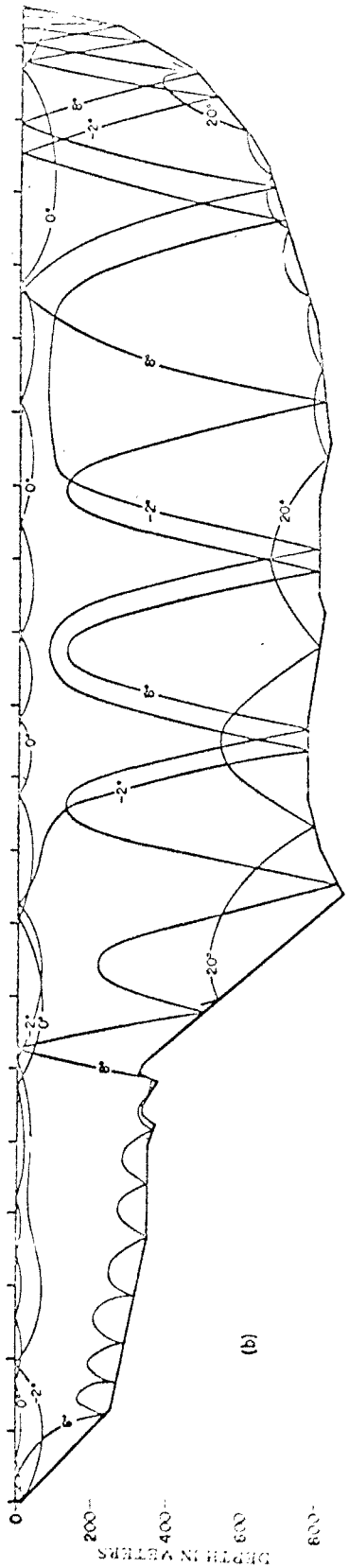

Fig. 3. Sound ray paths along 25° 44' on 28-29 Nov. 1961

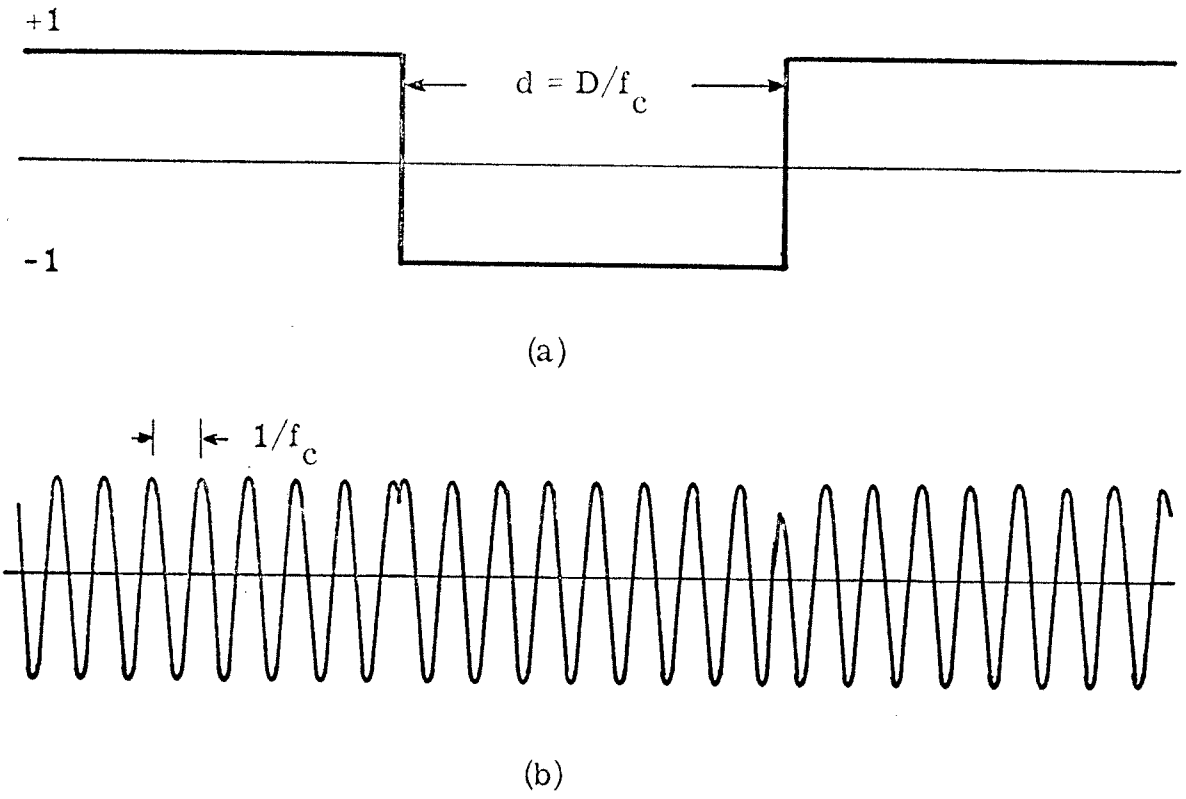

Fig. 4. A complement-phase modulated signal
(a) a portion of the modulating waveform
(b) the resulting transmission

Evidently

$$d = D/f_c$$

Furthermore, when the number of cycles of carrier per digit D is integer-valued, the signal is periodic with period

$$T = Ld = LD/f_c$$

where L is the number of digits in one period of the modulating sequence.

The RMS power spectrum of a typical (CPM) signal is shown in Fig. 5 for the special case $L = 15$ and $D = 8$. It is seen that this spectrum has a $\sin(x)/x$ envelope except at the carrier frequency. It can easily be shown that approximately half of the total power is contained at the carrier frequency with the other half contained in the sideband frequencies.

For the specific signal used in the experiment,

$$f_c = 420 \text{ Hz}$$
$$D = 8 \text{ cycles/digit}$$
and
$$L = 63 \text{ digits}$$

with the result that the digit duration and the period were

$$d = 0.019 \text{ seconds}$$
and
$$T = 1.2 \text{ seconds}$$

Furthermore, the frequency line spacing Δf and the effective signal band B (frequency spread between the spectral zeros on either side of the carrier) were

$$\Delta f = 1/T = 0.8333 \text{ Hz}$$
$$B = 2/d = 105 \text{ Hz}$$

Finally, it can be shown that there are 125 spectral lines lying within the signal band.

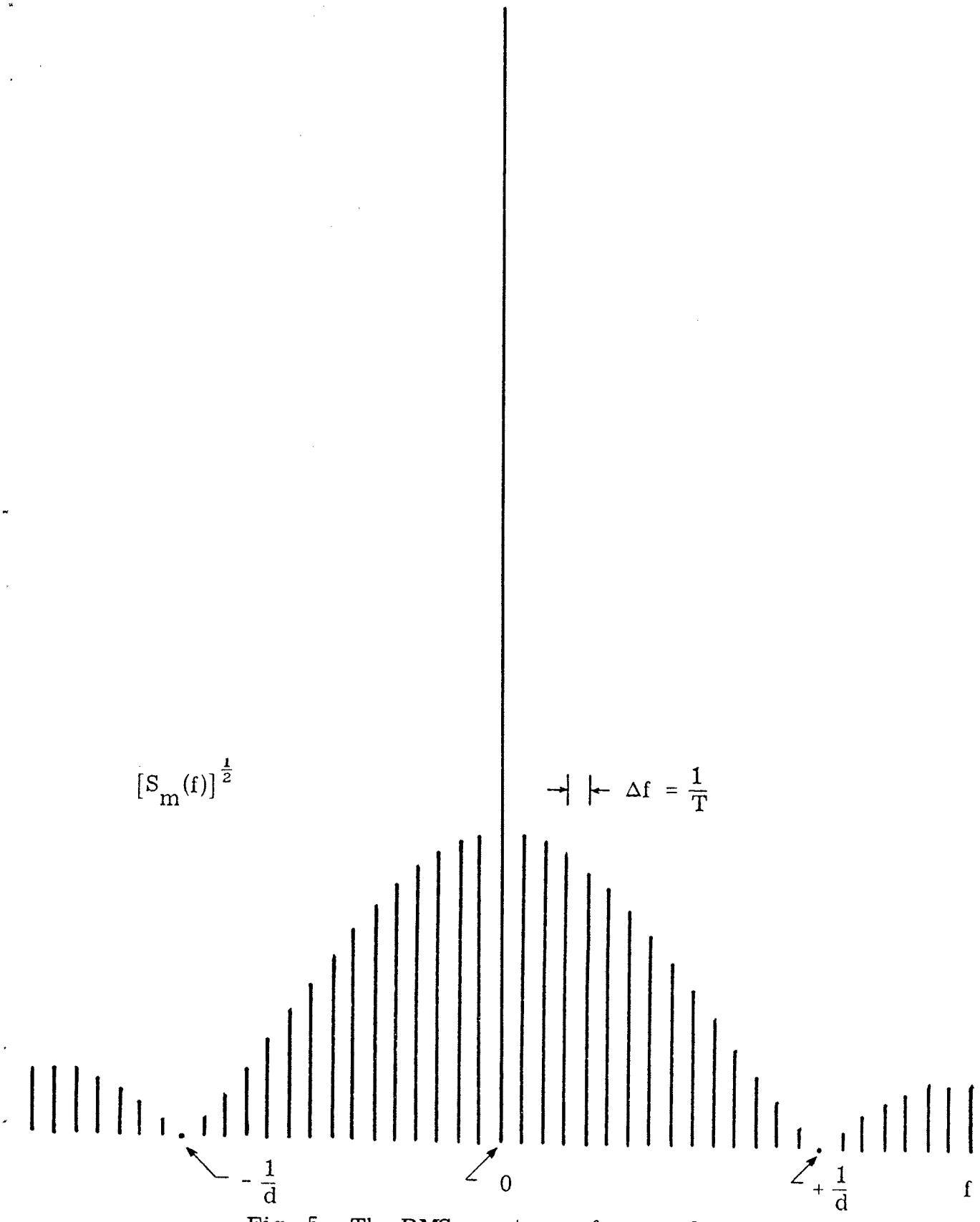

Fig. 5. The RMS spectrum of a complement-phase modulated signal for L = 15 and D = 8

1.3 The Quantities Measured

The quantities measured in the November 1970 experiment can be grouped into three categories: (1) signal power, noise power and carrier angle measurements, (2) forward-scattered surface reverberation measurements, and (3) multipath structure measurements. These measurements are obtained using digital processing techniques implemented by a digital computer located at each receiving site. (See Section 1.4.) Each of the measurements is computed and recorded every 100 seconds on the basis of 80 seconds of data. (The remaining 20 seconds are used solely for computations.) The specific quantities measured are described in the following paragraphs.

1.3.1 Power and Angle Measurements.

C Power. The C power measurement is a measure of the power present in the carrier of the received signal. It is determined as that power passing through a digital processing filter with a frequency response, $H_C(f)$, as illustrated in Fig. 6(a).[2] Note that due to the narrow bandwidth,[3] (0.013 Hz), $H_C(f)$ passes only the carrier frequency and none of the sideband frequencies present in the spectrum of the transmitted signal.

[2] Only the main lobes of the frequency responses of the processing filters in Fig. 6 are illustrated since these lobes contain almost all of the total power.

[3] By bandwidth we mean 1/2 the frequency spread between the two zeros on either side of the center frequency of the main lobe.

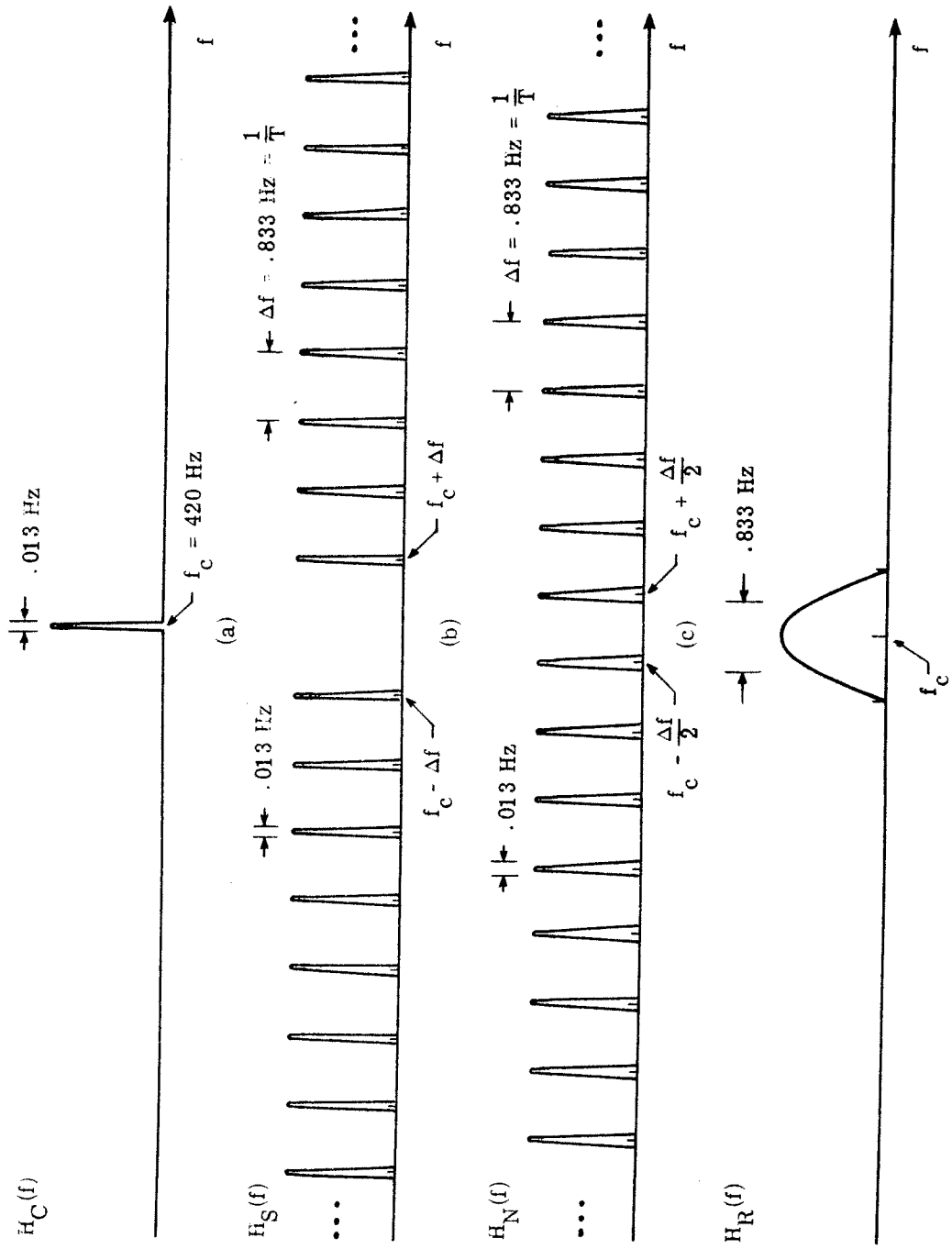

Fig. 6. The frequency responses of the digital processing filter

N Power. The N power measurement is a measure of the noise power contained within the signal band: $f_c - B/2 \leq |f| \leq f_c + B/2$. It is determined as that power passing through the digital processing filter with a frequency response, $H_N(f)$, as illustrated in Fig. 6(c).[4] Such a filter is often referred to as a comb filter. Note that each "tooth" in $H_N(f)$ is centered midway between the spectral lines in the signal spectrum, and the bandwidth of each tooth is again 0.013 Hz.

S Power. The S power measurement is a measure of the signal power within the signal band, excluding the carrier power. It is determined as that power passing through the digital processing filter with frequency response $H_S(f)$ as illustrated in Fig. 6(b). This filter is recognized as a comb filter with a tooth missing at the carrier frequency. The remaining teeth are aligned with the line frequencies of the transmitted signal. The bandwidth of each tooth is 0.013 Hz.

Carrier Angle (A). The carrier angle is a measure of the relative difference between the phase of the output of the carrier processing filter and the phase of the local reference oscillator (see Section 1.4).

1.3.2 Surface Reverberation Measurements. The effect of surface reverberation is to scatter some of the power of a transmitted

[4] The filter $H_N(f)$ is used to calculate the noise power only at the Bimini receiving site. An equivalent, but different, technique is used for the 7-mile data.

frequency into sidebands on either side of that frequency. It is felt that this scattered power should lie between 0.1 Hz and 0.4 Hz on either side of the transmitted frequency, depending on the spectrum of the surface waves. For the signal used in the experiment, the spacing between the lines in the power spectrum is $\Delta f = 0.8333$ Hz so that the sideband line frequencies do not interfere with the power scattered from the carrier frequency. Thus, the effect of surface reverberation can be measured by computing the power spectrum at the output of the processing filter whose frequency spectrum, $H_R(f)$, is shown in Fig. 6(d). Note that the bandwidth of $H_R(f)$ is large enough to include the power scattered by surface reverberation but small enough to exclude the power in the signal sidebands.

In addition to computing the reverberation or "reverb" spectra, the total power at the output of $H_R(f)$ minus the carrier power is also computed. This power, referred to as the reverb power or R power, is a measure of the power in the sidebands of the reverb spectrum.

1.3.3 Multipath Structure Measurements. The magnitude of the cross-correlation function between the demodulated reception and a pulse-compression reference is computed to measure the multipath structure of the channel. In the absense of noise, this function has a triangular peak of width, $2d = 0.038$ seconds, centered at the arrival time of each transmission path $\mathrm{mod}(T)$, and an amplitude proportional

to the amplitude of the signal received over that path. For example, the cross-correlation function for the special case of only two transmission paths is shown in Fig. 7. Note that this is the same function as would be obtained if a single, large, one-digit pulse were transmitted once every T seconds and received through a matched filter.

As a measure of the time stability of the channel multipath structure, the zero-delay complex cross-correlation coefficient between the demodulated received signal and a previously stored replica of the received signal is calculated for each data set. When this coefficient falls below a set value, indicating a marked change in the multipath structure, the current signal becomes the replica, and the new multipath picture is displayed. Otherwise, the previous replica is displayed and retained in storage. The changing magnitude of the correlation coefficient is an indicator of how fast the multipath structure is changing.

1.4 The Equipment Configuration

The configuration of the equipment used in the experiment is shown in Figs. 8 and 9. Figure 8 illustrates the configuration used in the generation and transmission of the signals and in the processing of the reception from the 7-mile phone at Miami. Figure 9 shows the configuration used in the processing of the reception at Bimini.

The operation of the equipment in Fig. 8 is as follows. The frequency standard (accurate to 1 part in 10^{10}) provides a 100 KHz

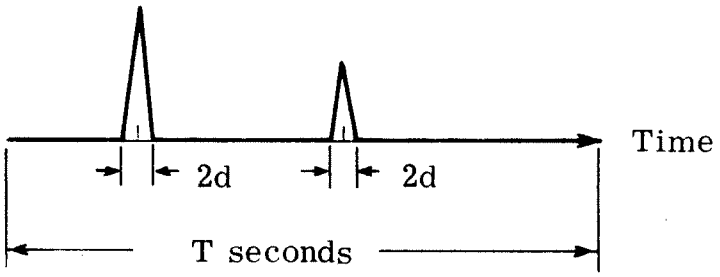

Fig. 7. A multipath display for two transmission paths

reference signal which is converted to a 1680 Hz (= 4x carrier frequency) clock signal by the frequency synthesizer and then passed through an isolation amplifier. One output of the isolation amplifier is used as a reference for the digital modulator whose output, after filtering, is the CPM signal described in the preceding section. This signal is amplified and then transmitted down the Miami-Bimini range. The reception at the 7-mile hydrophone is amplified and transmitted back to the RSMAS laboratory. There it is filtered and amplified and then processed by the LINC-8 computer. The other output of the isolation amplifier provides a clock signal to the LINC-8 computer for use in sampling the reception.

The receiving equipment at Bimini (Fig. 9) operates in essentially the same way as the receiving equipment at Miami. The receptions from both the deep and the shallow hydrophones are

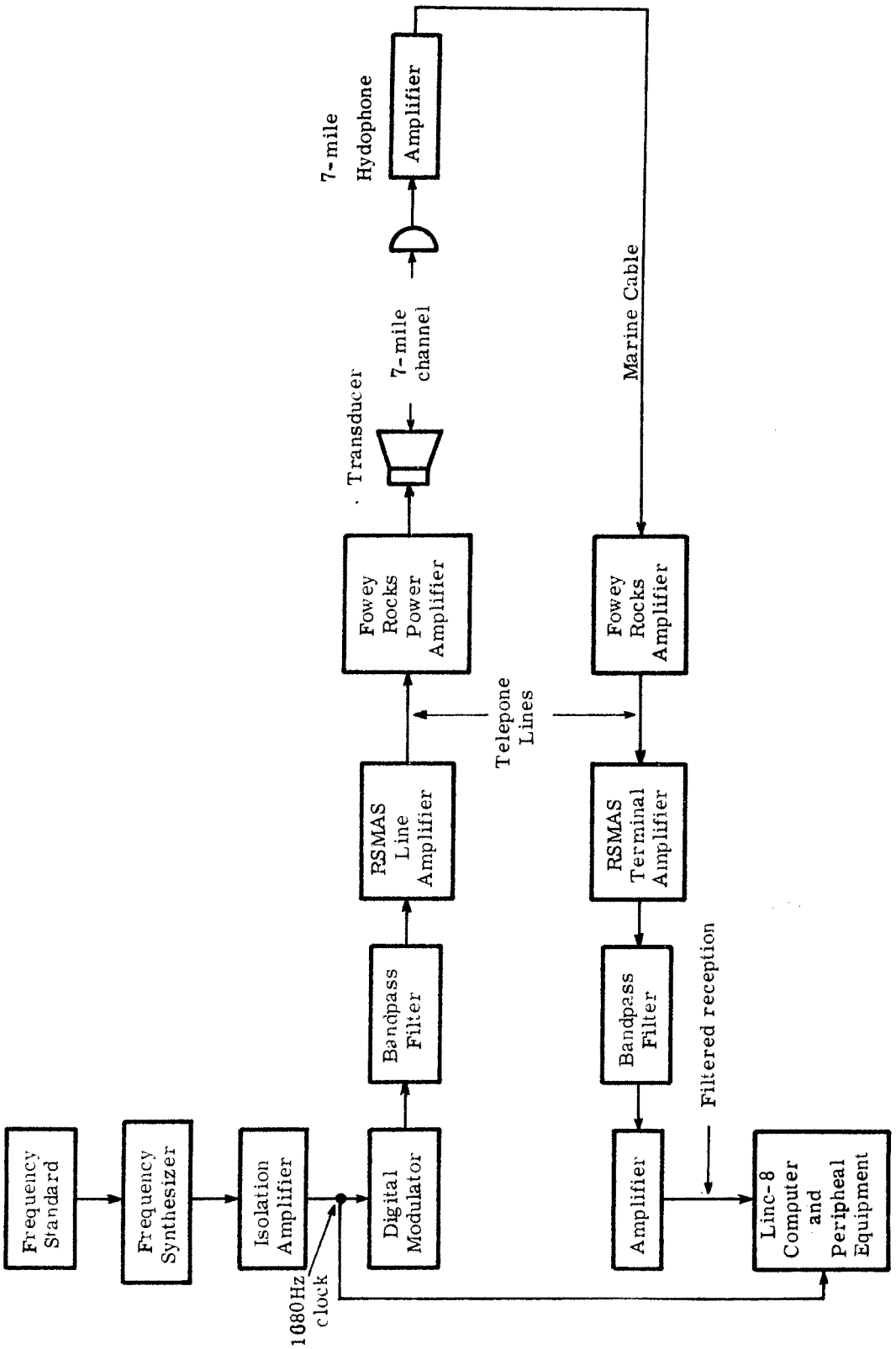

Fig. 8. Equipment configuration at RSMAS (Miami)

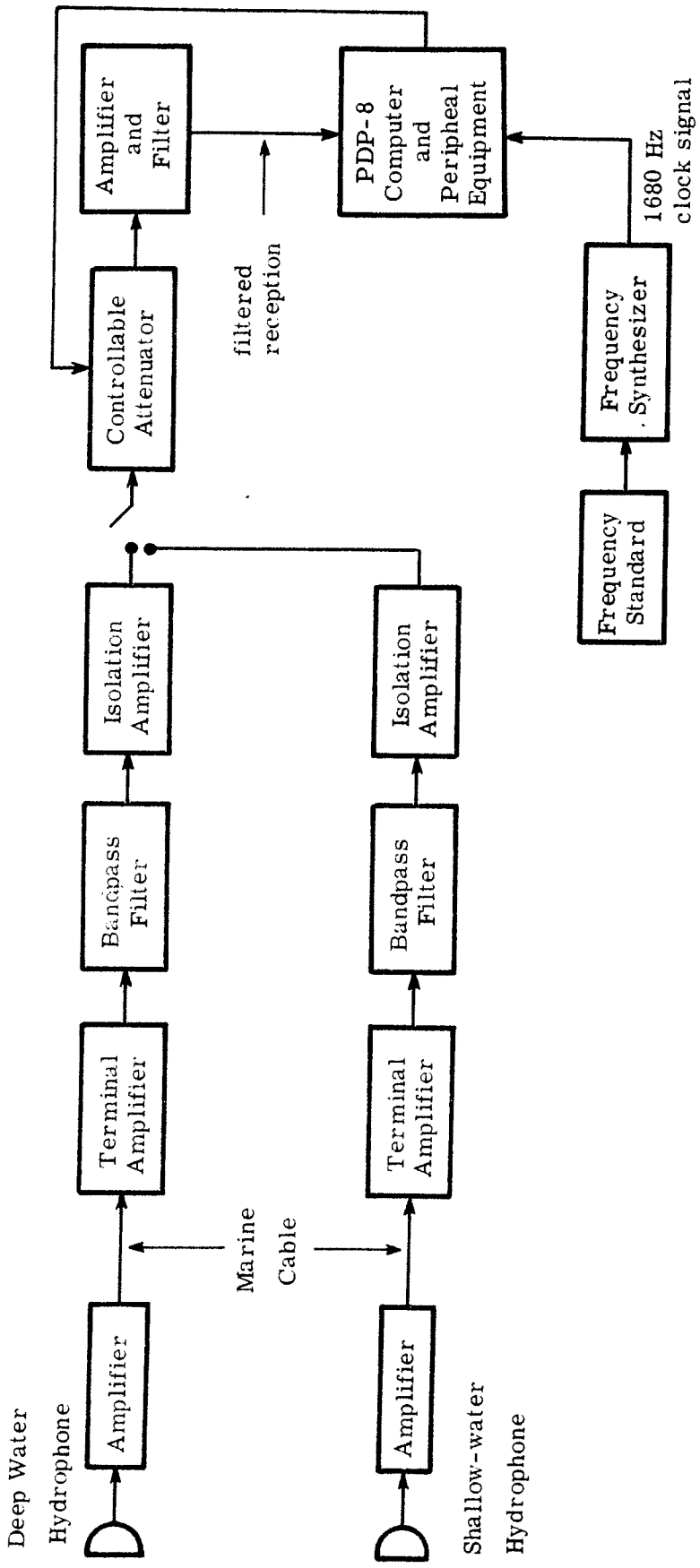

Fig. 9. Equipment configuration at Bimini

transmitted to the laboratory at Bimini and then amplified and filtered. The reception from one of the two hydrophones then enters an attenuator whose attenuation is controlled by the past signal level into the PDP-8 computer. The output of the controllable attenuator is first amplified and filtered and then processed by the computer. The coherent clock signal for the computer is obtained from a frequency standard and synthesizer identical to that employed at Miami.

The digital computers appearing in Figs. 8 and 9 are used to implement the processing filters and to calculate the reverb spectra and multipath displays as discussed in Section 2.3. In this capacity, these computers function as indicated in Fig. 10.

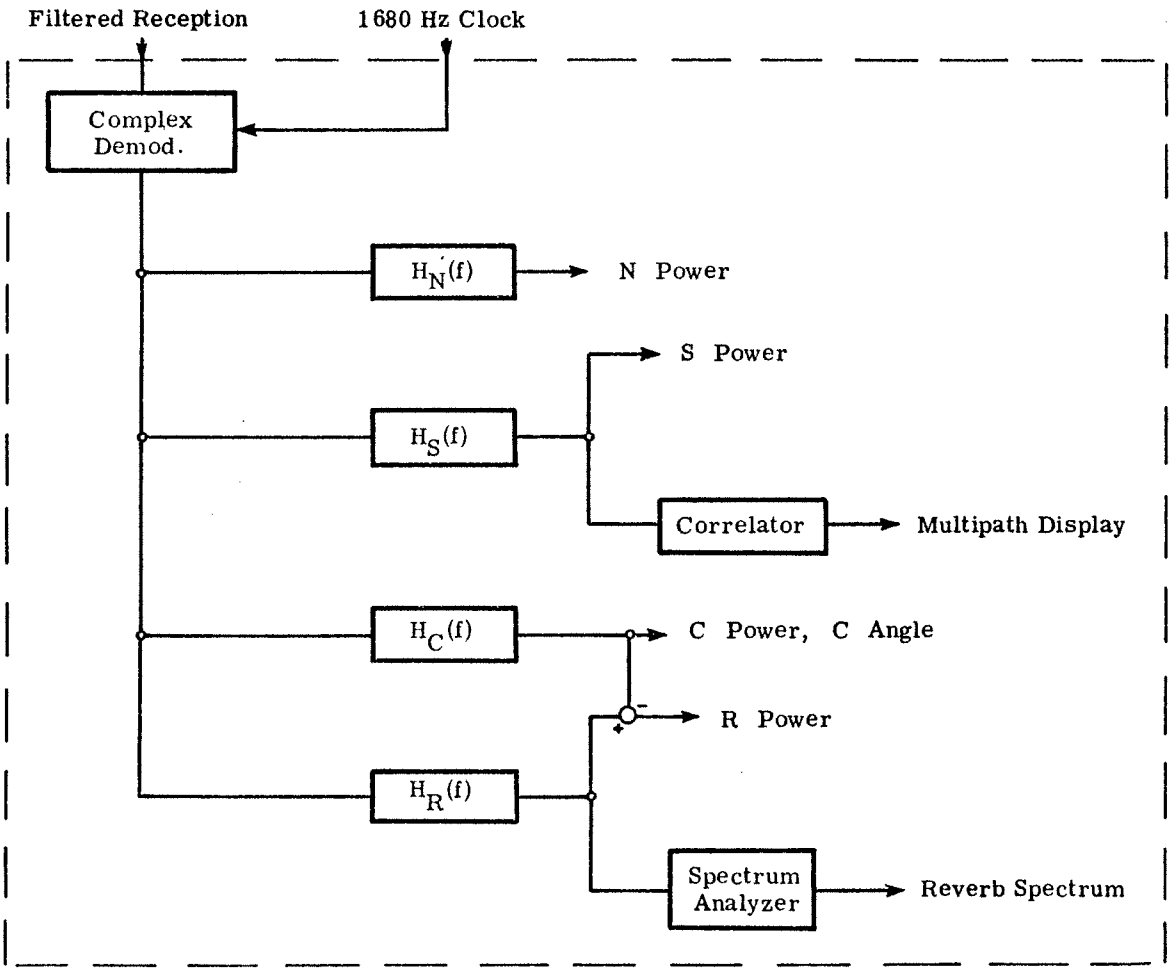

Fig. 10. Block diagram of the digital processing implementation

Chapter 2

THE PRELIMINARY ANALYSIS OF THE DATA

Measurements of all of the quantities discussed in Section 1.3 were made at Miami from the 7-mile hydrophone for 20 days. At Bimini, approximately 8 days of measurements were taken from the deep-water hydrophone and 11 days of measurements were taken from the shallow-water hydrophone. This chapter presents the preliminary analysis of the data from 15 of the 20 days, excluding the carrier angle and the correlation-coefficient measurements which will be discussed in a later report.

2.1 The Power Measurements

The power measurements, expressed in decibels relative to an arbitrary reference, have been plotted as continuous functions of time. (Continuity has been obtained by linear interpolation between the discrete data points.) Two different vertical scales have been used. In the one case, the vertical scaling is determined as if the gain of each of the processing filters in Fig. 6 is equal to unity. These plots are referred to as the unity-gain plots (UG). In the other case, the vertical scaling has been determined as if the product of the gain and the bandwidth of each of the processing filters were constant. These plots are referred to as the constant gain-bandwidth (CGB) plots. The CGB plots have the property that the approximate signal-to-noise ratio

(in dB) at the output of the processing filters $H_C(f)$, $H_S(f)$ and $H_R(f)$ can be obtained simply by subtracting N power from C, S or R power respectively.

UG and CGB plots of the power measurement for the complete experiment are found in Appendices A through D. In this section the essential features of these plots are summarized.

2.1.1 The Mean Powers. The general character of each of the power measurements is best illustrated in terms of a slowly varying component and the amount of additional variation about this component. The slowly varying component or "mean power" has been estimated by computing a sliding average. The amount of variation about the mean power has been estimated by computing a sliding standard deviation. In the following paragraphs the mean powers, based on a three-hour averaging time, are discussed. For notational convenience, the mean powers are distinguished from the actual measured powers by using a subscript "m". For example, C_m denotes the mean carrier power obtained by averaging the carrier power measurement C. The standard deviations about the means are discussed in Section 2.1.5.

Figures 11(a) and 11(b) illustrate the mean powers from the Bimini data plotted on a CGB scale. The deep hydrophone mean powers appear in Fig. 11(a) for 14 November through the evening of 17 November. During this period, the mean sideband power is relatively

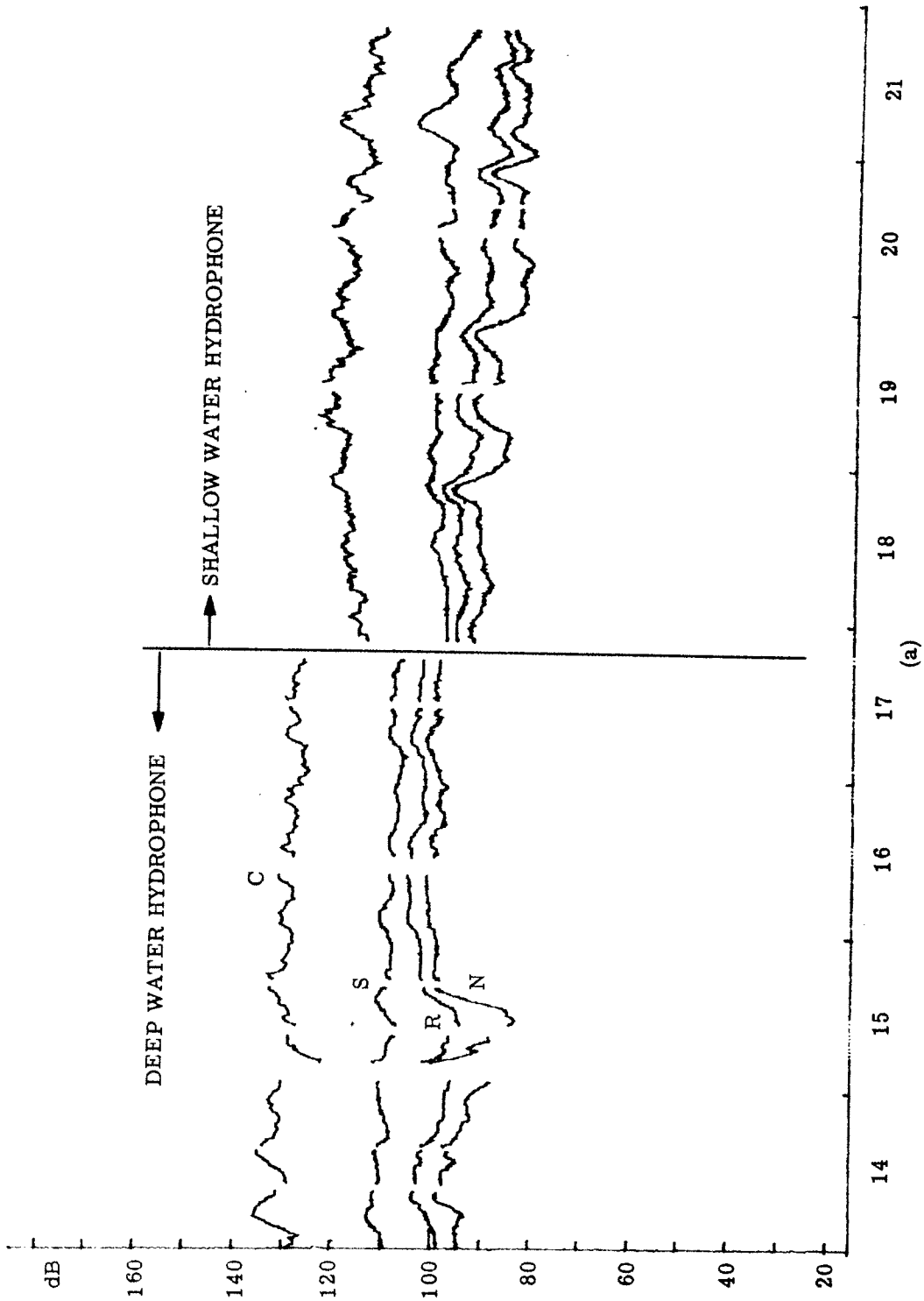

Fig. 11. Mean powers: Fowey Rocks to Bimini

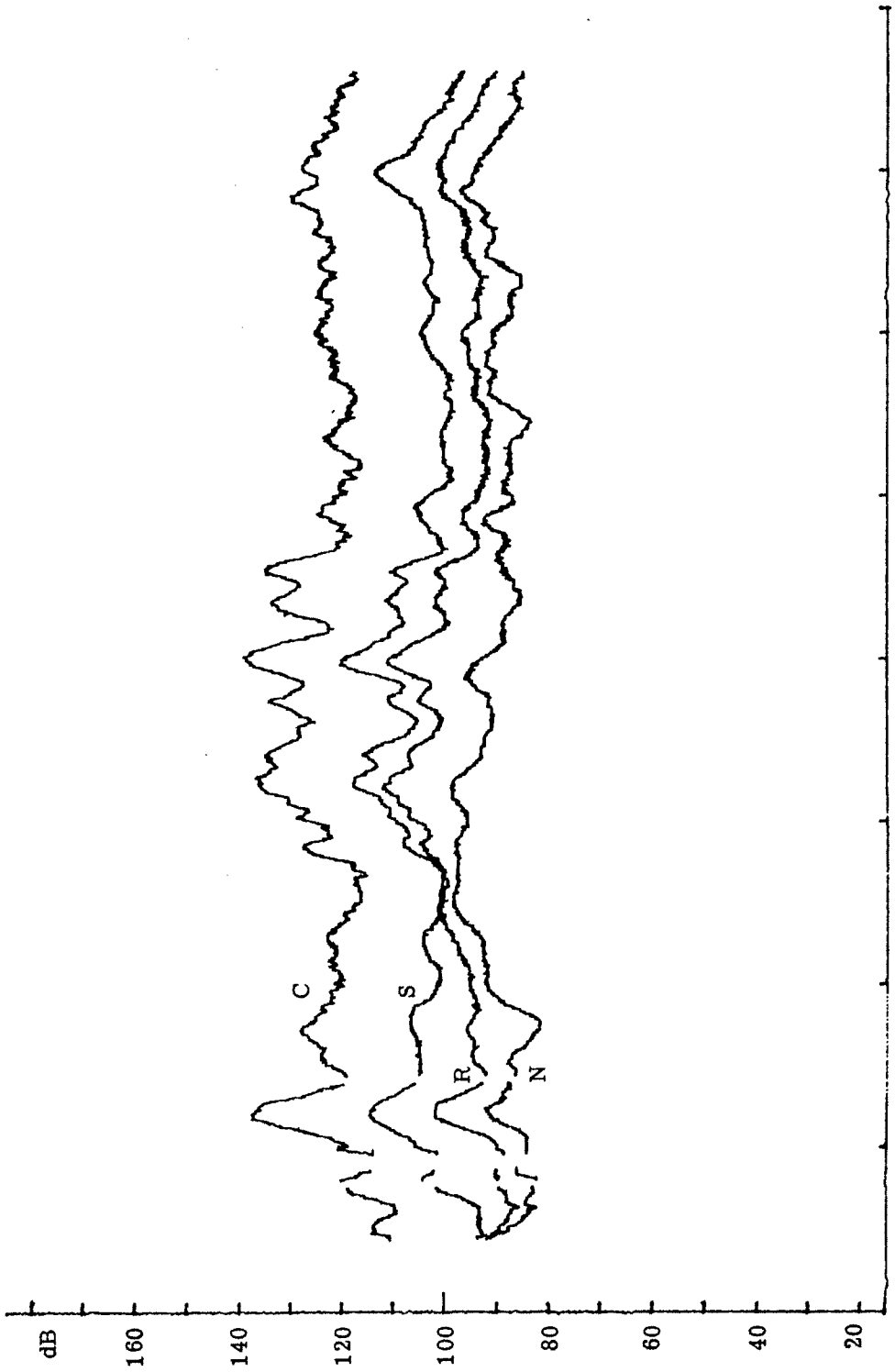
dB
160
140
120
100
80
60
40
20
C
S
R
N
22
23
24
25
26
27
28
29
(b)
DATE: NOVEMBER 1970

Fig. 11. (Cont.)

constant around 110 dB and the mean carrier power varies somewhat more around the value of 130 dB. There appears to be only a small correlation between C_m and S_m. The mean noise power reaches a low on 15 November, then abruptly rises 15 dB to a new value and remains at that new value with very little variation for the remainder of the deep-water data. In the period preceding the jump, N_m shows a significant amount of variation. The mean reverb power, R_m, with the exception of a short period on 15 November, exceeds N_m by less than 8 dB and both R_m and N_m appear to be highly correlated.

The remaining Bimini data were taken from the shallow hydrophone. The mean powers constitute the rest of Fig. 11(a) and all of Fig. 11(b). For approximately half of the time, the sideband power is reasonably constant around 105 dB , but, during the remaining time, S_m varies considerably with local maxima from 10 to 20 dB higher than the nominal value.[5] During the period of stable sideband power, C_m is also reasonably stable and there appears to be some correlation between the two. During the periods of high sideband power, however, C_m is also quite high and the two powers are highly correlated.

---

[5] The difference in the power levels between the deep hydrophone power measurements and the shallow hydrophone power measurements can be attributed to the gain settings of the amplifiers in the pre-processing equipment.

The shallow water mean noise power exhibits two different kinds of behavior. On the one hand, N_m suffers an abrupt 15 dB gain and then does not return to its original value for a period of several days [see 22 November, Fig. 11(b)]. This is similar to the jump in the deep hydrophone noise power except there is more variation following the jump. In contrast to the "jump type" variations in the shallow-hydrophone noise power, there are several instances where N_m rises about 10 dB and then immediately returns to the original value. These "roll-type" variations seldom last longer than several hours.

The behavior of the shallow-water reverb power during the periods of stable S_m is much like the behavior of the deep hydrophone reverb power. It maintains a fairly constant value except during the rolls in noise power. During the periods of high S_m, however, the reverb power is also high and the three powers S_m, C_m, and R_m all vary together.

Figures 12(a) and 12(b) illustrate the mean powers for the 7-mile data. The most striking feature of these plots is the high degree of stability in all four powers in contrast to the instability of the corresponding powers from the Bimini data. It is noted that the mean sideband power varies less than 10 dB during the course of the experiment, and the range of variation in the mean carrier power is only slightly greater. It should also be noted that although C_m

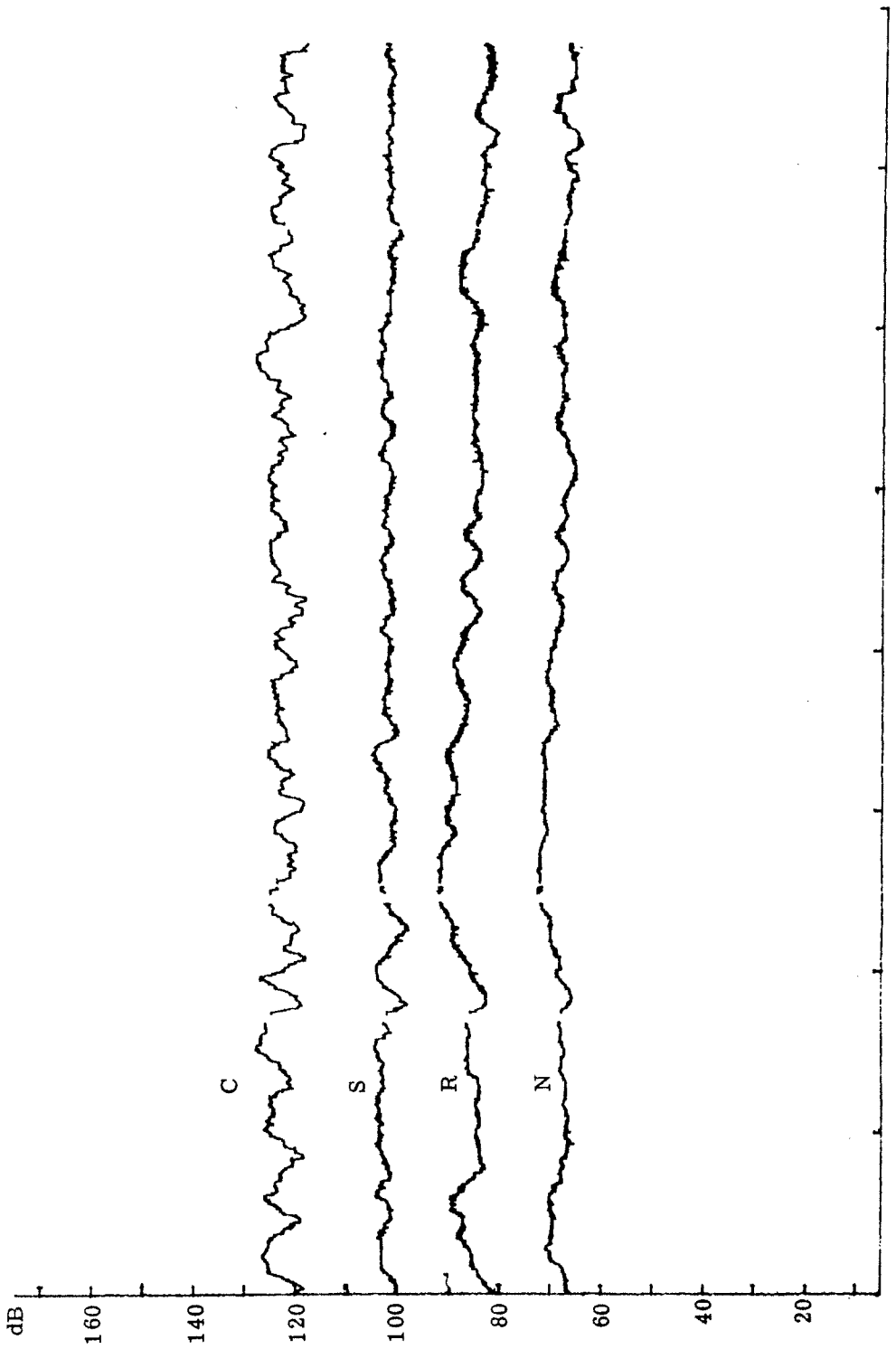

Fig. 12. Mean powers: Fowey Rocks to 7-mile

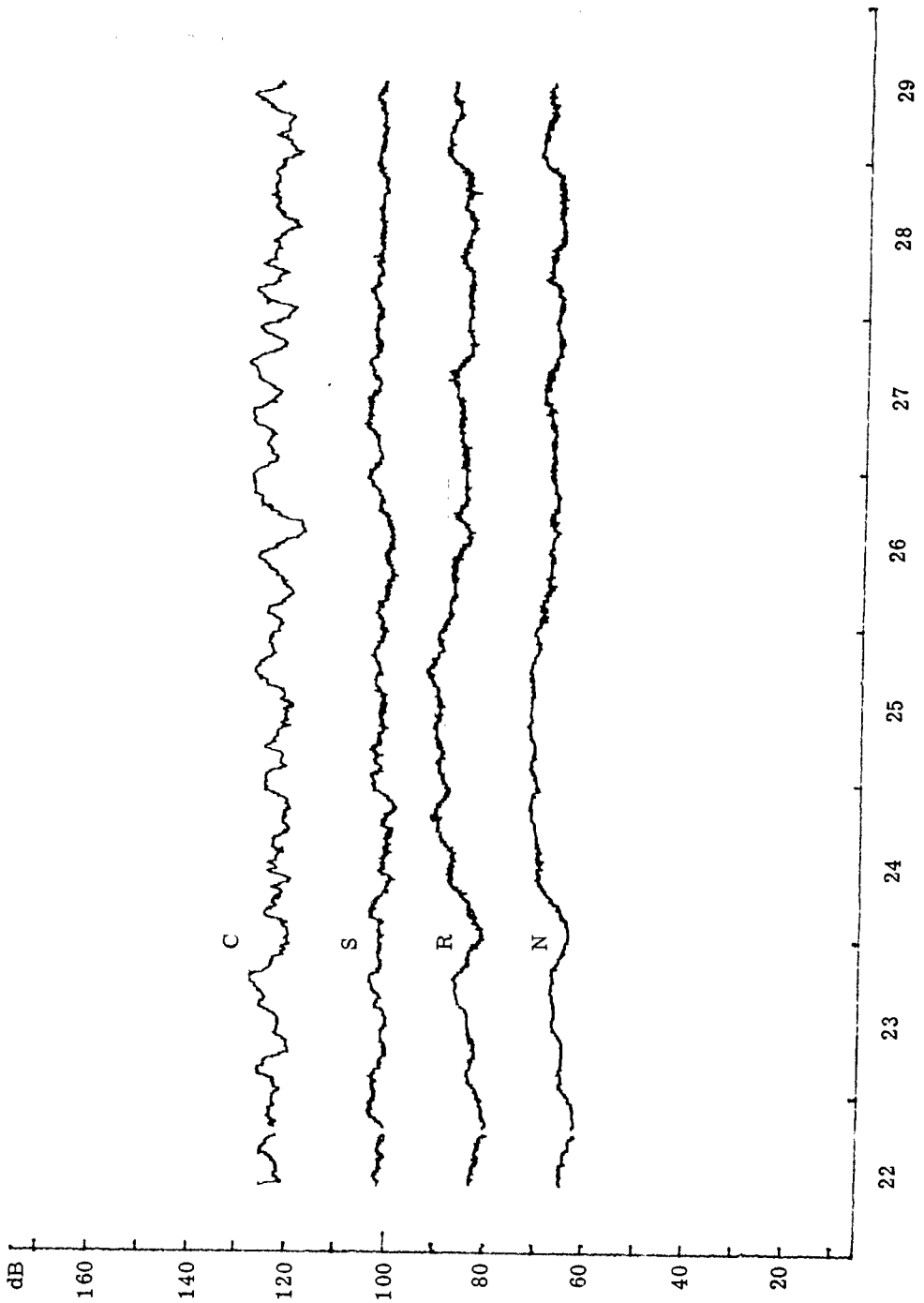
dB
160
140
120
100
80
60
40
20
C
S
R
N
22
23
24
25
26
27
28
29
DATE: NOVEMBER 1970

Fig. 12. (Cont.)

and S_m are only slightly correlated, the mean reverb power and the mean noise power show a substantial correlation.

In the above paragraphs we have discussed the plots of the four mean powers from each receiving site. These plots present the general characteristics of the power measurements for all 19 days of data in terms of two plots for each receiving site. In order to investigate the local behavior of the power measurements, however, it is necessary to examine specific examples of the CGB plots from the appendixes. This is done in the next three subsections.

2.1.2 The Carrier Power and the Sideband Power Measurements. Figures 13(a) and 13(b) illustrate two CGB plots of the carrier power and the sideband power taken from the stable S-power portion of the Bimini shallow hydrophone data. It is seen that C power varies over a wide range with most of the variation consisting of sharp, deep fades of up to 30 dB. The rate at which these fades occur varies from as little as one fade per two hours to as much as two fades per hour with an average fade rate of approximately one fade per hour. The amount of variation in the sideband power is small, with several periods during which S power varies less than 3 dB in 3 hours.

Figures 14(a) and 14(b) illustrates two CGB plots of the carrier power and the sideband power taken from the high S-power portion of the Bimini data. In Fig. 14(a), S rises to 118 dB ,

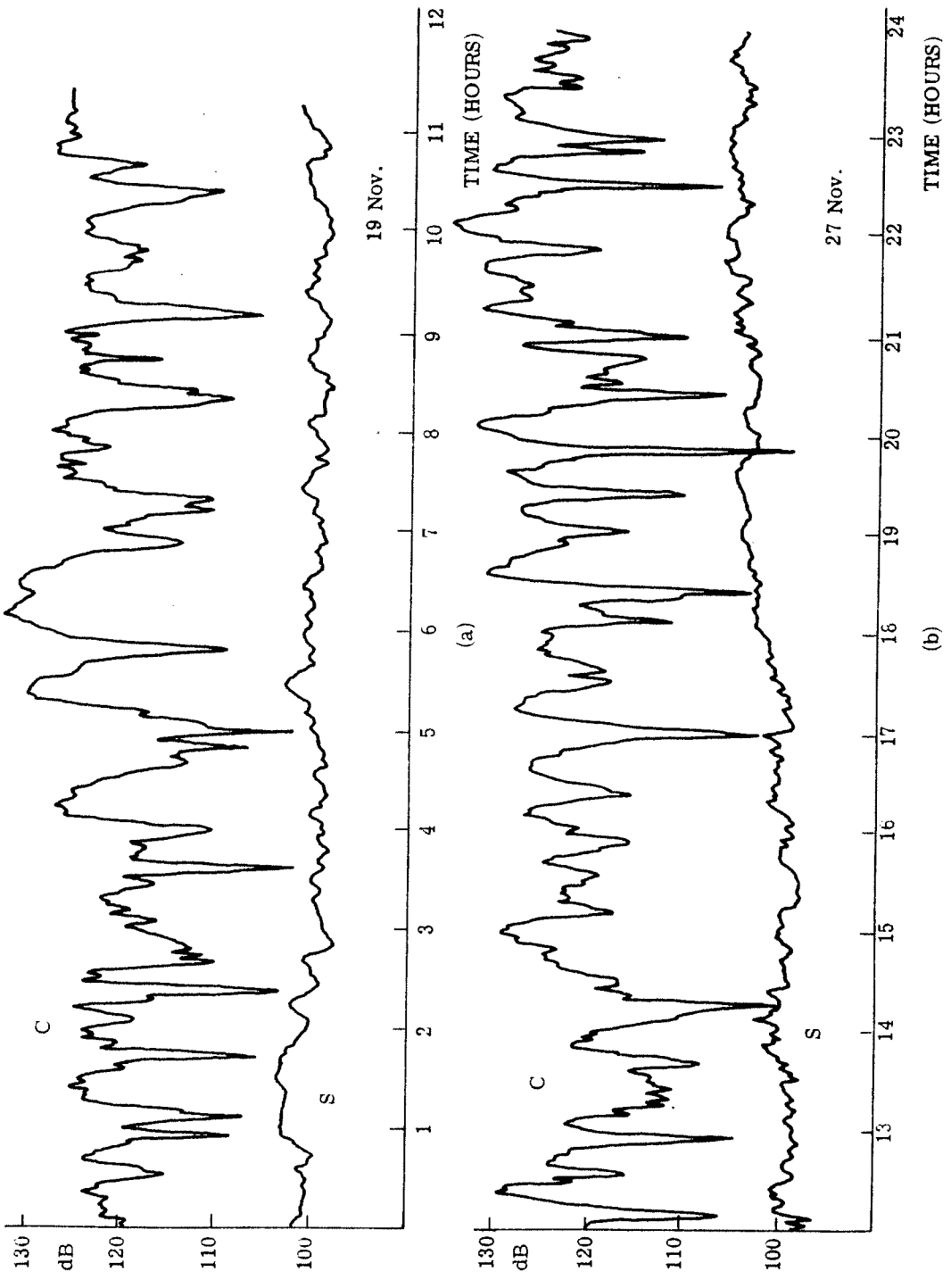

Fig. 13. Carrier and sideband powers: Fowey Rocks to Bimini

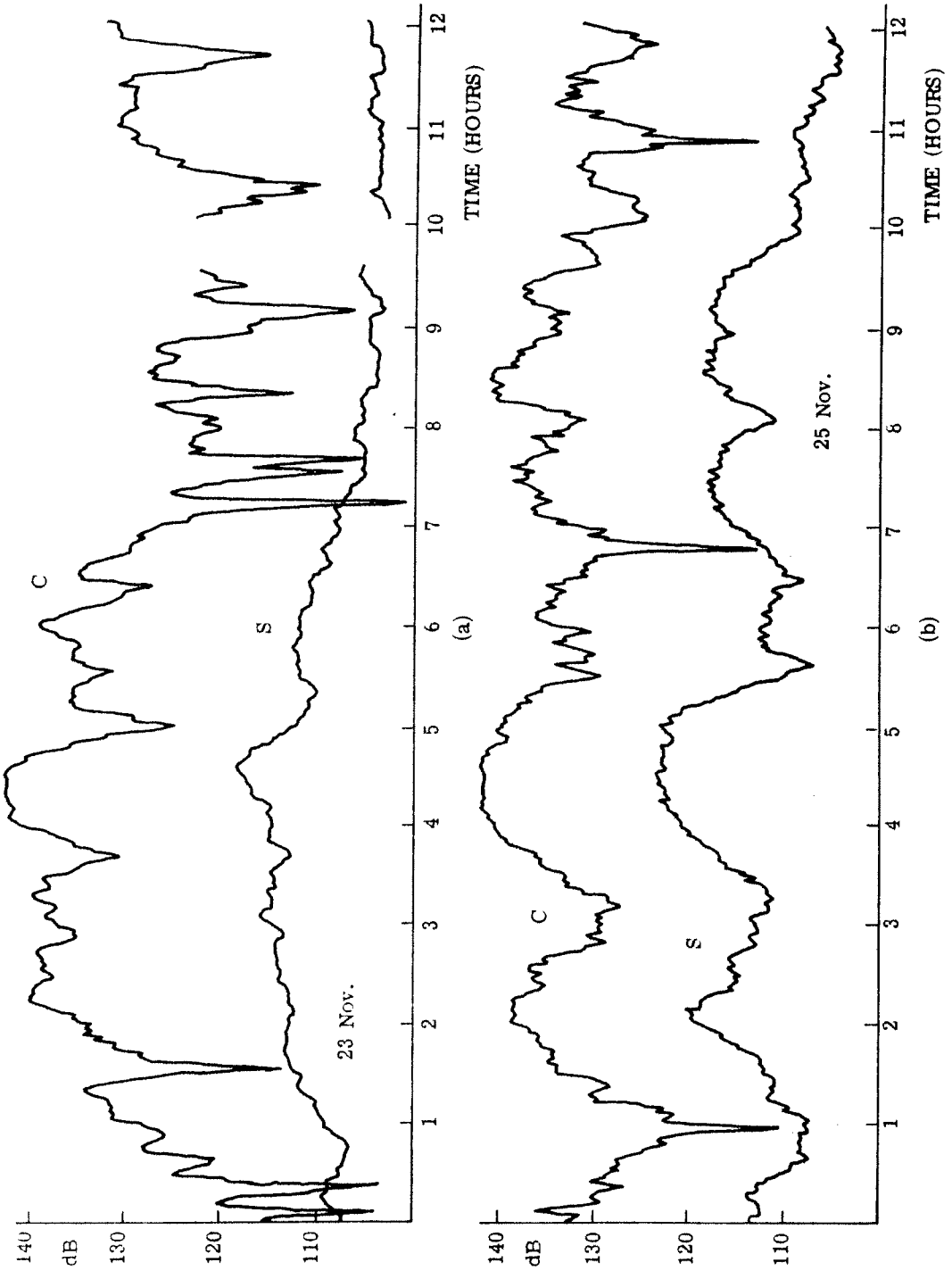

Fig. 14. Carrier and sideband powers: Fowey Rocks to Bimini

18 dB higher than its nominal value, and in Fig. 14(b) S rises to 124 dB. In both Figs. 14(a), (b), it is noted that the carrier power is well above its nominal value, that the C-power fade rate is considerably less than its nominal value, and that both C power and S power are highly correlated.

The C- and S-power measurements taken from the 7-mile data have much the same general character as the C- and S-power measurements taken from the stable S portion of the Bimini data. The 7-mile C power also has fades as deep as 30 dB and the 7-mile S power also has only a small amount of variation.

There are, however, two significant differences between the 7-mile C and S powers and the Bimini C and S powers. First, the 7-mile C power fade rate, (on the average), is noticeably less than the Bimini C-power fade rate. Figures 15(a) and 15(b) illustrate two representative CGB plots of C and S power from the 7-mile data. It is seen that there are several periods of over three hours where at most one deep fade occurs. There are, of course, many periods from the 7-mile data with a high C-power fade rate [for example between 1500 hrs and 2000 hrs in Fig. 15(a)], but a cursory examination of all the data from both sites indicates that the 7-mile C-power fade rate is approximately half the Bimini C-power fade rate.

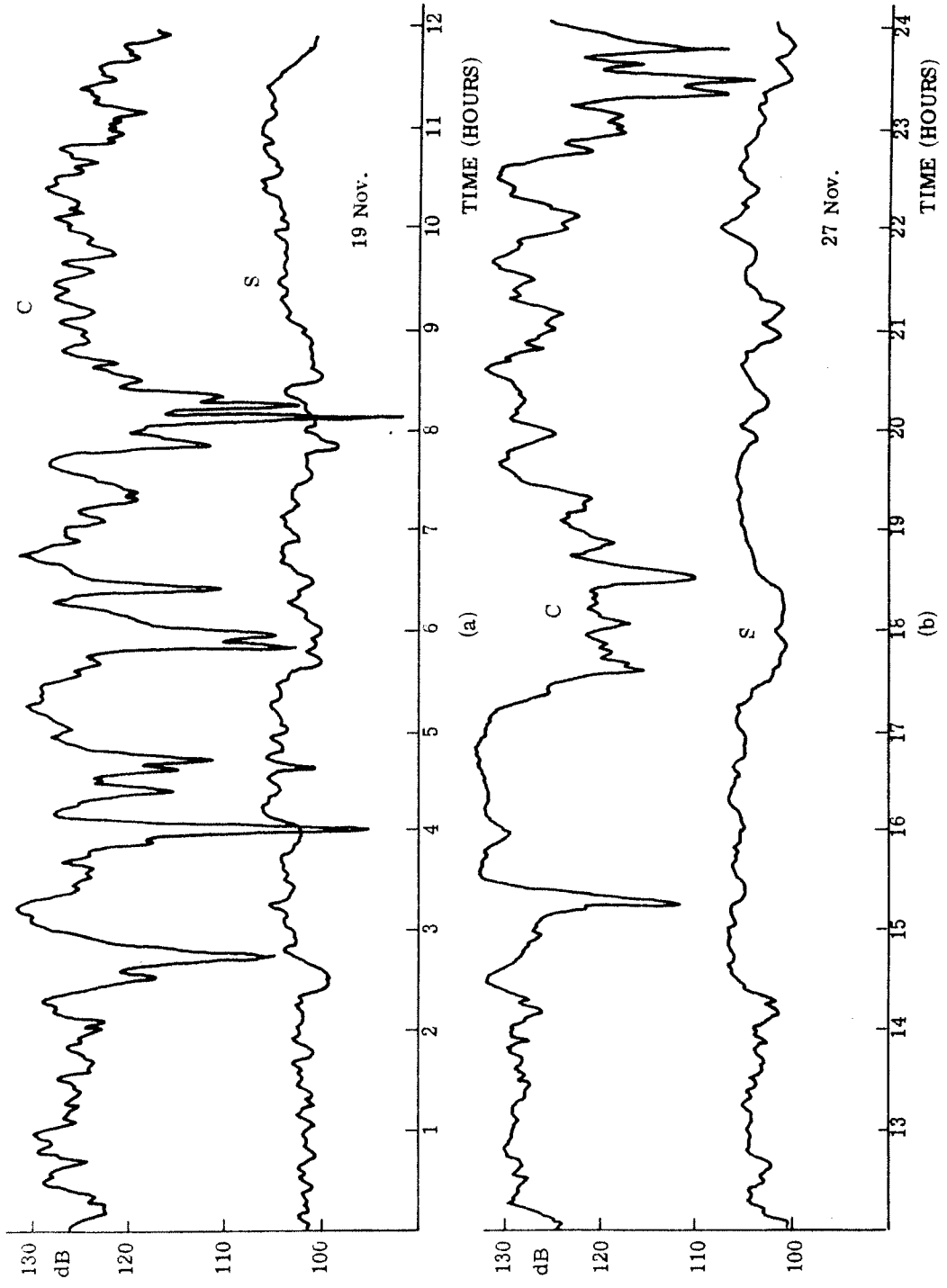

Fig. 15. Carrier and sideband powers: Fowey Rocks to 7-mile

The second major distinction between the 7-mile C and S powers and the Bimini C and S powers lies in the dependency of the C-power fade rate on the level of S power. In the 7-mile data, the C-power fade rate appears to be independent of the level of S power. In the Bimini data, however, the C-power fade rate is much lower during the periods of high S power than it is during the periods of stable S power.

2.1.3 The Noise Power Measurements. The Bimini noise power measurement varies over a range of 30 dB during the course of the experiment. Part of this variation consists of changes between 10 and 15 dB in the mean N power due to "jumps" and "rolls" as discussed in Section 2.1.1. In addition, there are large isolated 20 to 30 dB spikes which can be attributed to local shipping noise. Finally, there is a small portion of the Bimini data during which 5 to 10 dB spikes occur at a rate of from three to five spikes an hour.

To illustrate these different behaviors, four different 12 hour segments of the Bimini noise power are presented in Figs. 16(a) to 16(d). Figure 16(a) illustrates a jump of 18 dB in the noise power. Note that N power is considerably more stable after the jump than before the jump. Figure 16(b) shows the noise power over the same 12-hour period a day later. The N power measurement has remained

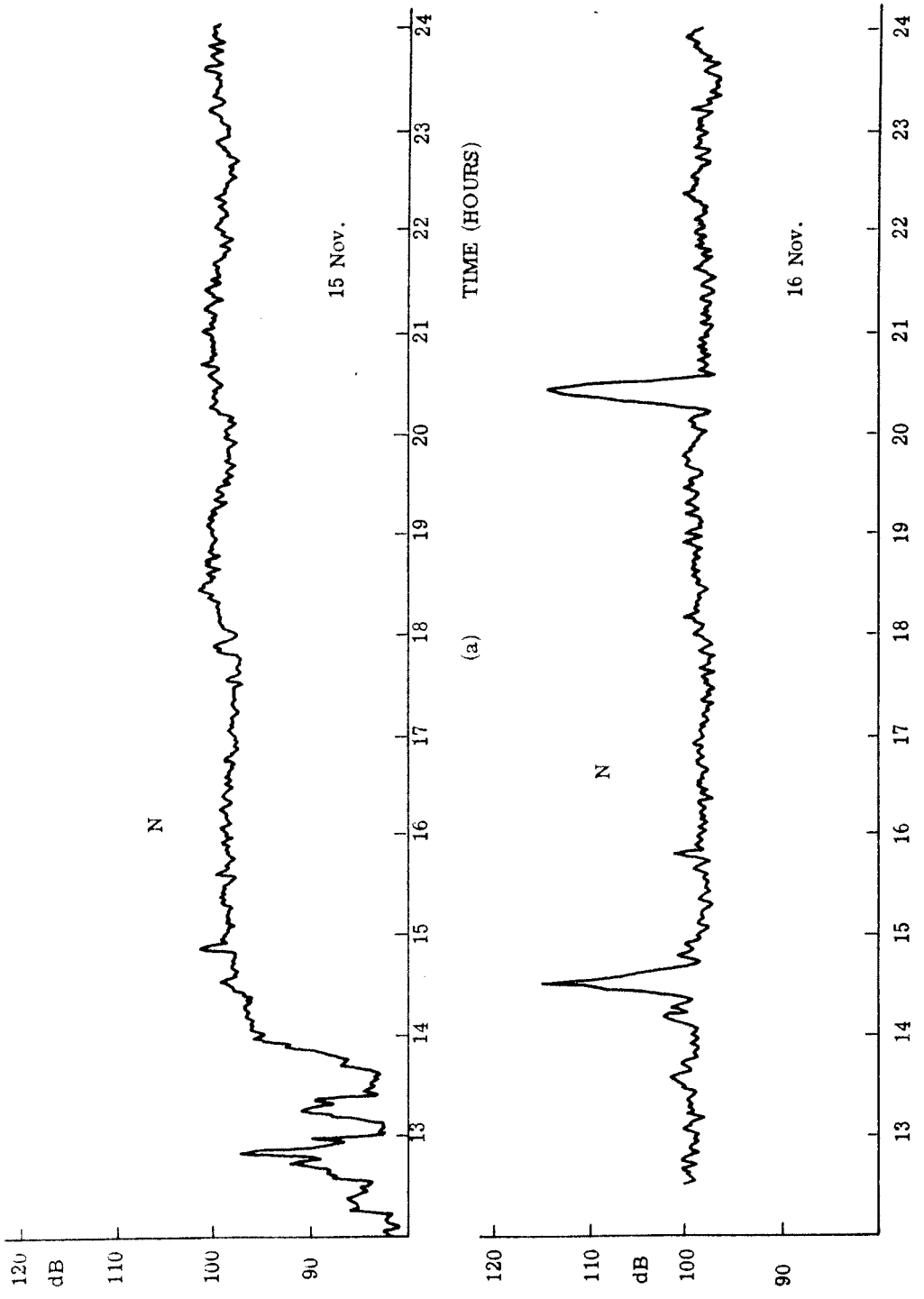

Fig. 16. Noise power: Fowey Rocks to Bimini

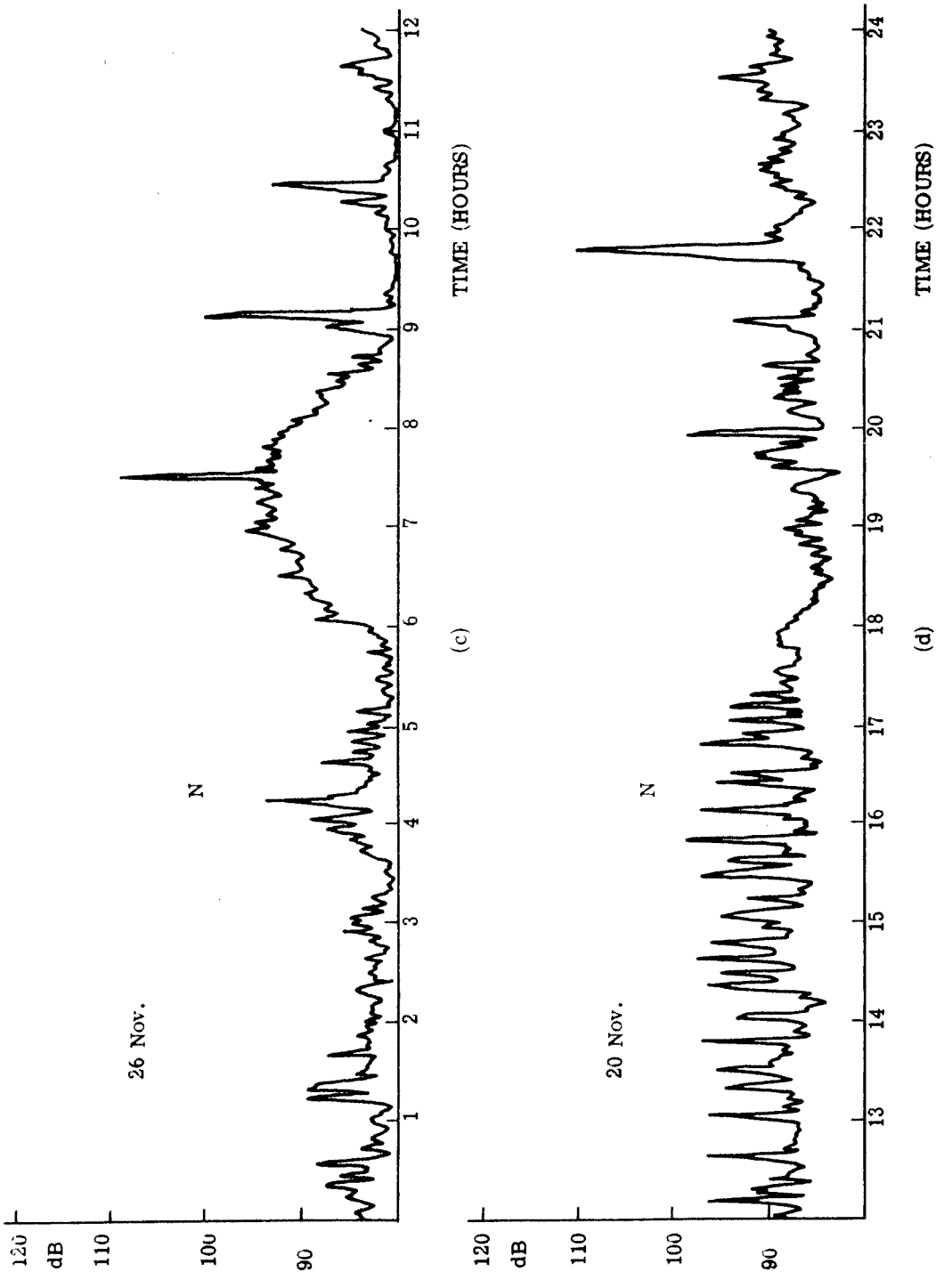
26 Nov.
N
dB
120
110
100
90
1
2
3
4
5
6
7
8
9
10
11
12
TIME (HOURS)
(c)
20 Nov.
N
dB
120
110
100
90
13
14
15
16
17
18
19
20
21
22
23
24
TIME (HOURS)
(d)

Fig. 16. (Cont.)

at the same level and there is still very little variation about this level. The two sharp peaks are examples of local shipping noise. Figure 16(c) illustrates that portion of the Bimini data during which the large, closely spaced spikes occur. It is unlikely that these spikes are due to local shipping noise in the light of their high repetition rate and the time of day when they occur. Figure 16(d) illustrates a roll variation in the noise power. At 1800 hours, the level of the noise power increases 15 dB and then returns to its original level, all within a period of three hours. These roll variations occur fairly often at different times in the shallow-water data. It is interesting to note, however, that on most of the days when shallow-hydrophone data were taken, a roll began between 1730 and 1800 hours and lasted from two to three hours. (See the figures for the first 12 hours for November 18 to 22, 25, 26, and 28 in Appendix A.) It is reasonable to assume that these rolls can be attributed to biological activity.

The 7-mile N power measurement differs from the Bimini N power measurement in two ways. First, as mentioned in Section 2.1.2, there are no appreciable jump or roll type variations in the 7-mile noise power. Second, the large, closely spaced, spiked variations that occur only once in the Bimini N power, occur six

times in the 7-mile N power with each occurrence lasting from 6 to 24 hours. In the remaining portion of 7-mile noise power data, there is only a small amount of variation with the exception of occasional shipping noise spikes. Figures 17 and 18 illustrate different 12-hour segments that are typical of the 7-mile noise power measurement.

2.1.4 The Reverb Power Measurements. The Bimini reverb power can be viewed as consisting of small amplitude variations about the mean R power of Fig. 11, Section 2.1.1. As mentioned in Section 2.1.1, R power varies according to N power during the periods of stable S power and varies according to S power during the period of high S power. Detailed examples of this dependency of R power on N power and on S power appear in Fig. 19(a) and (b) respectively. It should be noted that the level of R power in Fig. 19(b) is from 10 to 20 dB higher than the level of R power in Fig. 19(a).

The 7-mile reverb power resembles the 7-mile noise power in behavior. The two mean powers vary together during the whole experiment as discussed in Section 2.1.1. Moreover, the 7-mile R power also has long periods during which large amplitude, closely spaced spikes occur and long periods when there is only a small amount of variation about the mean value. In fact, there is a high correlation between the amount of variation in R power and the amount

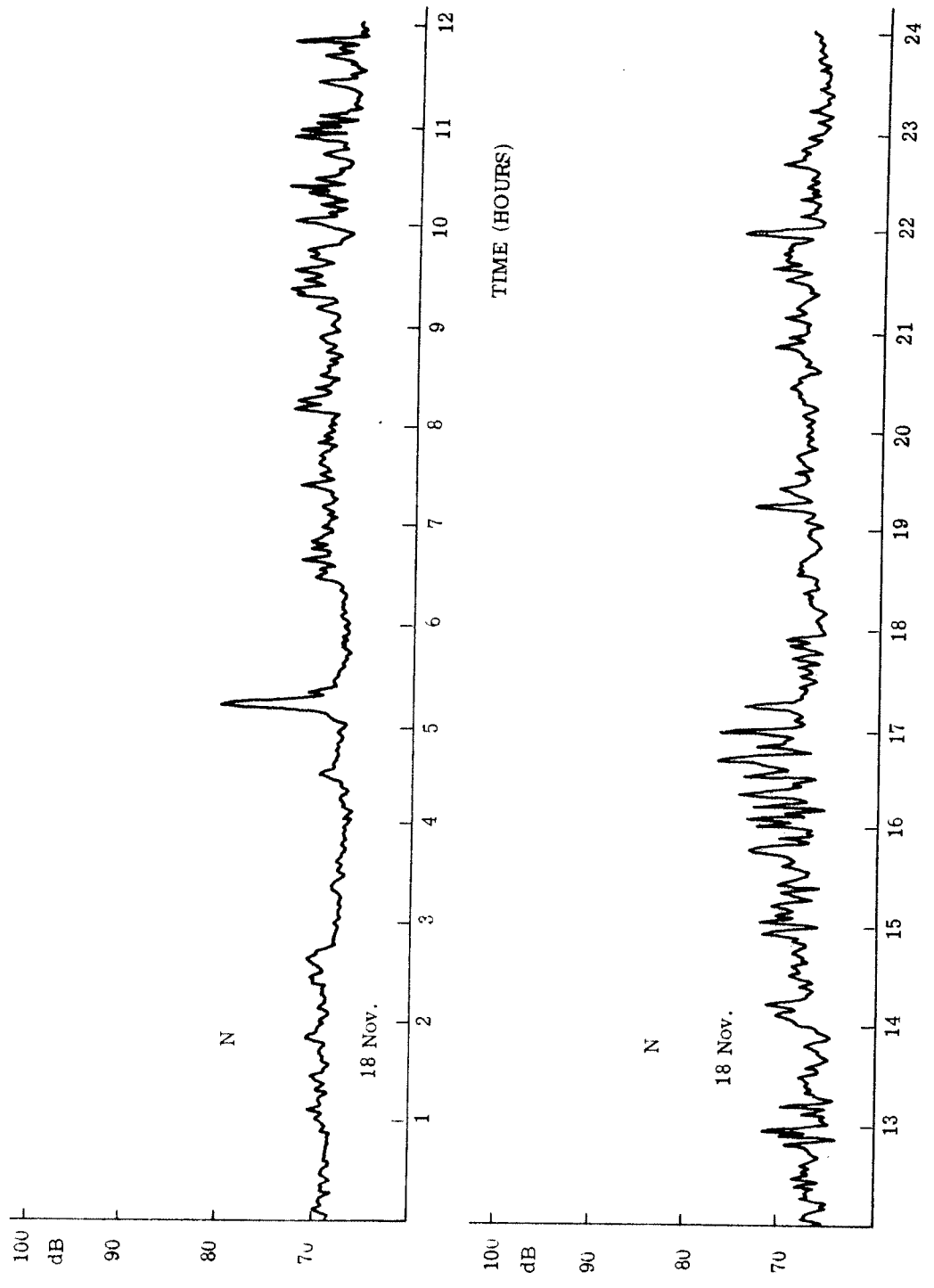

Fig. 17. Noise power: Fowey Rocks to 7-mile

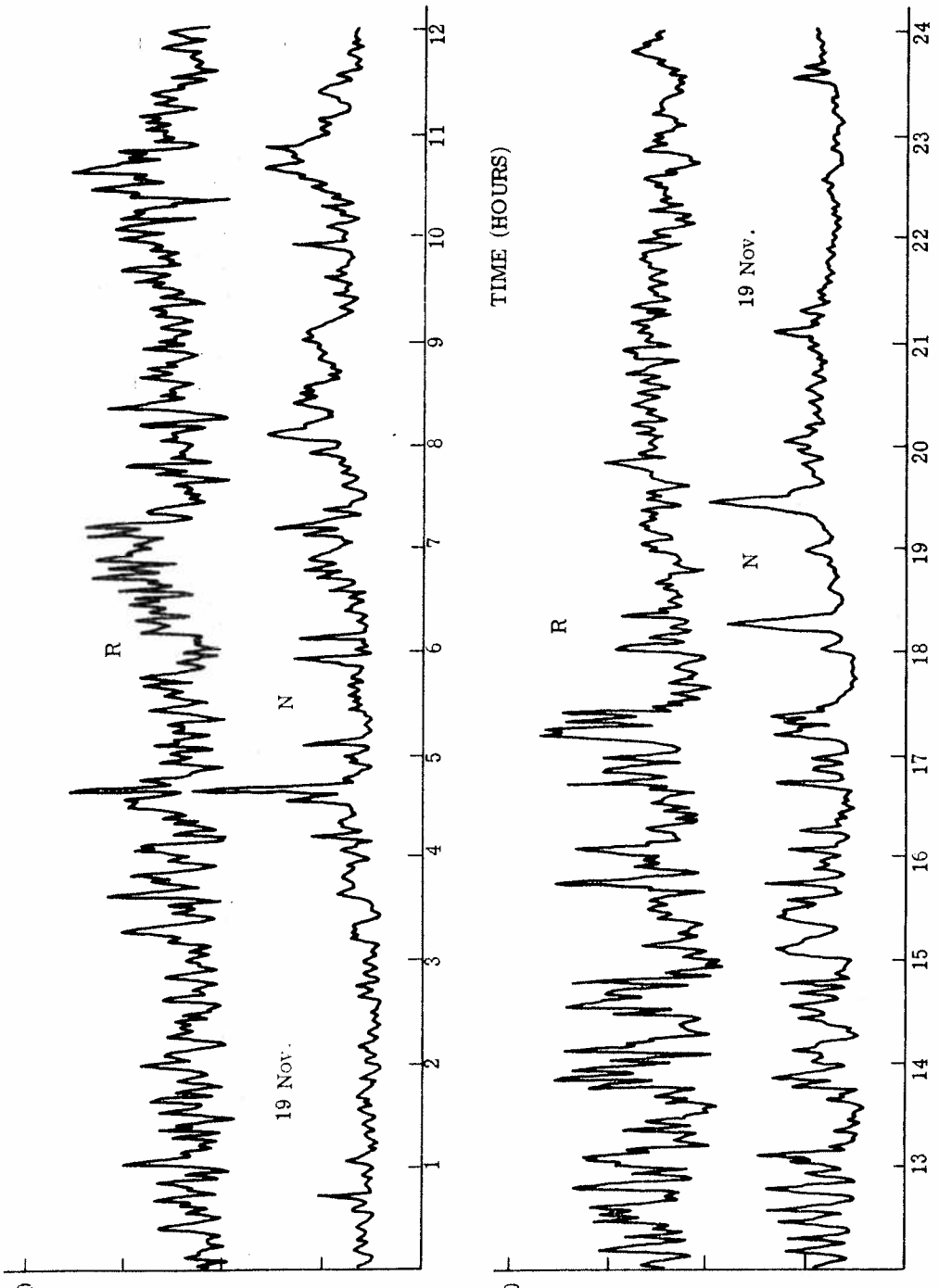

Fig. 18. Reverb and noise powers: Fowey Rocks to 7-mile

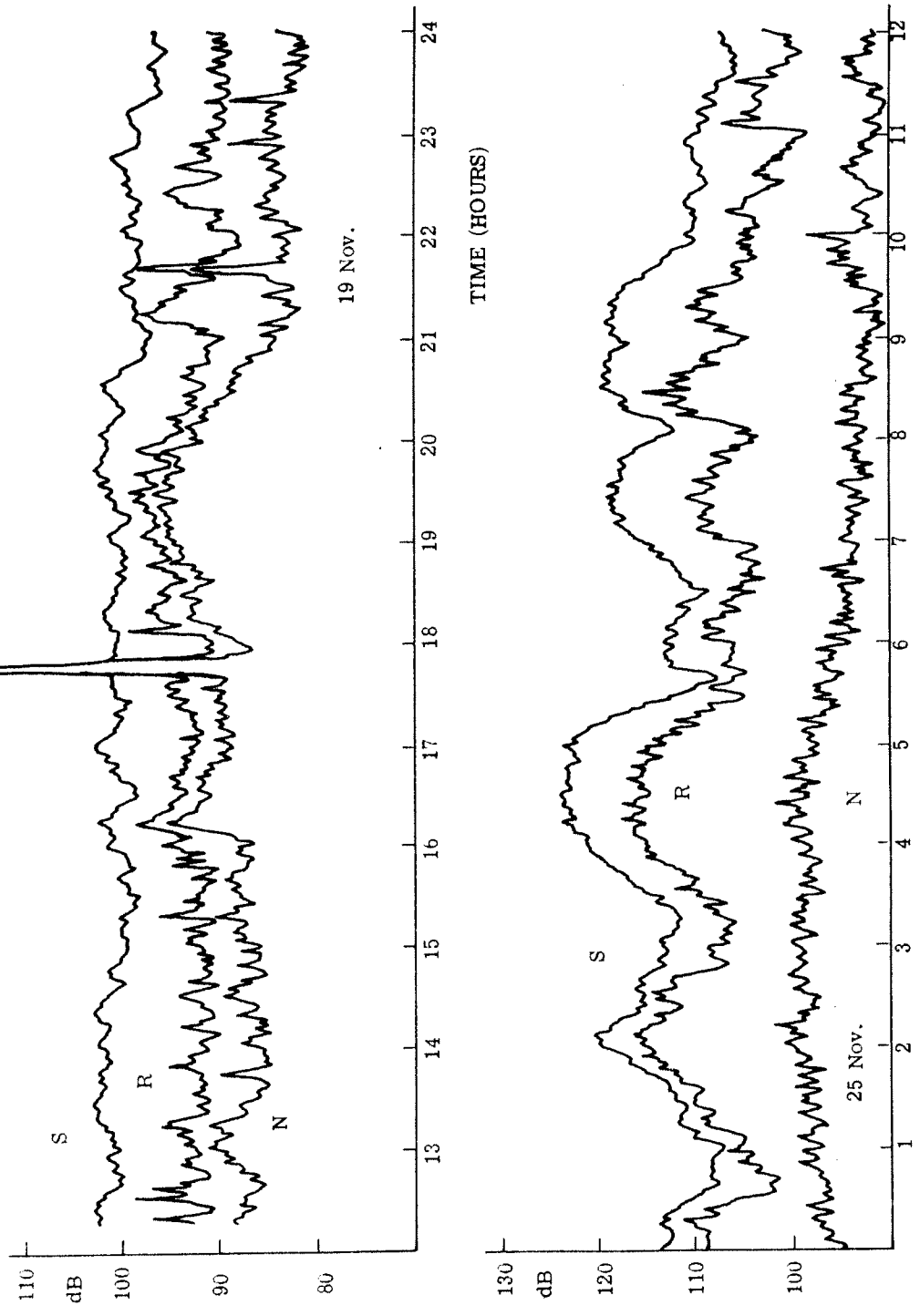

Fig. 19. Reverb, sideband and noise powers: Fowey Rocks to Bimini

of variation in N power. This is apparent in Fig. 18 which illustrates the two power measurements from 19 November. It is also noted from Fig. 18 that the R power signal-to-noise ratio is exceptionally high. We will return to this point in Section 2.2.

2.1.5 The Standard Deviations About the Mean Powers. In the above paragraphs, the power measurements have been described in terms of the slowly varying mean powers and specific examples of the CGB plots illustrating the character of the variations about the means. As a quantitative measure of this variation, sliding standard deviations for each power have been computed using a 25-minute averaging time. For notational convenience the standard deviation of each power is denoted by a "σ" with a subscript denoting the power; for example, σ_N denotes the standard deviation of the N power measurement.

The plot of the standard deviations for the Bimini powers is illustrated in Fig. 20. The fades in C power appear as sharp spikes in σ_C. Thus, those periods during which the spikes in σ_C occur less frequently correspond to the periods of low C-power fade rates. The jump and roll type variations in N power do not appear in σ_N. However, the period during which the large, closely spaced spikes occur, appears as a 3 dB increase in the level of σ_N [compare the morning of 25 November in Figs. 16(c) and 20(b)]. The shipping noise

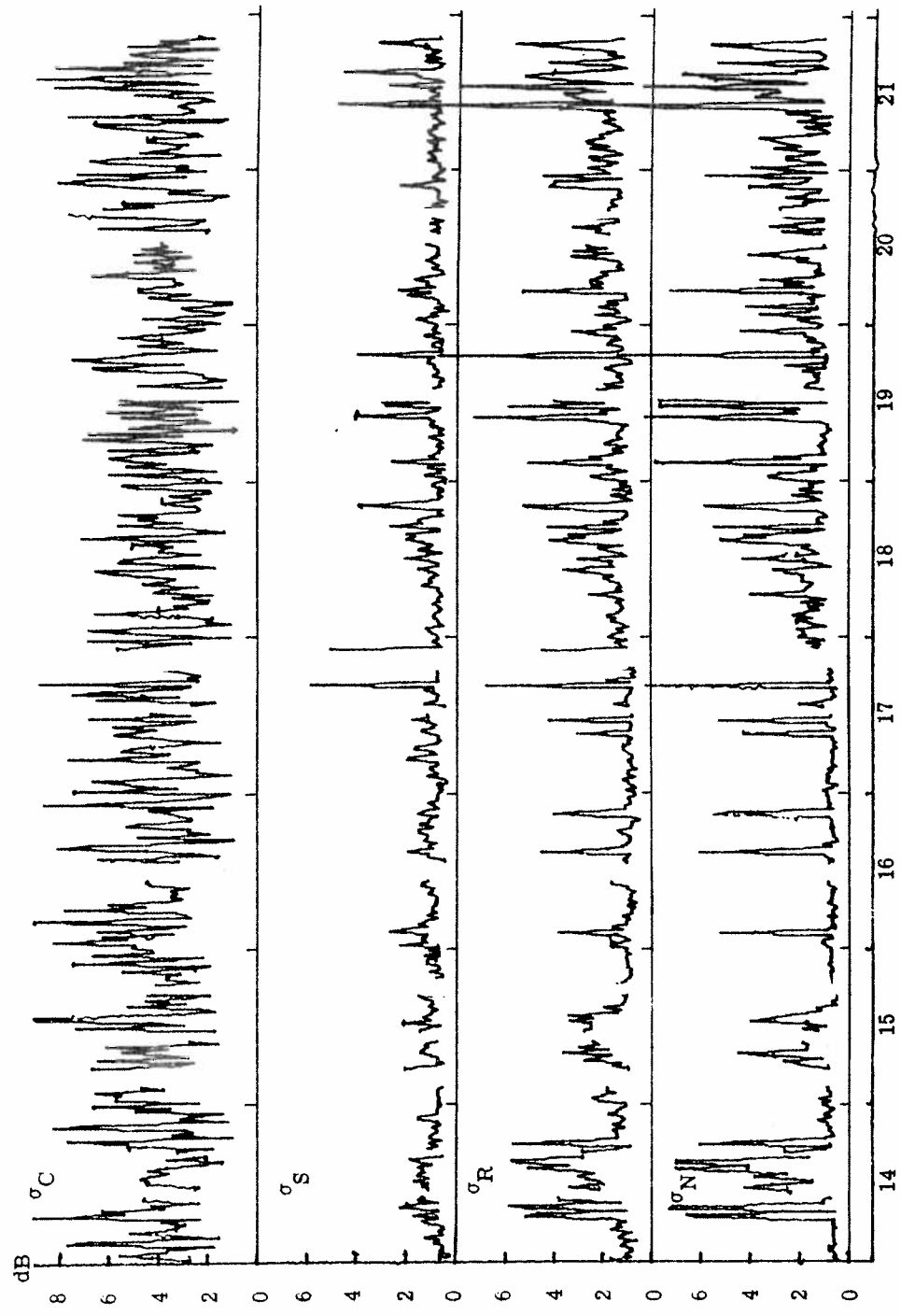

Fig. 20. Standard deviations: Fowey Rocks to Bimini

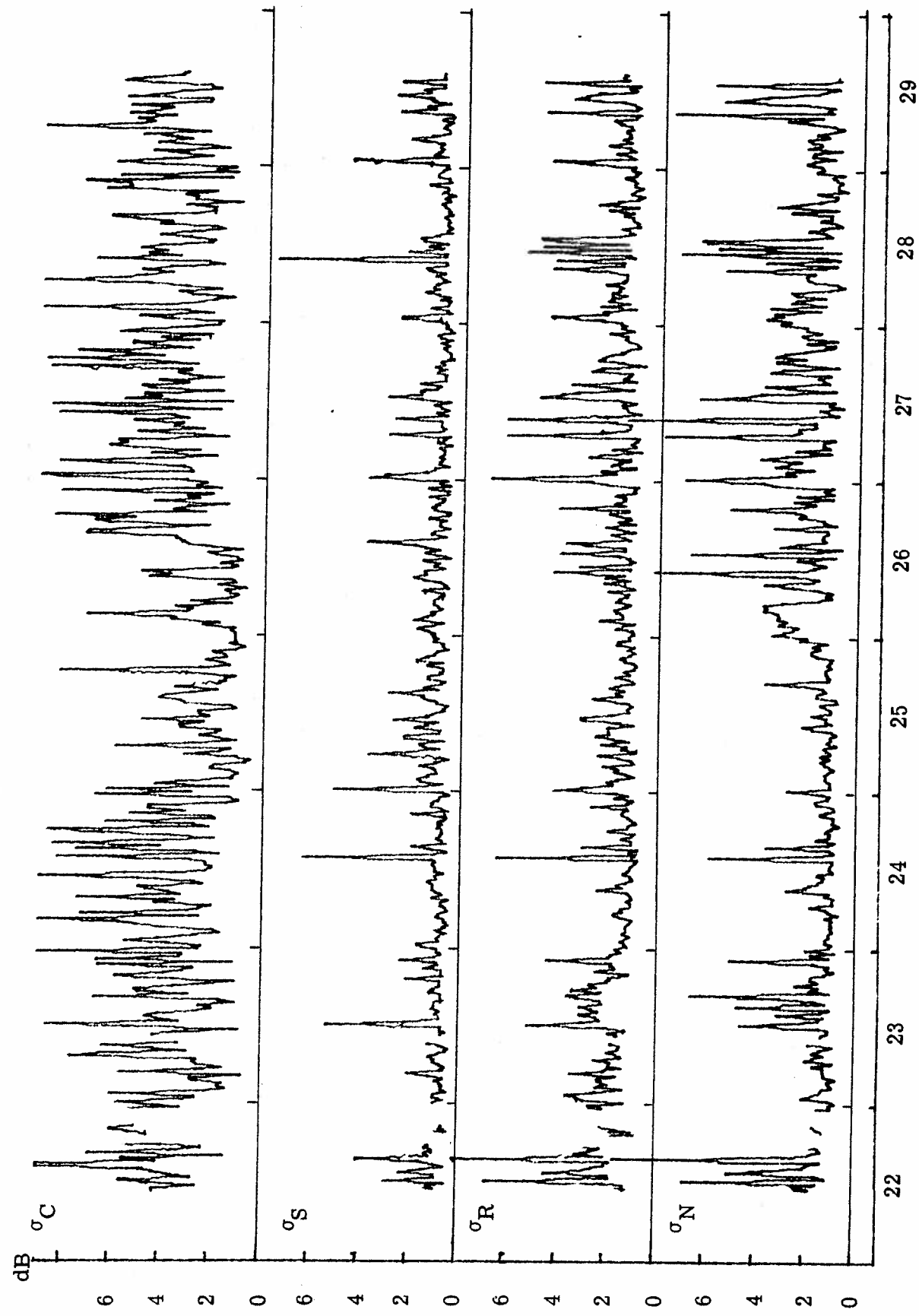
dB
σ_C
σ_S
σ_R
σ_N
6
4
2
0
22
23
24
25
26
27
28
29
DATE NOV. 1970

Fig. 20. (Cont.)

in N power also appear as spikes in σ_N. It is noted that some of these also appear in σ_S and σ_R when S power and R power become noise-driven by the large shipping noise spikes.

An important point to be noted in Fig. 20 is that, with the exception of the shipping noise spikes, σ_S is reasonably constant. This indicates that the amount of variation in the sideband power is essentially the same throughout the experiment. The same statement holds for both R and N power, if two 6-hour segments, one on 15 November and one on 23 November, are excluded from σ_R, and one 6-hour segment on 26 November is excluded from σ_N.

Figure 21 illustrates the standard deviations for the 7-mile power measurements. The lower 7-mile C-power fade rate is indicated by the smaller number of spikes in σ_C. Note also that the average level of the 7-mile σ_C is significantly less than the average level of the Bimini σ_C indicating less variation in the 7-mile C power. It is also seen that the spikes in σ_N due to shipping noise are smaller than those in the Bimini σ_N. Also, none of these spikes appear in σ_S and only a few appear in σ_R. This is a result of the higher signal-to-noise ratios at the 7-mile hydrophone.

Special attention should be given to the behavior of σ_R and σ_N in Fig. 21. Both σ_R and σ_N have frequent periods during which they rise several dB. These increases in σ_R and σ_N are the result of large amounts of variation about the average levels. The high

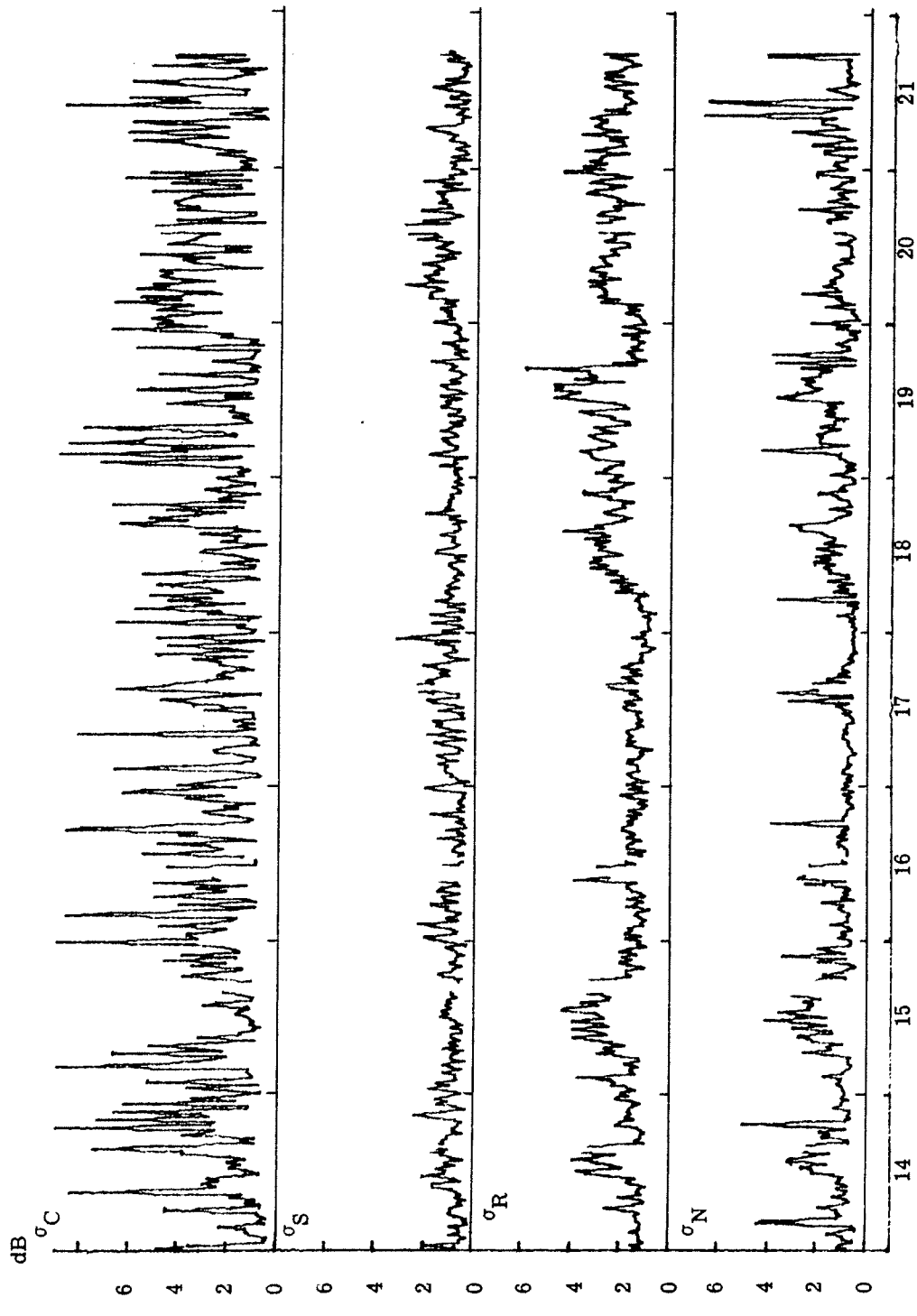

Fig. 21. Standard deviations: Fowey Rocks to 7-mile

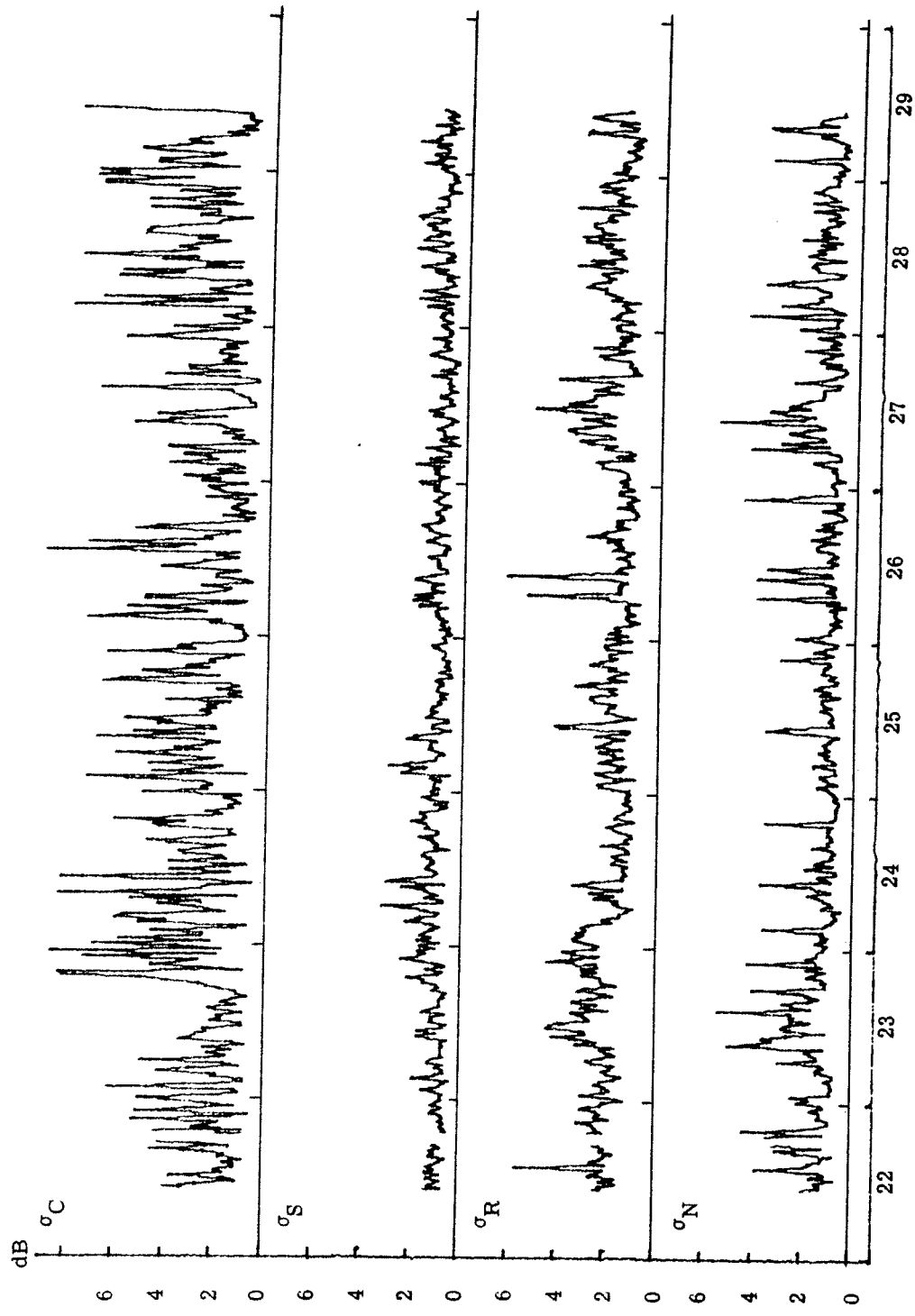
dB
σ_C
σ_S
σ_R
σ_N
6
4
2
0
22
23
24
25
26
27
28
29
DATE NOV. 1970

Fig. 21. (Cont.)

correlation between these periods of increase in σ_R and σ_N is apparent.

2.2 The Surface Reverberation Spectra

In the preceding section the behavior of the reverb power at both receiving sites was discussed qualitatively. In this section, examples of the surface reverberation (reverb) spectra are presented and discussed.

Recall from Section 1.3 that the reverb spectrum is that portion of the received spectrum contained within a bandwidth of 0.833 Hz centered about the carrier frequency. Thus, the reverb spectrum contains the power in the carrier frequency line, the power scattered from the carrier line by the surface reverberation, and that portion of the noise power normally lying within the reverb bandwidth. To illustrate the decomposition of the reverb spectrum into its components, displays from each receiving site are presented in Fig. 22. The tick marks on the frequency axis of each display are separated by 0.1 Hz and the amplitude is expressed in dB with the two vertically spaced tick marks indicating a difference of 20 dB. Figure 24(a) shows the spectrum when only noise is present, and Fig. 24(b) shows the spectrum when both signal and noise are present, both displays are taken from the Bimini data. It is seen that when only noise is present, the carrier line appears as a dot above the center frequency and the reverb power appears in sidebands about the carrier line.

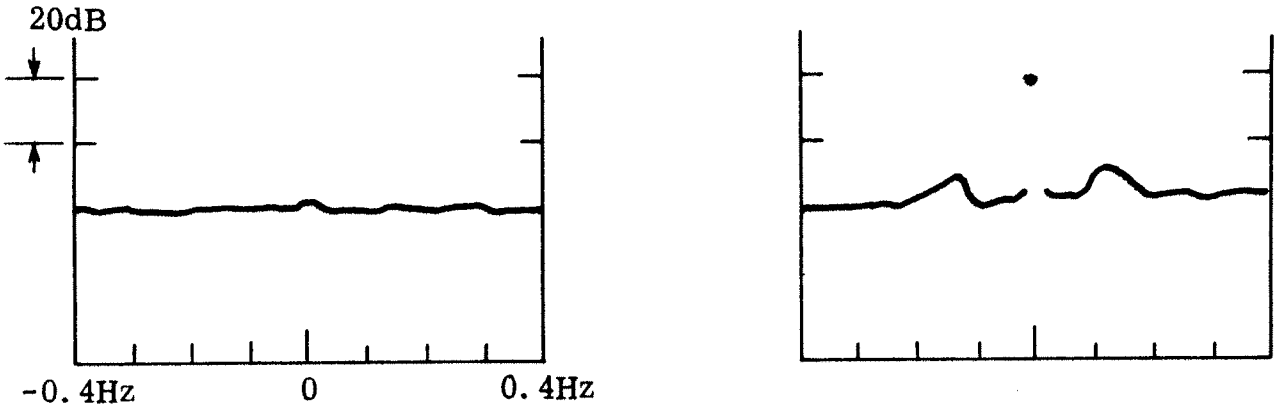

Fig. 22. Reverb spectra displays: Fowey Rocks to Bimini

Figure 23(a) and (b) show two displays taken from the 7-mile data at two different times when no signal was transmitted. Notice that there is a 0.2 Hz bandwidth over which the spectrum level is 20 dB higher than the level in the remaining portion of the reverb bandwidth. Note also that the center frequency of each excursion is different. It is doubtful that these excursions are characteristic of the ocean noise, and until a more complete investigation is made, they must be attributed to signal leakage somewhere in the 7-mile processing equipment. It might also be mentioned that the additional power present in the display of Figs. 23(a) and (b) would account for as much as 13 dB of the 7-mile R power measurement.

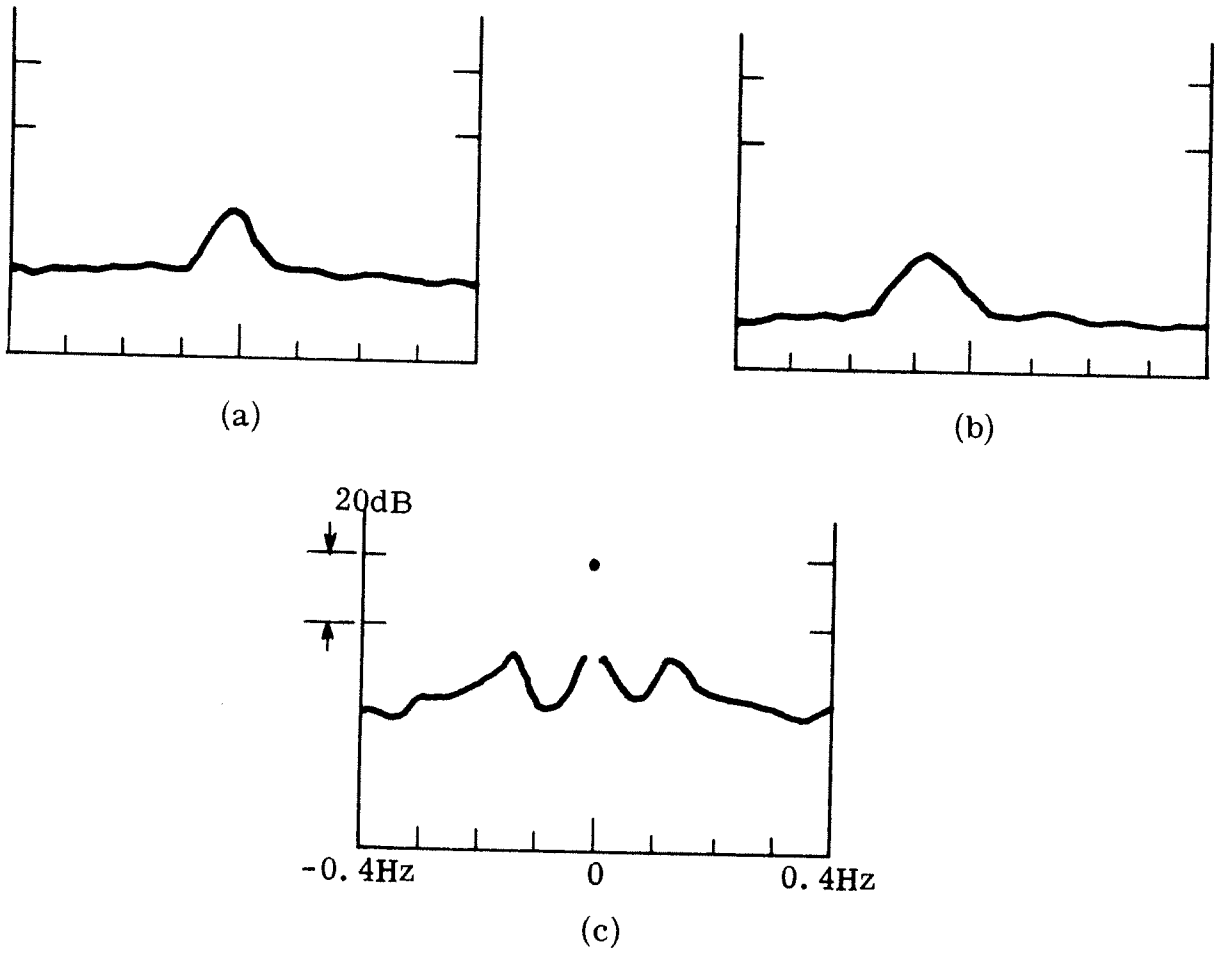

Fig. 23. Reverb spectra displays: Fowey Rocks to 7-mile

Figure 23(c) illustrates a typical 7-mile reverb display when signal is also present. It is not possible to determine what percentage of the sidebands must be attributed to signal leakage in the equipment.

We begin the description of the reverb displays with examples from the Bimini data. As might be expected, the most significant reverb sidebands occur in the large S power portion of the data since during this period R power is also quite large. As examples of the

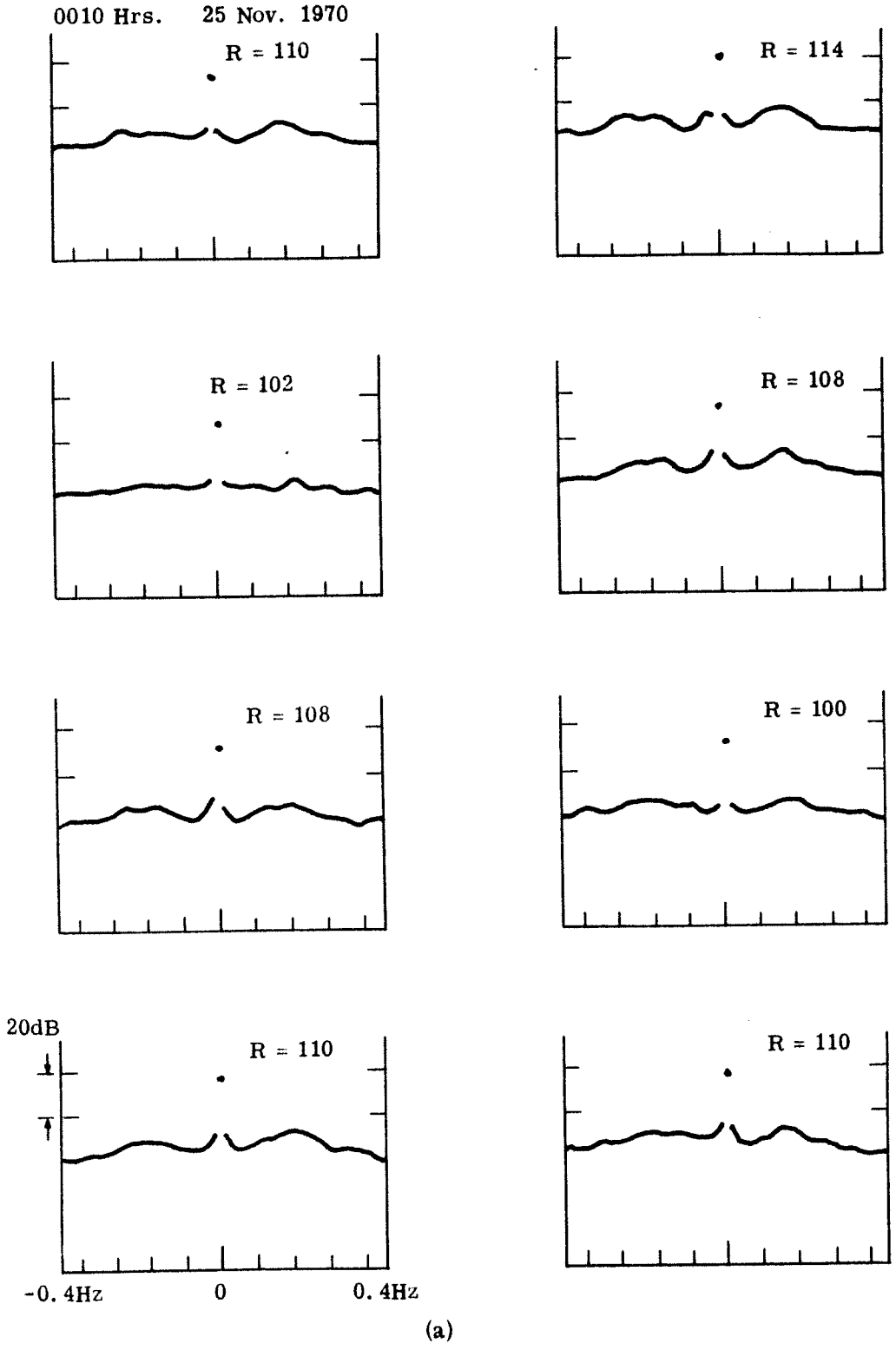

Fig. 24. Reverb spectra displays: Fowey Rocks to Bimini

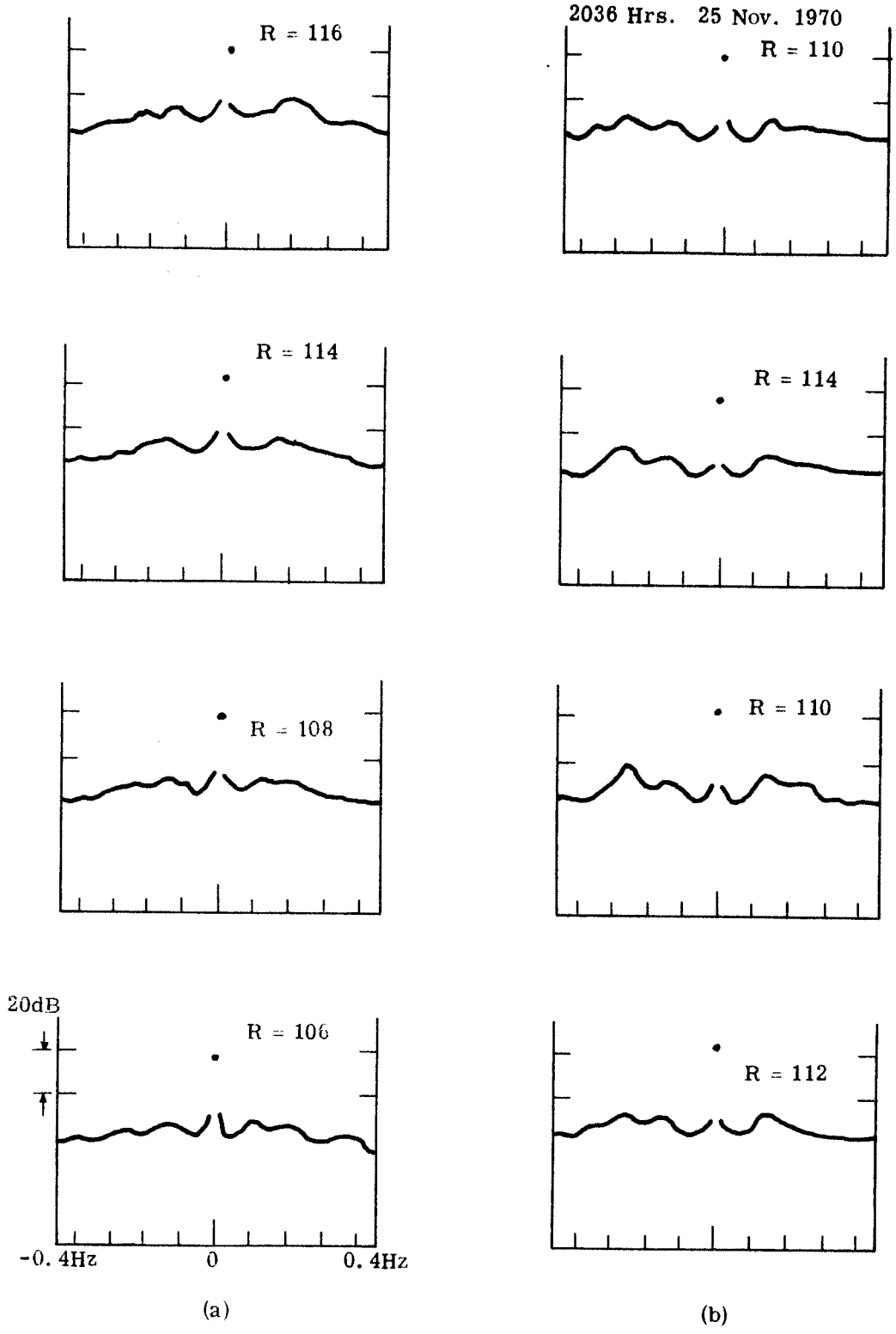
R = 116
2036 Hrs. 25 Nov. 1970
R = 110
R = 114
R = 114
R = 108
R = 110
20dB
R = 106
R = 112
-0.4Hz
0
0.4Hz
(a)
(b)

Fig. 24. (Cont.)

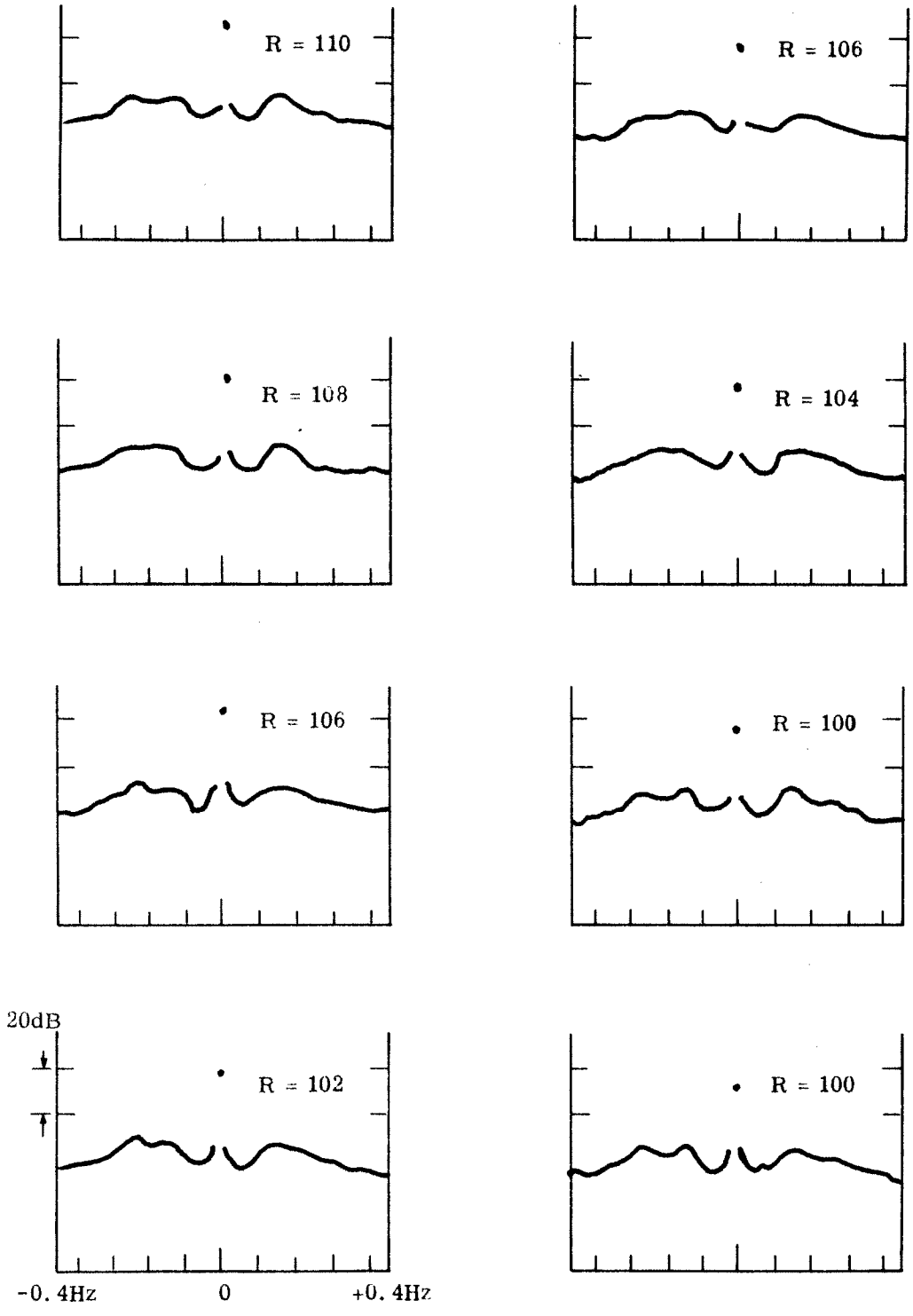

(b)

Fig. 24. (Cont.)

reverb displays during this period, two sequences of displays taken over different 6-hour intervals appear in Figs. 24(a) and 24(b). The first display in the upper left-hand corner of Fig. 24 was taken at 0010 hours on 25 November. The first display in Fig. 24(b) was taken at 2036 hours, also on 25 November. Successive displays in all of the sequences of displays illustrated in this section are taken at 30 minute intervals. The value of R power at the time when each display was taken is written to the left of the display. It is seen from Fig. 24 that the amplitude of the reverb sidebands depends on the value of the corresponding R-power measurement. For these displays it appears that the reverb sidebands are centered about ± 0.2 Hz on either side of the carrier with most of the power in each sideband confined to a 0.2 Hz bandwidth.

Although the largest reverb sidebands occur during the high S-power portion of the Bimini data, there are also periods from the stable S-power data during which reasonably well-defined reverb sidebands appear. Figure 25 illustrates two, 4-hour sequences of reverb displays taken from different periods of the stable S-power data. The first display in the sequence in Fig. 25(a) was taken at 0400 hours on 14 November and the first display in Fig. 25(b) was taken at 0255 hours on 18 November. As above, the amplitude of the reverb sidebands depends on the corresponding value of R power. In contrast to the reverb displays taken from the high S-power data,

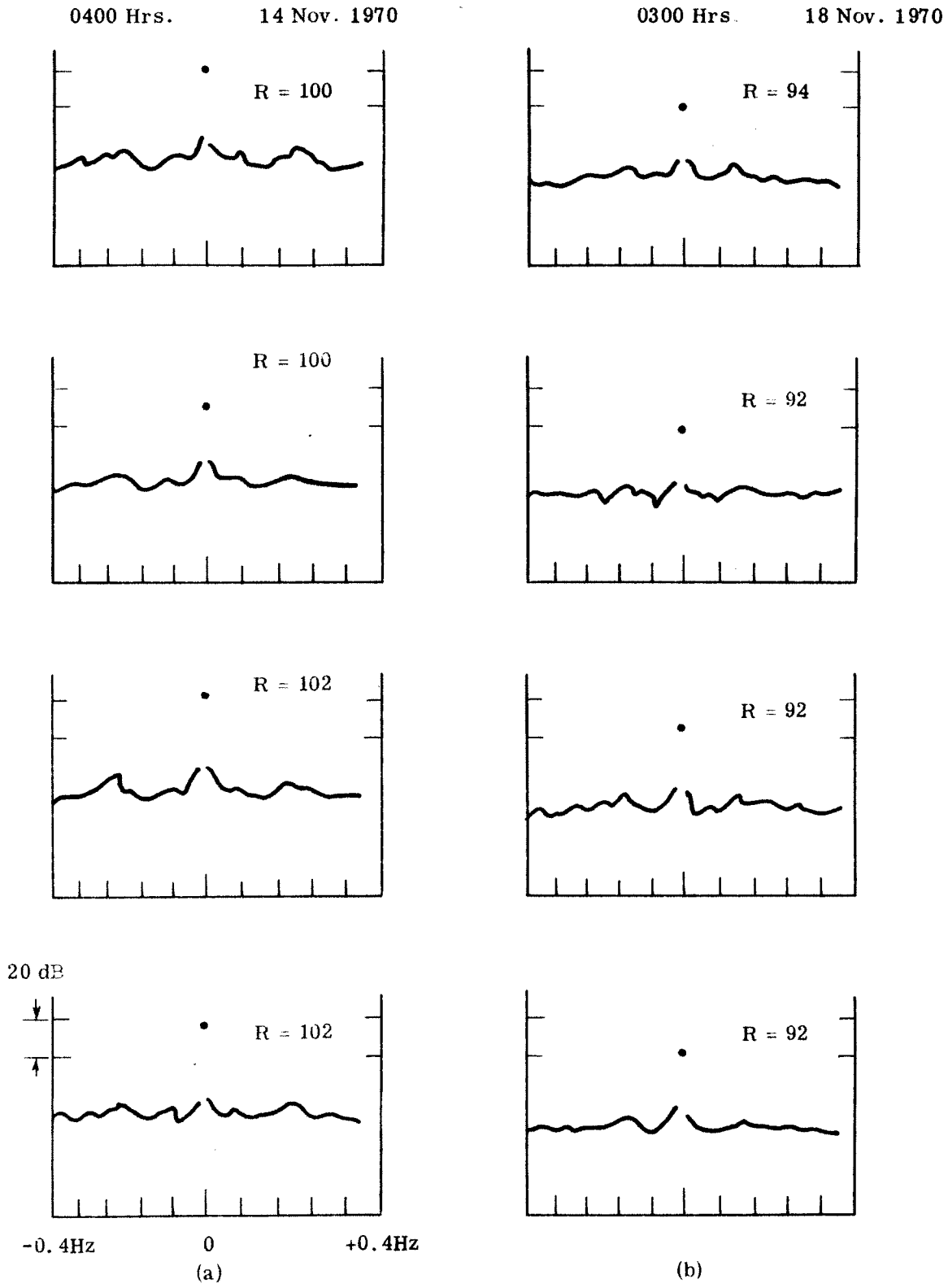

Fig. 25. Reverb spectra displays: Fowey Rocks to Bimini

however, the bandwidth of each sideband is only about 0.1 Hz. Also note that the center frequencies of the reverb sidebands in Fig. 25(a) are from 0.05 to 0.1 Hz larger than the center frequencies for the other Bimini reverb spectra. The reverb displays in Fig. 25 are typical of much of the stable S-power Bimini data, although there are long periods in this portion of the data where no noticeable reverb sidebands appear.

The reverb spectra from the 7-mile data generally have a more definite structure than do those from the Bimini data. The amplitudes of the sidebands are larger and the shape of the sidebands varies less during the course of the experiment. Figures 26(a) to 26(d) illustrate four sequences of reverb spectra taken on four different days. (The time when the first display in each sequence was taken is indicated at the top of the display.) The amplitudes of the reverb sidebands in these displays ranges from 10 to 25 dB and the sideband center-frequencies vary between $\pm$ 0.12 to $\pm$ 0.25. These reverb displays illustrate the complete range of behavior of the 7-mile reverb spectra.

2.3 The Multipath Structure Displays

The displays of the multipath structure are obtained as the magnitude of the cross-correlation between the demodulated reception and a pulse-compression reference (see Section 1.3). The length

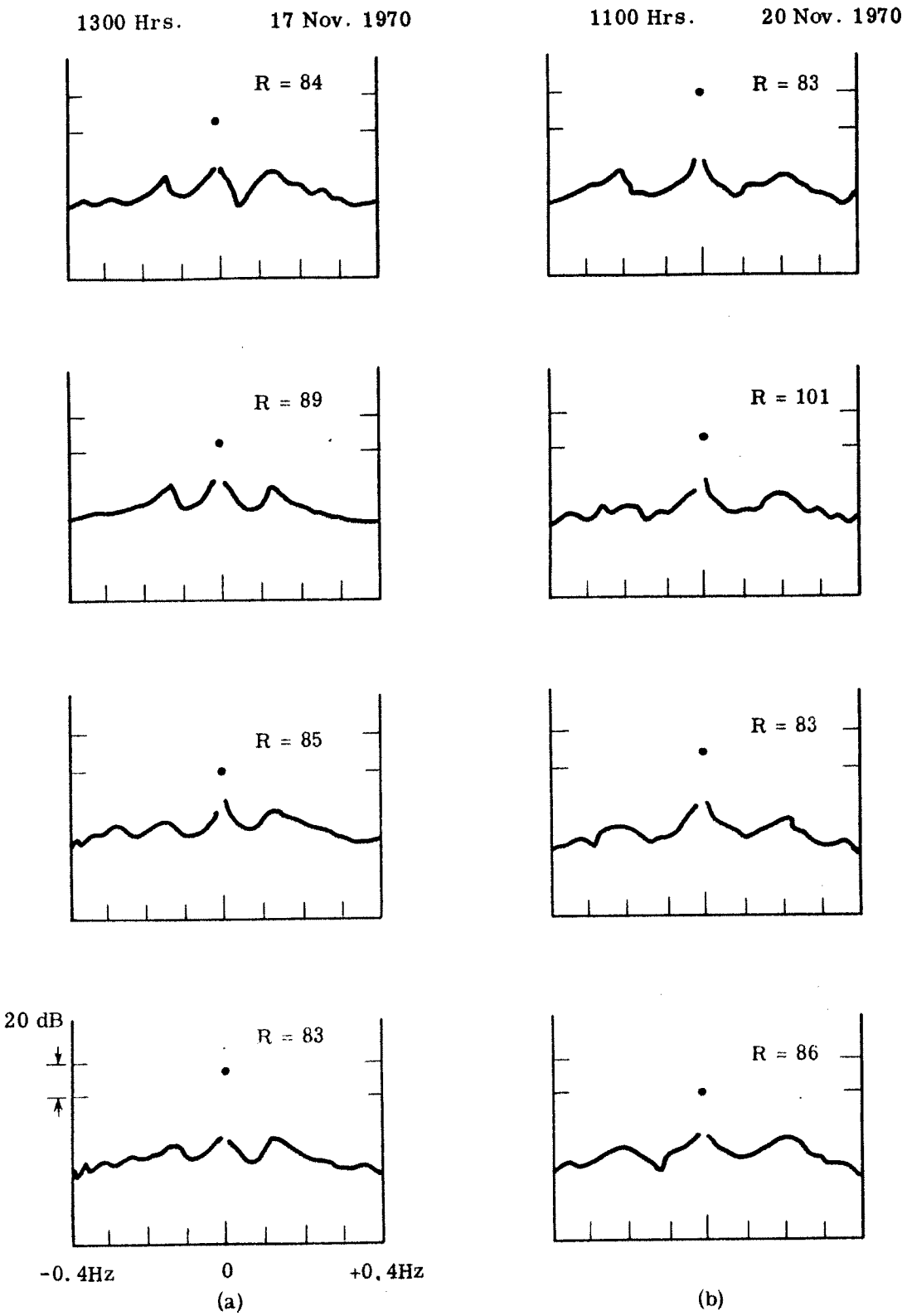

Fig. 26. Reverb spectra displays: Fowey Rocks to 7-mile

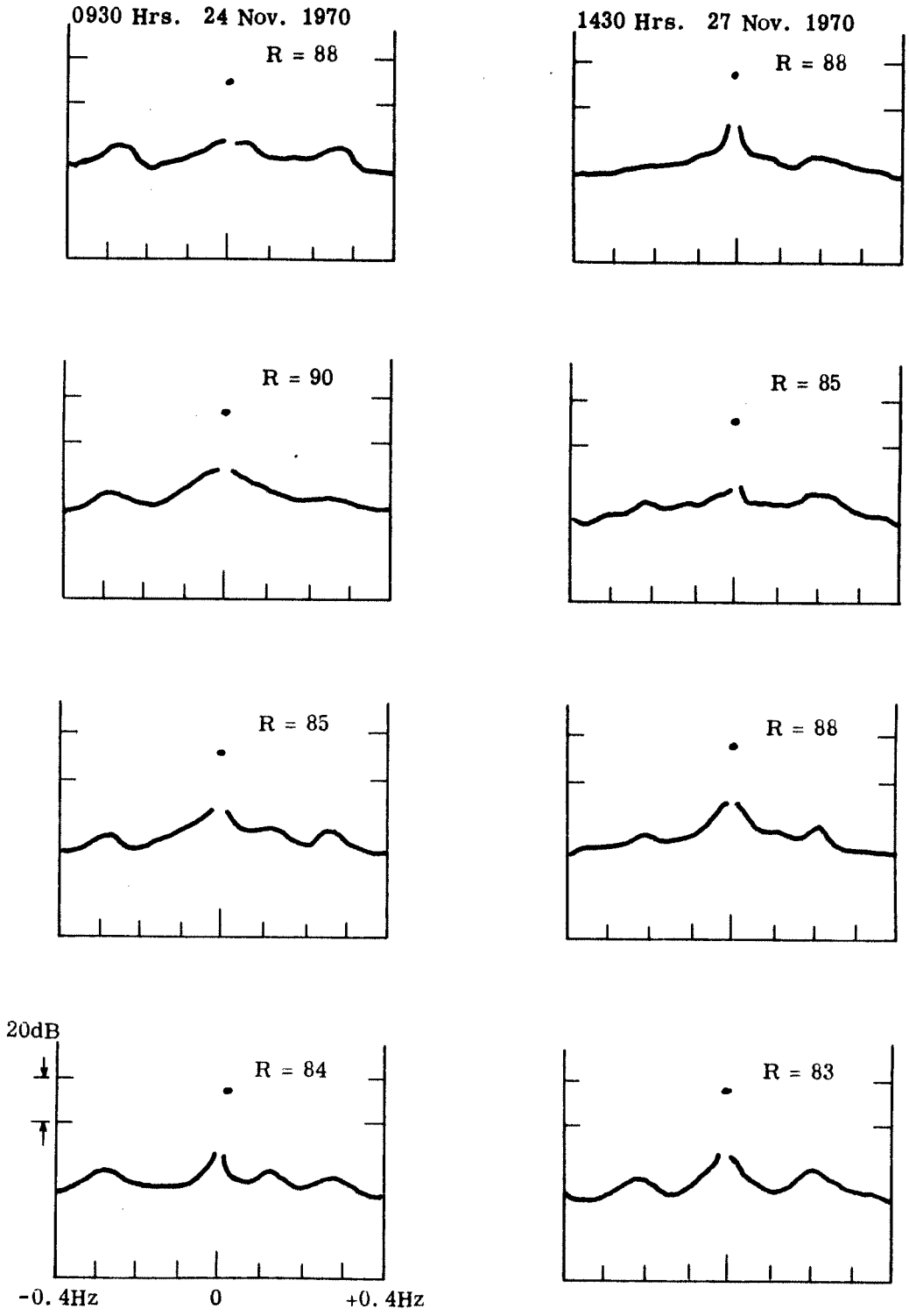
0930 Hrs. 24 Nov. 1970
R = 88
1430 Hrs. 27 Nov. 1970
R = 88
R = 90
R = 85
R = 85
R = 88
20dB
R = 84
R = 83
-0. 4Hz
0
+0. 4Hz

Fig. 26. (Cont.)

of the time delay axis in these displays is equal to the period of the transmission, 1.2 seconds, and the duration of a single peak in the display is $2d = 0.038$ seconds. (The duration of a single peak is indicated on the display in the lower left-hand corner in each figure.) The vertical scaling for the multipath displays is determined only up to a factor which is a power of two. Thus, care must be used in comparing the relative strengths of arrival peaks in different displays.

The multipath displays from the Bimini data indicate a wide variation in the complexity of the multipath structure. The most complex structure occurs during the period of stable S power. Figures 27(a) and 27(b) illustrate two sequences of multipath displays taken from this portion of the Bimini data. The multipath displays in Fig. 27(a) were taken from the shallow water data at 5-minute intervals beginning at 0050 hours on 16 November. The corresponding values of S power appear to the left of each display. There are two main arrival peaks occurring close together, preceded by a varying number of small amplitude arrival peaks. The overall power in the minor arrival peaks is the greatest for the small value of S power.

The multipath displays in Fig. 27(b) were taken from the deep water data at 5-minute intervals beginning at 0352 hours on 14 November. The multipath structure in these displays is quite complicated. Each display shows many transmission paths, all of approximately the same strength. Although a significant portion of the Bimini

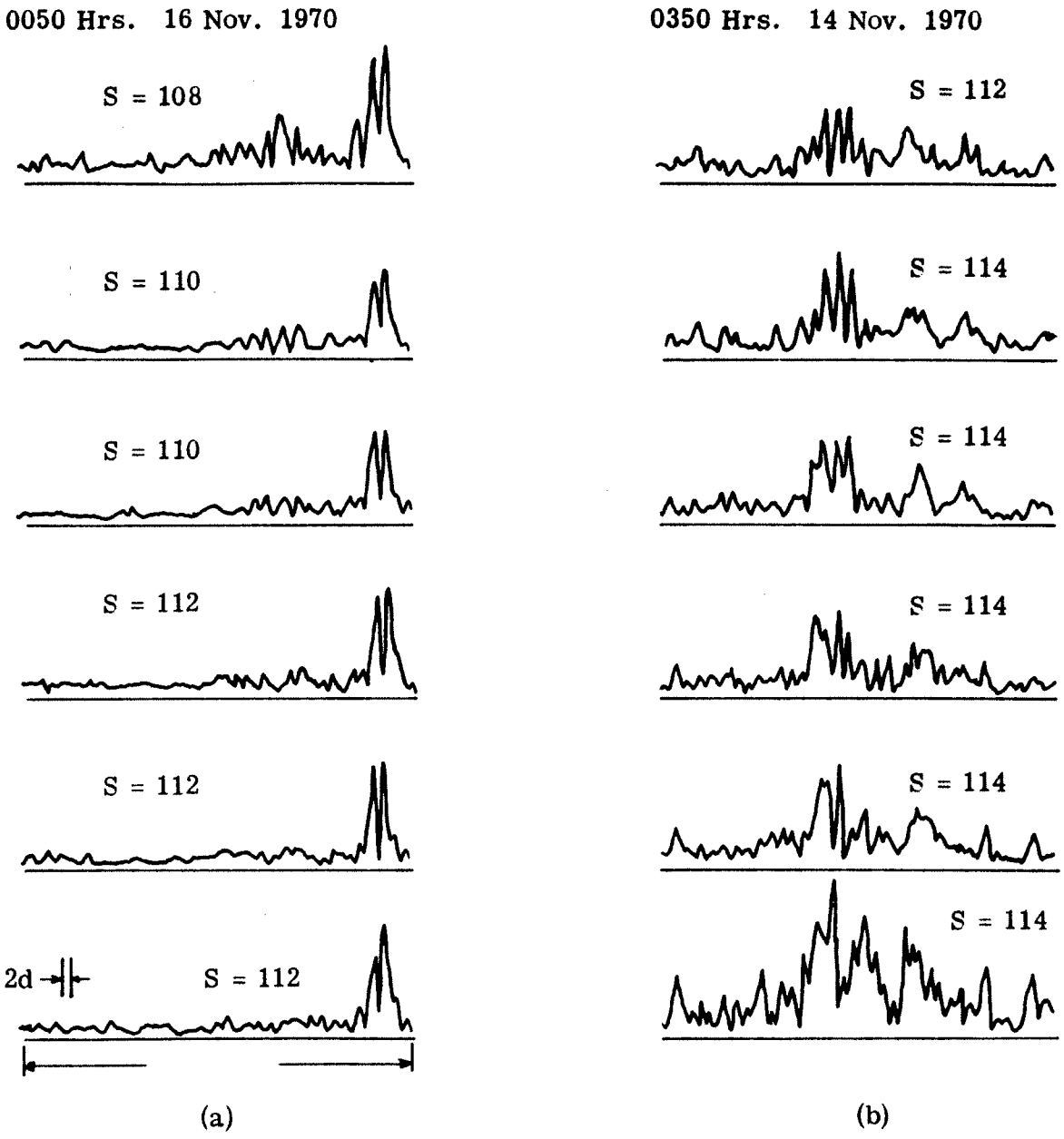

Fig. 27. Multipath structure displays: Fowey Rocks to Bimini

data has a multipath structure as complicated as that appearing in Fig. 27(b), there are only a few instances where the multipath structure becomes more complicated.

The least complicated multipath structure occurs during the high S-power portion of the Bimini data. Figure 28 illustrates a sequence of multipath displays taken every 30 minutes beginning at 0010 hours on 25 November. For the high values of S power, the multipath displays indicate only one major arrival peak, and in several of these displays there are no smaller arrival peaks at all. For the lower values of S power, however, more than one major arrival peak appears.

The multipath displays from the 7-mile data are less complicated and more stable than those from the Bimini data. Figures 29(a) to 29(d) illustrate four sequences of multipath displays taken on different days. The times at which the first display in each sequence were taken are the same as those for the reverb spectra in Fig. 27. The successive display in each sequence were taken at 15-minute intervals. It is seen that with few exceptions, each display indicates one major transmission path preceded by from two to four minor transmission paths. This behavior is typical of the 7-mile data multipath structure.

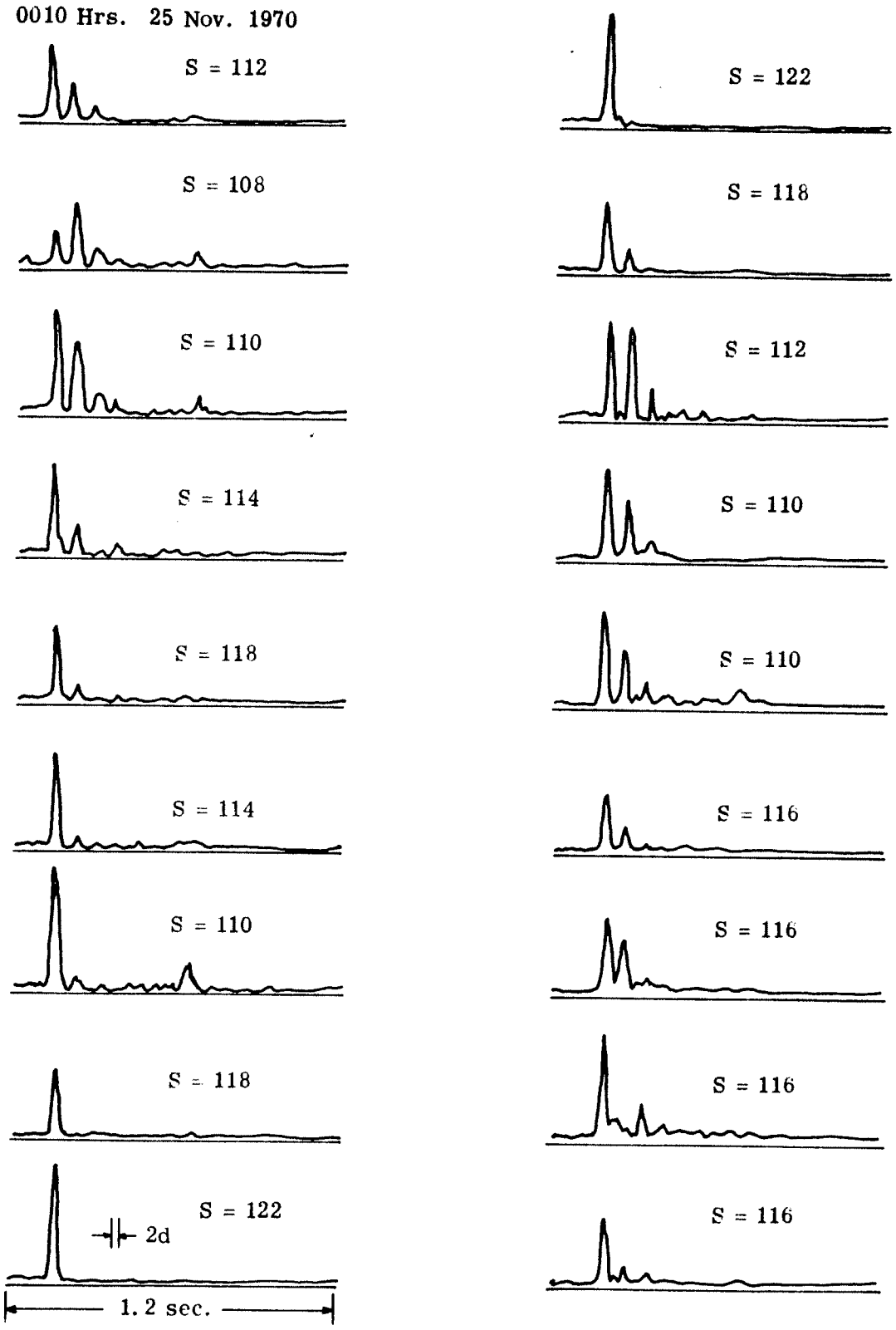

Fig. 28. Multipath structure displays: Fowey Rocks to Bimini

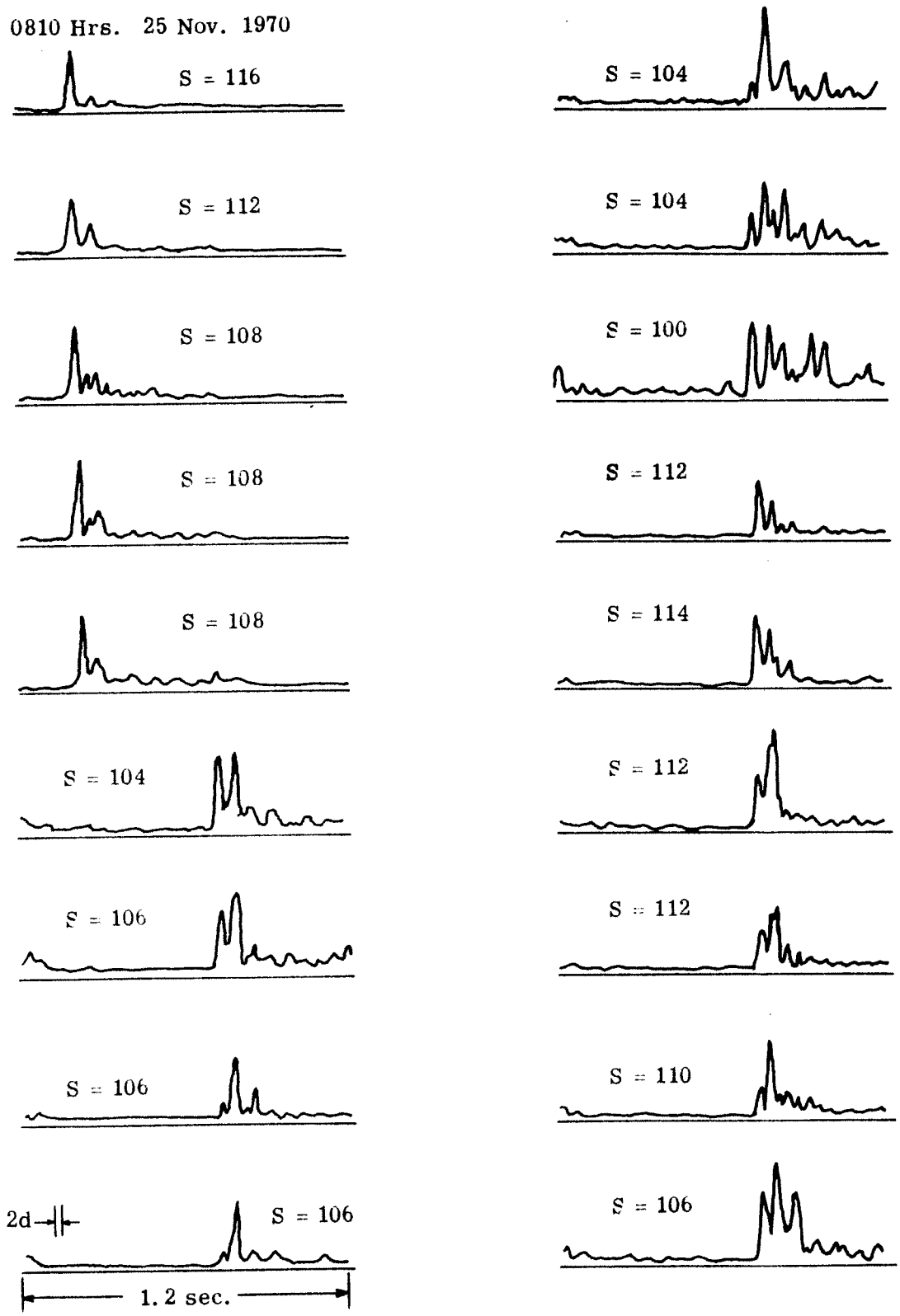
0810 Hrs. 25 Nov. 1970
S = 116
S = 112
S = 108
S = 108
S = 108
S = 104
S = 106
S = 106
2d
S = 106
1.2 sec.
S = 104
S = 104
S = 100
S = 112
S = 114
S = 112
S = 112
S = 110
S = 106

Fig. 28. (Cont.)

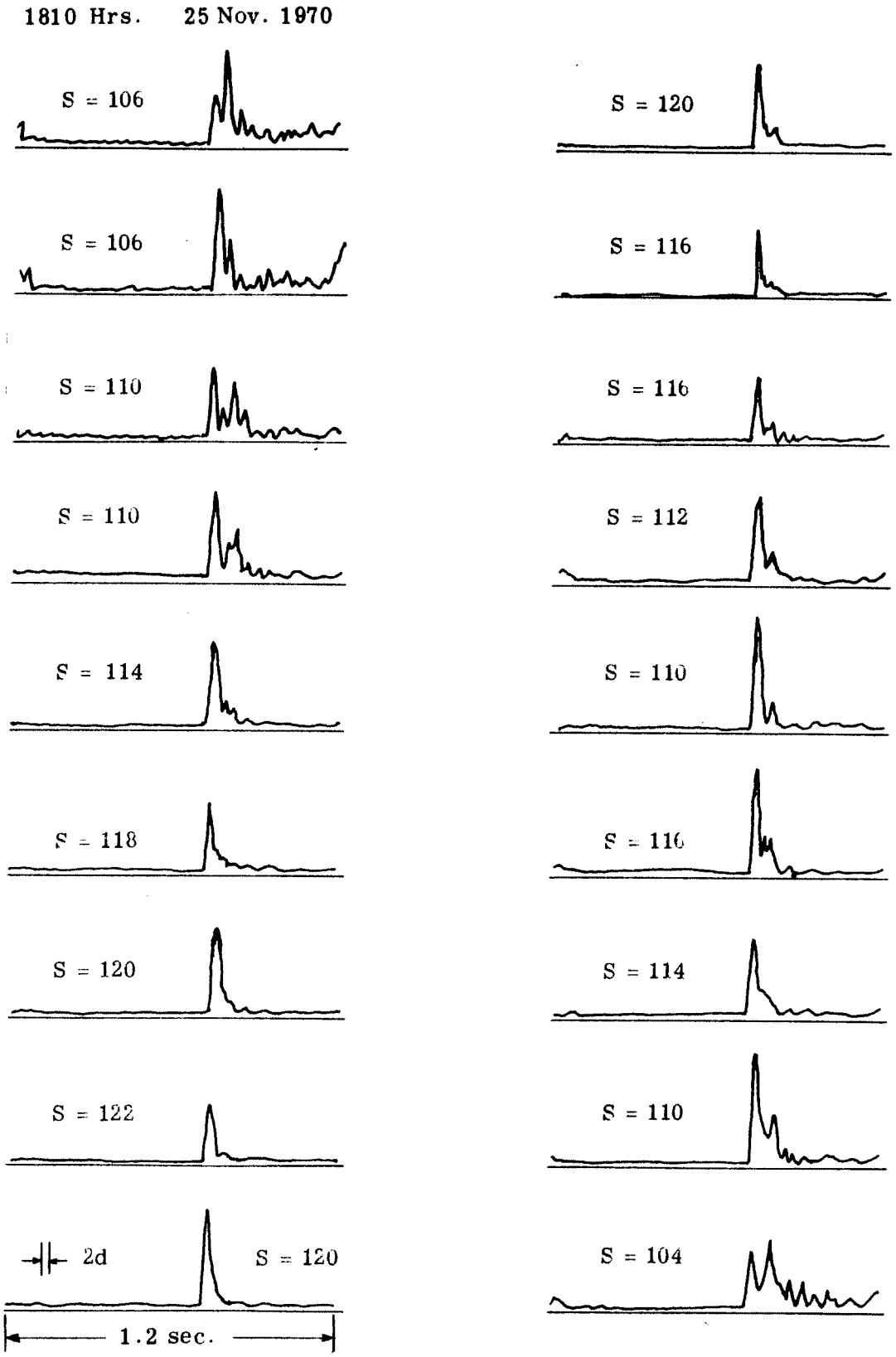
1810 Hrs. 25 Nov. 1970
S = 106
S = 106
S = 110
S = 110
S = 114
S = 118
S = 120
S = 122
2d
S = 120
1.2 sec.
S = 120
S = 116
S = 116
S = 112
S = 110
S = 116
S = 114
S = 110
S = 104

Fig. 28. (Cont.)

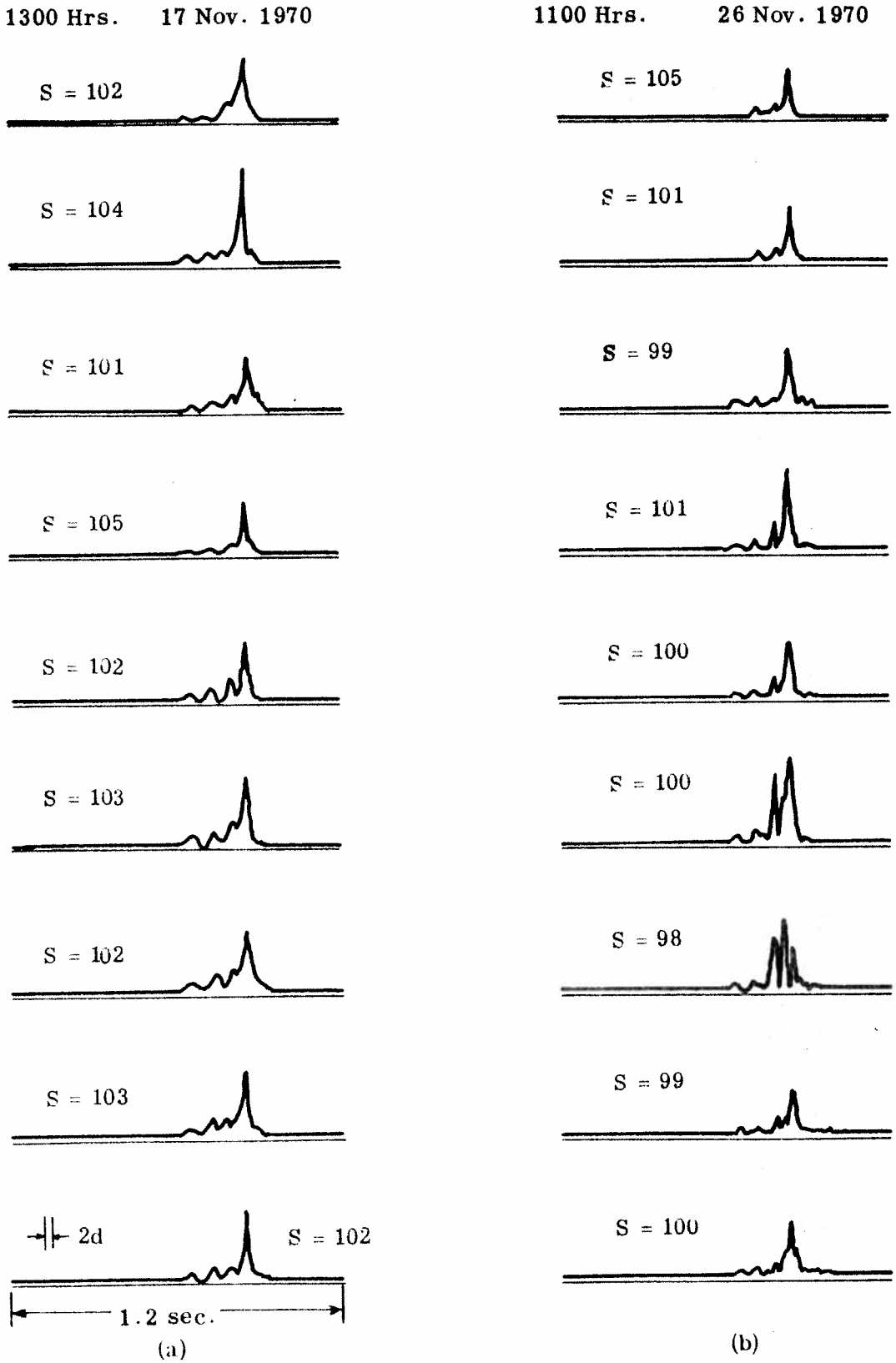

Fig. 29. Multipath structure displays: Fowey Rocks to 7-mile

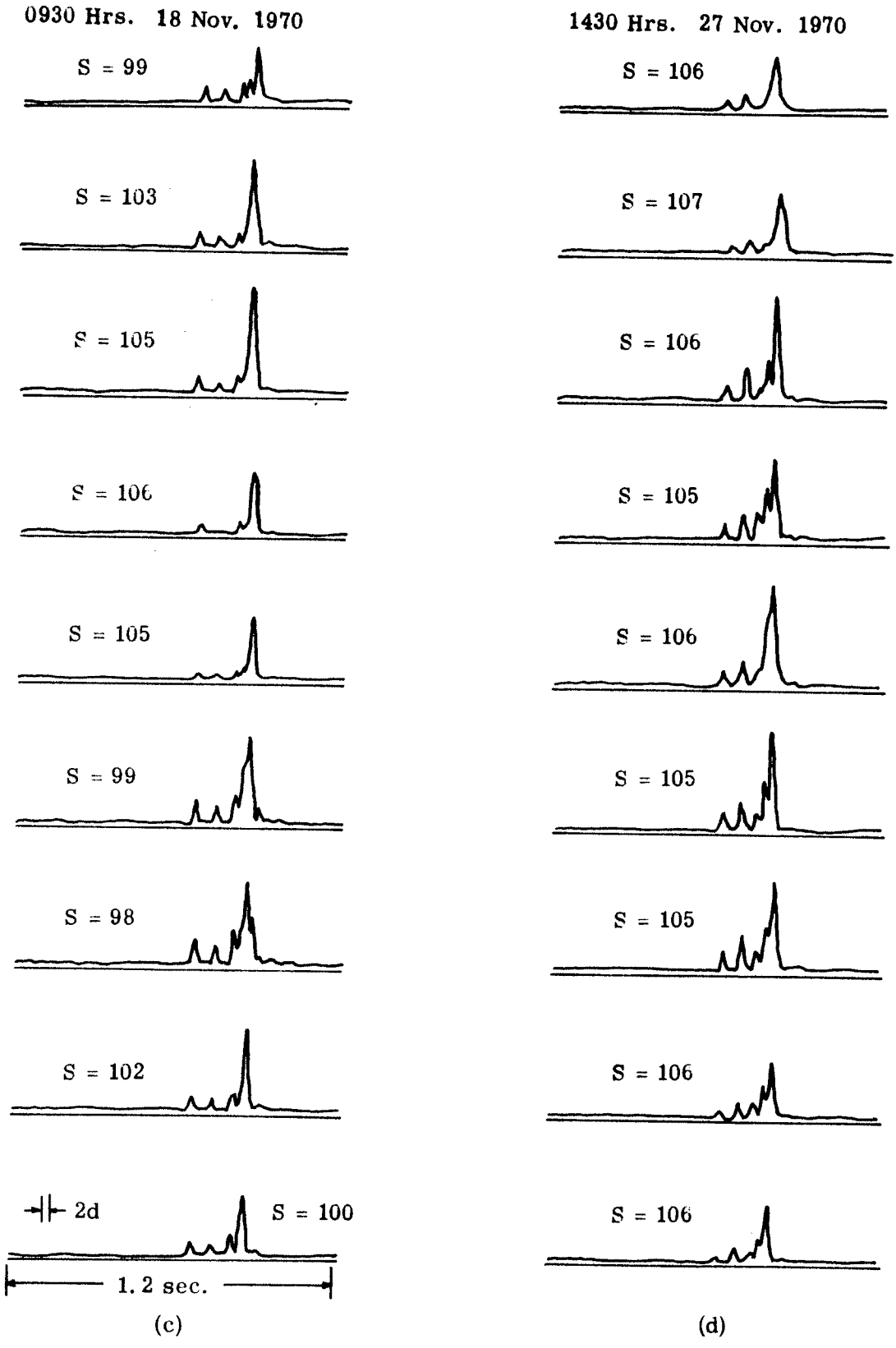
0930 Hrs. 18 Nov. 1970
S = 99
S = 103
S = 105
S = 106
S = 105
S = 99
S = 98
S = 102
2d
S = 100
1.2 sec.
(c)
1430 Hrs. 27 Nov. 1970
S = 106
S = 107
S = 106
S = 105
S = 106
S = 105
S = 105
S = 106
S = 106
(d)

Fig. 29. (Cont.)

2.4 Environmental Measurements

During the course of the experiment, water temperature and tide level readings were made at the Bimini receiving site. Also wind speed and direction at Bimini were recorded during much of the experiment. In this section we present the results of these measurements along with a general description of the weather conditions during the experiment. Other environmental measurements were also made at the Miami receiving site, but the results of these will be deferred to a later report.

With the exception of two cold periods, the weather during the experiment was generally mild with daytime temperatures in the mid 70's and light breezes ranging from 3 to 15 knots. The first of the two cold fronts reached Bimini around noon on 15 November, bringing cool, windy weather which lasted through 18 November. During this time, the daytime temperatures were in the mid 60's and the winds were between 10 and 22 knots out of the northwest. The second, and most severe cold front began on the evening of 23 November and lasted until 25 November. During this time the daytime temperatures dropped into the low 60's and the winds ranged from 15 to 30 knots out of the northeast.

The water temperature readings at the Bimini receiving site were taken from a thermistor string located approximately one mile from shore. The five different readings, labelled T_1, T_2, T_3, T_4,

and T_5, were taken at depths of 118 ft., 348 ft. 486 ft., 624 ft. and 759 ft. respectively. Plots of these readings appear in Fig. 30.

The Bimini tide level was measured in feet above a reference point at a post located several yards from shore. The plot of these measurements appears in Fig. 31. The wind velocities in knots for those days when the measurements are available is also indicated in Fig. 31.

2.5 Summary of the Preliminary Analysis

The Bimini Data. At the Bimini receiving site, 4 days of data were taken from the deep hydrophone and 11 1/2 days of data were taken from the shallow hydrophone. These periods, along with the times on the other main events that occurred at the Bimini receiving site, are illustrated in Fig. 32. We consider the deep hydrophone data first. The general behavior of the three signal powers C, S and R does not change during the deep hydrophone data even during the cold weather period that occurred between 15 November and 18 November. The carrier power suffers sharp, deep fades occurring at an average rate of about one fade per hour. The sideband power is reasonably stable with local variations confined to a 10 dB range. Reverb power is also quite stable with its load variations also limited to a 10 dB range, although the frequency of these variations is greater than those in S power. Typical signal-to-noise

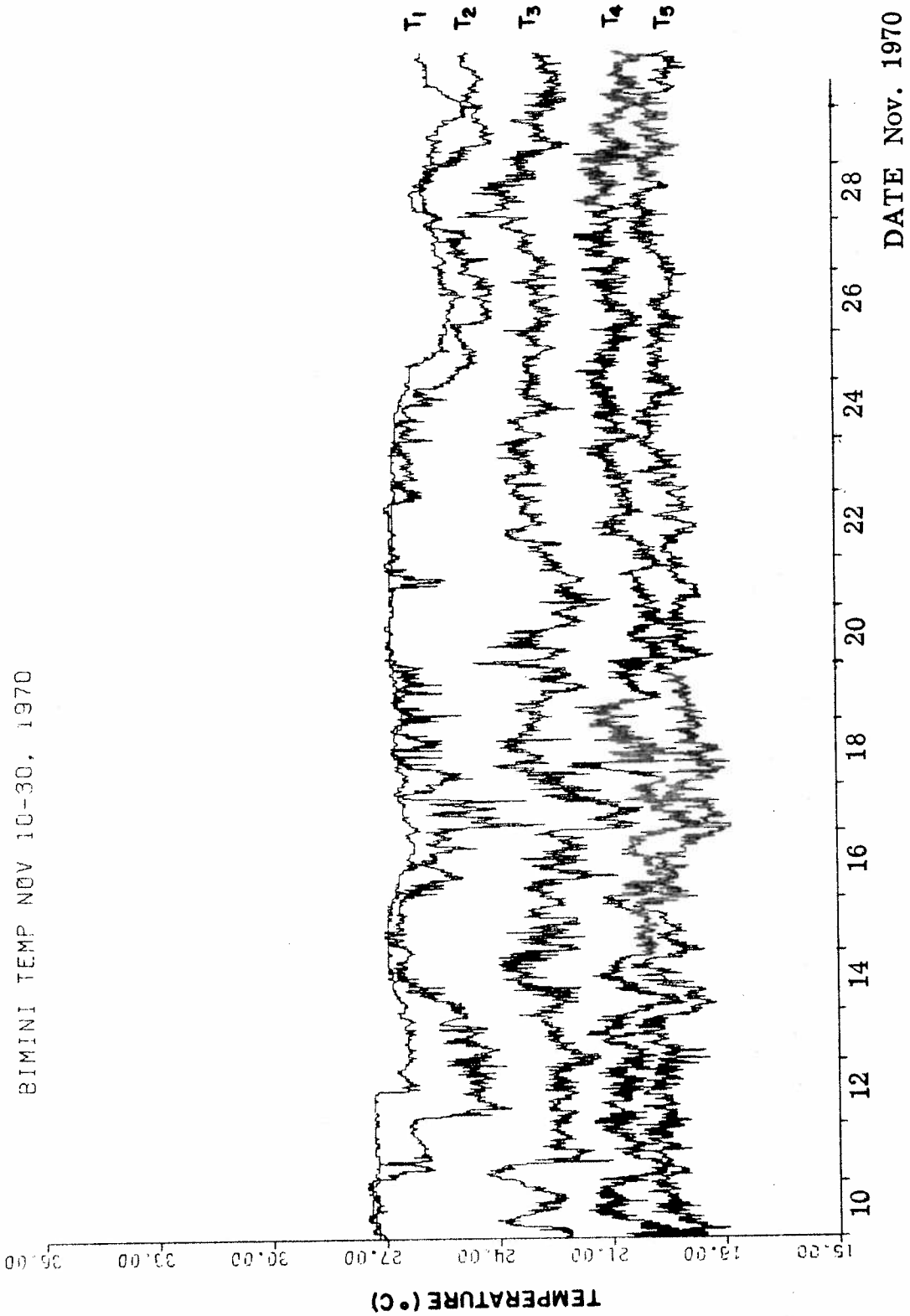

Fig. 30. Water temperatures at Bimini

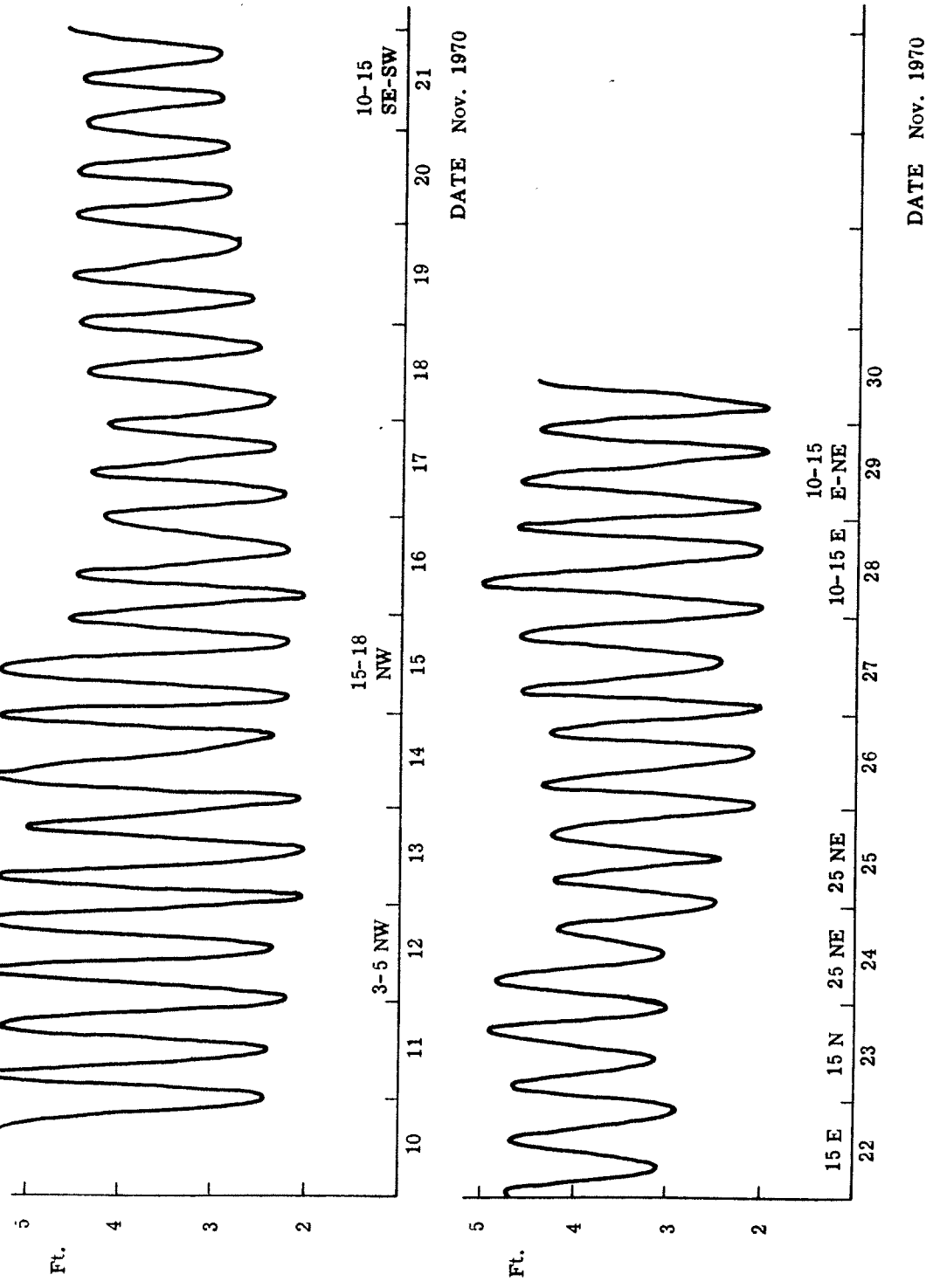

Fig. 31. Tide level at Bimini

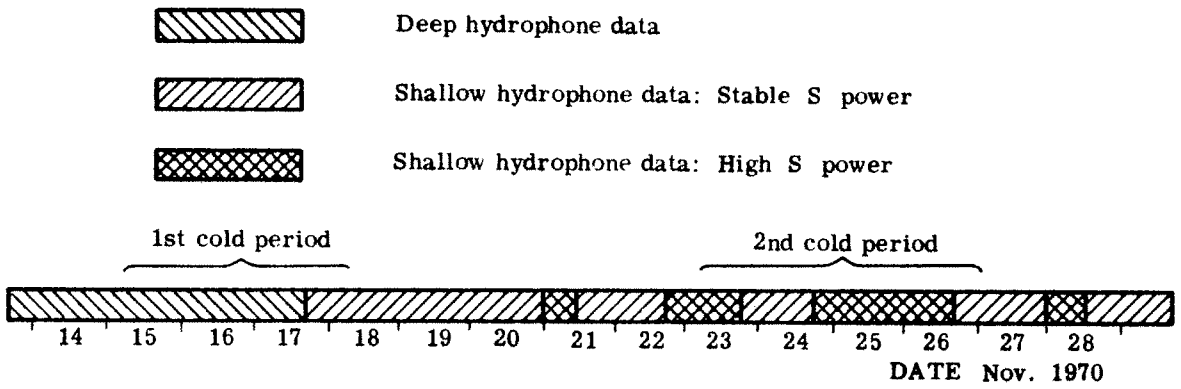

Fig. 32. The times of the main events at Bimini

ratios for C, S and R power are 40 dB, 20 dB and 3 to 10 dB respectively.

The reverb spectra from much of the deep hydrophone data do not have measurable sidebands although there are a few periods during the first cold front when sidebands do become noticeable with amplitudes as large as 10 dB . The multipath displays generally exhibit a complicated structure with many arrival peaks.

The most significant feature of the deep water noise power is the abrupt 15 dB increase that occurs on 15 November. The time at which this jump occurs coincides with a sharp increase in the wind velocity as the first cold front reached Bimini, suggesting that the

added 15 dB of noise power can be attributed to surface noise. After the jump occurs, N power becomes extremely stable with local variations (excluding shipping noise spikes) confined to a 3 dB range. Before the jump, N power is considerably less stable.

The shallow hydrophone data, with the exception of the noise power, is best described by considering the periods of stable S power and the periods of high S power separately. During the stable S-power period, the three signal powers C S and R have the same general behavior as the signal powers from the deep hydrophone data. In fact, the only noticeable difference is that the local variations in R power are slightly more dramatic than those in the deep hydrophone R power. Typical signal-to-noise ratios for C, S and R are 40 dB , 15 dB and 5 to 10 dB , respectively. The reverb spectra and multipath displays from this period also have the same general structure as those from the deep hydrophone data.

During the high S power period, all three signal powers C, S and R are from 10 to 20 dB higher than at other times. The carrier power fade rate drops to as low as one fade per six hours. Sideband power becomes considerably less stable and all three powers are highly correlated. The signal-to-noise ratios for C, S and R reach highs of 50 dB, 35 dB and 25 dB respectively.

The second cold front began about one day before the most dramatic period of high S power. When S power reaches its highest

values, the water temperature reading closest to the surface, T_1, reaches its lowest values, thus suggesting that at least some large increases in S power may be due to increased surface ducting.

The reverb spectra from the high S-power period generally have well defined sidebands with amplitudes between 5 and 20 dB depending on the corresponding level of R power. The multipath displays indicate only one major transmission path with at most only a few minor transmission paths. The clarity and stability of the multipath displays are greatest when the corresponding S power is large.

The noise power from the shallow hydrophone data exhibits several distinct kinds of variation in addition to shipping noise. As in the shallow hydrophone noise power, there is a sharp 15 dB jump of surface noise that occurs as the wind velocity increases at the beginning of the second cold front. Also there is a series of 10 to 15 dB "rolls" in the mean level of the noise power many of which occur in a regular diurnal pattern suggesting a biological origin. Finally, there is a short 6-hour period during which large closely spaced spikes occur.

The 7-mile Data. The 7-mile data exhibit much greater stability than do the Bimini data. The mean power levels and the reverb and multipath displays show little variation, even during the cold weather periods. The carrier power fades although as severe

as the Bimini carrier power fades, occur only about half as often. The sideband power is almost identical in behavior to the Bimini deep hydrophone sideband power. Typical signal-to-noise ratios for C and S power are 30 dB and 50 dB respectively.

Although the mean reverb and noise powers are considerably more stable than those from the Bimini data, there are many periods where large, closely spaced spikes occur. (This happens only once for a short period in the Bimini noise power and not at all in the Bimini reverb power.) Moreover, these spikes often, although not always, appear in both the 7-mile power measurements at the same time.

The reverb displays from the 7-mile data resemble those from the high S-power periods of the Bimini data. Reverb sidebands with amplitudes ranging from 5 to 10 dB and center frequencies between ± 0.1 and $+0.25$ are consistently evident. The multipath displays, almost without exception, show one major transmission path, preceded by at most 3 minor arrival peaks.

APPENDIX A

Appendix A contains the constant gain x bandwidth plots of the carrier, sideband reverb and noise powers from the Bimini data.

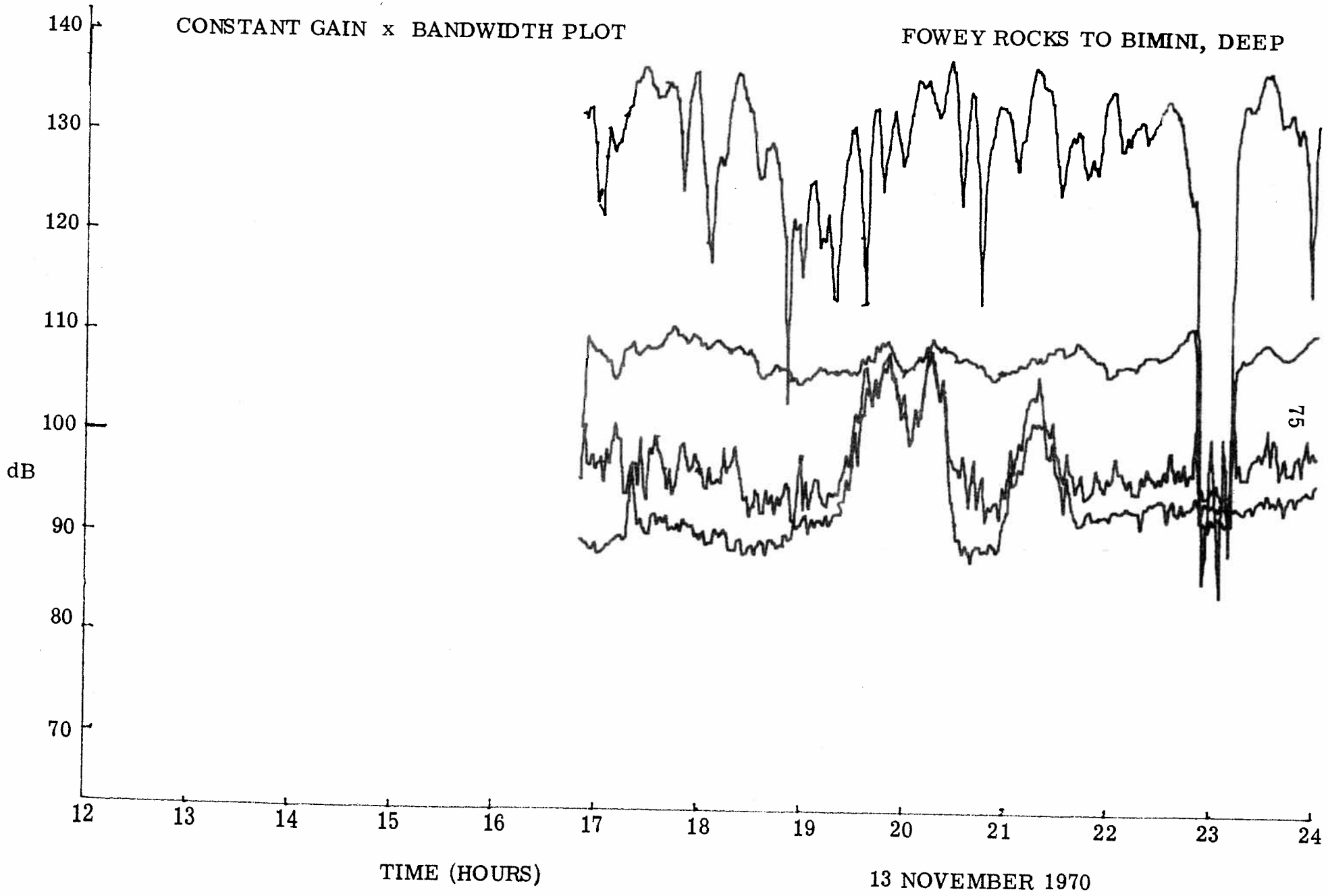
CONSTANT GAIN x BANDWIDTH PLOT
FOWEY ROCKS TO BIMINI, DEEP
140
130
120
110
100
90
80
70
dB
75
12
13
14
15
16
17
18
19
20
21
22
23
24
TIME (HOURS)
13 NOVEMBER 1970

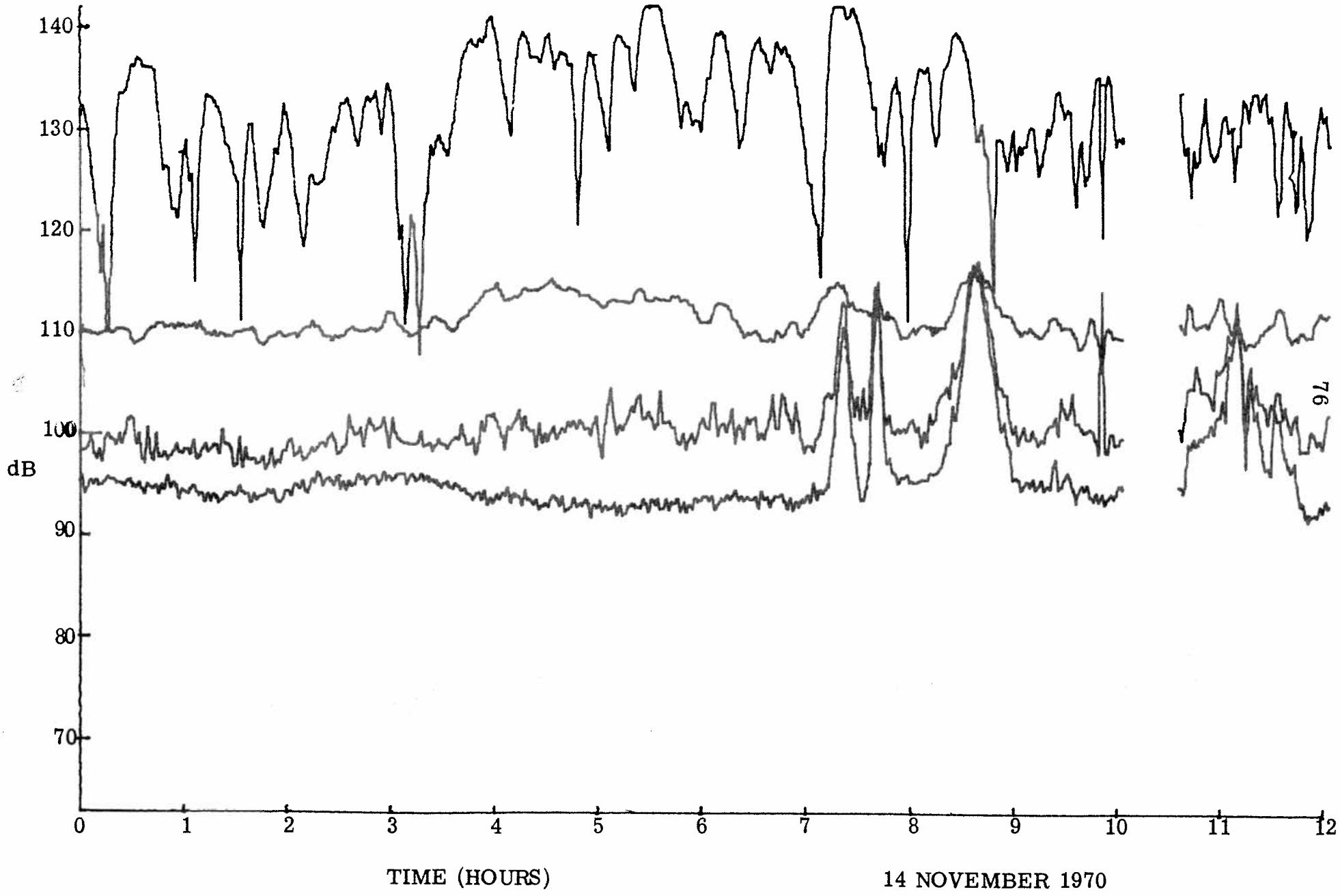
CONSTANT GAIN x BANDWIDTH PLOT
FOWEY ROCKS TO BIMINI, DEEP
140
130
120
110
100
90
80
70
dB
0
1
2
3
4
5
6
7
8
9
10
11
12
TIME (HOURS)
14 NOVEMBER 1970
76

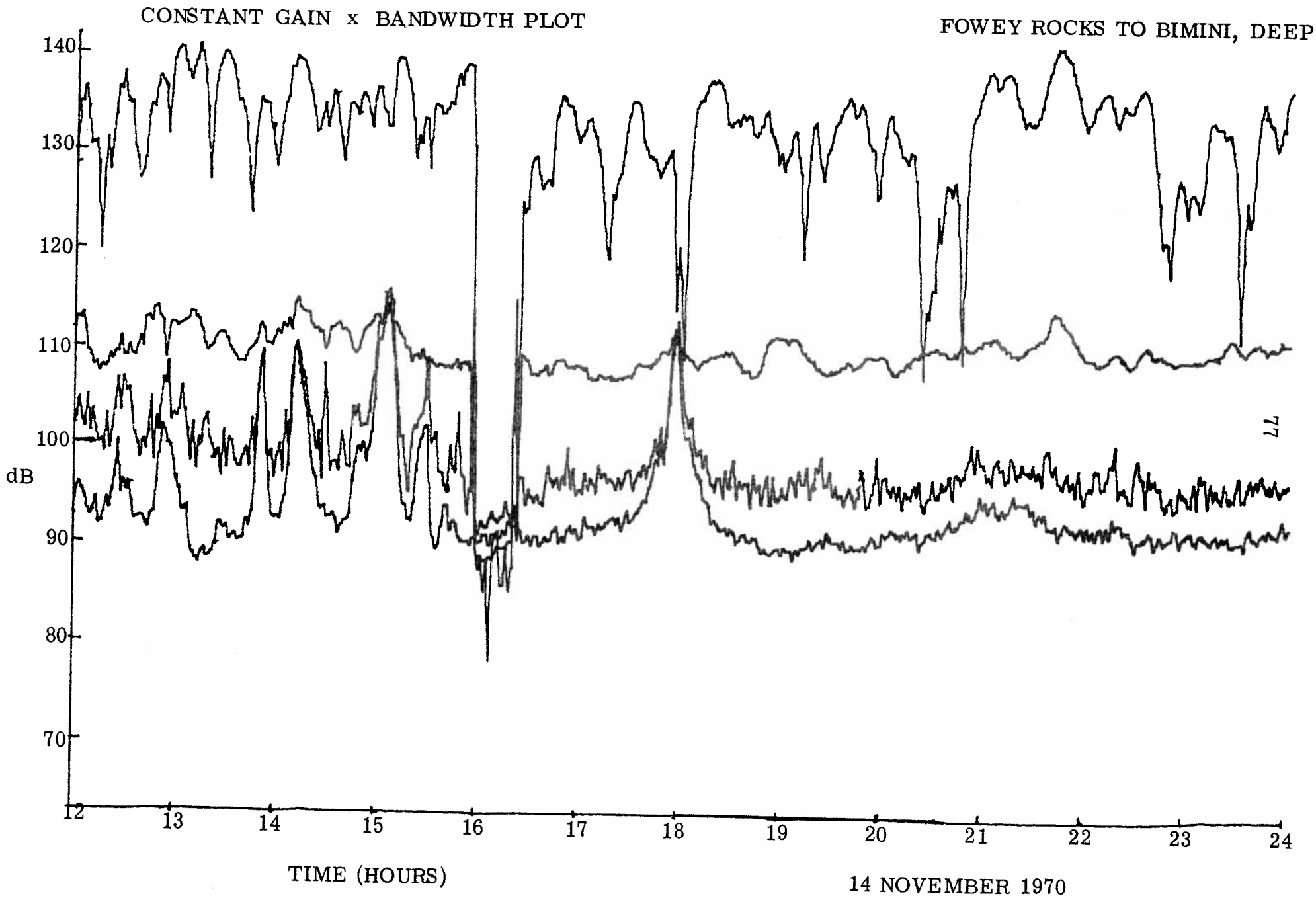
CONSTANT GAIN x BANDWIDTH PLOT
FOWEY ROCKS TO BIMINI, DEEP
140
130
120
110
100
90
80
70
dB
77
12
13
14
15
16
17
18
19
20
21
22
23
24
TIME (HOURS)
14 NOVEMBER 1970

CONSTANT GAIN x BANDWIDTH PLOT

FOWEY ROCKS TO BIMINI, DEEP

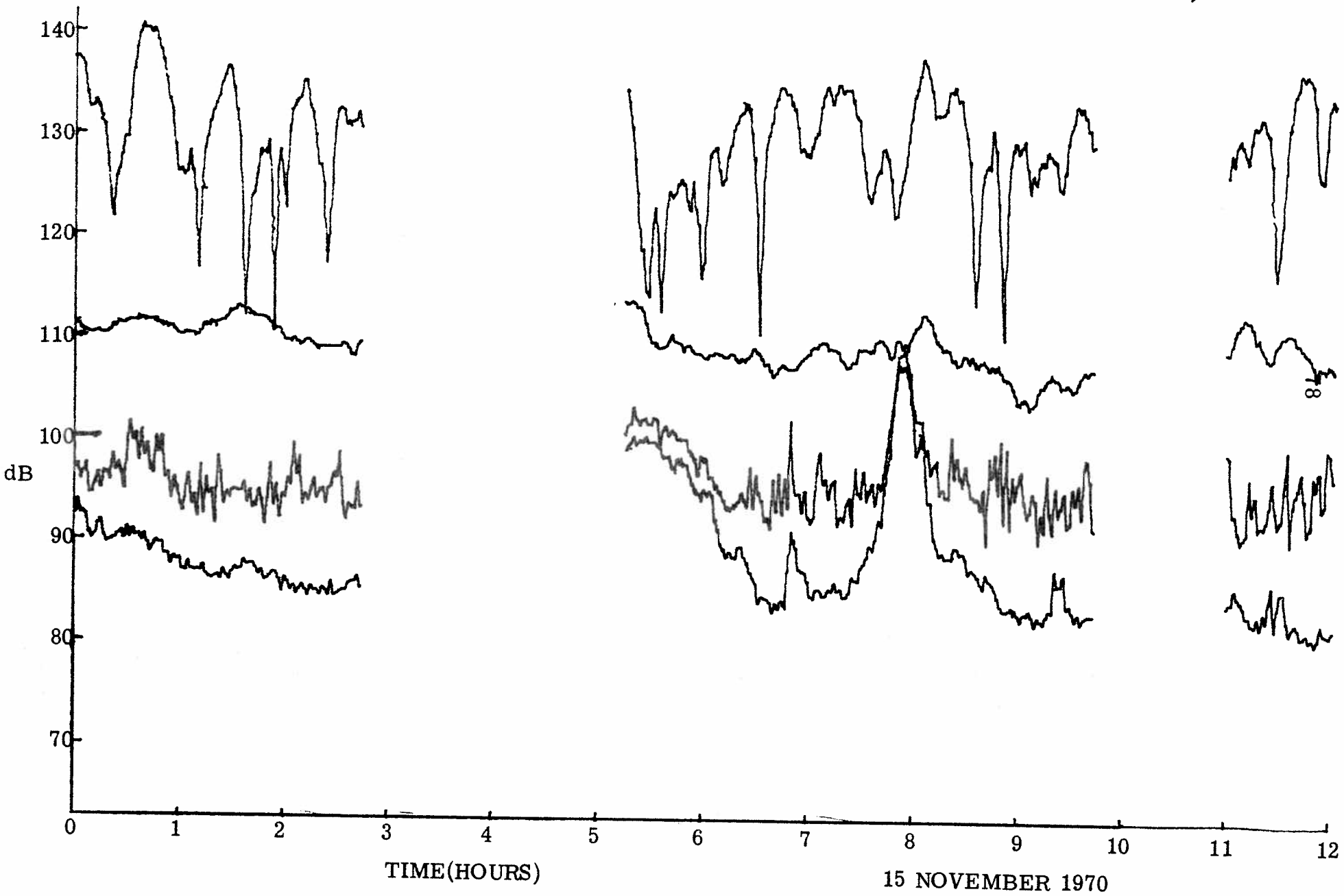

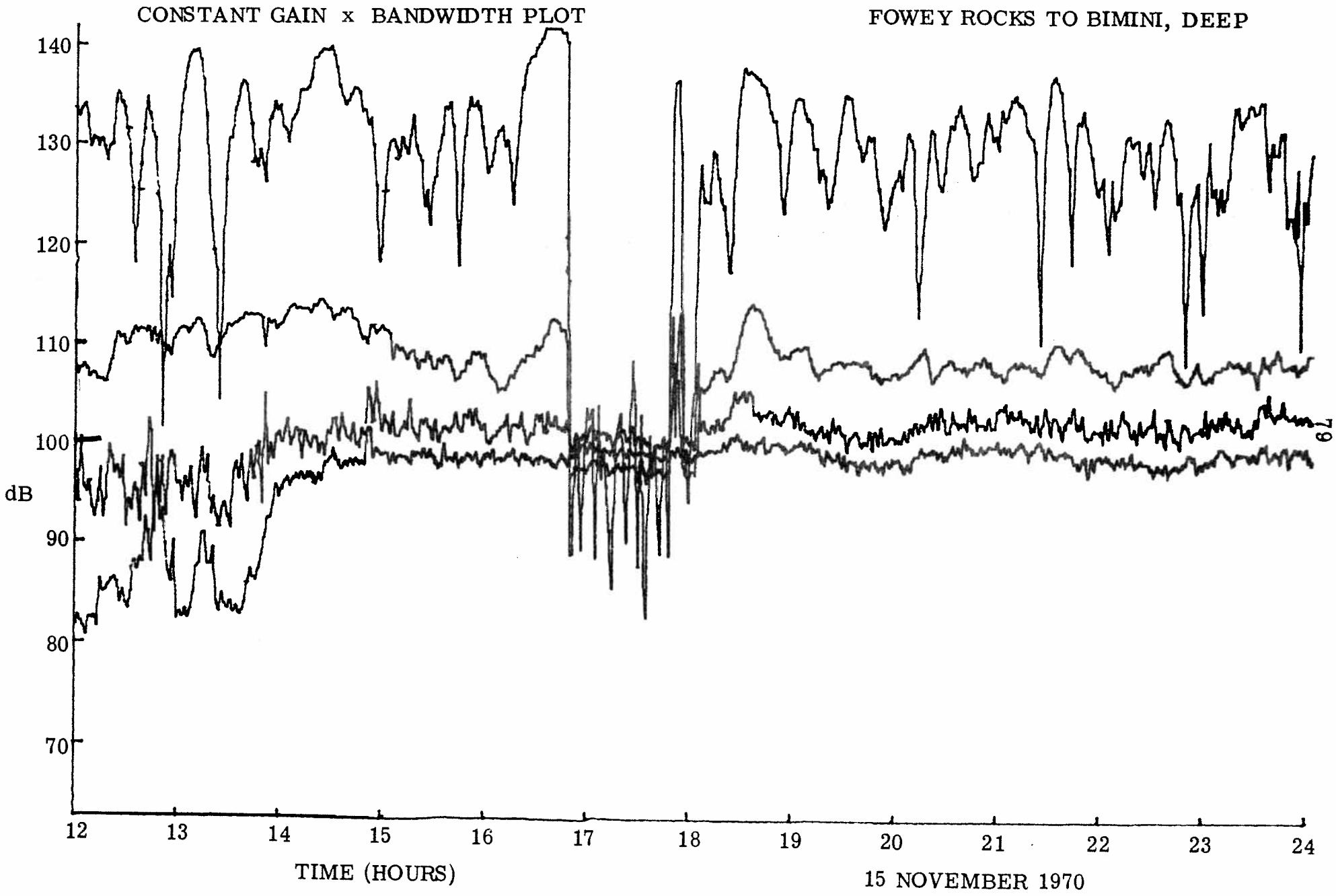
CONSTANT GAIN x BANDWIDTH PLOT
FOWEY ROCKS TO BIMINI, DEEP
140
130
120
110
100
90
80
70
dB
12
13
14
15
16
17
18
19
20
21
22
23
24
TIME (HOURS)
15 NOVEMBER 1970
79

CONSTANT GAIN x BANDWIDTH PLOT

FOWEY ROCKS TO BIMINI, DEEP

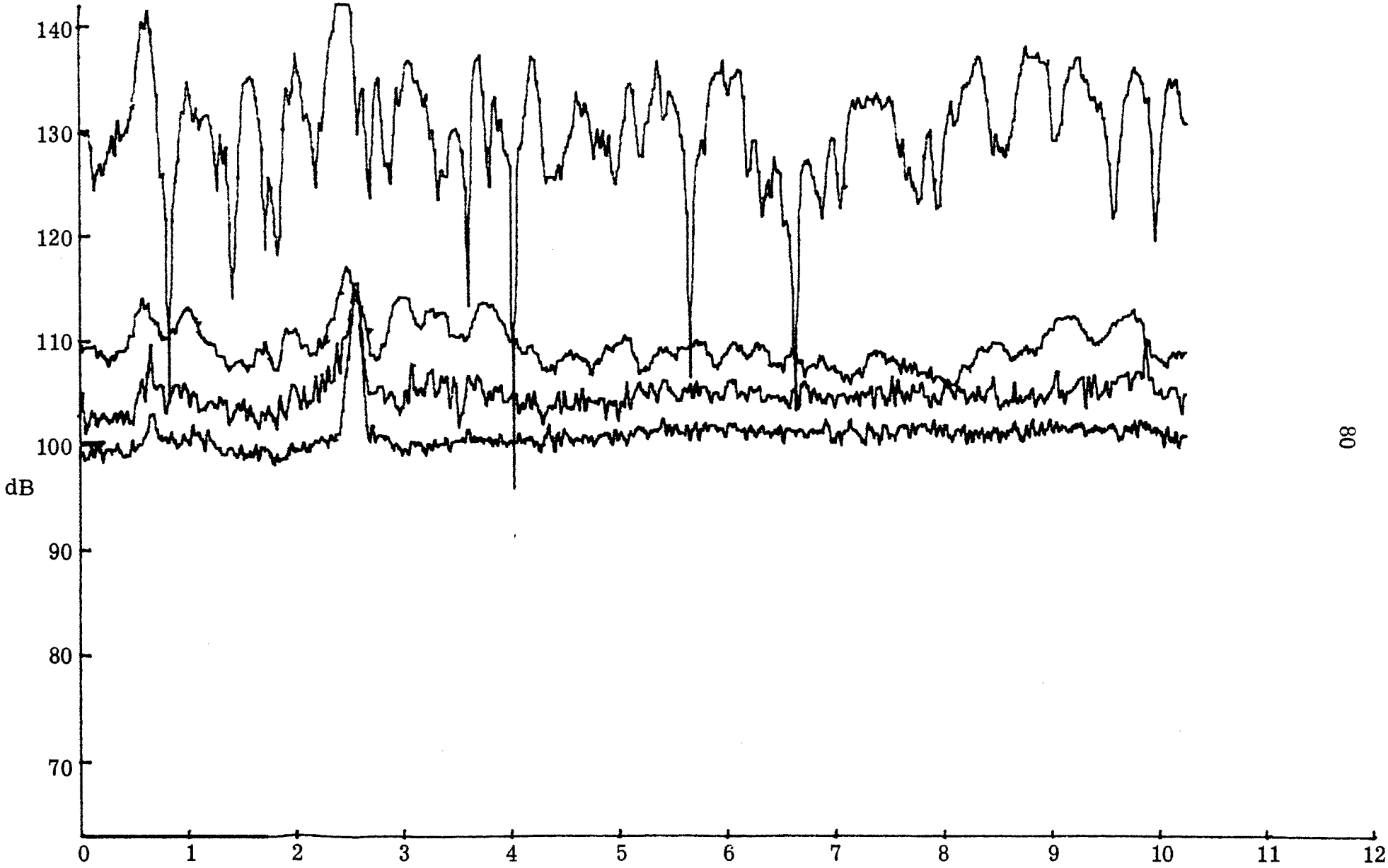

16 NOVEMBER 1970

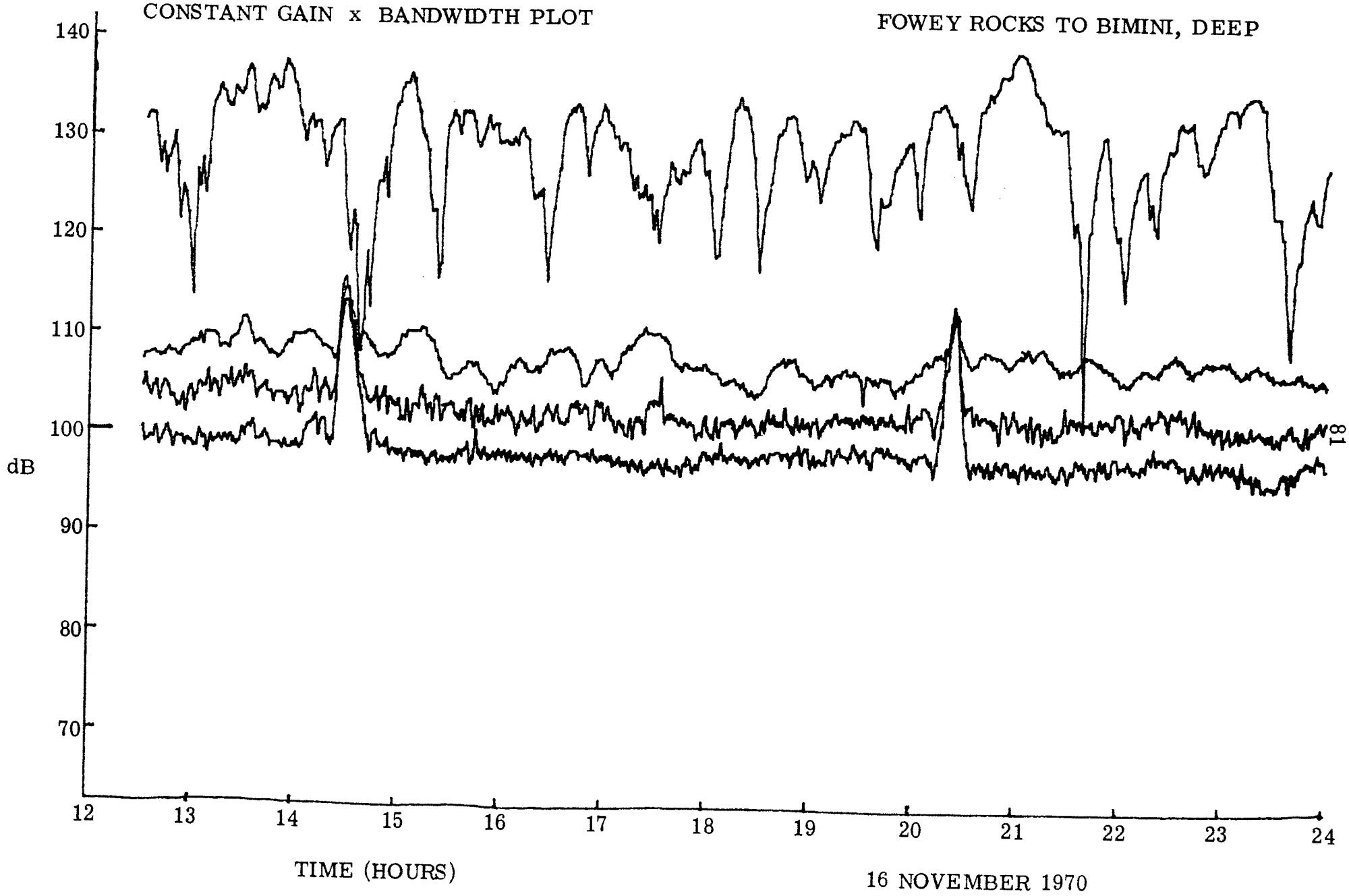
CONSTANT GAIN x BANDWIDTH PLOT
FOWEY ROCKS TO BIMINI, DEEP
140
130
120
110
100
90
80
70
dB
181
12
13
14
15
16
17
18
19
20
21
22
23
24
TIME (HOURS)
16 NOVEMBER 1970

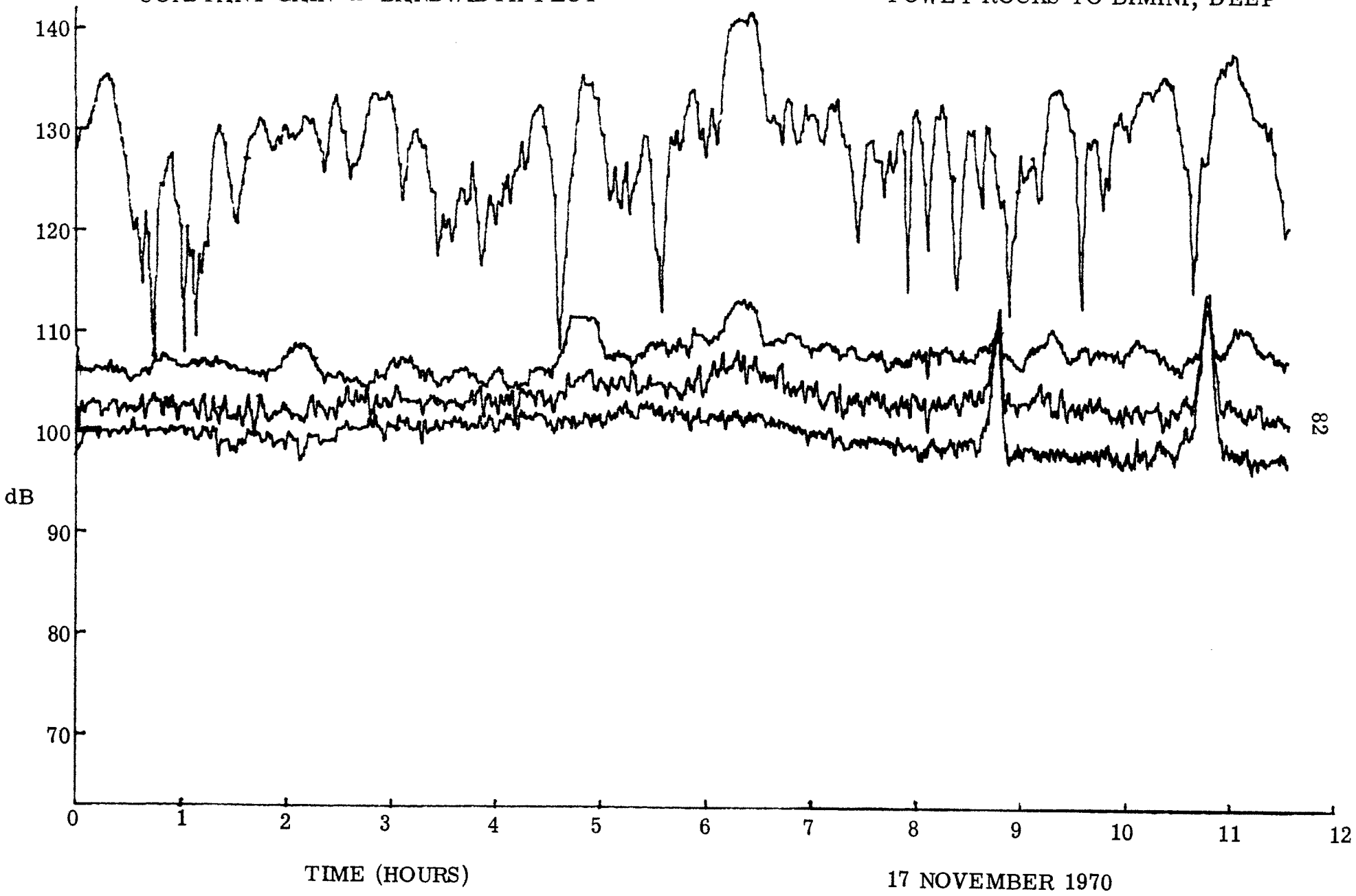
CONSTANT GAIN x BANDWIDTH PLOT
FOWEY ROCKS TO BIMINI, DEEP
140
130
120
110
100
dB
90
80
70
0
1
2
3
4
5
6
7
8
9
10
11
12
TIME (HOURS)
17 NOVEMBER 1970
82

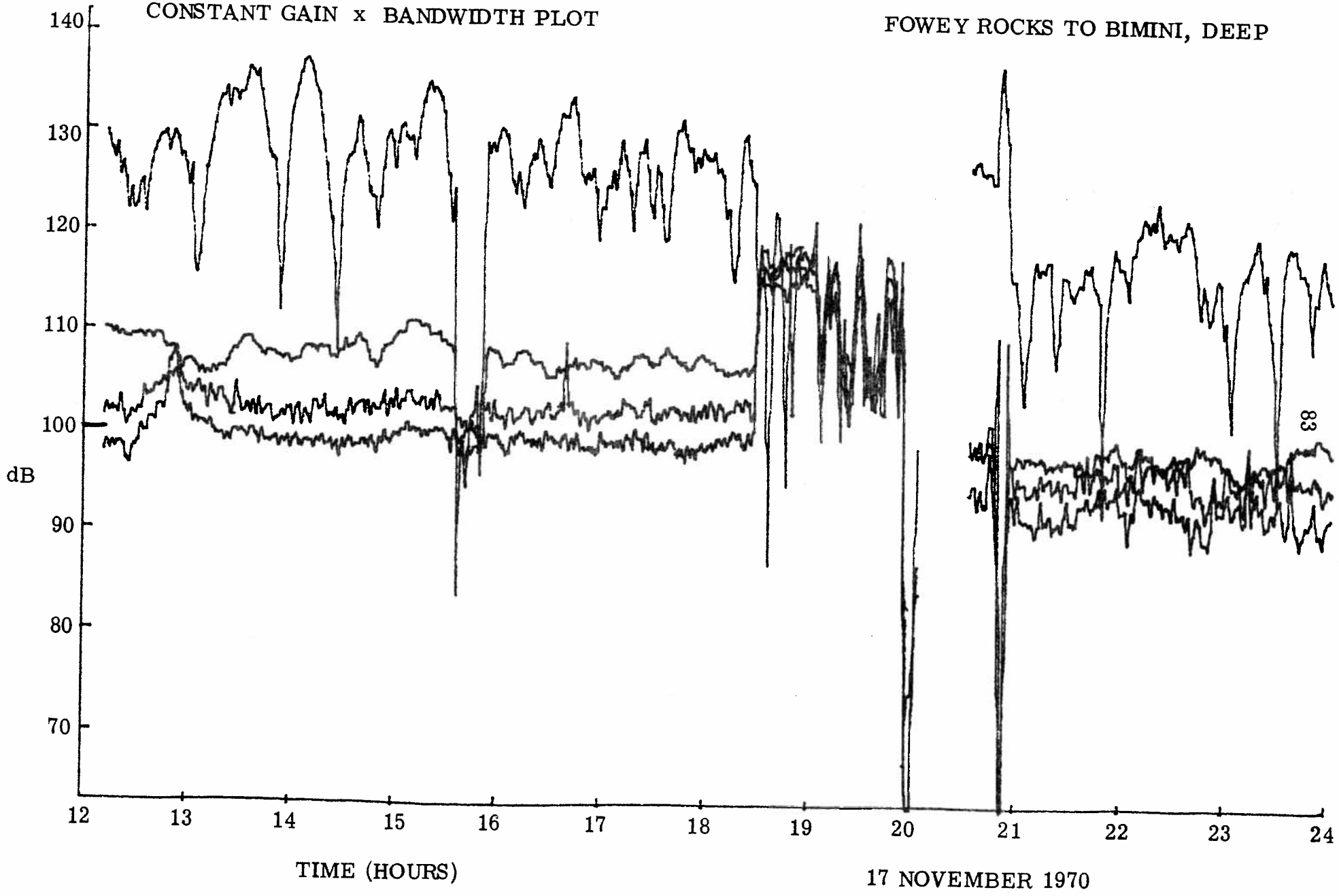
CONSTANT GAIN x BANDWIDTH PLOT
FOWEY ROCKS TO BIMINI, DEEP
140
130
120
110
100
90
80
70
dB
12
13
14
15
16
17
18
19
20
21
22
23
24
TIME (HOURS)
17 NOVEMBER 1970
83

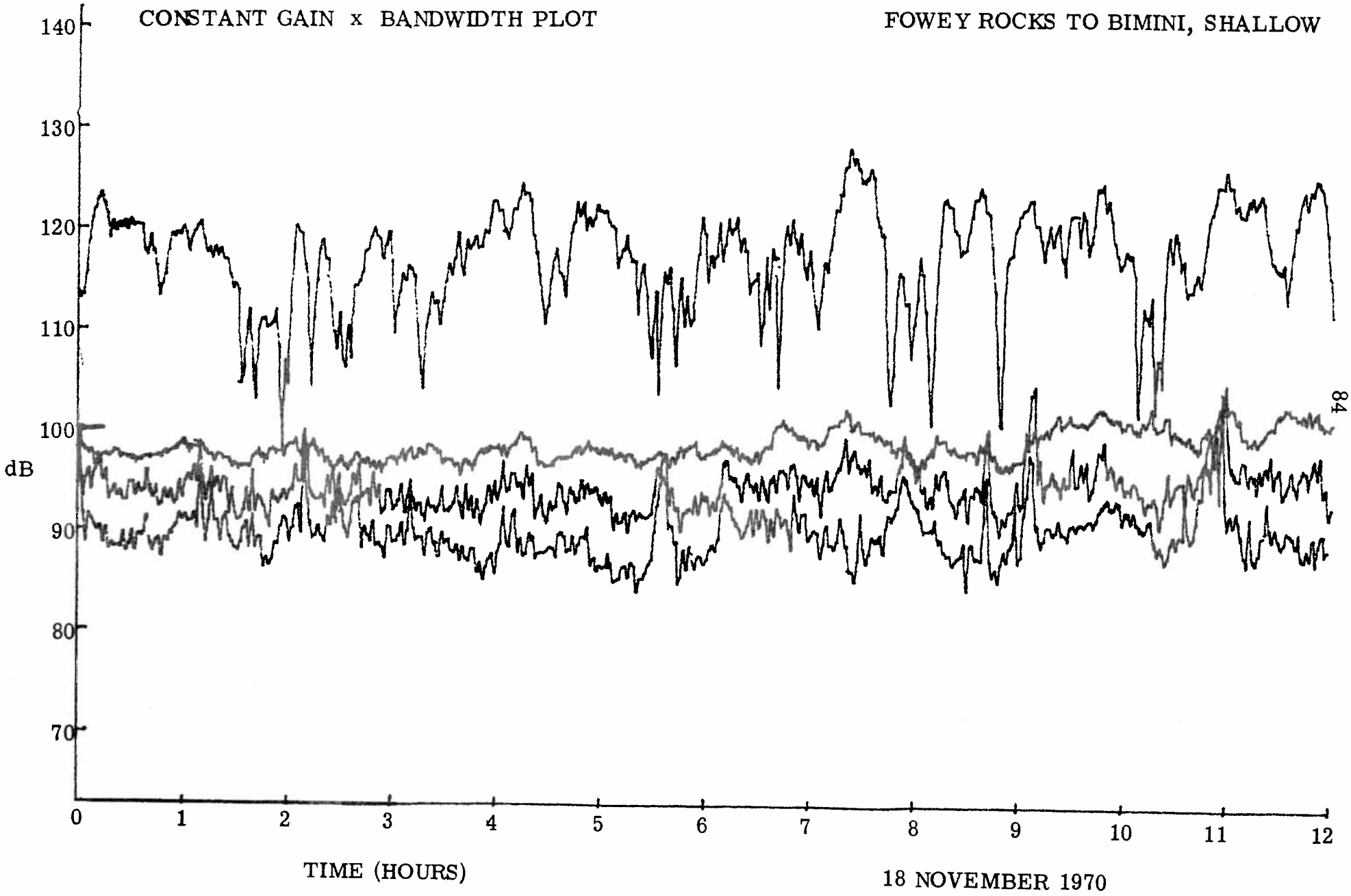
CONSTANT GAIN x BANDWIDTH PLOT
FOWEY ROCKS TO BIMINI, SHALLOW
140
130
120
110
100
90
80
70
dB
84
0
1
2
3
4
5
6
7
8
9
10
11
12
TIME (HOURS)
18 NOVEMBER 1970

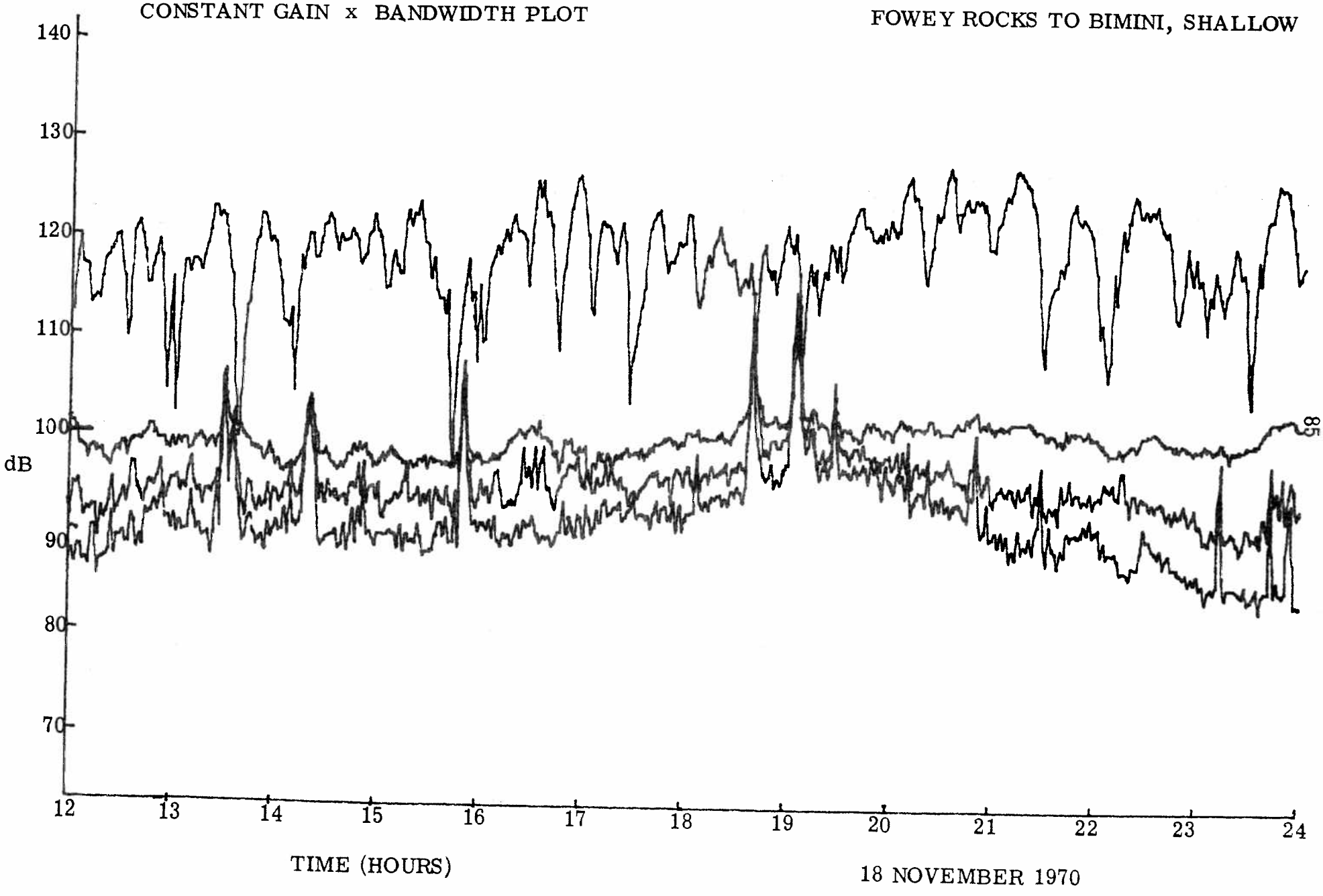
CONSTANT GAIN x BANDWIDTH PLOT
FOWEY ROCKS TO BIMINI, SHALLOW
140
130
120
110
100
90
80
70
dB
85
12
13
14
15
16
17
18
19
20
21
22
23
24
TIME (HOURS)
18 NOVEMBER 1970

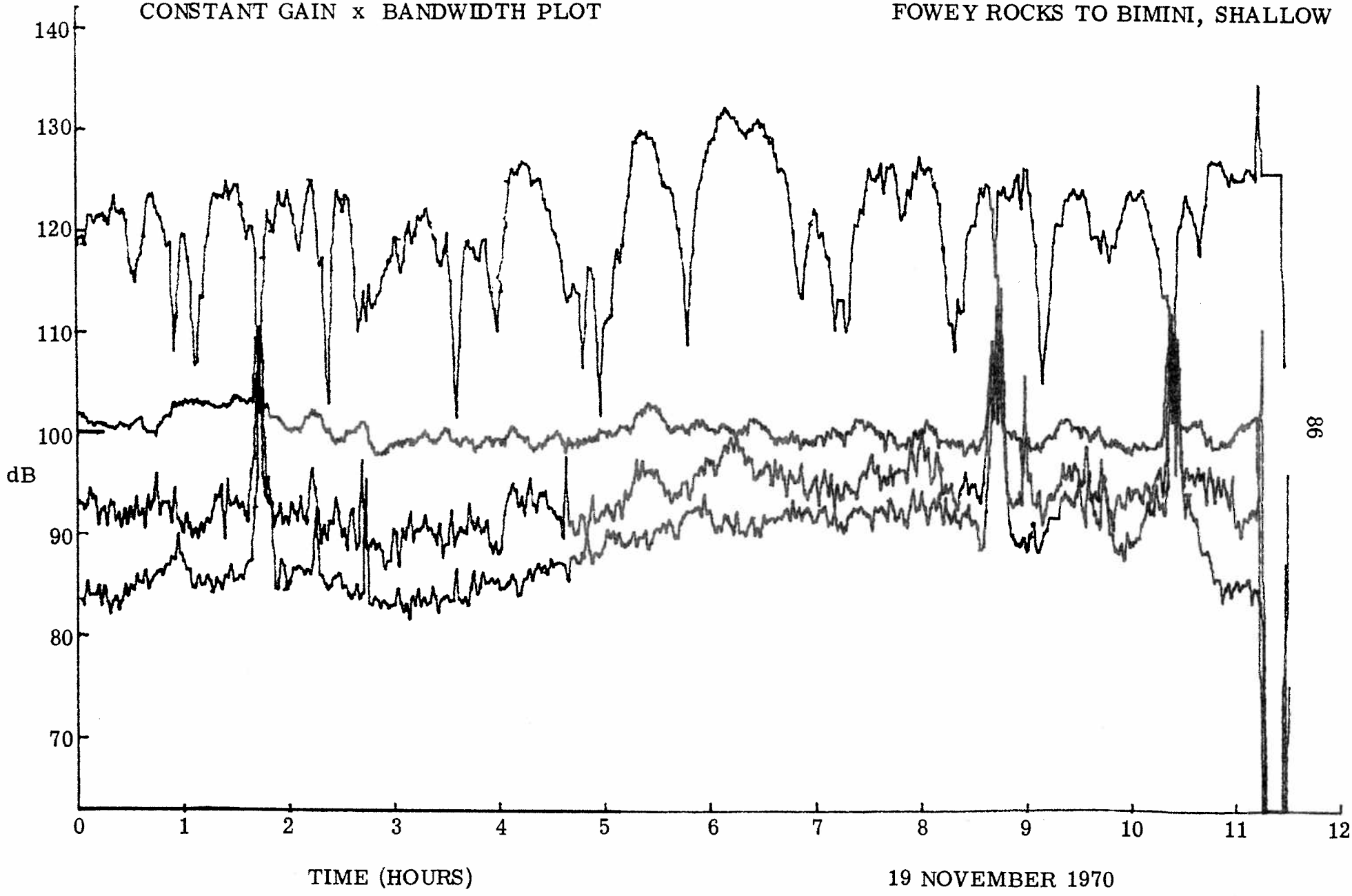
CONSTANT GAIN x BANDWIDTH PLOT
FOWEY ROCKS TO BIMINI, SHALLOW
140
130
120
110
100
90
80
70
dB
86
0
1
2
3
4
5
6
7
8
9
10
11
12
TIME (HOURS)
19 NOVEMBER 1970

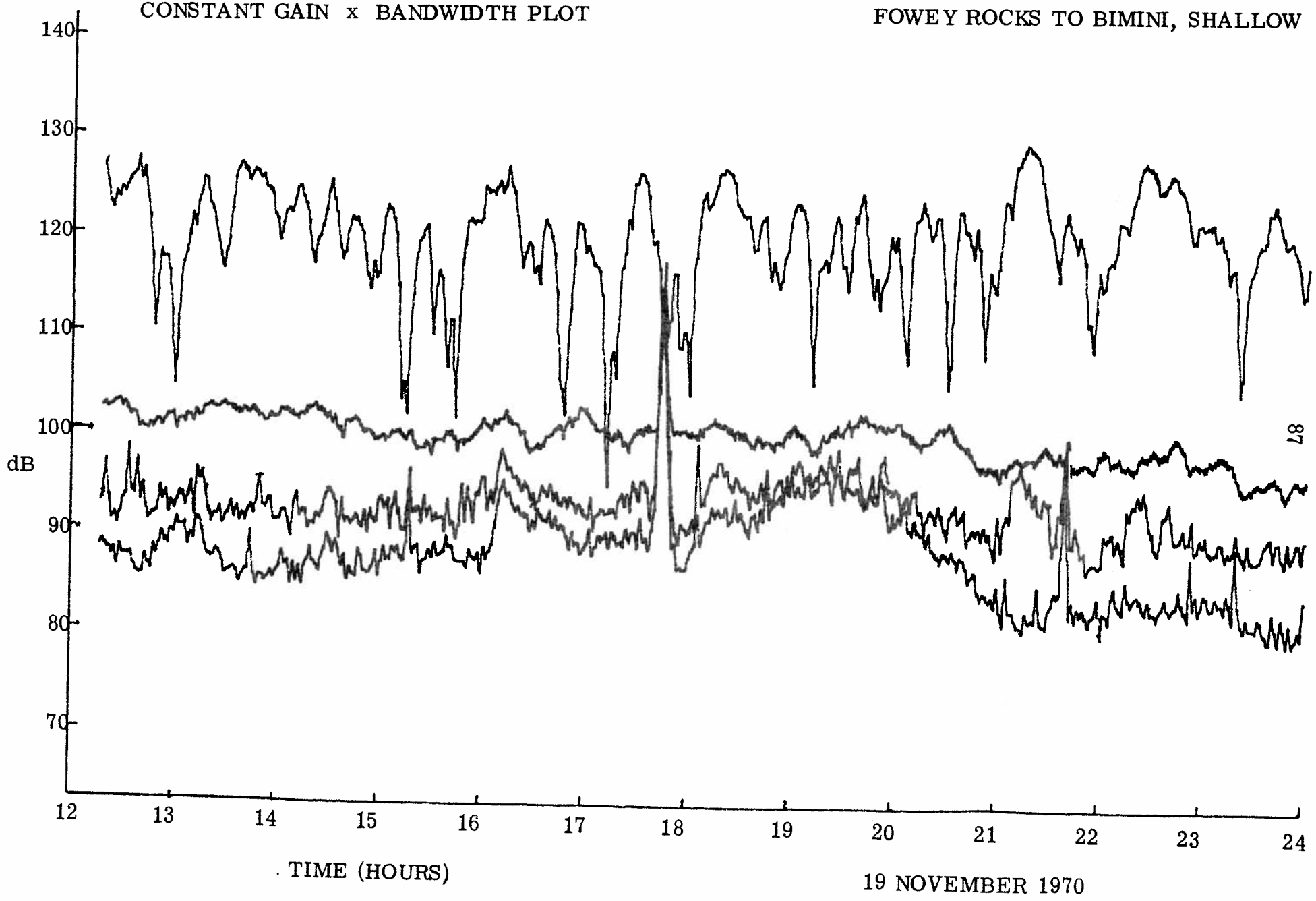
CONSTANT GAIN x BANDWIDTH PLOT
FOWEY ROCKS TO BIMINI, SHALLOW
140
130
120
110
100
90
80
70
dB
87
12
13
14
15
16
17
18
19
20
21
22
23
24
TIME (HOURS)
19 NOVEMBER 1970

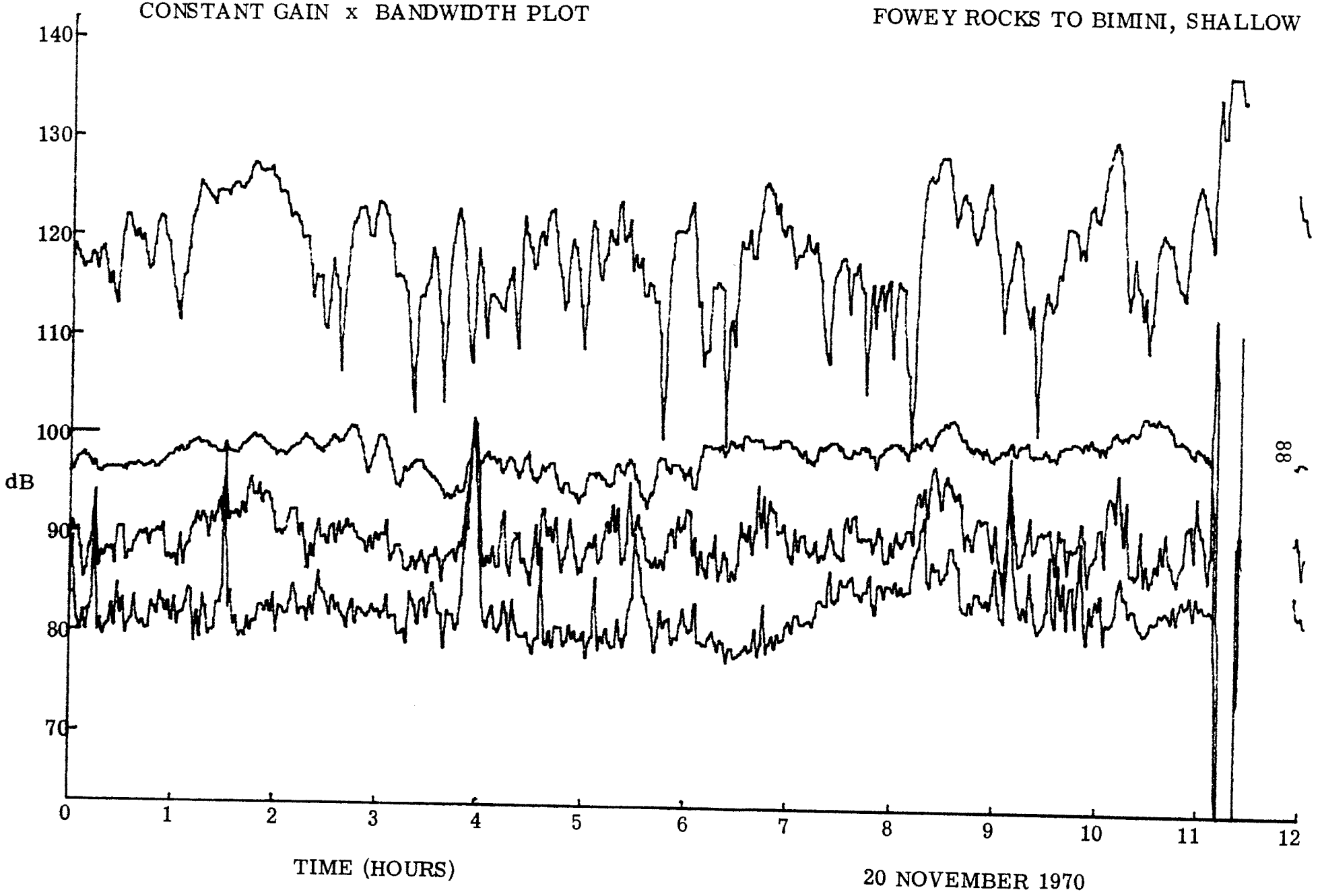
CONSTANT GAIN x BANDWIDTH PLOT
FOWEY ROCKS TO BIMINI, SHALLOW
140
130
120
110
100
90
80
70
dB
88
0
1
2
3
4
5
6
7
8
9
10
11
12
TIME (HOURS)
20 NOVEMBER 1970

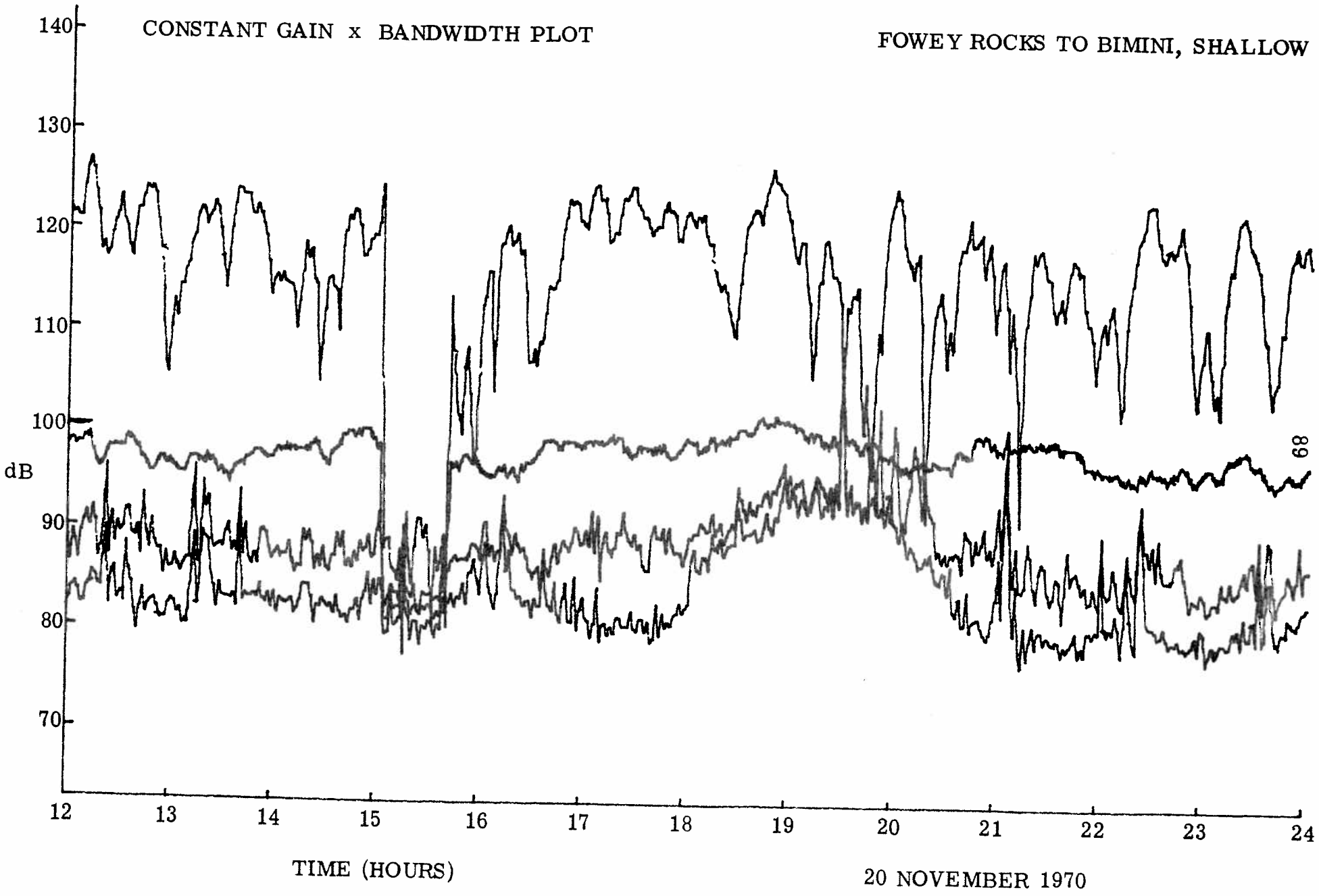
CONSTANT GAIN x BANDWIDTH PLOT
FOWEY ROCKS TO BIMINI, SHALLOW
140
130
120
110
100
90
80
70
dB
68
12
13
14
15
16
17
18
19
20
21
22
23
24
TIME (HOURS)
20 NOVEMBER 1970

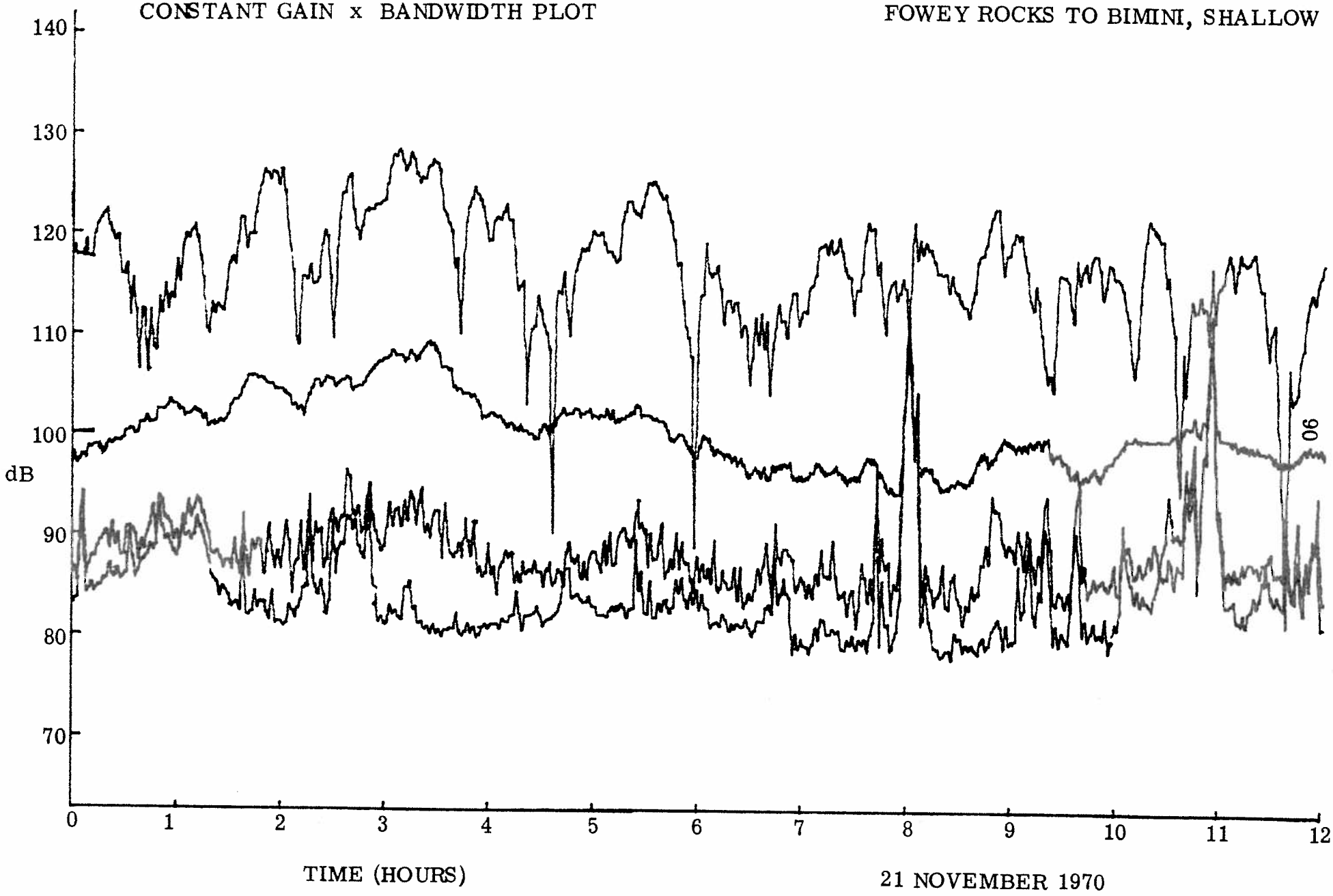
CONSTANT GAIN x BANDWIDTH PLOT
FOWEY ROCKS TO BIMINI, SHALLOW
140
130
120
110
100
90
80
70
dB
90
0
1
2
3
4
5
6
7
8
9
10
11
12
TIME (HOURS)
21 NOVEMBER 1970

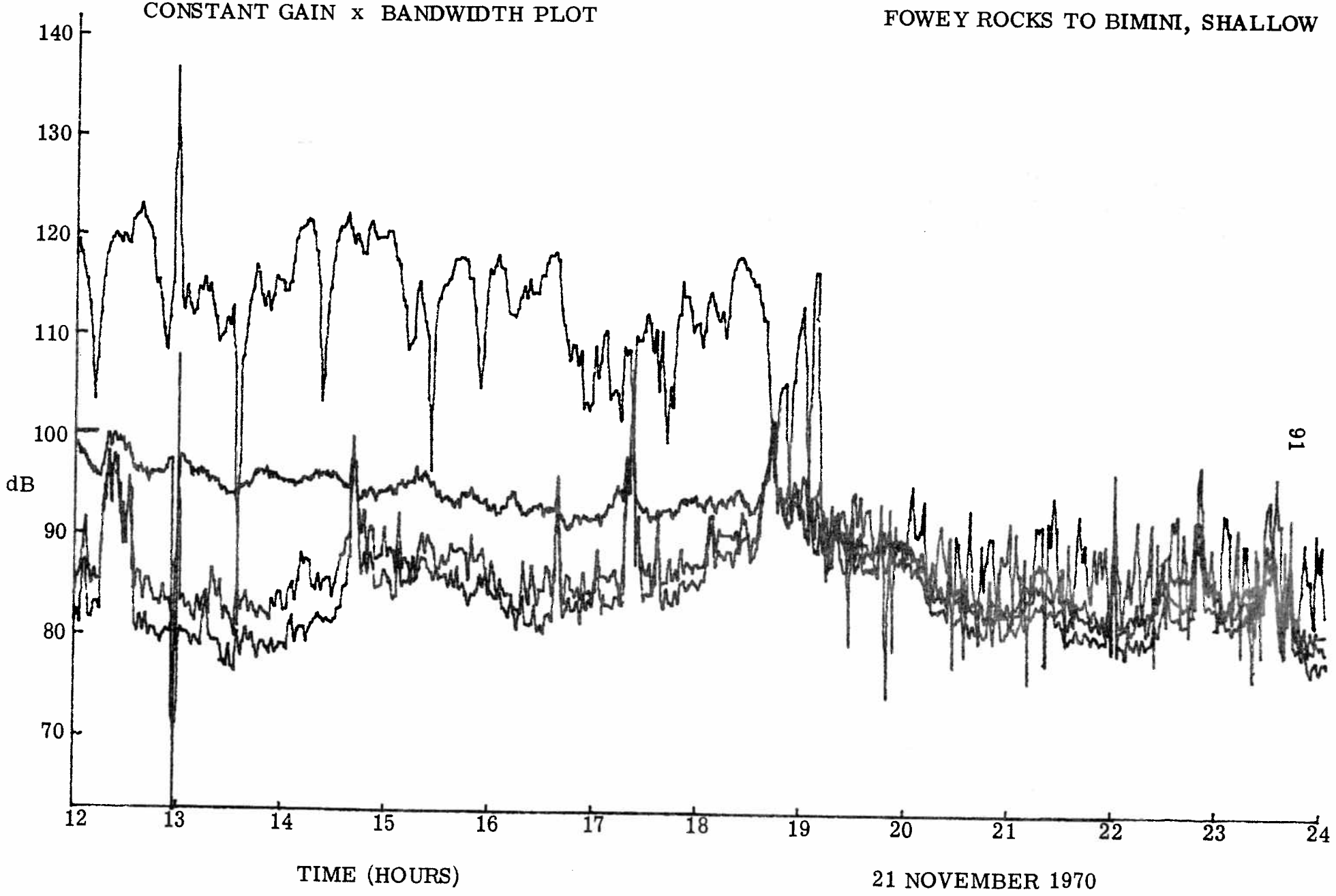
CONSTANT GAIN x BANDWIDTH PLOT
FOWEY ROCKS TO BIMINI, SHALLOW
140
130
120
110
100
90
80
70
dB
91
12
13
14
15
16
17
18
19
20
21
22
23
24
TIME (HOURS)
21 NOVEMBER 1970

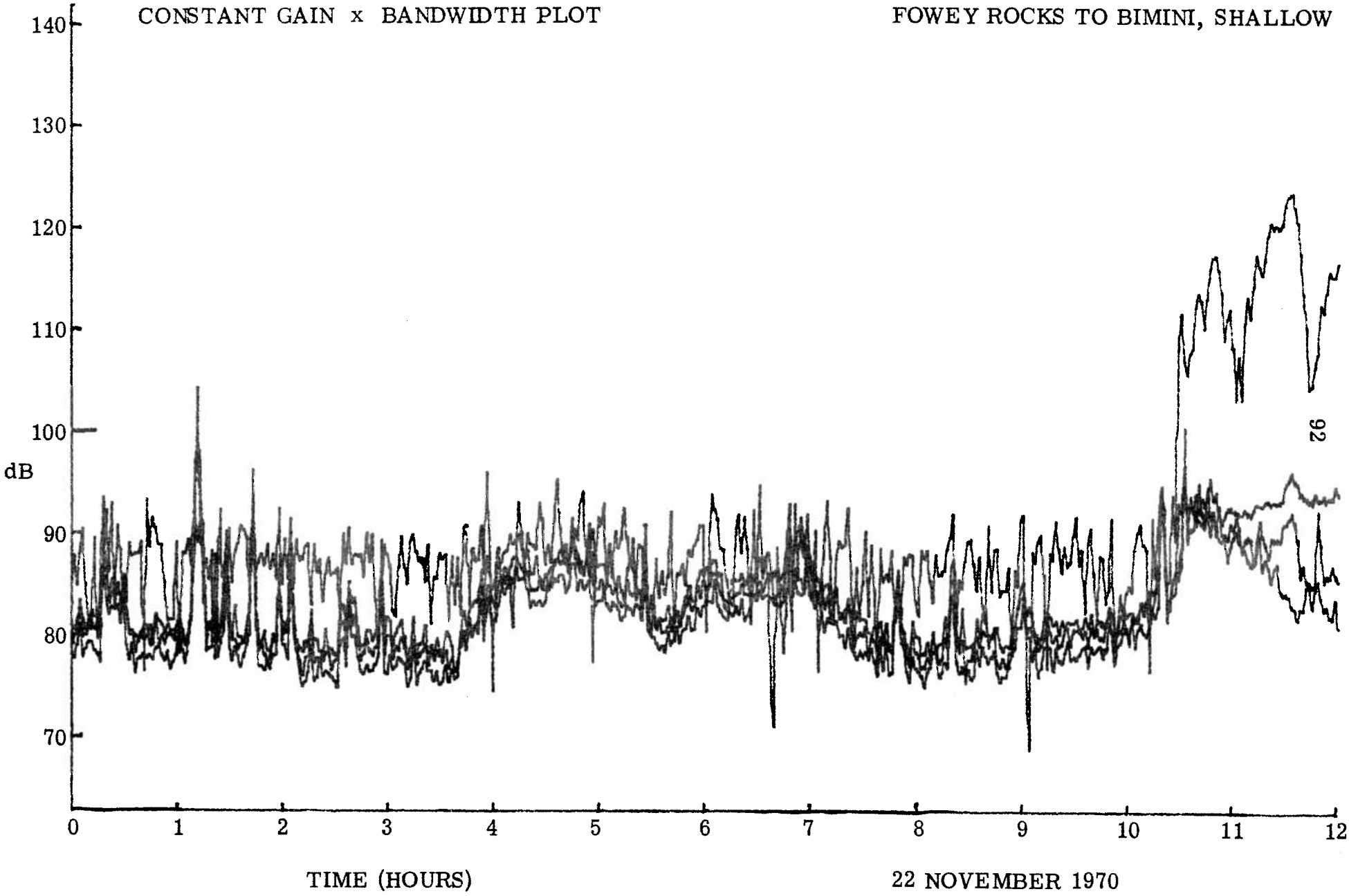
CONSTANT GAIN x BANDWIDTH PLOT
FOWEY ROCKS TO BIMINI, SHALLOW
140
130
120
110
100
90
80
70
dB
92
0
1
2
3
4
5
6
7
8
9
10
11
12
TIME (HOURS)
22 NOVEMBER 1970

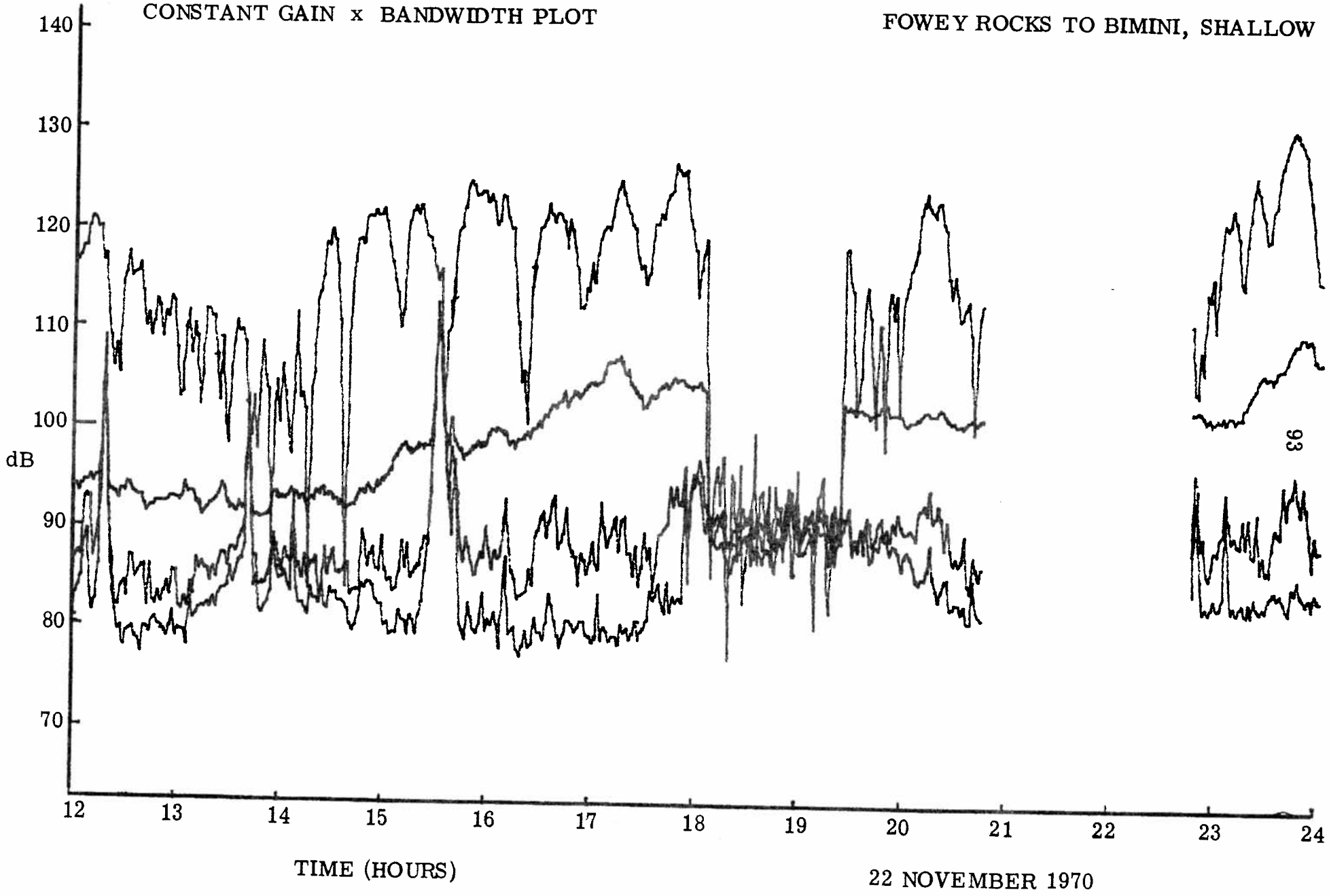
CONSTANT GAIN x BANDWIDTH PLOT
FOWEY ROCKS TO BIMINI, SHALLOW
140
130
120
110
100
90
80
70
dB
93
12
13
14
15
16
17
18
19
20
21
22
23
24
TIME (HOURS)
22 NOVEMBER 1970

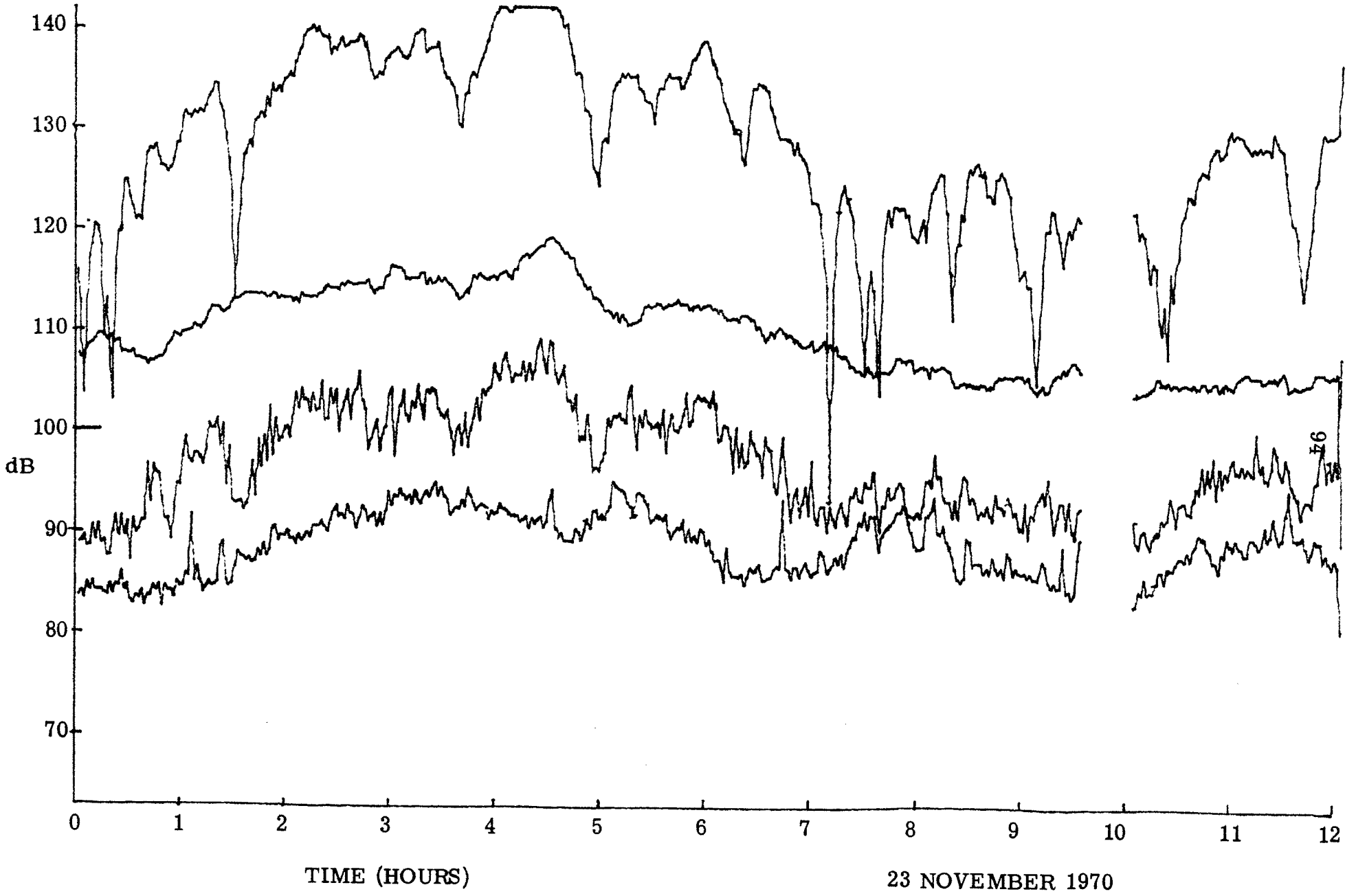
CONSTANT GAIN x BANDWIDTH PLOT
FOWEY ROCKS TO BIMINI, SHALLOW
140
130
120
110
100
90
80
70
dB
94
0
1
2
3
4
5
6
7
8
9
10
11
12
TIME (HOURS)
23 NOVEMBER 1970

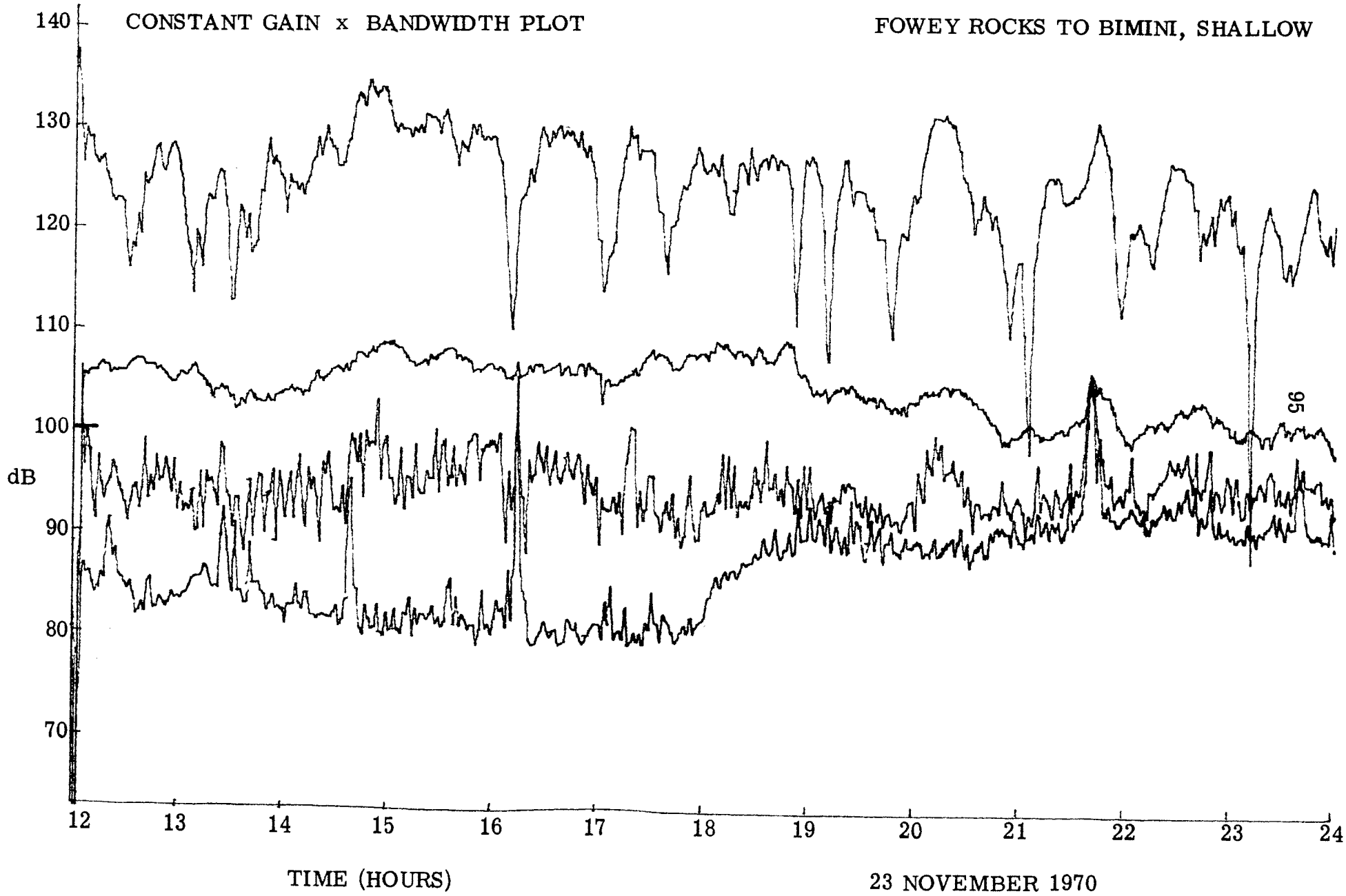
CONSTANT GAIN x BANDWIDTH PLOT
FOWEY ROCKS TO BIMINI, SHALLOW
140
130
120
110
100
90
80
70
dB
95
12
13
14
15
16
17
18
19
20
21
22
23
24
TIME (HOURS)
23 NOVEMBER 1970

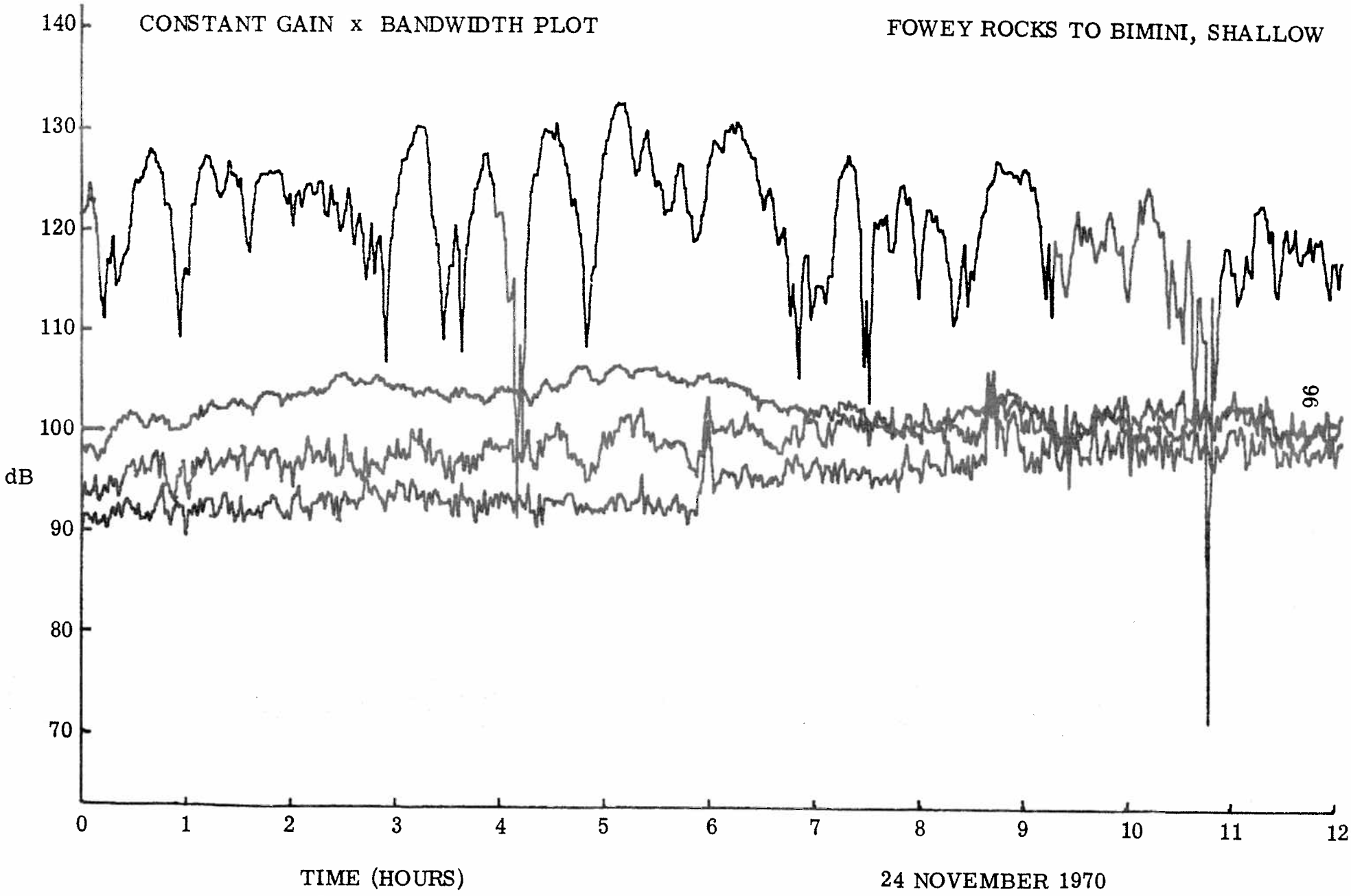
CONSTANT GAIN x BANDWIDTH PLOT
FOWEY ROCKS TO BIMINI, SHALLOW
140
130
120
110
100
90
80
70
dB
96
0
1
2
3
4
5
6
7
8
9
10
11
12
TIME (HOURS)
24 NOVEMBER 1970

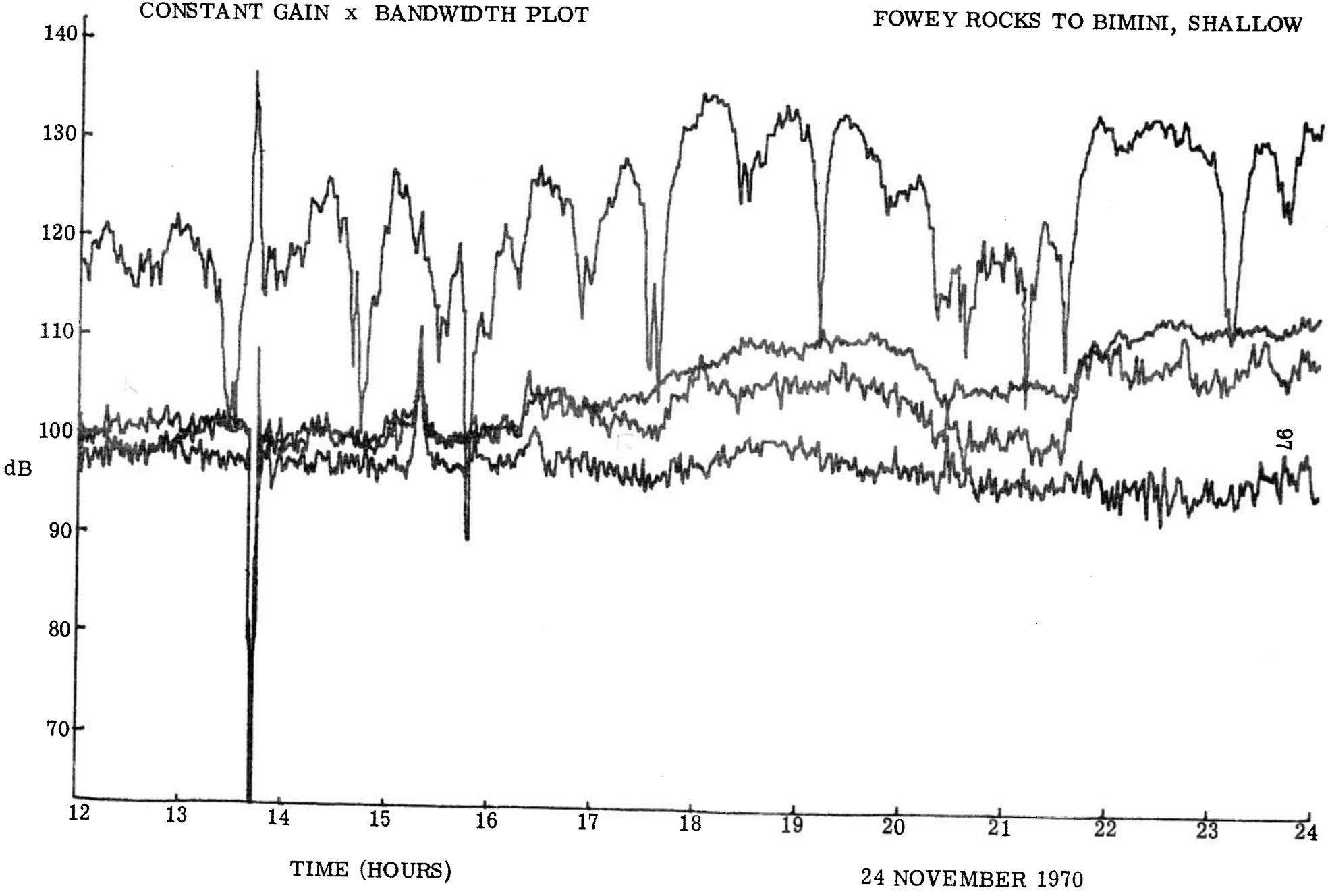
CONSTANT GAIN x BANDWIDTH PLOT
FOWEY ROCKS TO BIMINI, SHALLOW
140
130
120
110
100
90
80
70
dB
97
12
13
14
15
16
17
18
19
20
21
22
23
24
TIME (HOURS)
24 NOVEMBER 1970

CONSTANT GAIN x BANDWIDTH PLOT

FOWEY ROCKS TO BIMINI, SHALLOW

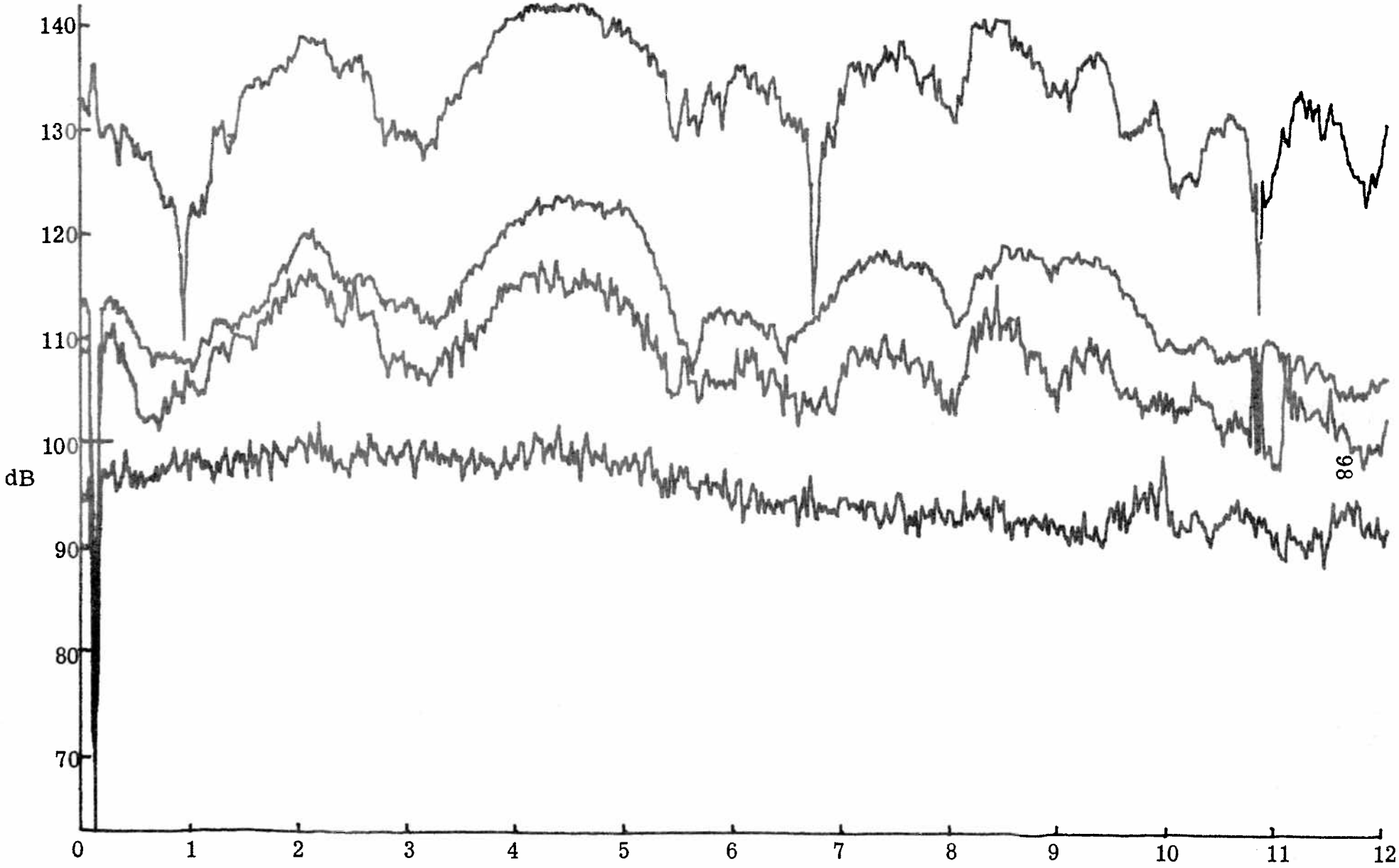

25 NOVEMBER 1970

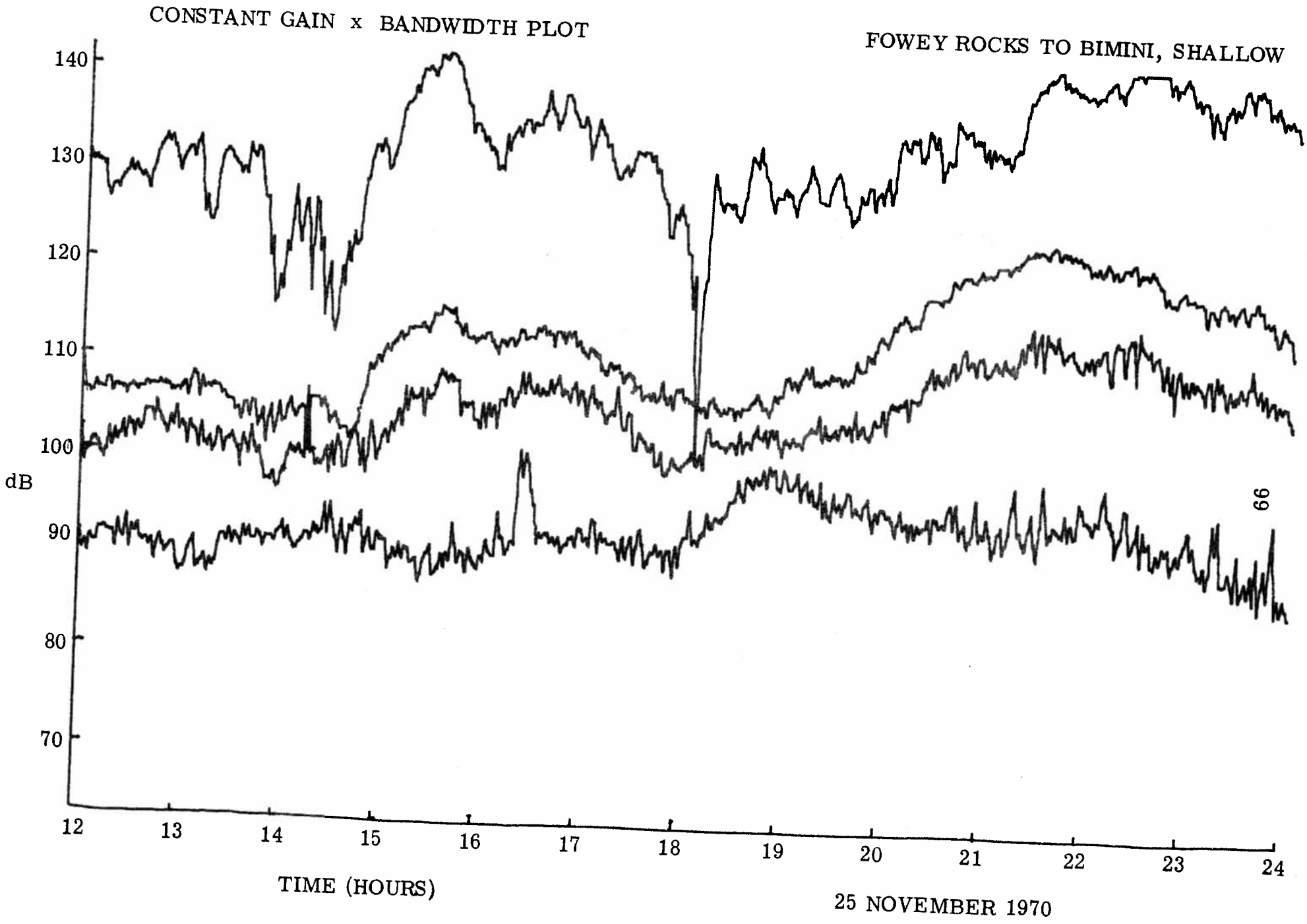
CONSTANT GAIN x BANDWIDTH PLOT
FOWEY ROCKS TO BIMINI, SHALLOW
140
130
120
110
100
90
80
70
dB
66
12
13
14
15
16
17
18
19
20
21
22
23
24
TIME (HOURS)
25 NOVEMBER 1970

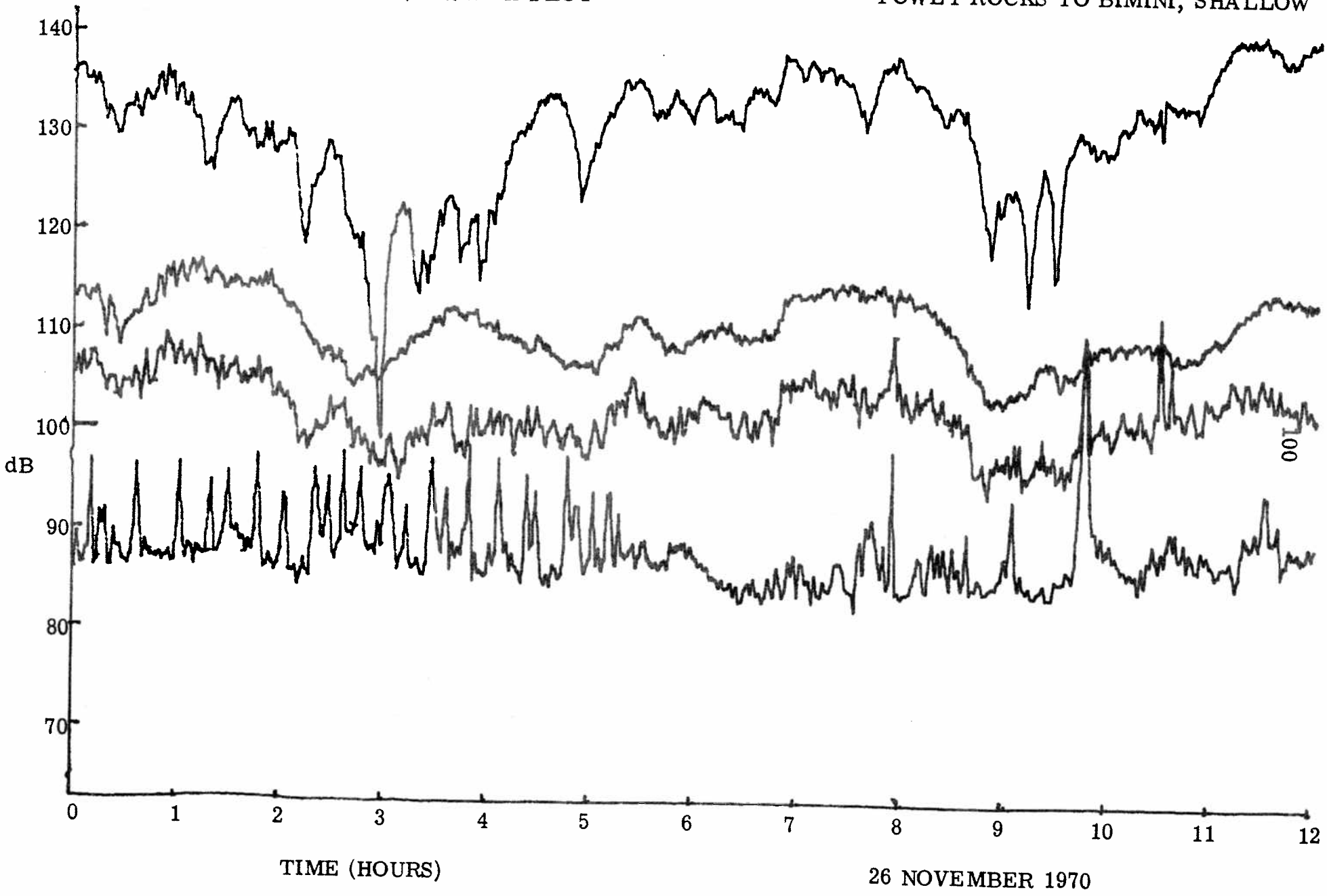
CONSTANT GAIN x BANDWIDTH PLOT
FOWEY ROCKS TO BIMINI, SHALLOW
140
130
120
110
100
90
80
70
dB
100
0
1
2
3
4
5
6
7
8
9
10
11
12
TIME (HOURS)
26 NOVEMBER 1970

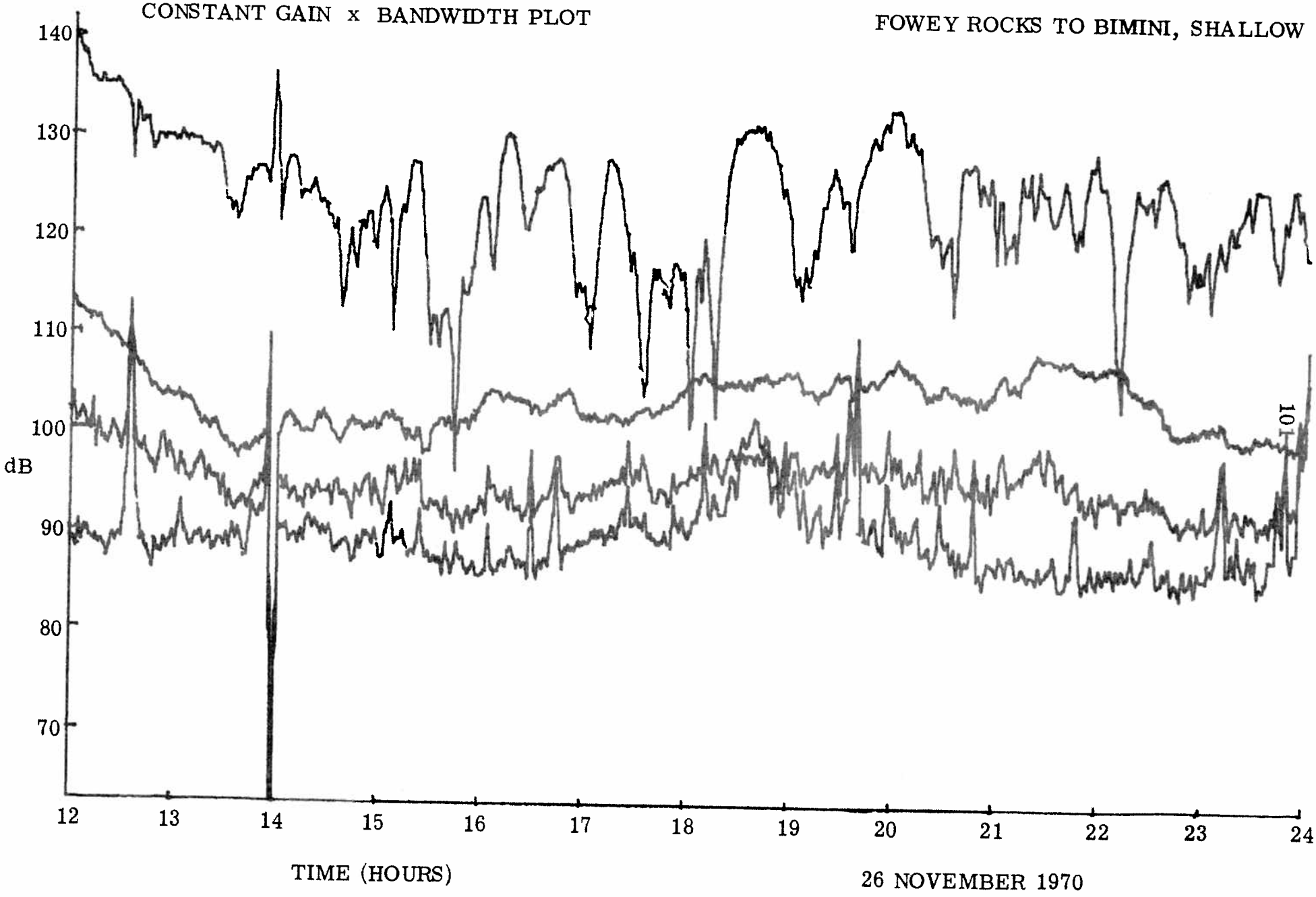
CONSTANT GAIN x BANDWIDTH PLOT
FOWEY ROCKS TO BIMINI, SHALLOW
140
130
120
110
100
90
80
70
dB
101
12
13
14
15
16
17
18
19
20
21
22
23
24
TIME (HOURS)
26 NOVEMBER 1970

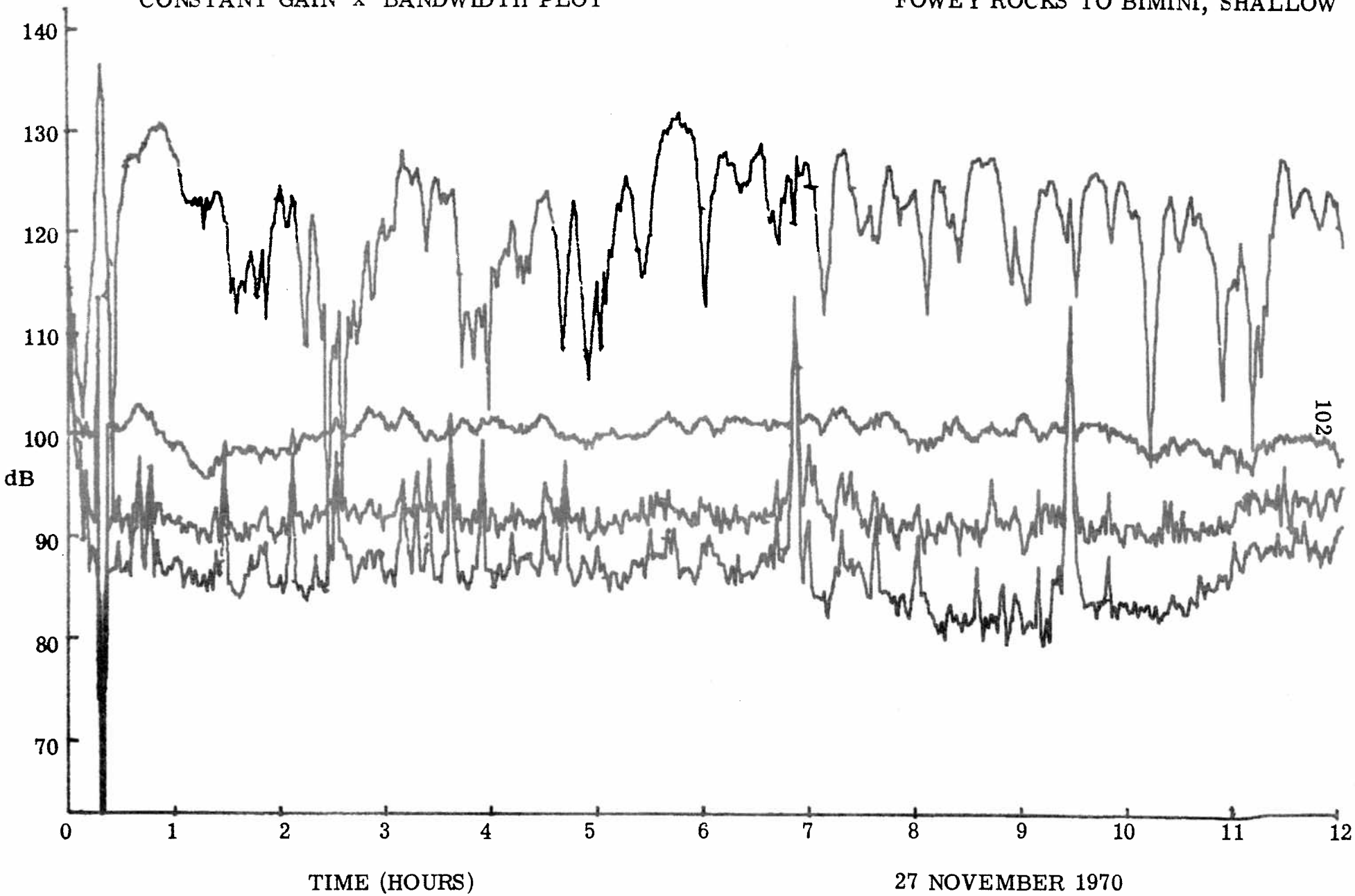
CONSTANT GAIN x BANDWIDTH PLOT
FOWEY ROCKS TO BIMINI, SHALLOW
140
130
120
110
100
90
80
70
dB
102
0
1
2
3
4
5
6
7
8
9
10
11
12
TIME (HOURS)
27 NOVEMBER 1970

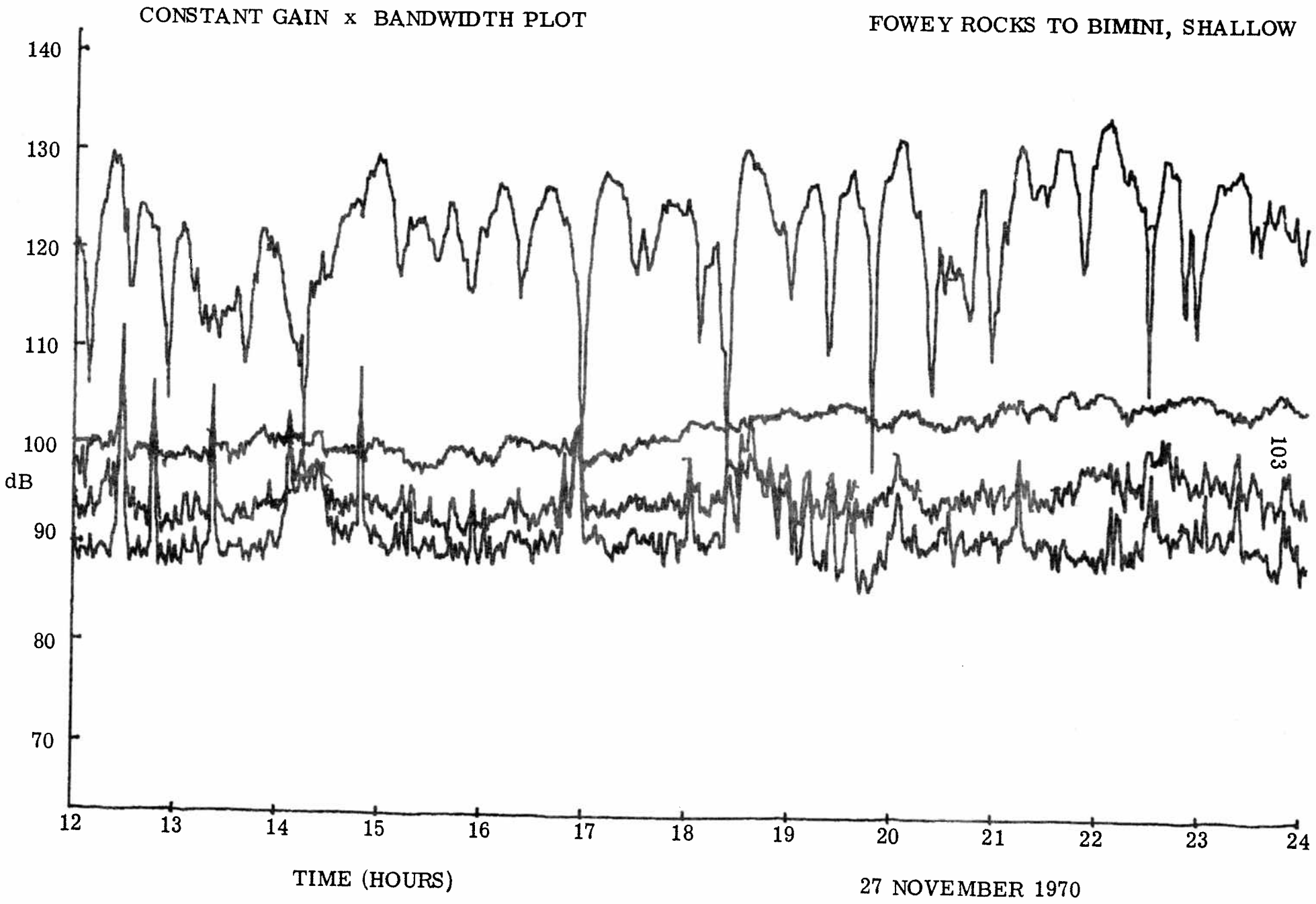
CONSTANT GAIN x BANDWIDTH PLOT
FOWEY ROCKS TO BIMINI, SHALLOW
140
130
120
110
100
90
80
70
dB
103
12
13
14
15
16
17
18
19
20
21
22
23
24
TIME (HOURS)
27 NOVEMBER 1970

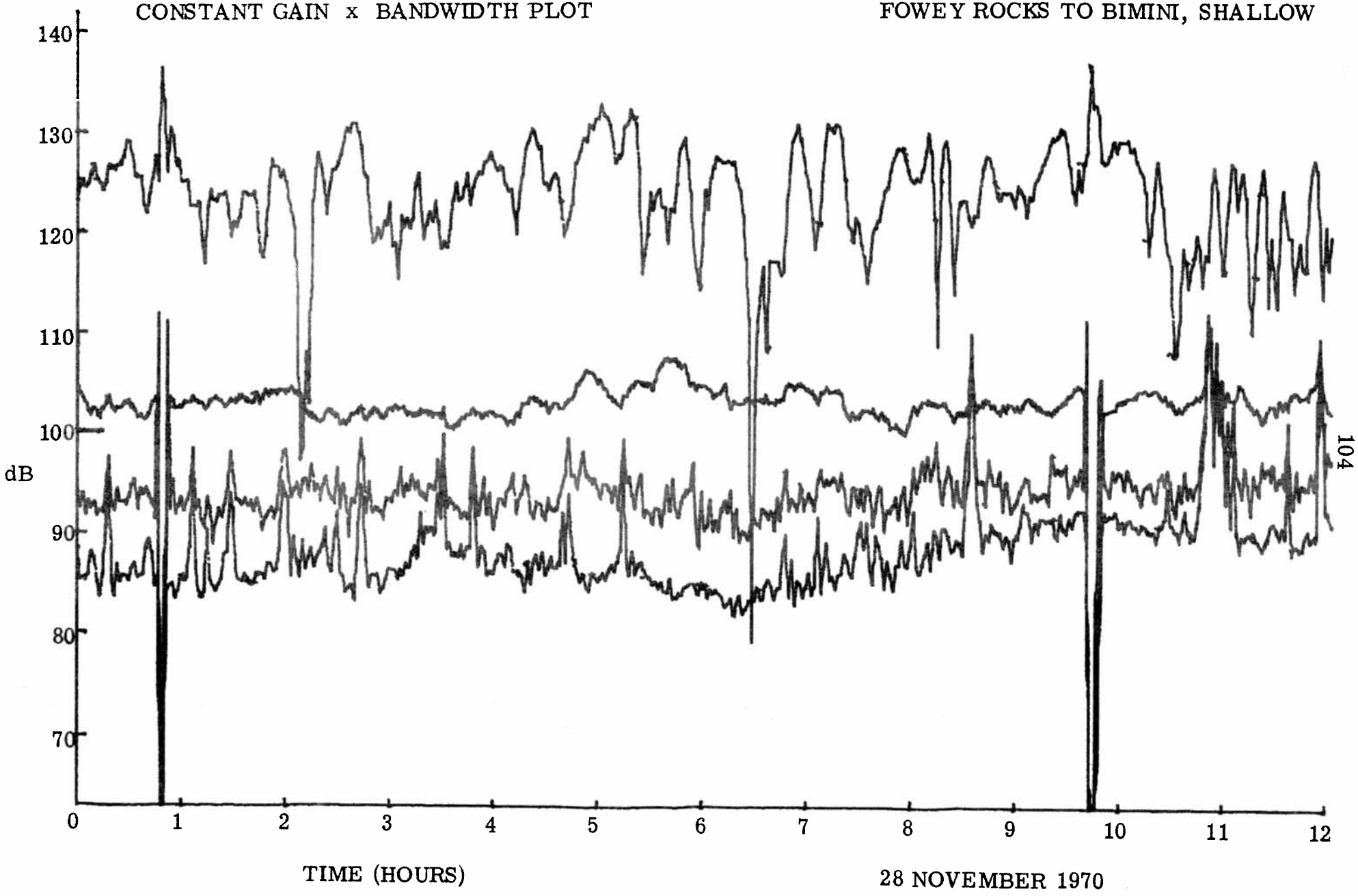
CONSTANT GAIN x BANDWIDTH PLOT
FOWEY ROCKS TO BIMINI, SHALLOW
140
130
120
110
100
90
80
70
dB
104
0
1
2
3
4
5
6
7
8
9
10
11
12
TIME (HOURS)
28 NOVEMBER 1970

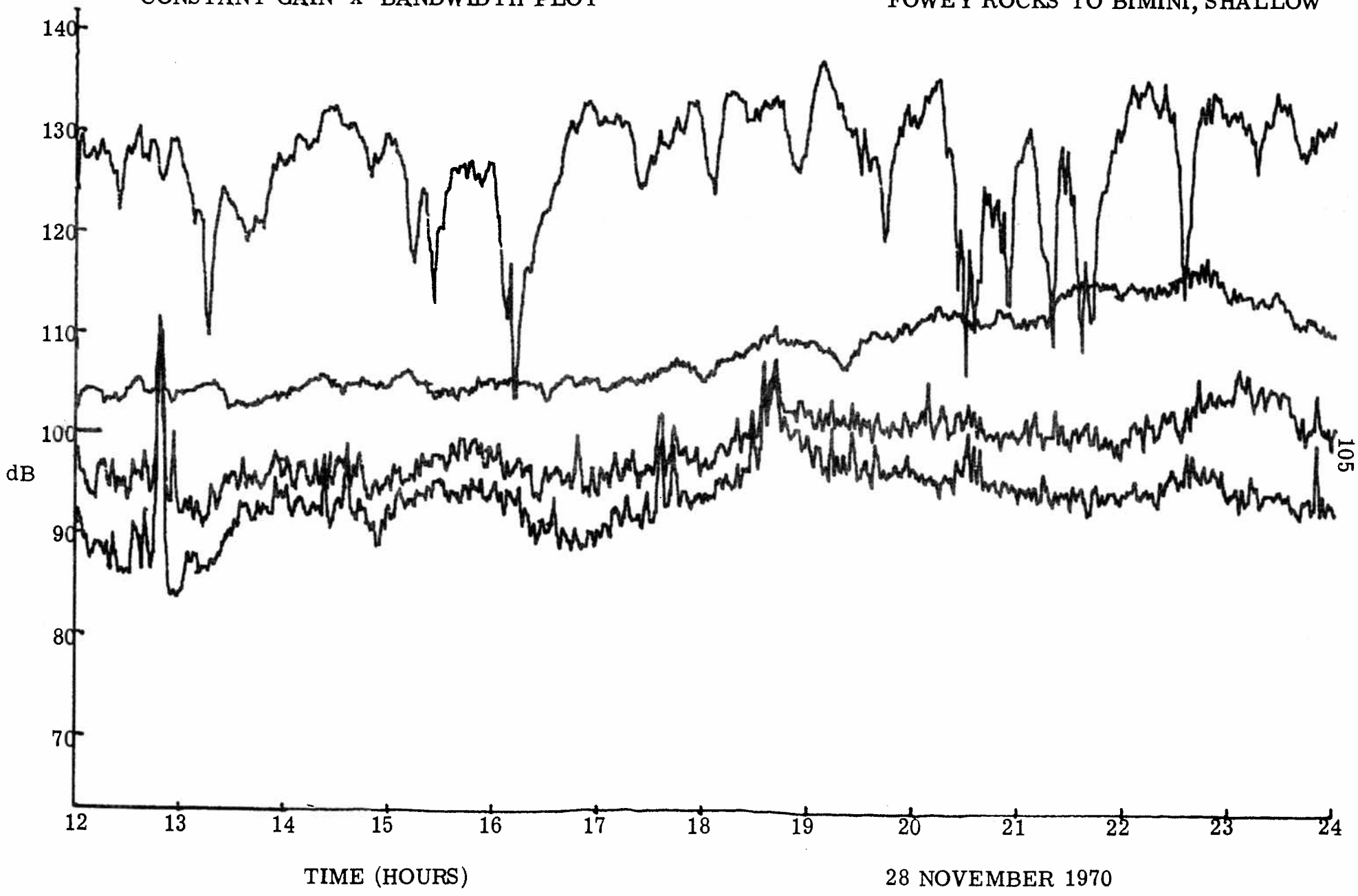
CONSTANT GAIN x BANDWIDTH PLOT
FOWEY ROCKS TO BIMINI, SHALLOW
140
130
120
110
100
90
80
70
dB
105
12
13
14
15
16
17
18
19
20
21
22
23
24
TIME (HOURS)
28 NOVEMBER 1970

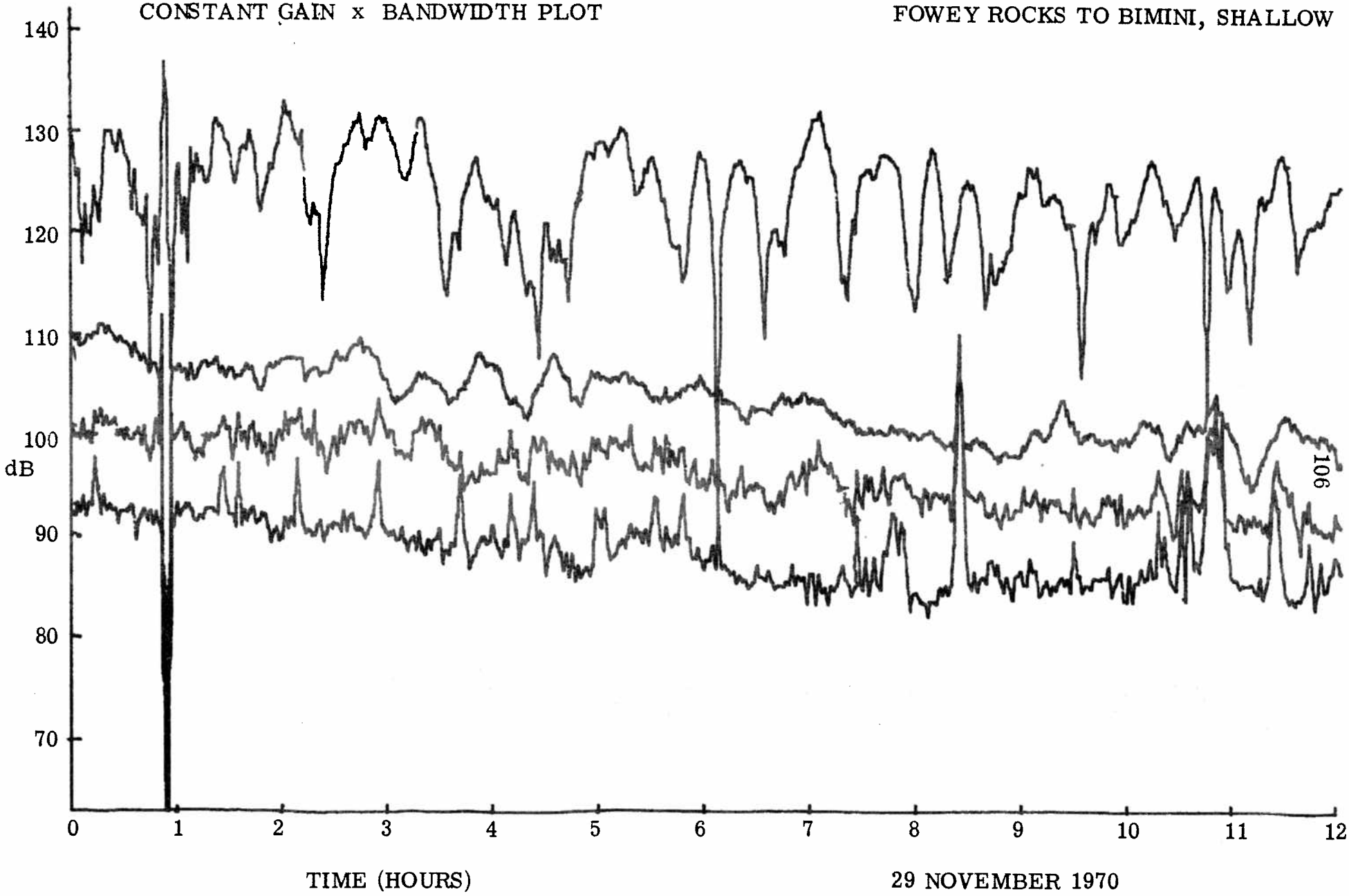
CONSTANT GAIN x BANDWIDTH PLOT
FOWEY ROCKS TO BIMINI, SHALLOW
140
130
120
110
100
90
80
70
dB
106
0
1
2
3
4
5
6
7
8
9
10
11
12
TIME (HOURS)
29 NOVEMBER 1970

APPENDIX B

Appendix B contains the unity gain plots of the carrier and sideband powers from the Bimini data.

UNITY GAIN PLOT

FOWEY ROCKS TO BIMINI, DEEP

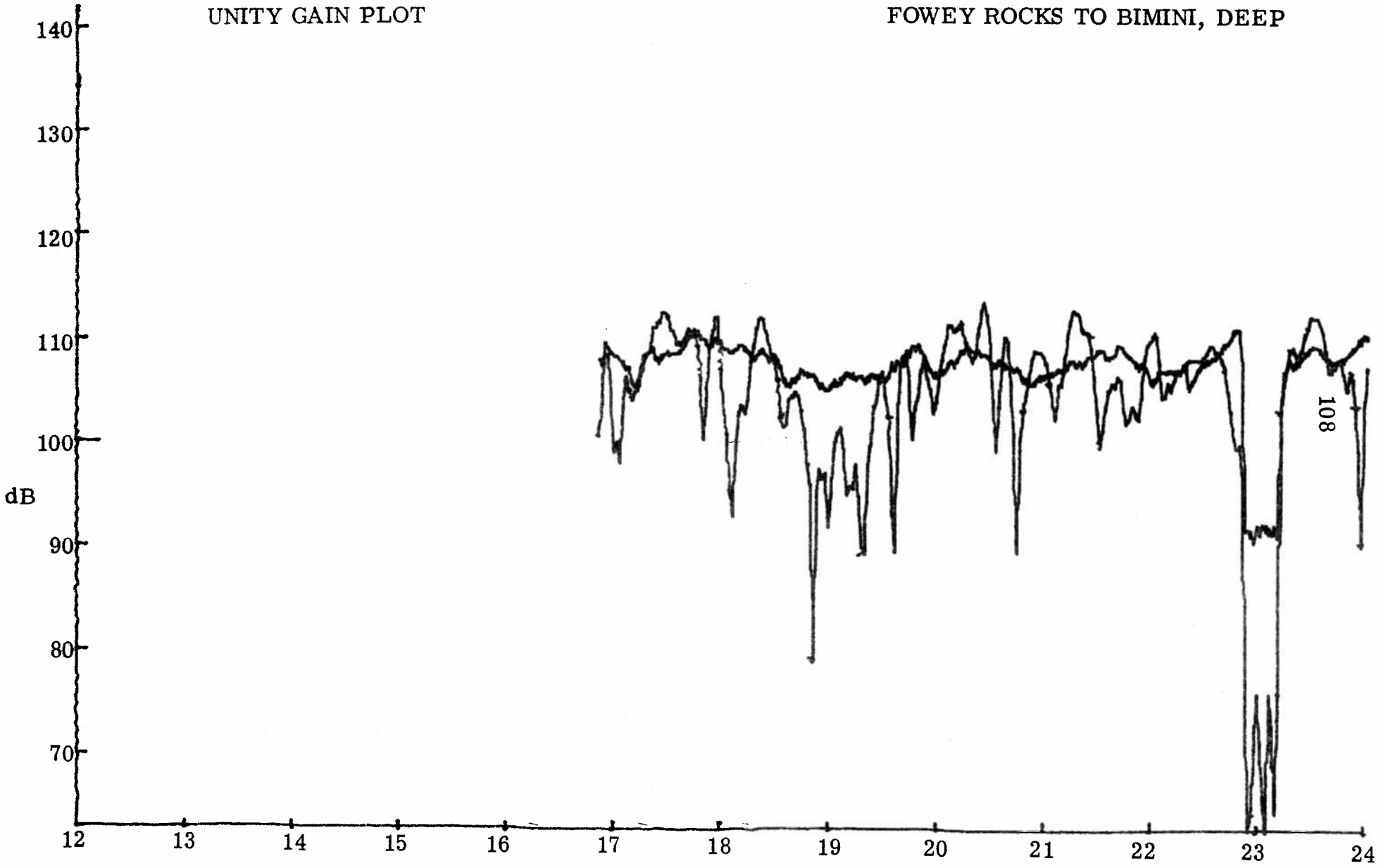

TIME (HOURS)

13 NOVEMBER 1970

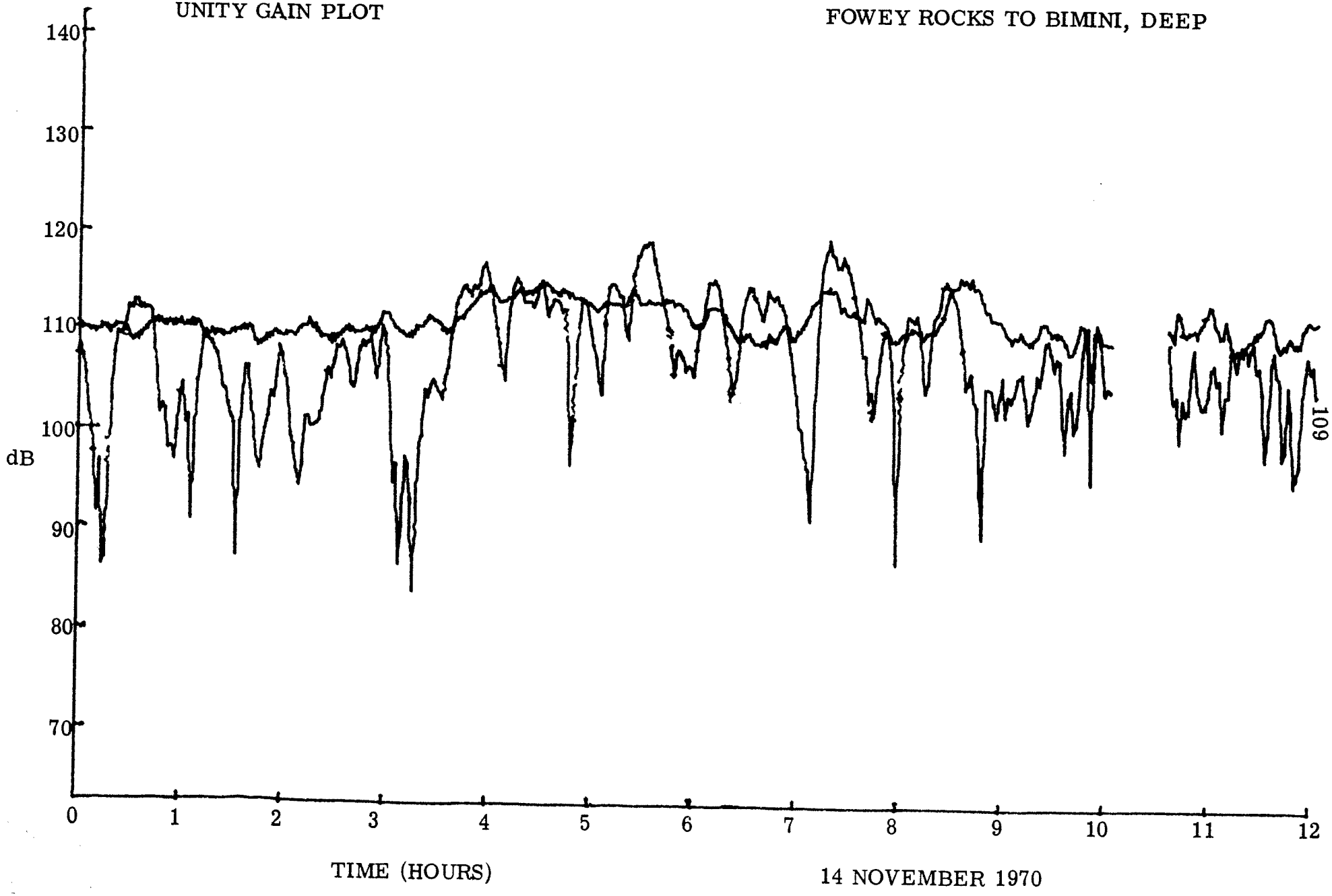
UNITY GAIN PLOT
FOWEY ROCKS TO BIMINI, DEEP
140
130
120
110
100
90
80
70
dB
109
0
1
2
3
4
5
6
7
8
9
10
11
12
TIME (HOURS)
14 NOVEMBER 1970

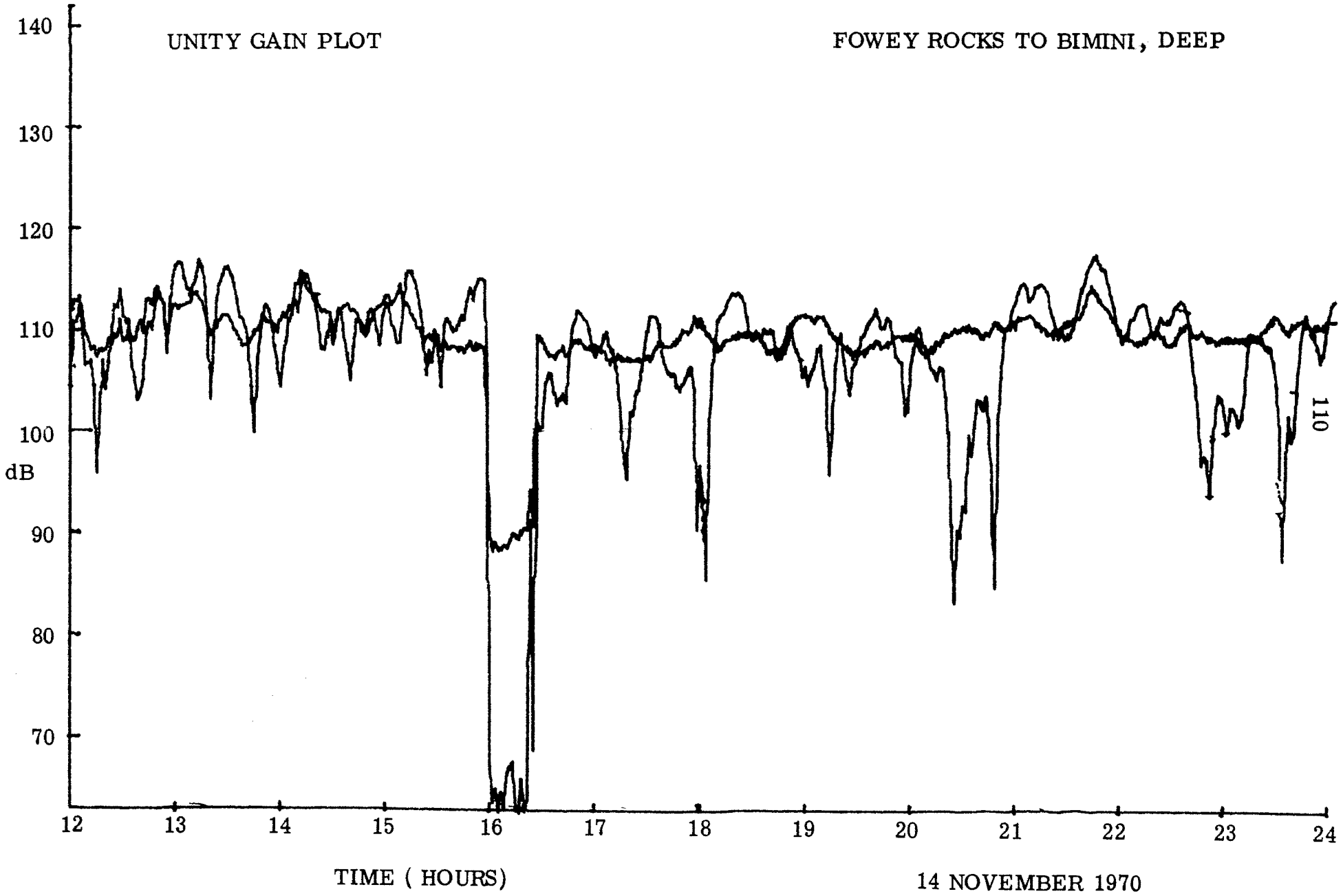
UNITY GAIN PLOT
FOWEY ROCKS TO BIMINI, DEEP
140
130
120
110
100
dB
90
80
70
110
12
13
14
15
16
17
18
19
20
21
22
23
24
TIME (HOURS)
14 NOVEMBER 1970

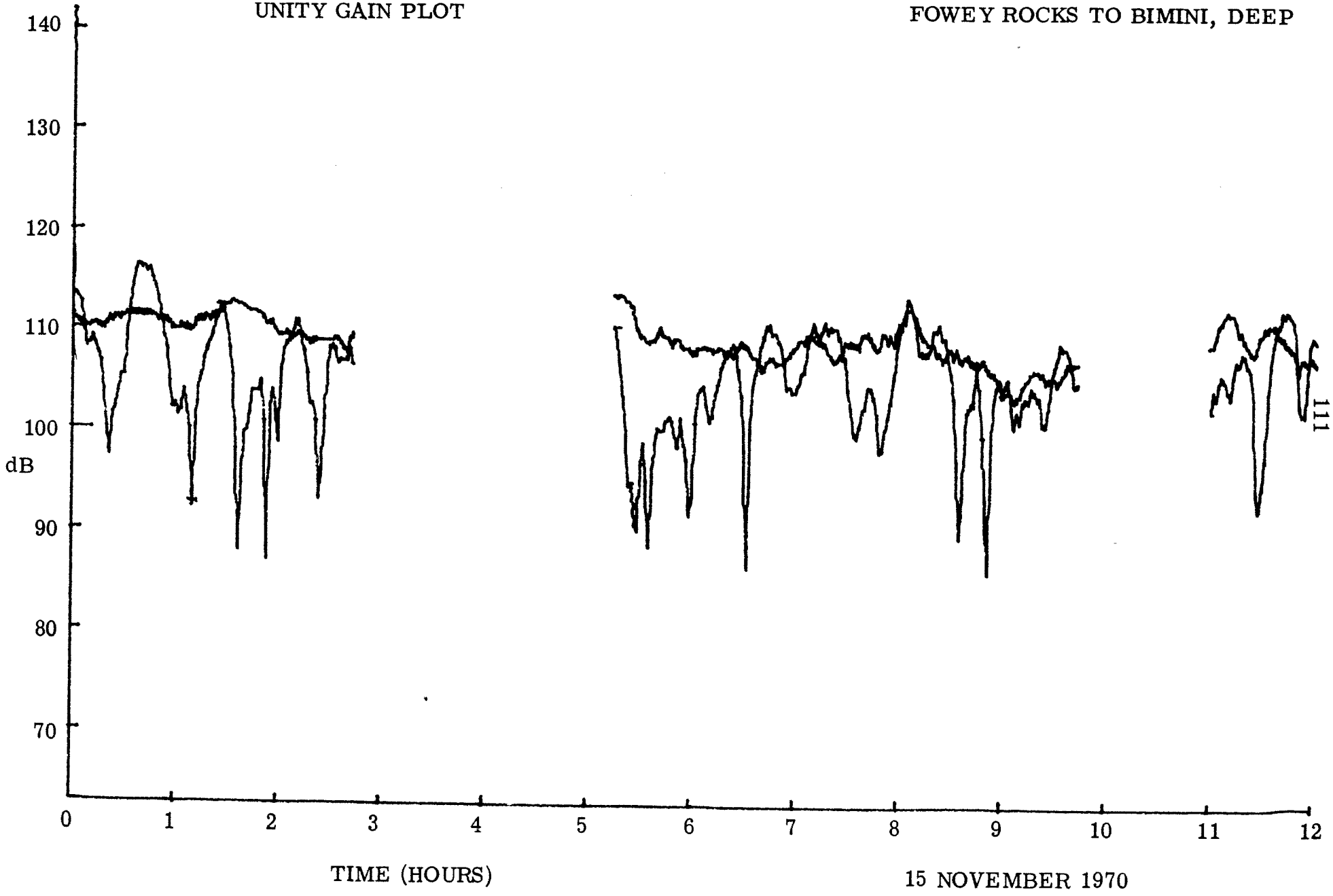
UNITY GAIN PLOT
FOWEY ROCKS TO BIMINI, DEEP
140
130
120
110
100
dB
90
80
70
0
1
2
3
4
5
6
7
8
9
10
11
12
TIME (HOURS)
15 NOVEMBER 1970
111

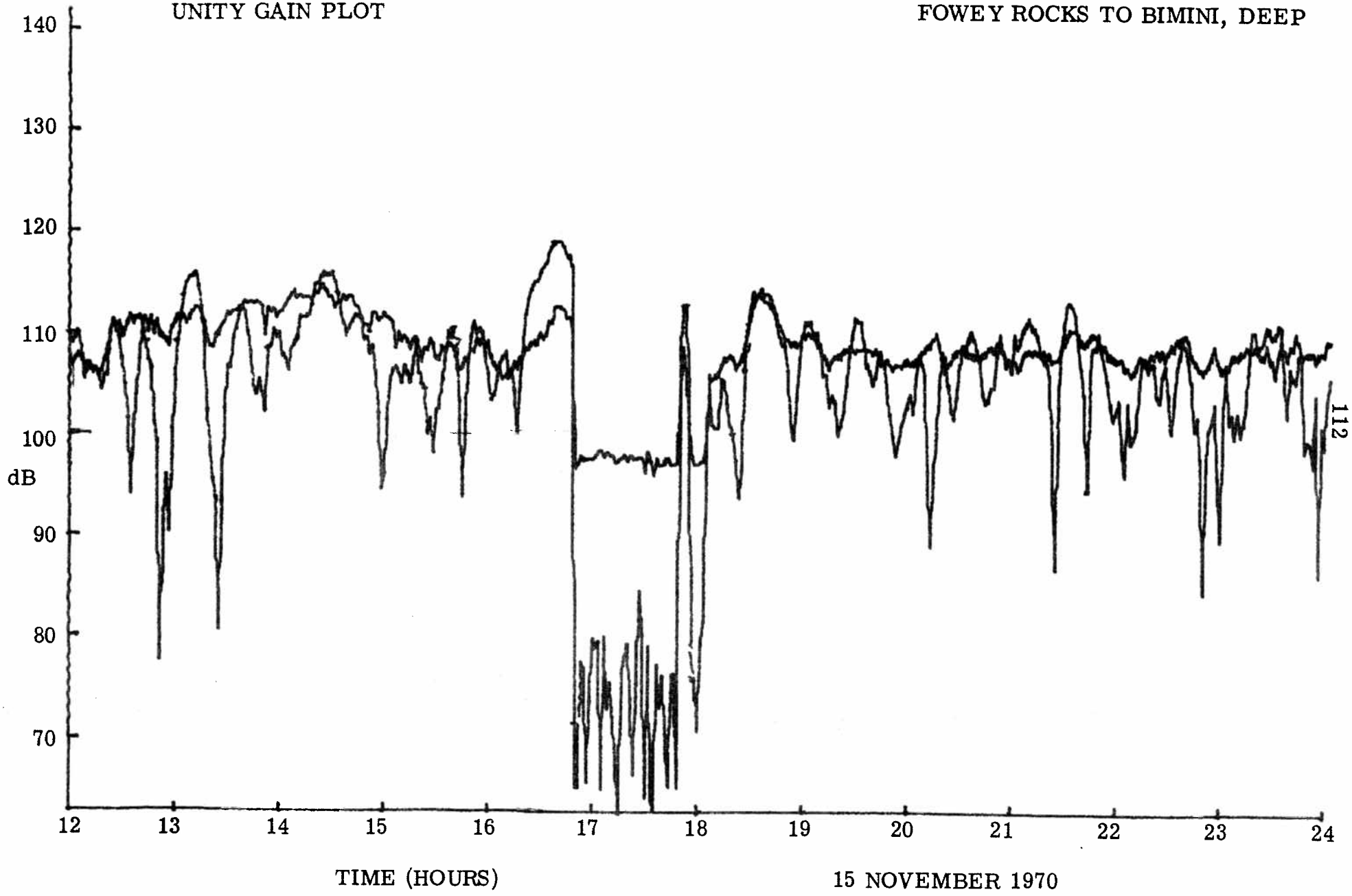
UNITY GAIN PLOT
FOWEY ROCKS TO BIMINI, DEEP
140
130
120
110
100
dB
90
80
70
112
12
13
14
15
16
17
18
19
20
21
22
23
24
TIME (HOURS)
15 NOVEMBER 1970

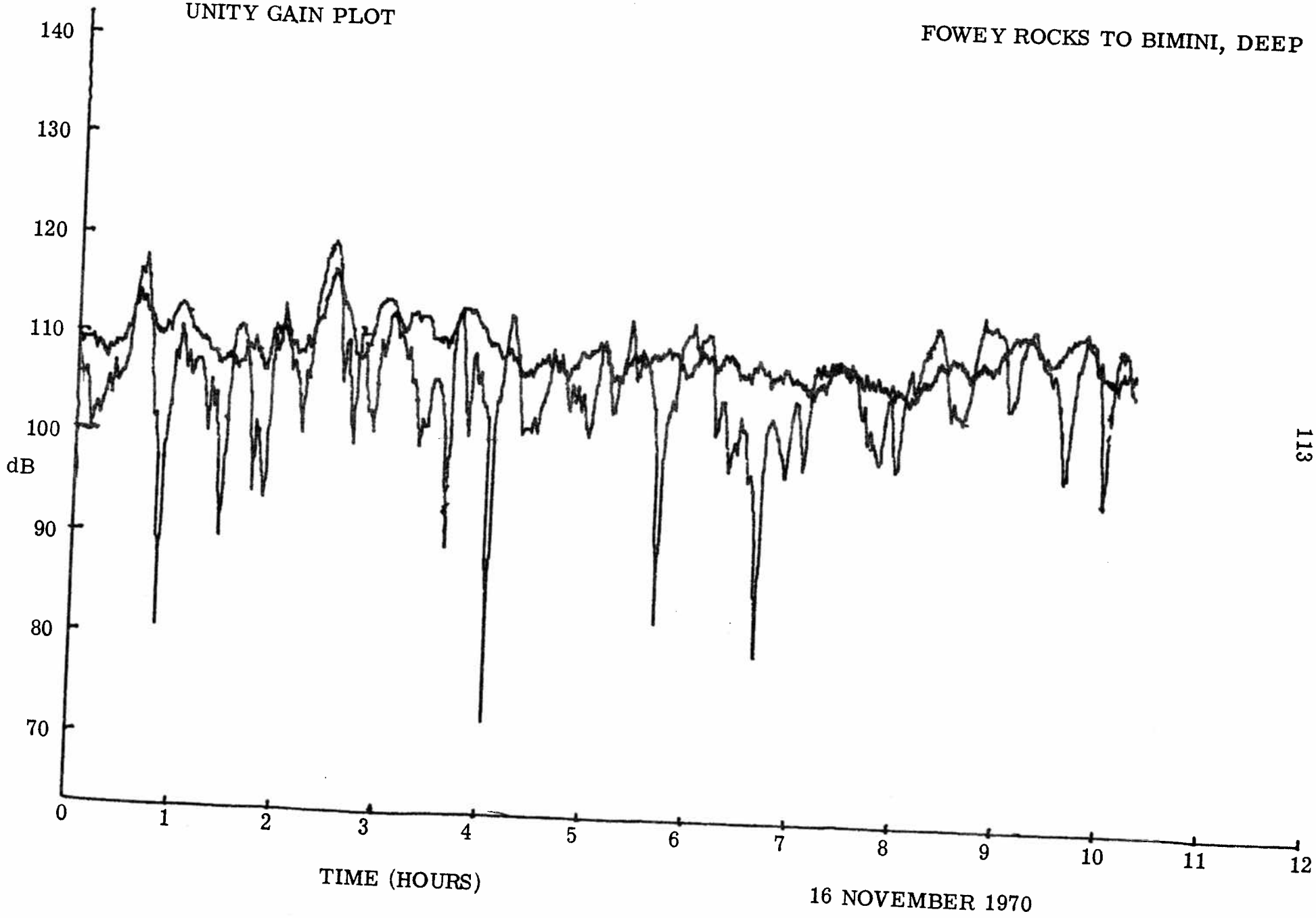
UNITY GAIN PLOT
FOWEY ROCKS TO BIMINI, DEEP
140
130
120
110
100
dB
90
80
70
0
1
2
3
4
5
6
7
8
9
10
11
12
TIME (HOURS)
16 NOVEMBER 1970

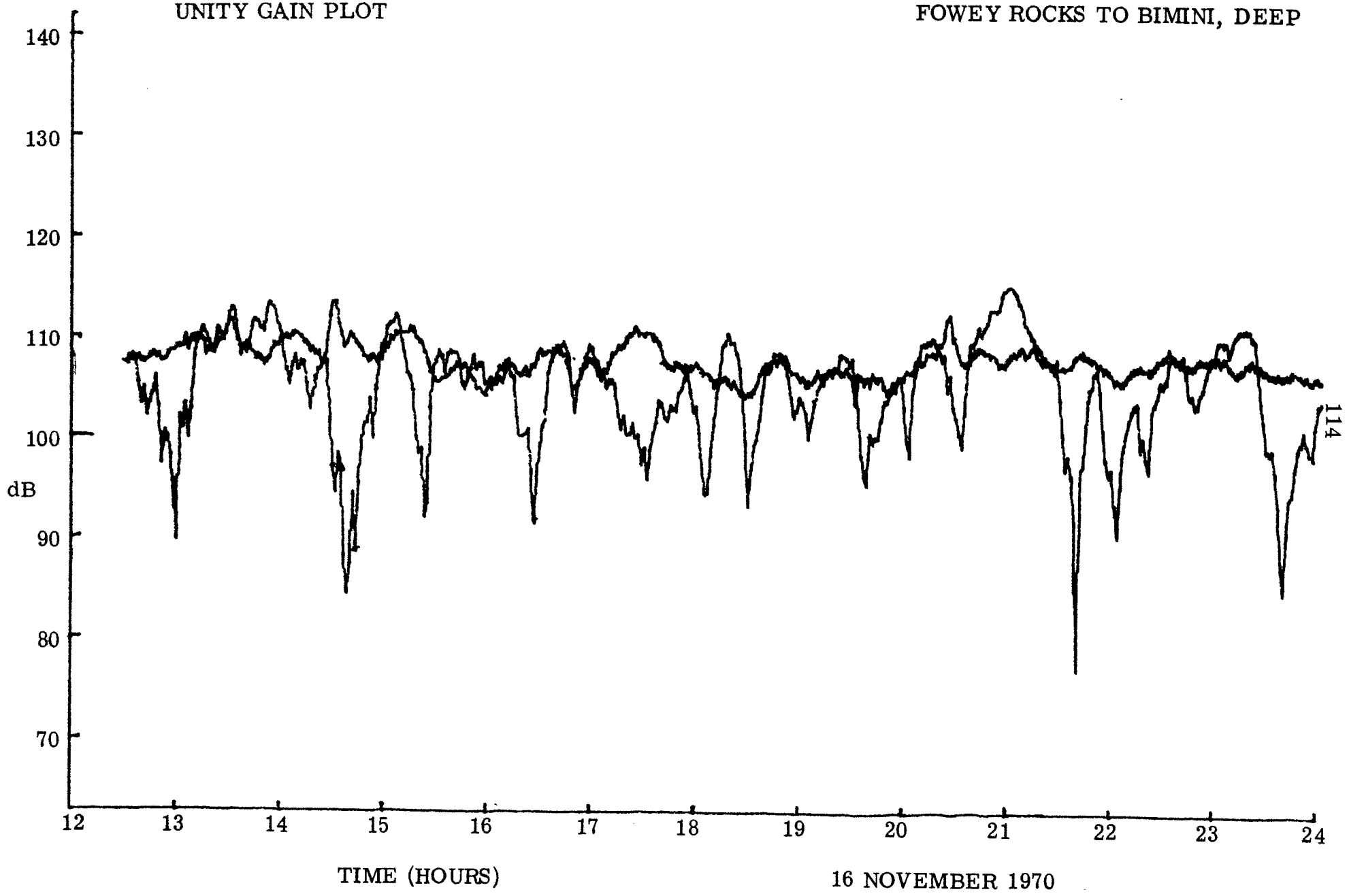
UNITY GAIN PLOT
FOWEY ROCKS TO BIMINI, DEEP
140
130
120
110
100
dB
90
80
70
114
12
13
14
15
16
17
18
19
20
21
22
23
24
TIME (HOURS)
16 NOVEMBER 1970

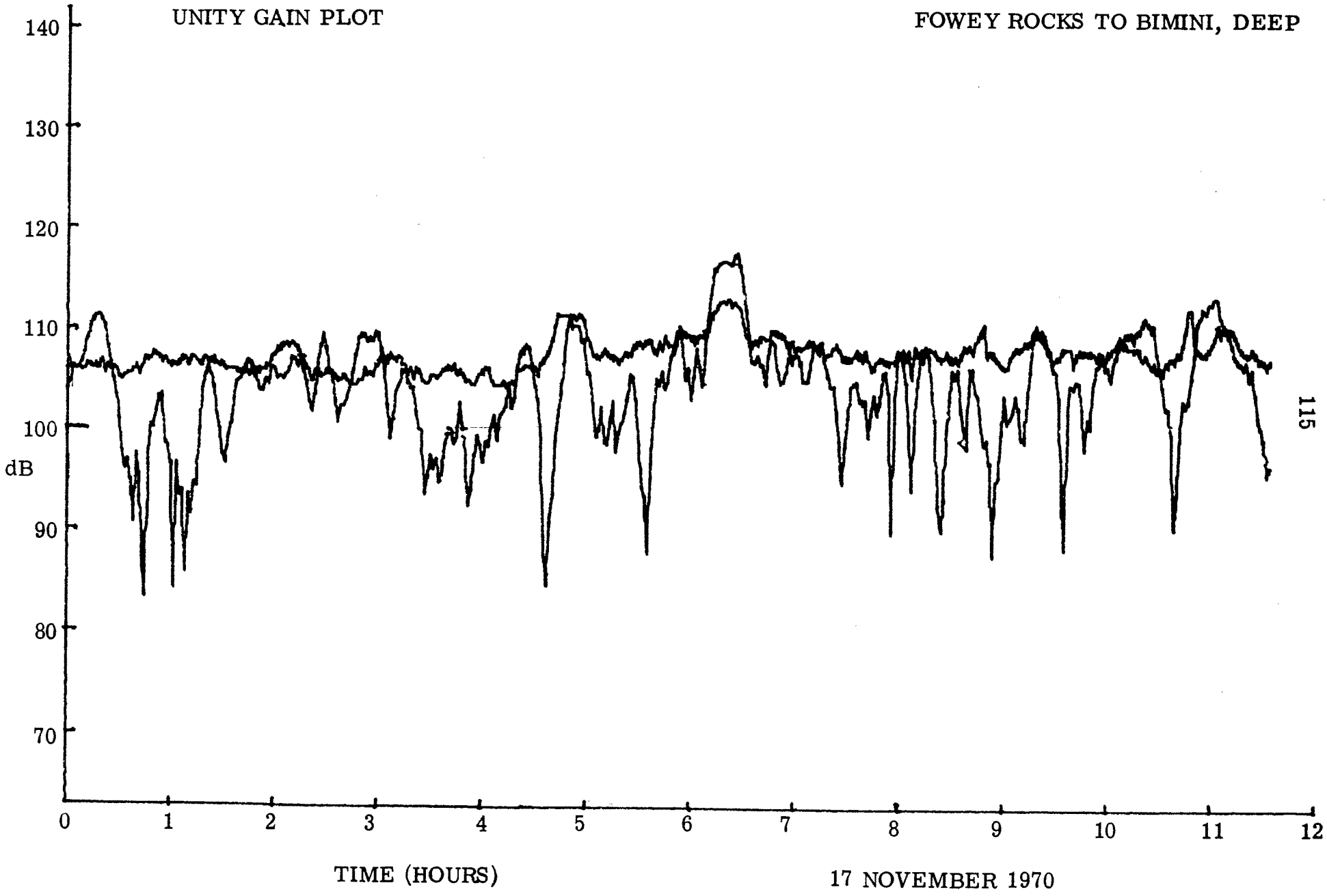
UNITY GAIN PLOT
FOWEY ROCKS TO BIMINI, DEEP
140
130
120
110
100
90
80
70
dB
115
0
1
2
3
4
5
6
7
8
9
10
11
12
TIME (HOURS)
17 NOVEMBER 1970

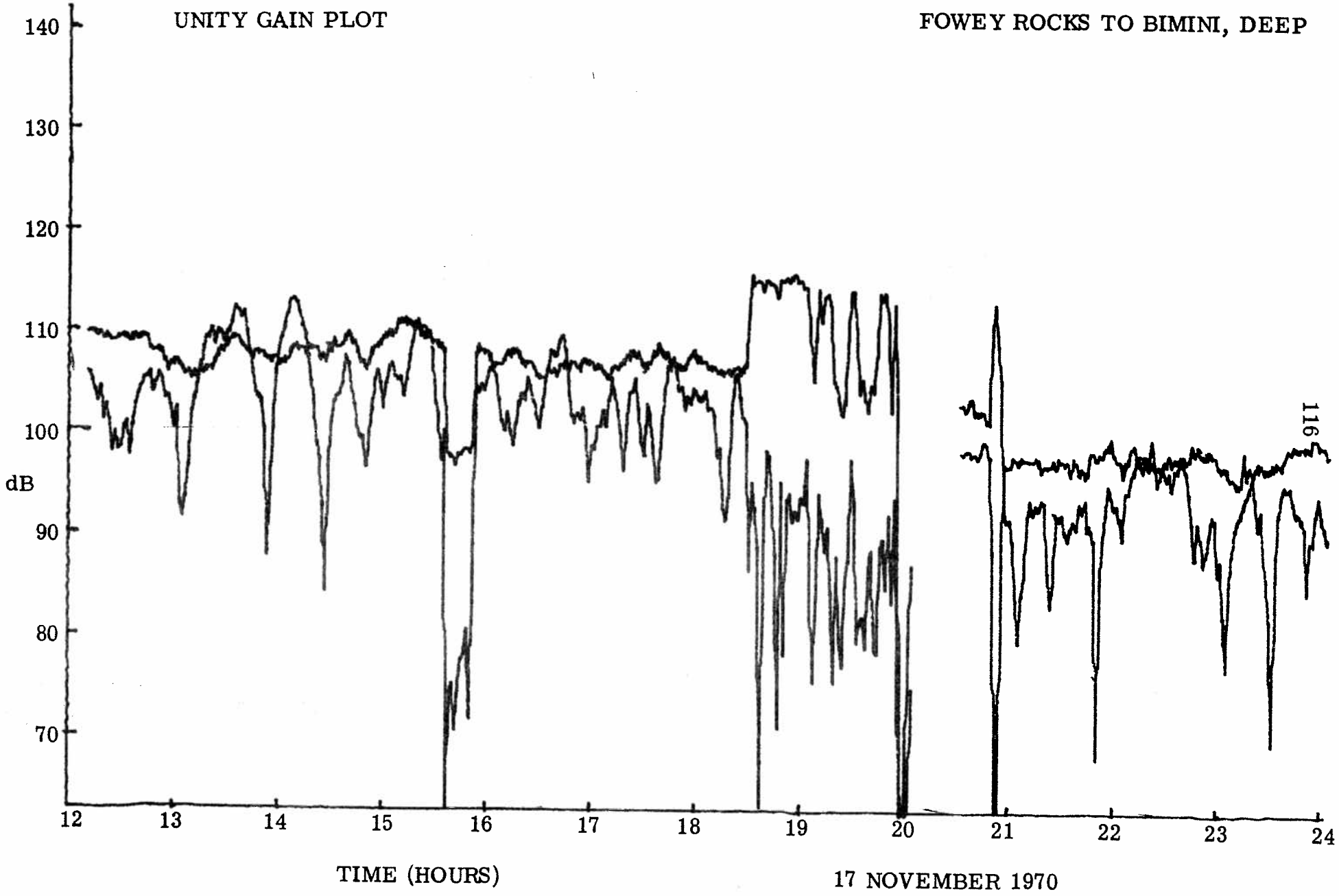
UNITY GAIN PLOT
FOWEY ROCKS TO BIMINI, DEEP
140
130
120
110
100
90
80
70
dB
116
12
13
14
15
16
17
18
19
20
21
22
23
24
TIME (HOURS)
17 NOVEMBER 1970

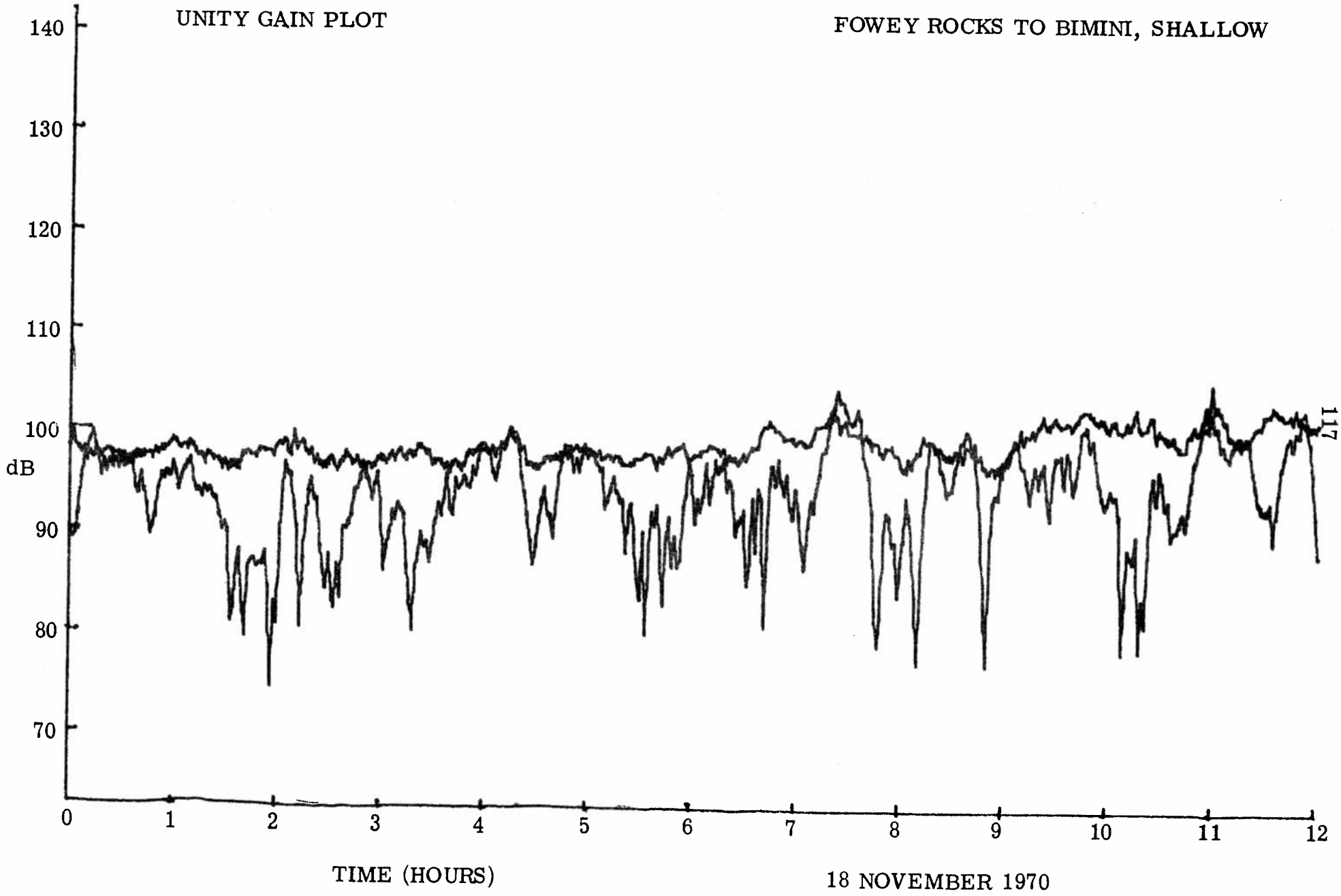
UNITY GAIN PLOT
FOWEY ROCKS TO BIMINI, SHALLOW
140
130
120
110
100
dB
90
80
70
117
0
1
2
3
4
5
6
7
8
9
10
11
12
TIME (HOURS)
18 NOVEMBER 1970

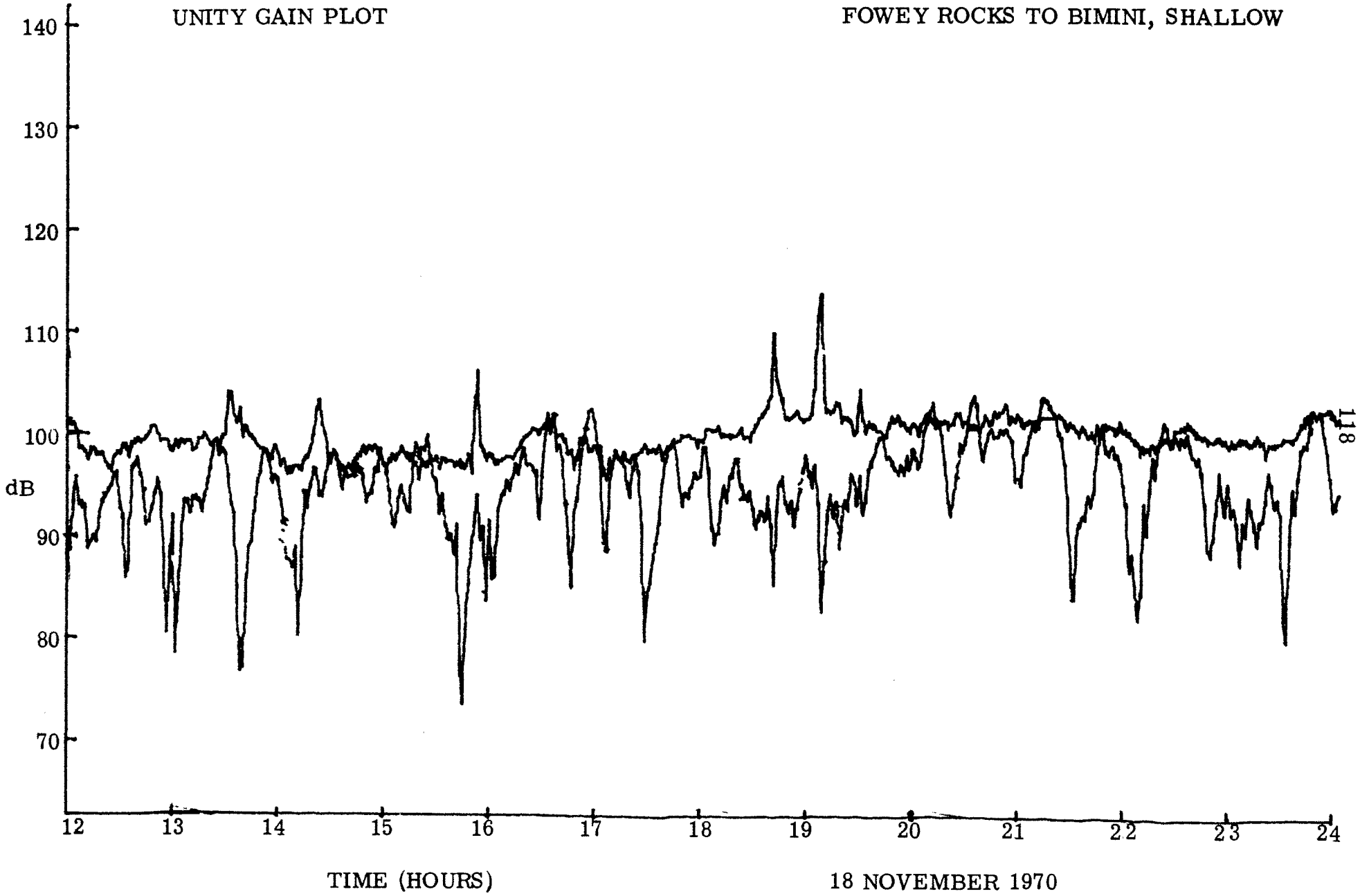
UNITY GAIN PLOT
FOWEY ROCKS TO BIMINI, SHALLOW
140
130
120
110
100
90
80
70
dB
118
12
13
14
15
16
17
18
19
20
21
22
23
24
TIME (HOURS)
18 NOVEMBER 1970

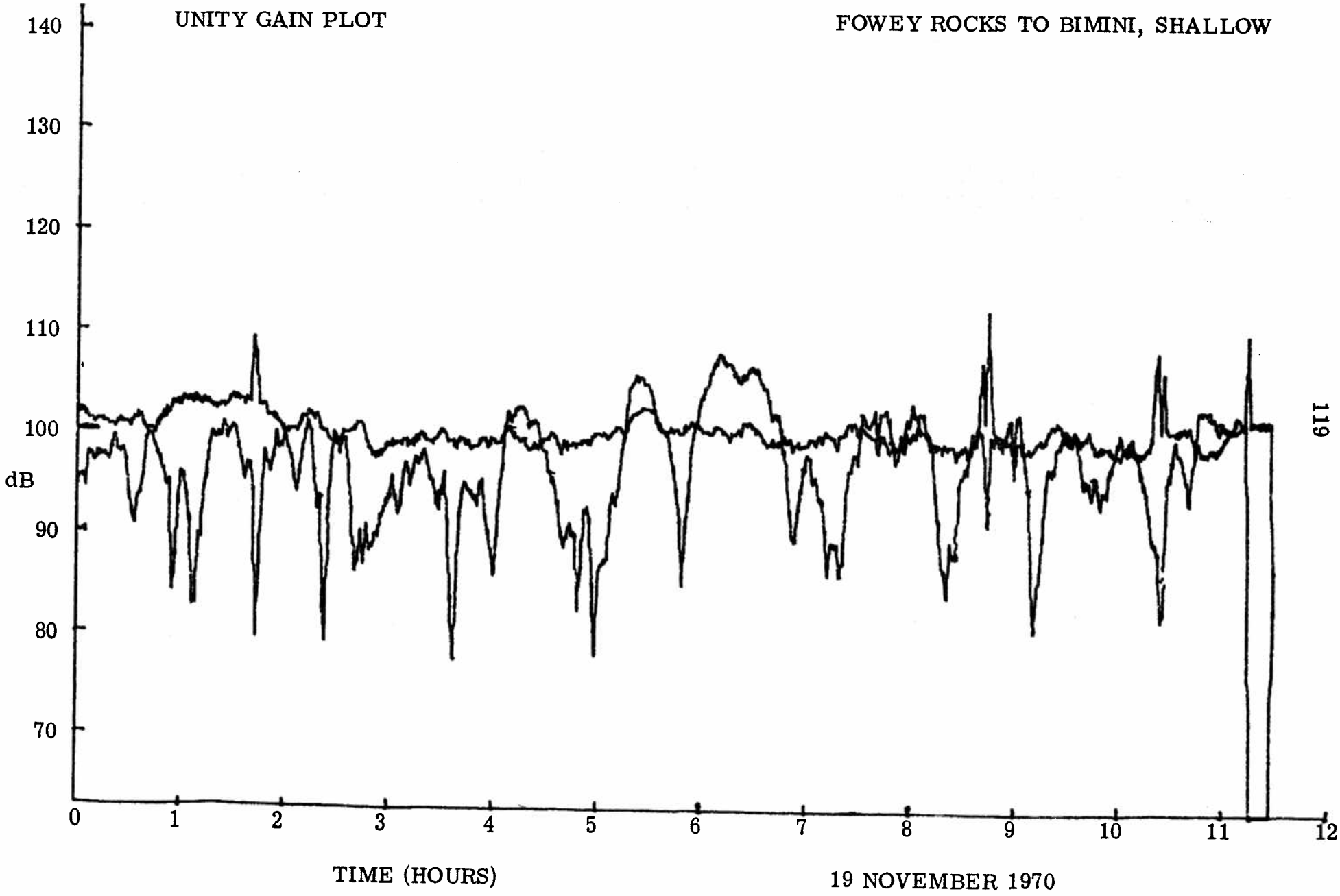
UNITY GAIN PLOT
FOWEY ROCKS TO BIMINI, SHALLOW
140
130
120
110
100
90
80
70
dB
119
0
1
2
3
4
5
6
7
8
9
10
11
12
TIME (HOURS)
19 NOVEMBER 1970

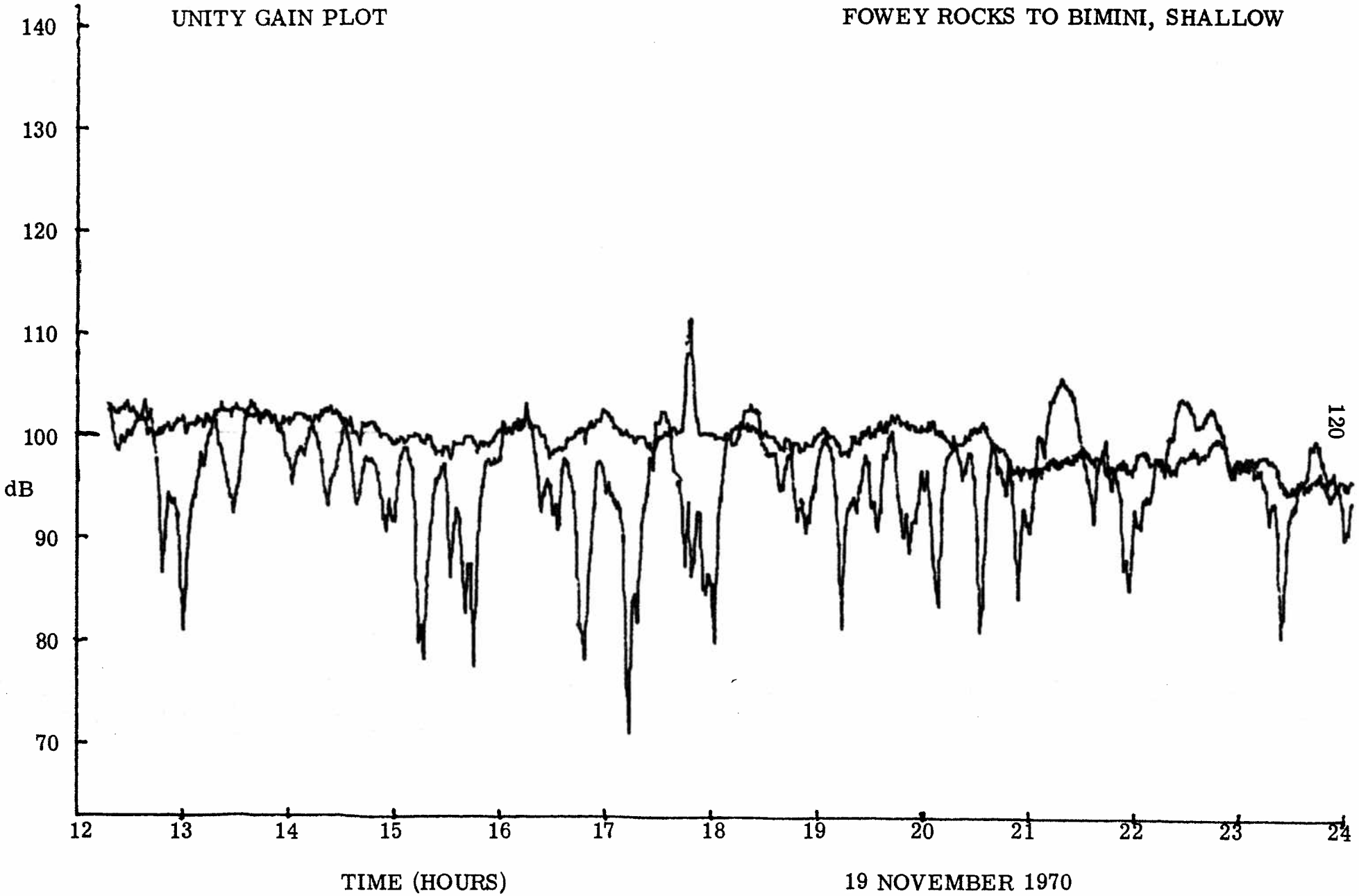
UNITY GAIN PLOT
FOWEY ROCKS TO BIMINI, SHALLOW
140
130
120
110
100
90
80
70
dB
120
12
13
14
15
16
17
18
19
20
21
22
23
24
TIME (HOURS)
19 NOVEMBER 1970

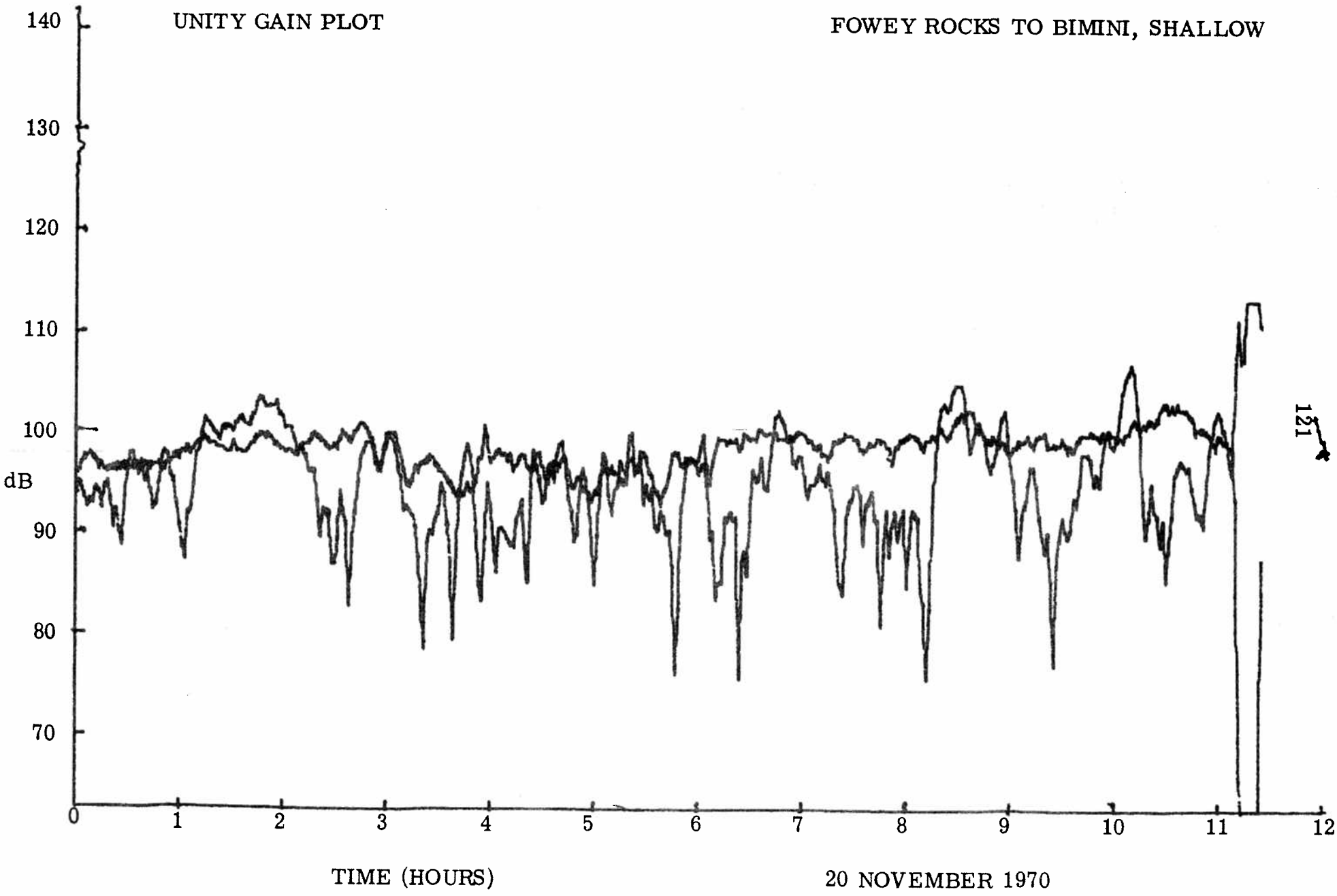
UNITY GAIN PLOT
FOWEY ROCKS TO BIMINI, SHALLOW
140
130
120
110
100
dB
90
80
70
121
0
1
2
3
4
5
6
7
8
9
10
11
12
TIME (HOURS)
20 NOVEMBER 1970

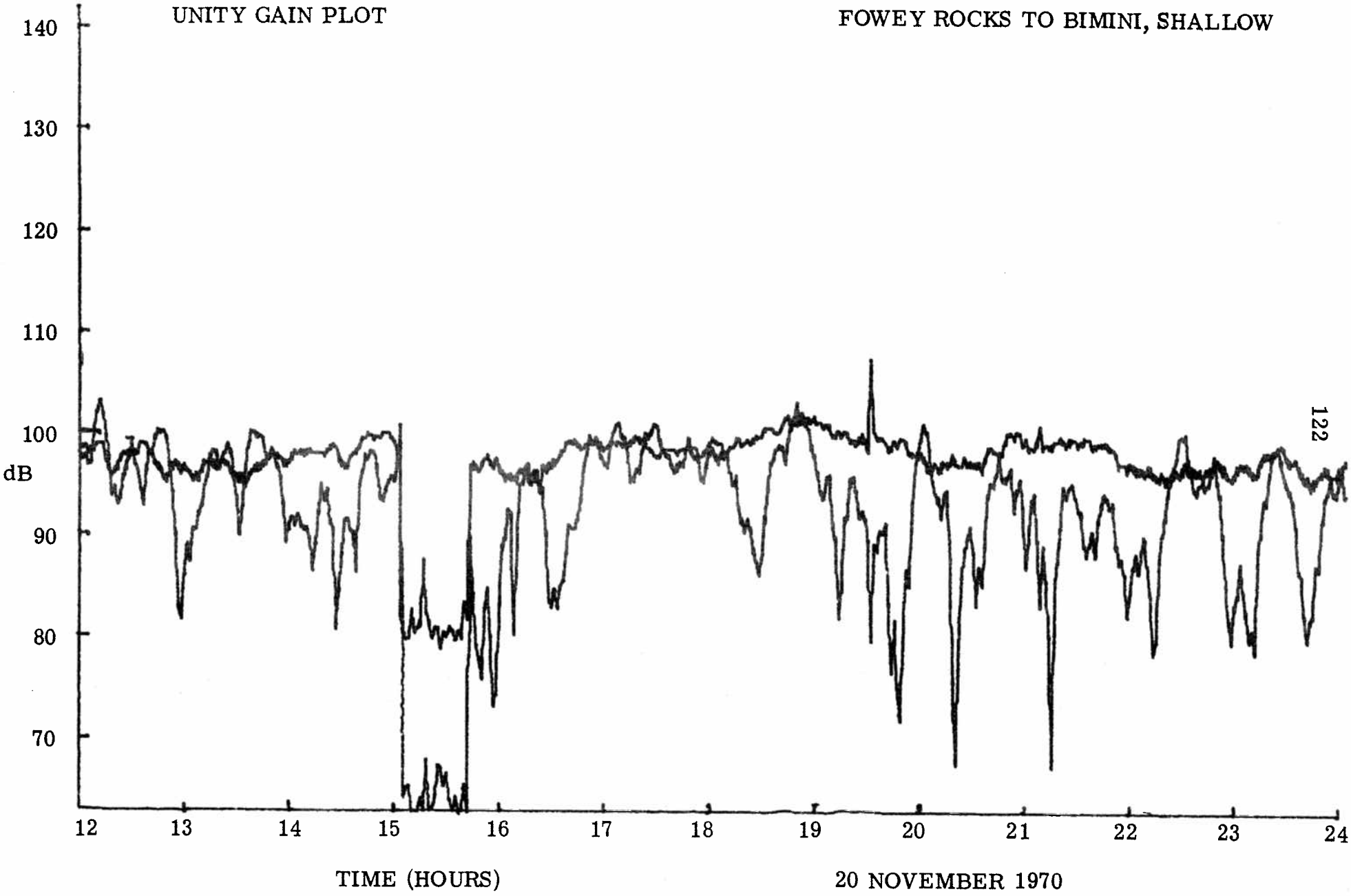
UNITY GAIN PLOT
FOWEY ROCKS TO BIMINI, SHALLOW
140
130
120
110
100
90
80
70
dB
122
12
13
14
15
16
17
18
19
20
21
22
23
24
TIME (HOURS)
20 NOVEMBER 1970

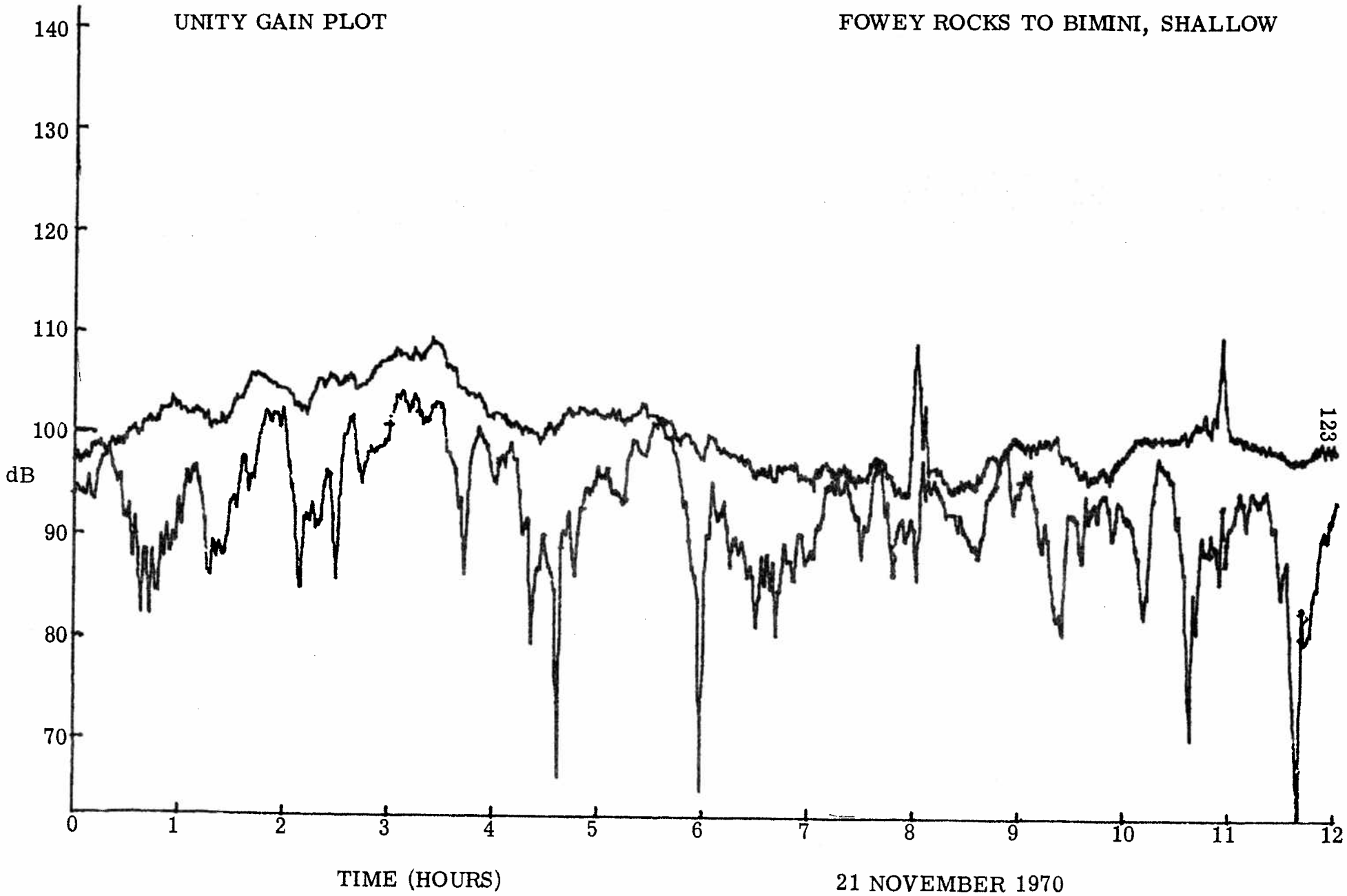
UNITY GAIN PLOT
FOWEY ROCKS TO BIMINI, SHALLOW
140
130
120
110
100
90
80
70
dB
123
0
1
2
3
4
5
6
7
8
9
10
11
12
TIME (HOURS)
21 NOVEMBER 1970

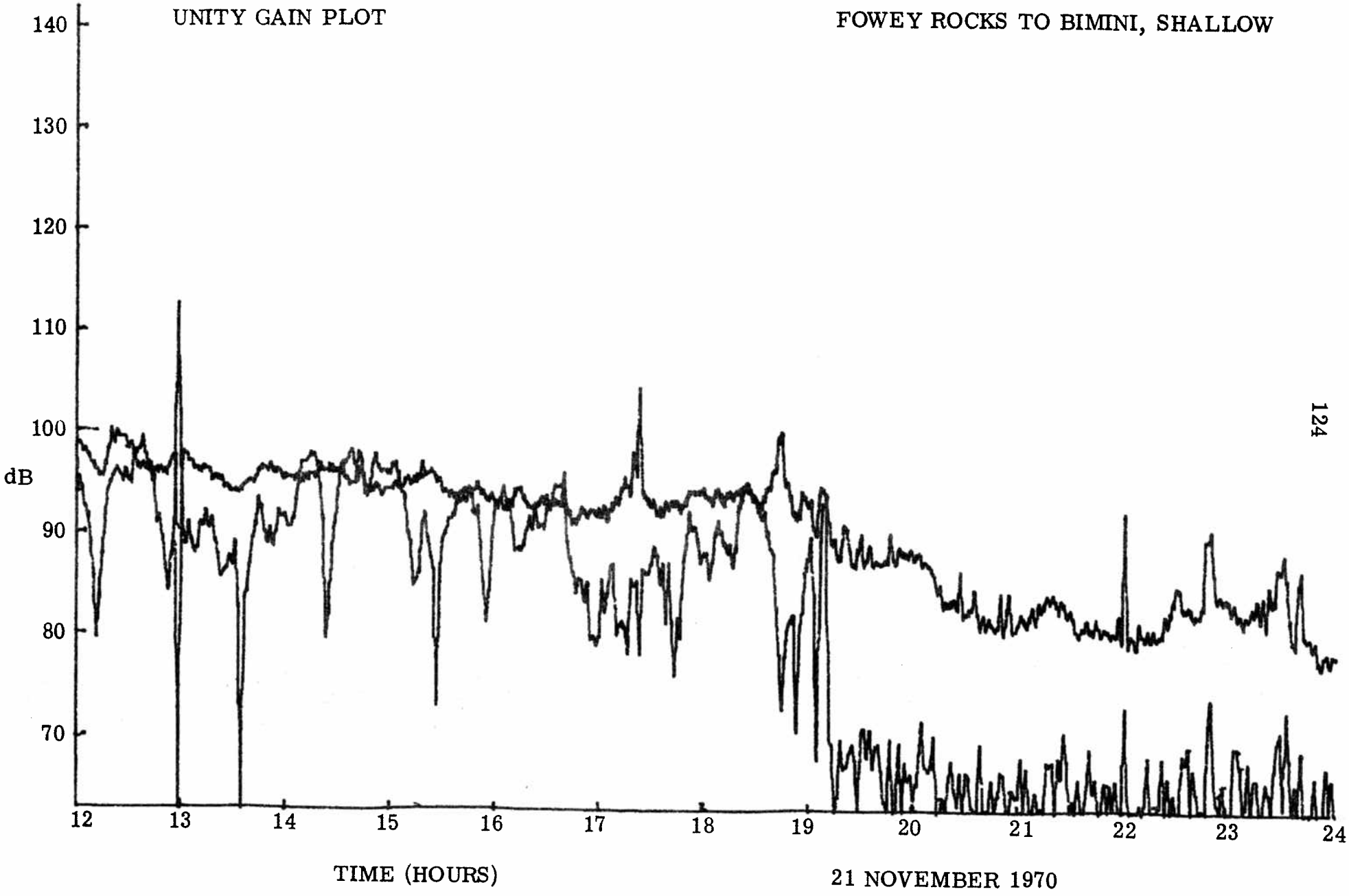
UNITY GAIN PLOT
FOWEY ROCKS TO BIMINI, SHALLOW
140
130
120
110
100
90
80
70
dB
12
13
14
15
16
17
18
19
20
21
22
23
24
TIME (HOURS)
21 NOVEMBER 1970
124

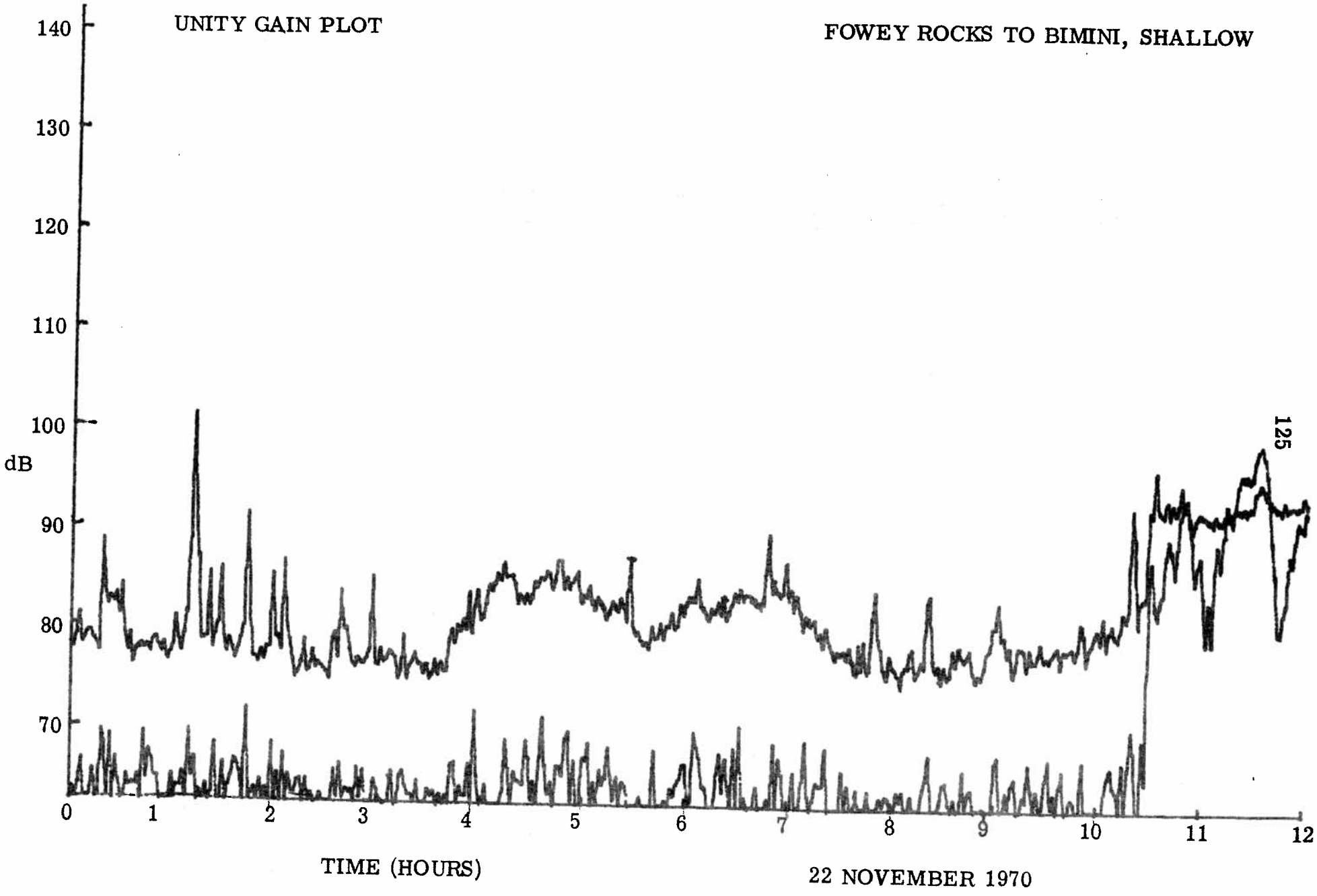
UNITY GAIN PLOT
FOWEY ROCKS TO BIMINI, SHALLOW
140
130
120
110
100
90
80
70
dB
125
0
1
2
3
4
5
6
7
8
9
10
11
12
TIME (HOURS)
22 NOVEMBER 1970

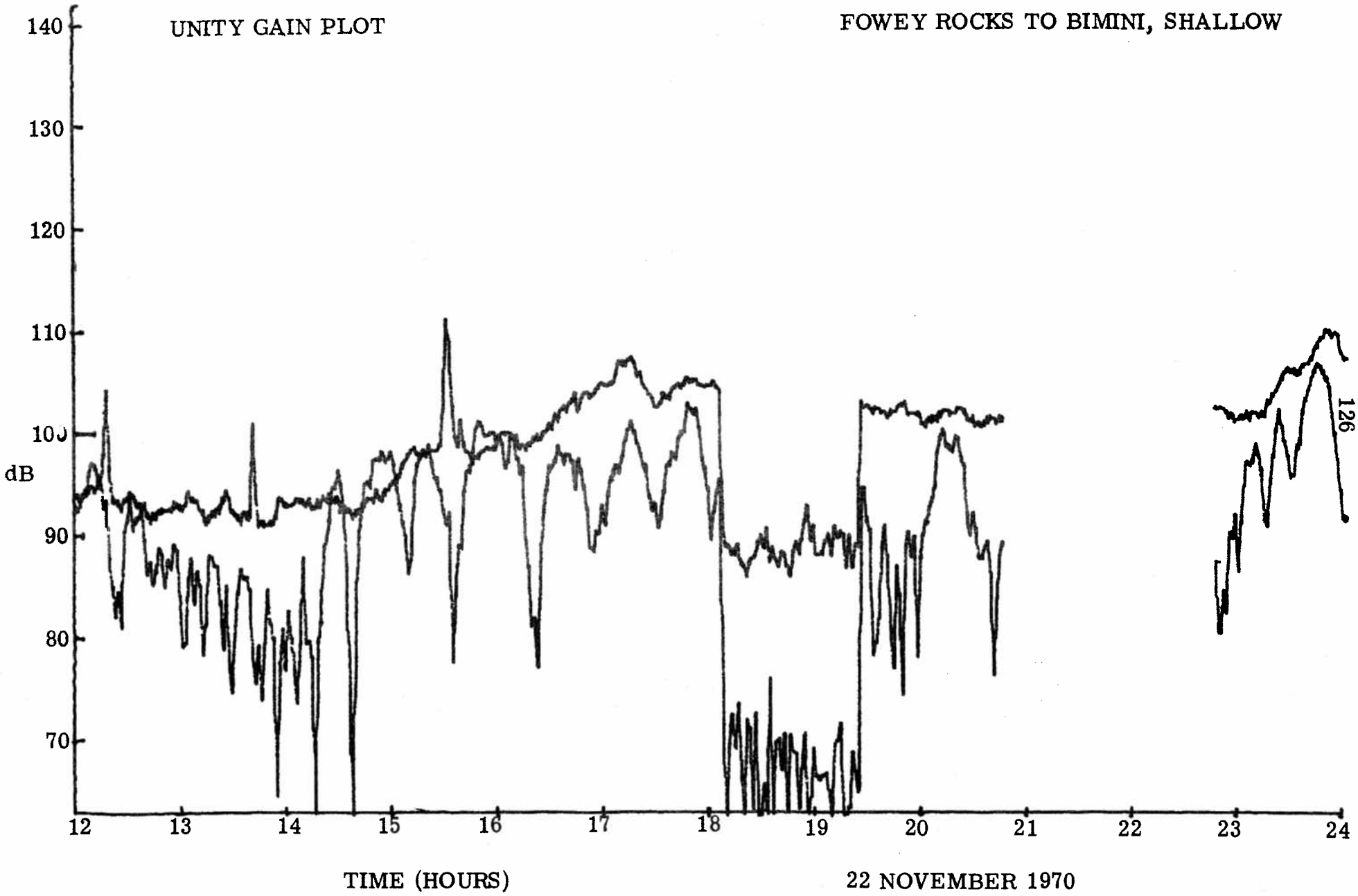
UNITY GAIN PLOT
FOWEY ROCKS TO BIMINI, SHALLOW
140
130
120
110
100
dB
90
80
70
126
12
13
14
15
16
17
18
19
20
21
22
23
24
TIME (HOURS)
22 NOVEMBER 1970

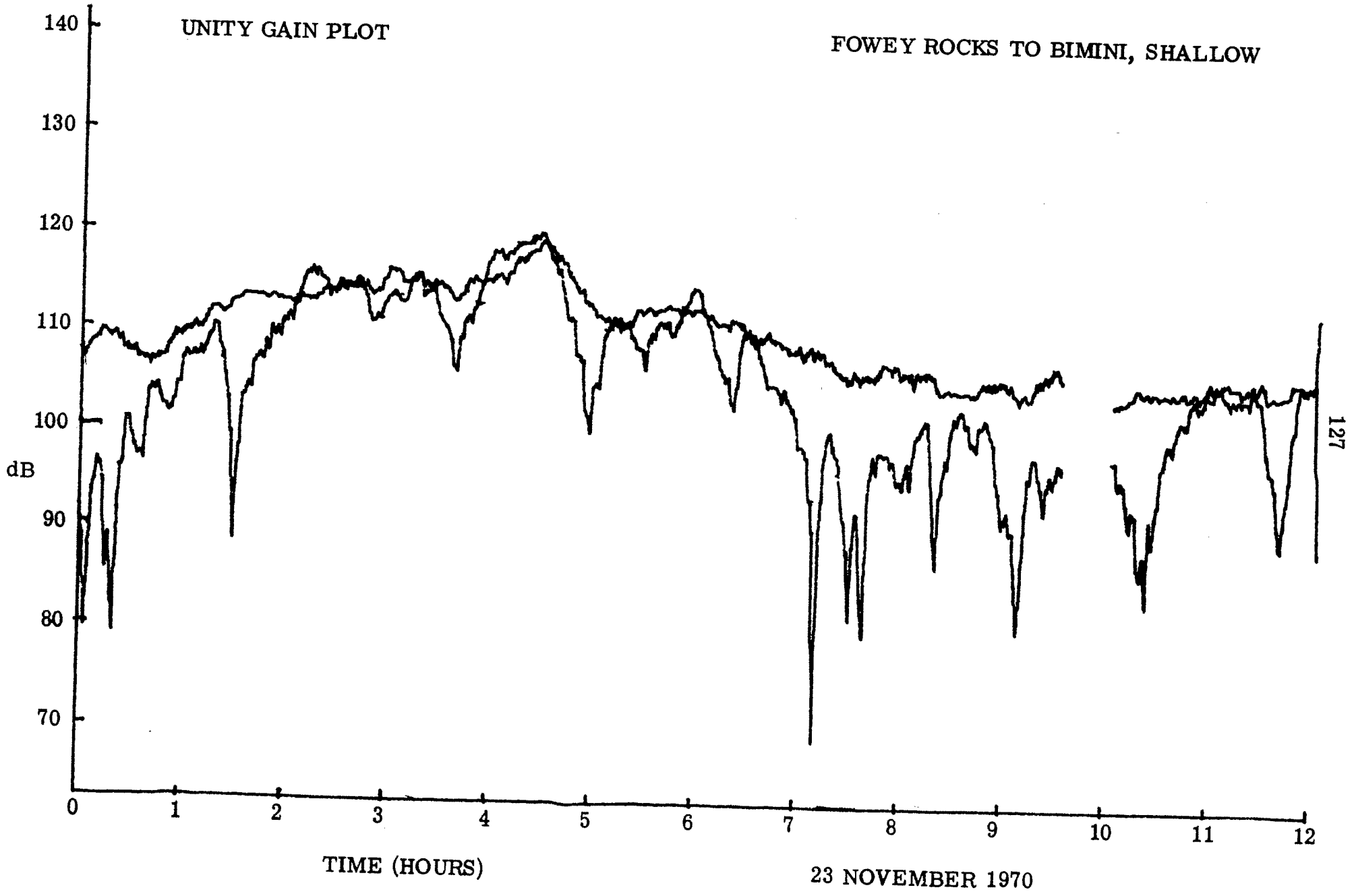
UNITY GAIN PLOT
FOWEY ROCKS TO BIMINI, SHALLOW
140
130
120
110
100
90
80
70
dB
127
0
1
2
3
4
5
6
7
8
9
10
11
12
TIME (HOURS)
23 NOVEMBER 1970

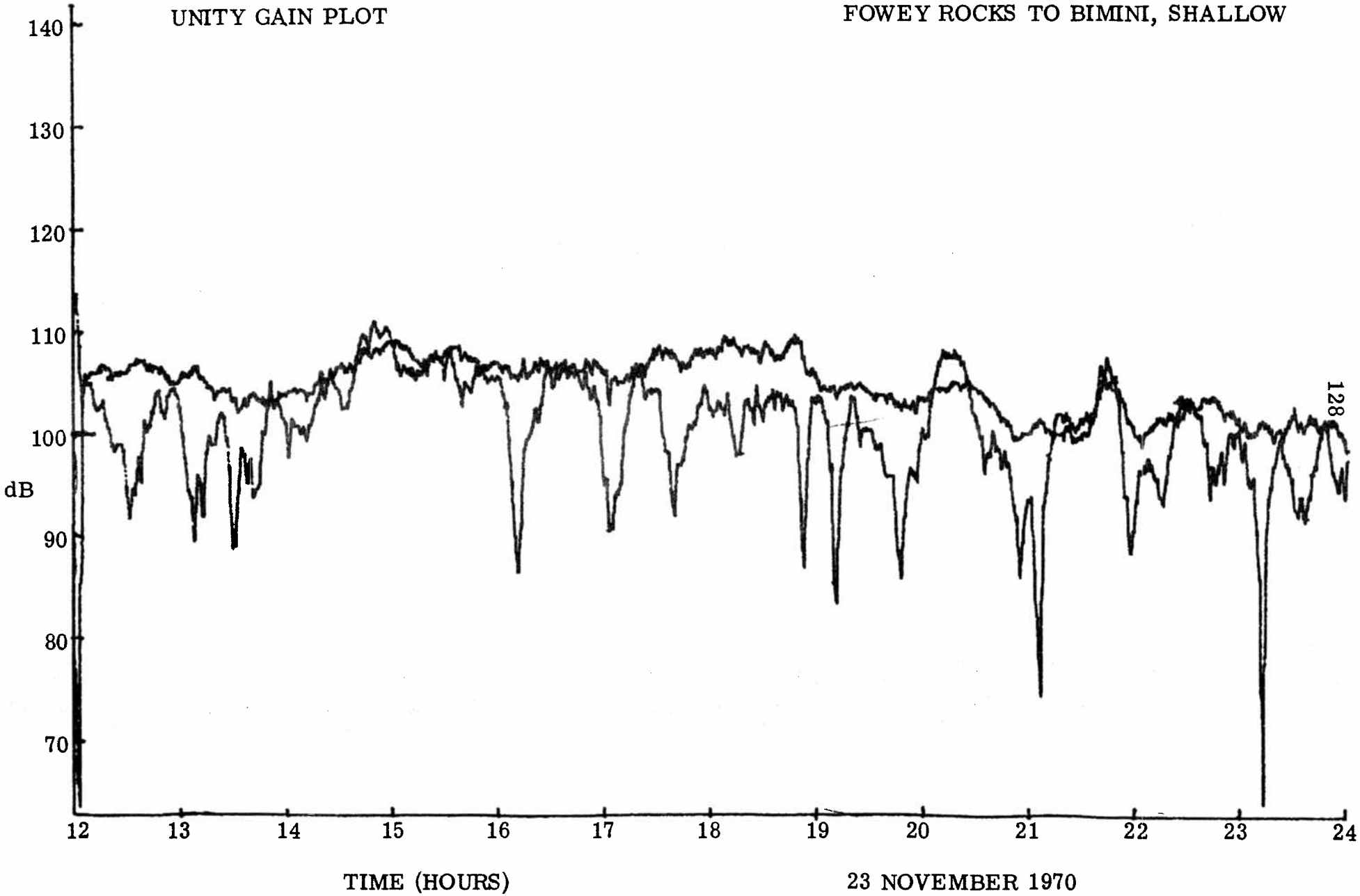
UNITY GAIN PLOT
FOWEY ROCKS TO BIMINI, SHALLOW
140
130
120
110
100
90
80
70
dB
128
12
13
14
15
16
17
18
19
20
21
22
23
24
TIME (HOURS)
23 NOVEMBER 1970

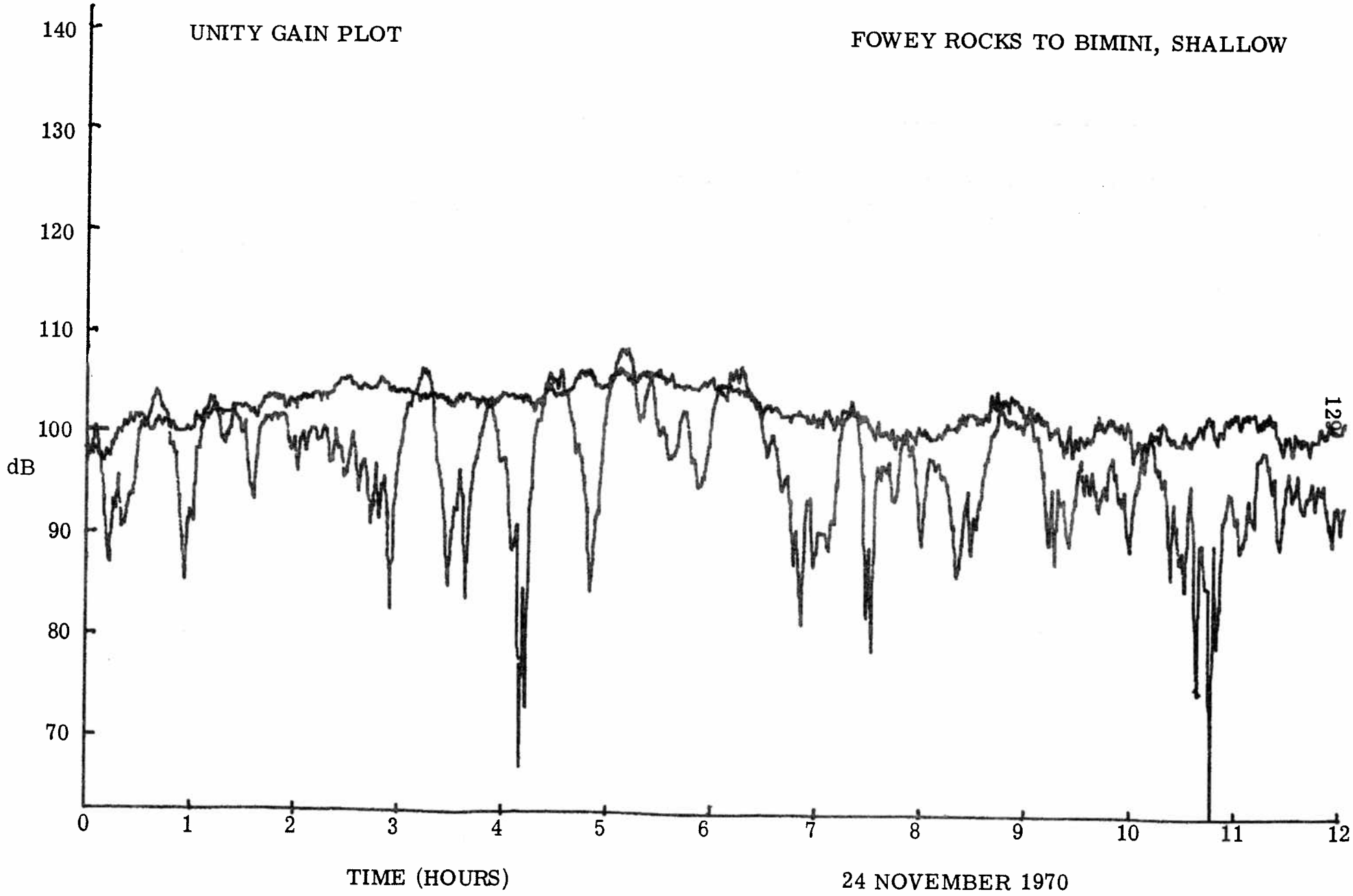
UNITY GAIN PLOT
FOWEY ROCKS TO BIMINI, SHALLOW
140
130
120
110
100
90
80
70
dB
0
1
2
3
4
5
6
7
8
9
10
11
12
TIME (HOURS)
24 NOVEMBER 1970
126

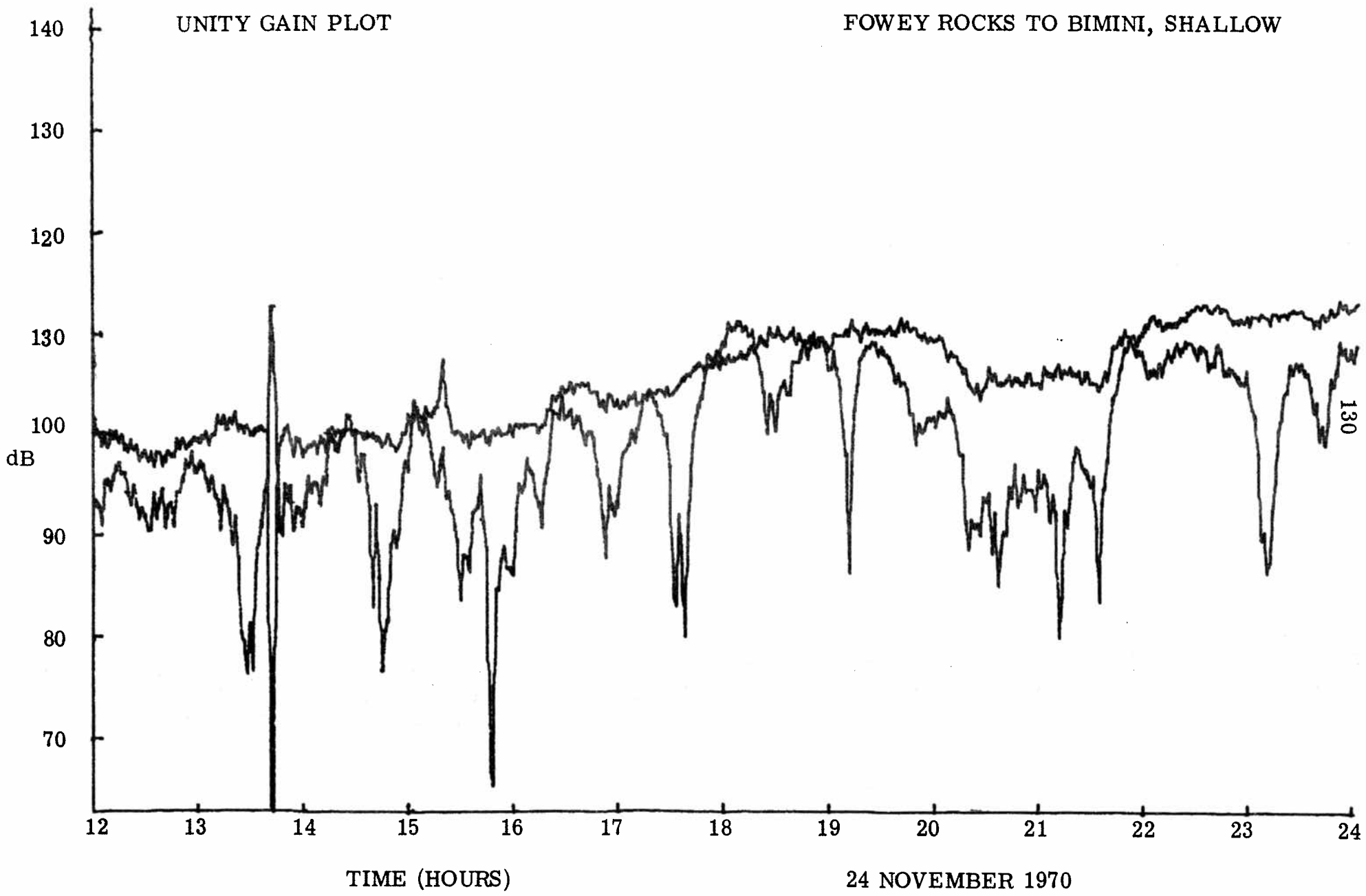
UNITY GAIN PLOT
FOWEY ROCKS TO BIMINI, SHALLOW
140
130
120
130
100
dB
90
80
70
130
12
13
14
15
16
17
18
19
20
21
22
23
24
TIME (HOURS)
24 NOVEMBER 1970

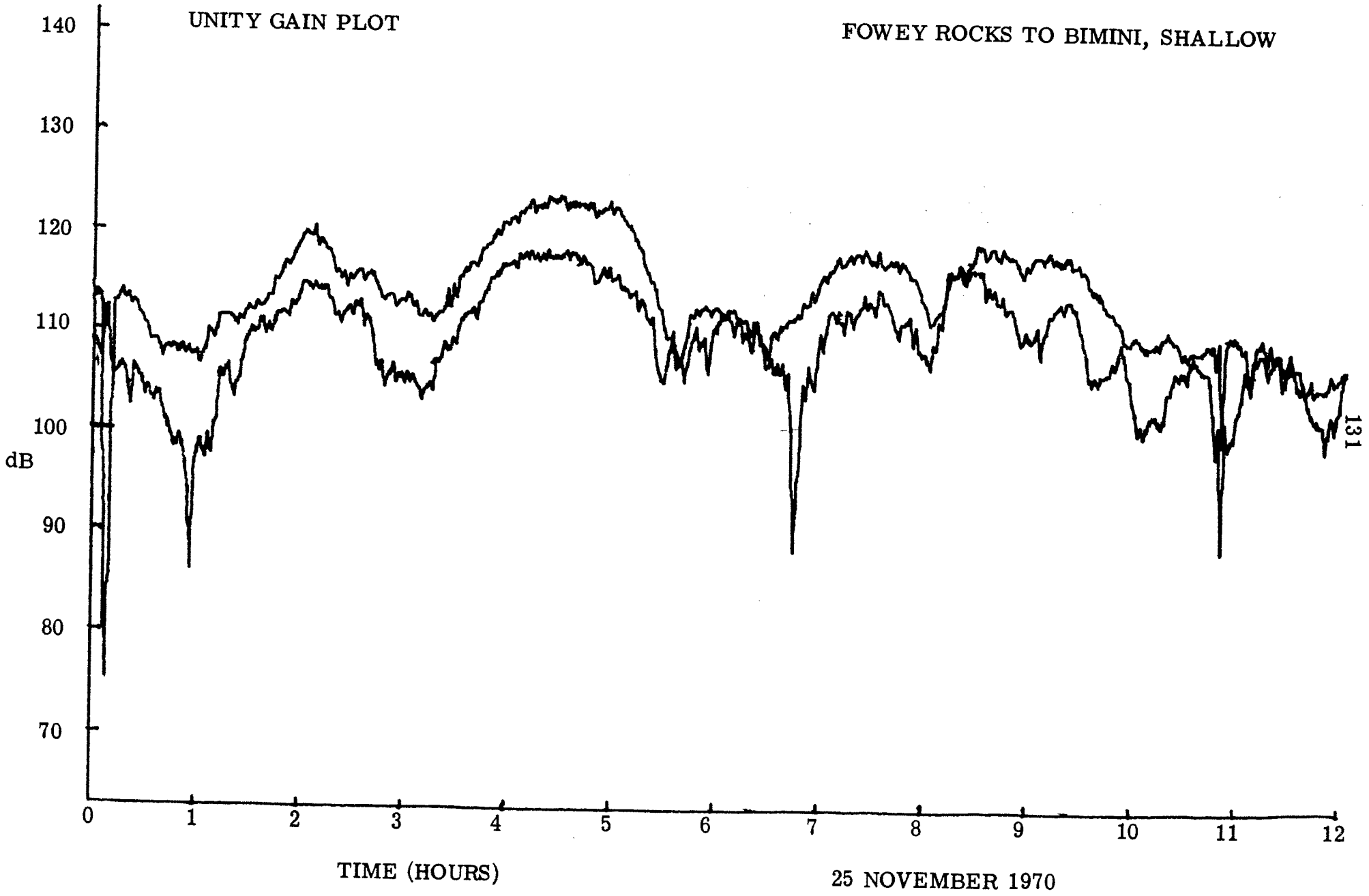
UNITY GAIN PLOT
FOWEY ROCKS TO BIMINI, SHALLOW
140
130
120
110
100
90
80
70
dB
131
0
1
2
3
4
5
6
7
8
9
10
11
12
TIME (HOURS)
25 NOVEMBER 1970

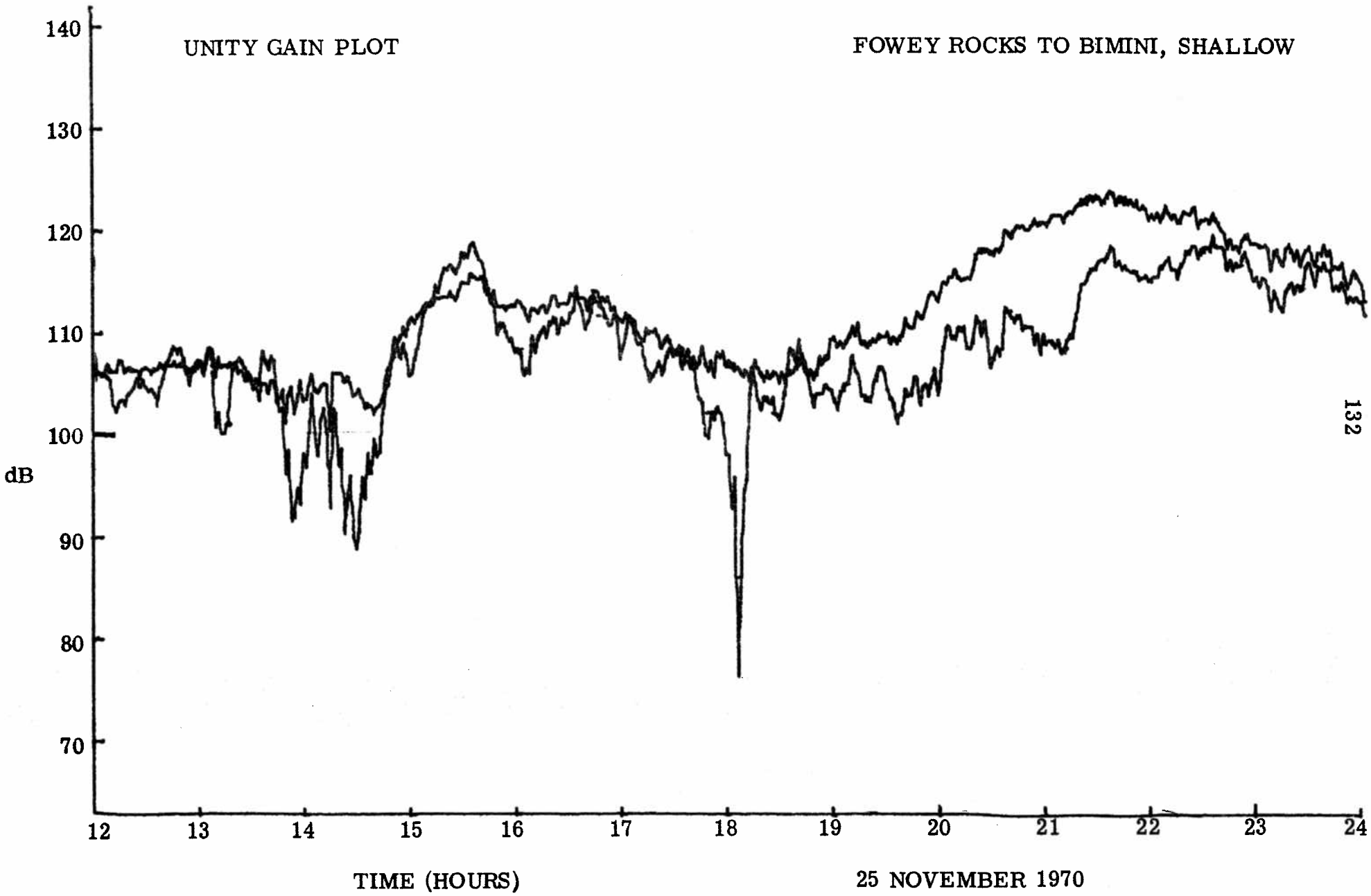
UNITY GAIN PLOT
FOWEY ROCKS TO BIMINI, SHALLOW
140
130
120
110
100
90
80
70
dB
132
12
13
14
15
16
17
18
19
20
21
22
23
24
TIME (HOURS)
25 NOVEMBER 1970

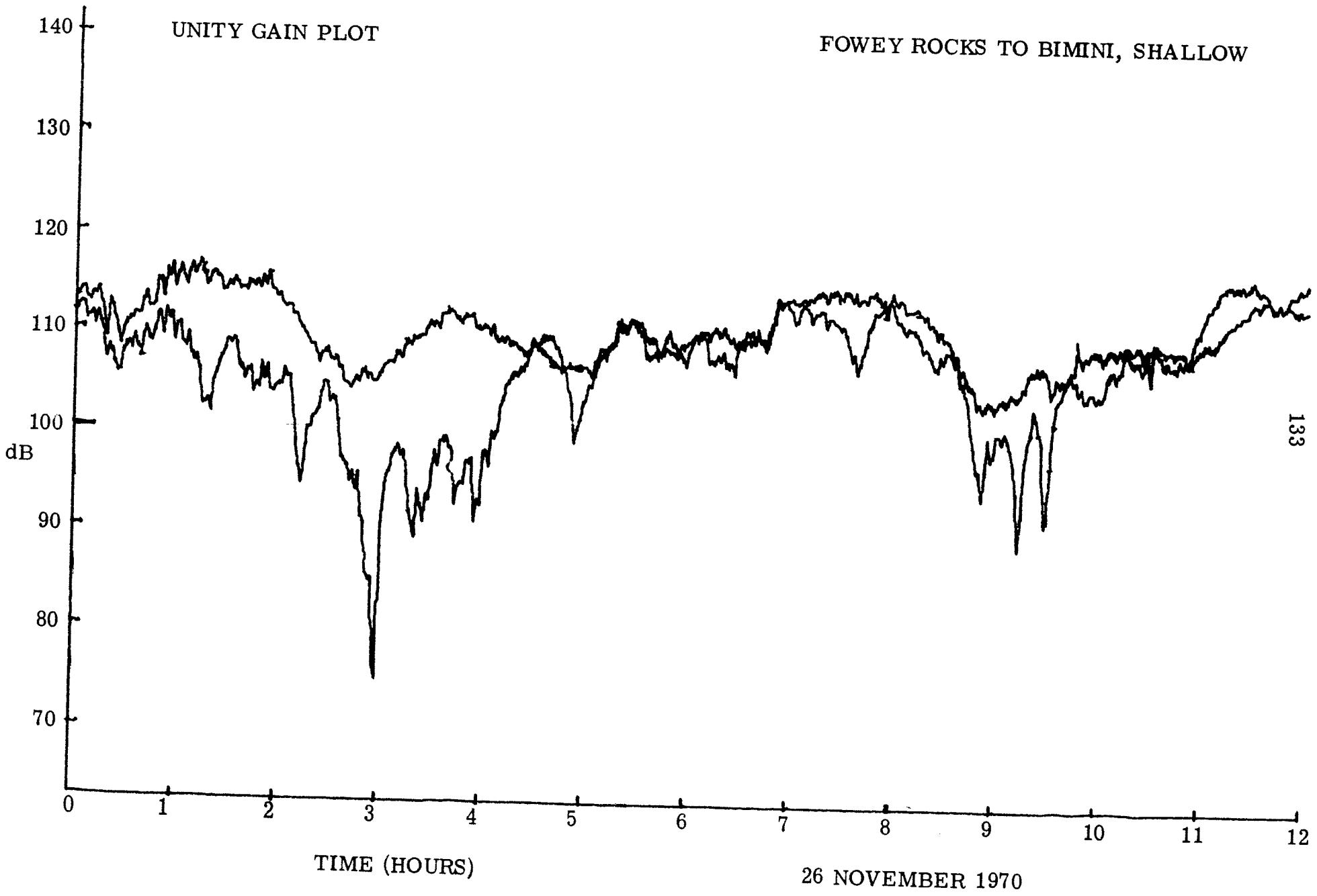
UNITY GAIN PLOT
FOWEY ROCKS TO BIMINI, SHALLOW
140
130
120
110
100
90
80
70
dB
133
0
1
2
3
4
5
6
7
8
9
10
11
12
TIME (HOURS)
26 NOVEMBER 1970

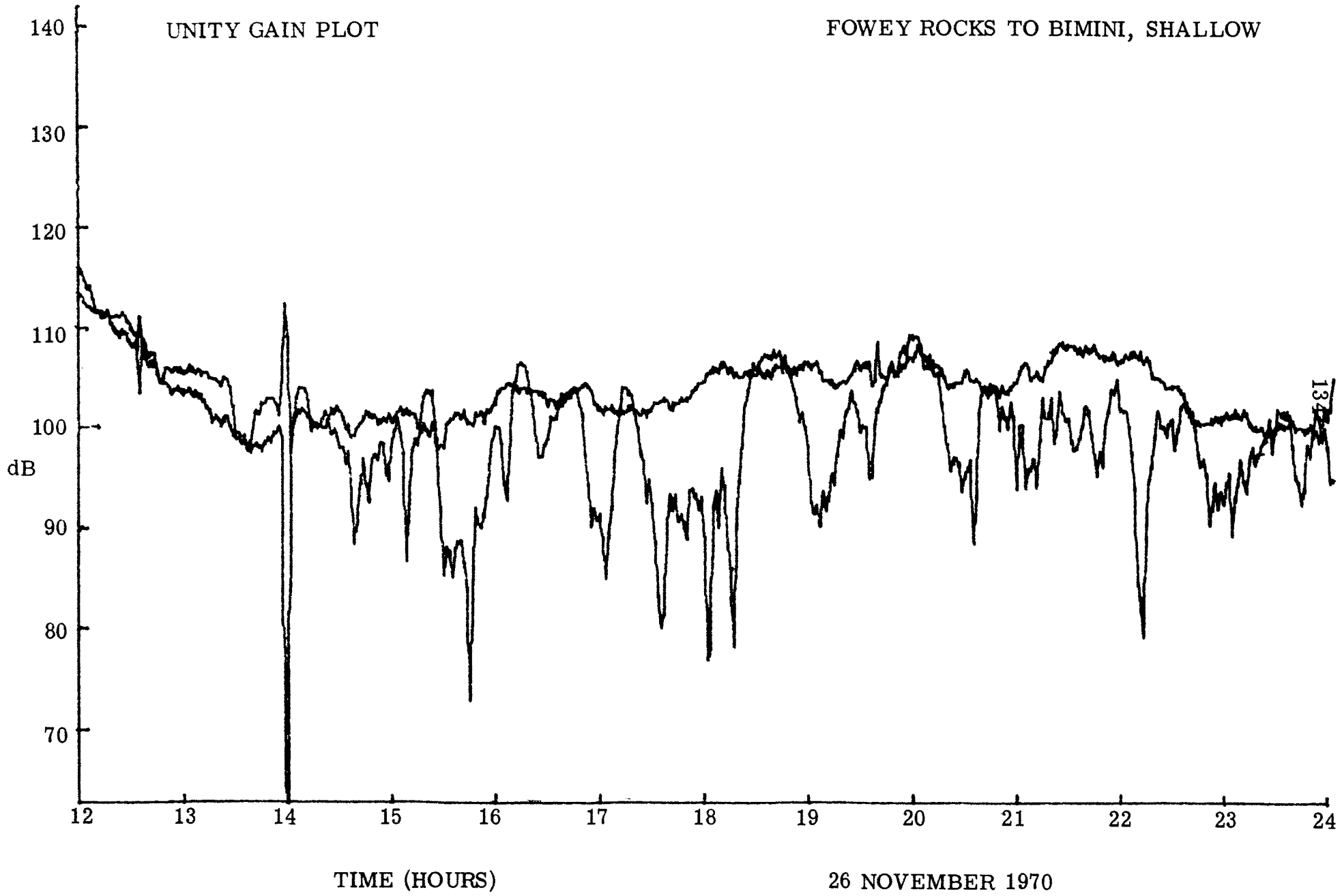
UNITY GAIN PLOT
FOWEY ROCKS TO BIMINI, SHALLOW
140
130
120
110
100
90
80
70
dB
134
12
13
14
15
16
17
18
19
20
21
22
23
24
TIME (HOURS)
26 NOVEMBER 1970

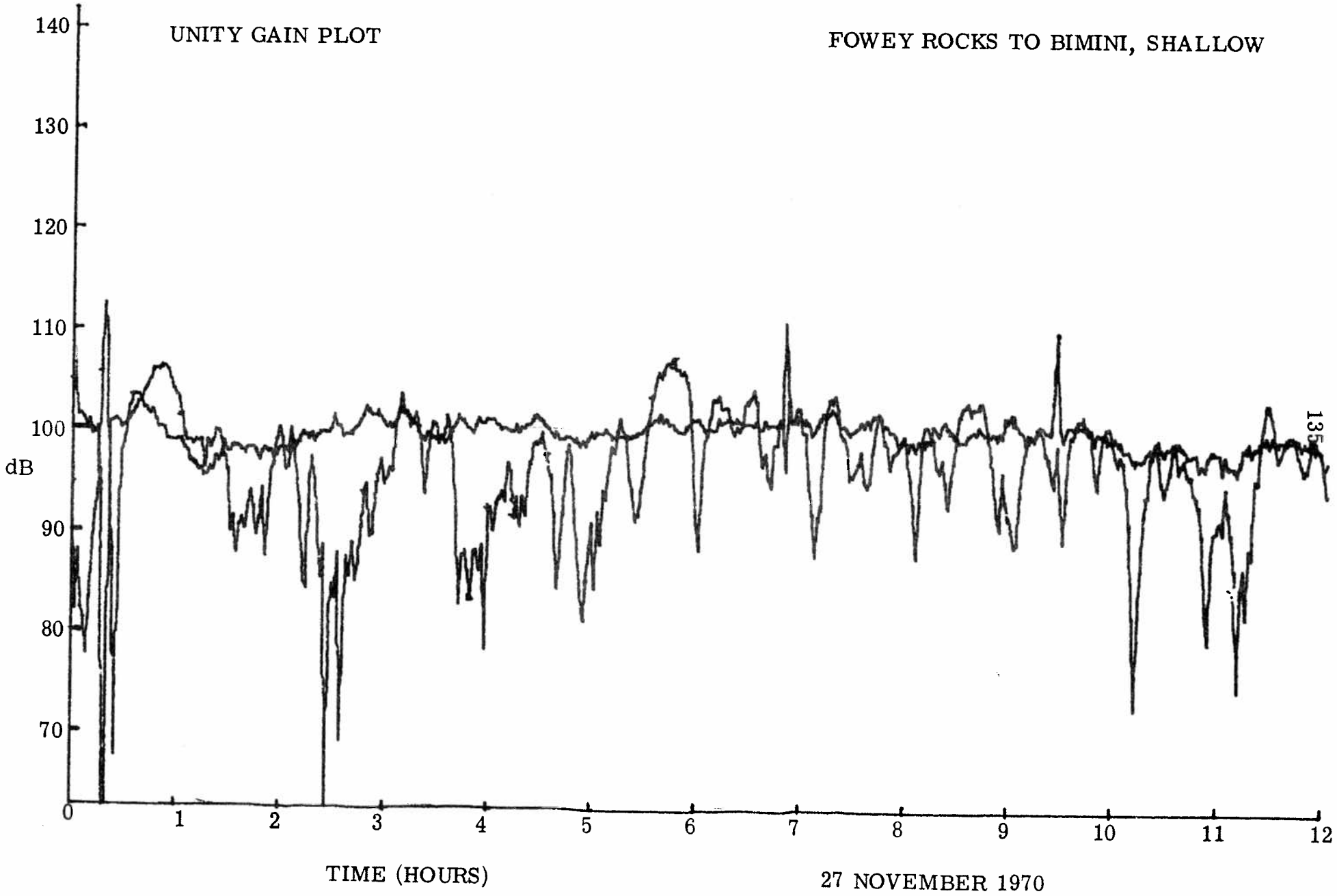
UNITY GAIN PLOT
FOWEY ROCKS TO BIMINI, SHALLOW
140
130
120
110
100
90
80
70
dB
0
1
2
3
4
5
6
7
8
9
10
11
12
135
TIME (HOURS)
27 NOVEMBER 1970

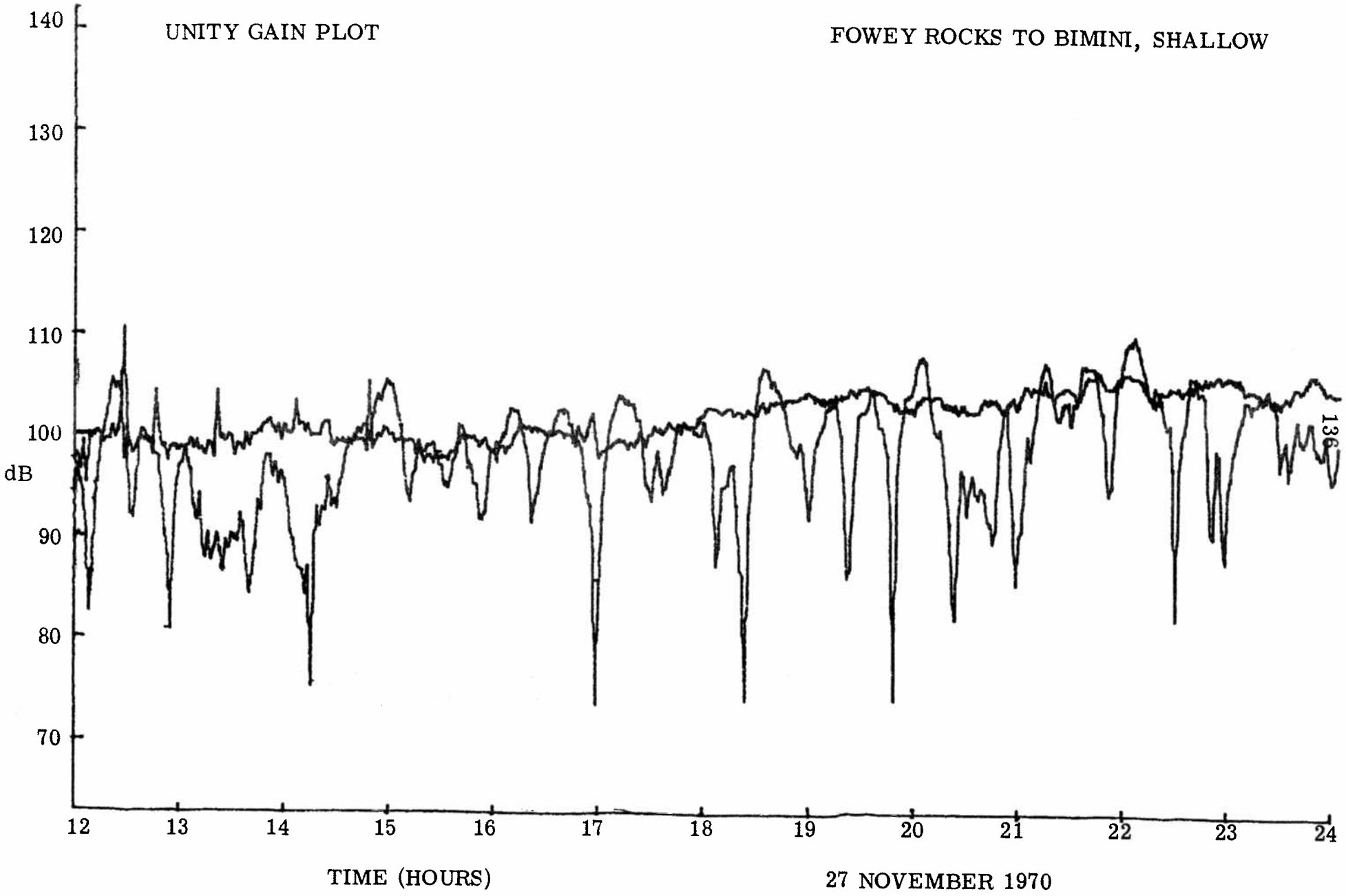
UNITY GAIN PLOT
FOWEY ROCKS TO BIMINI, SHALLOW
140
130
120
110
100
90
80
70
dB
136
12
13
14
15
16
17
18
19
20
21
22
23
24
TIME (HOURS)
27 NOVEMBER 1970

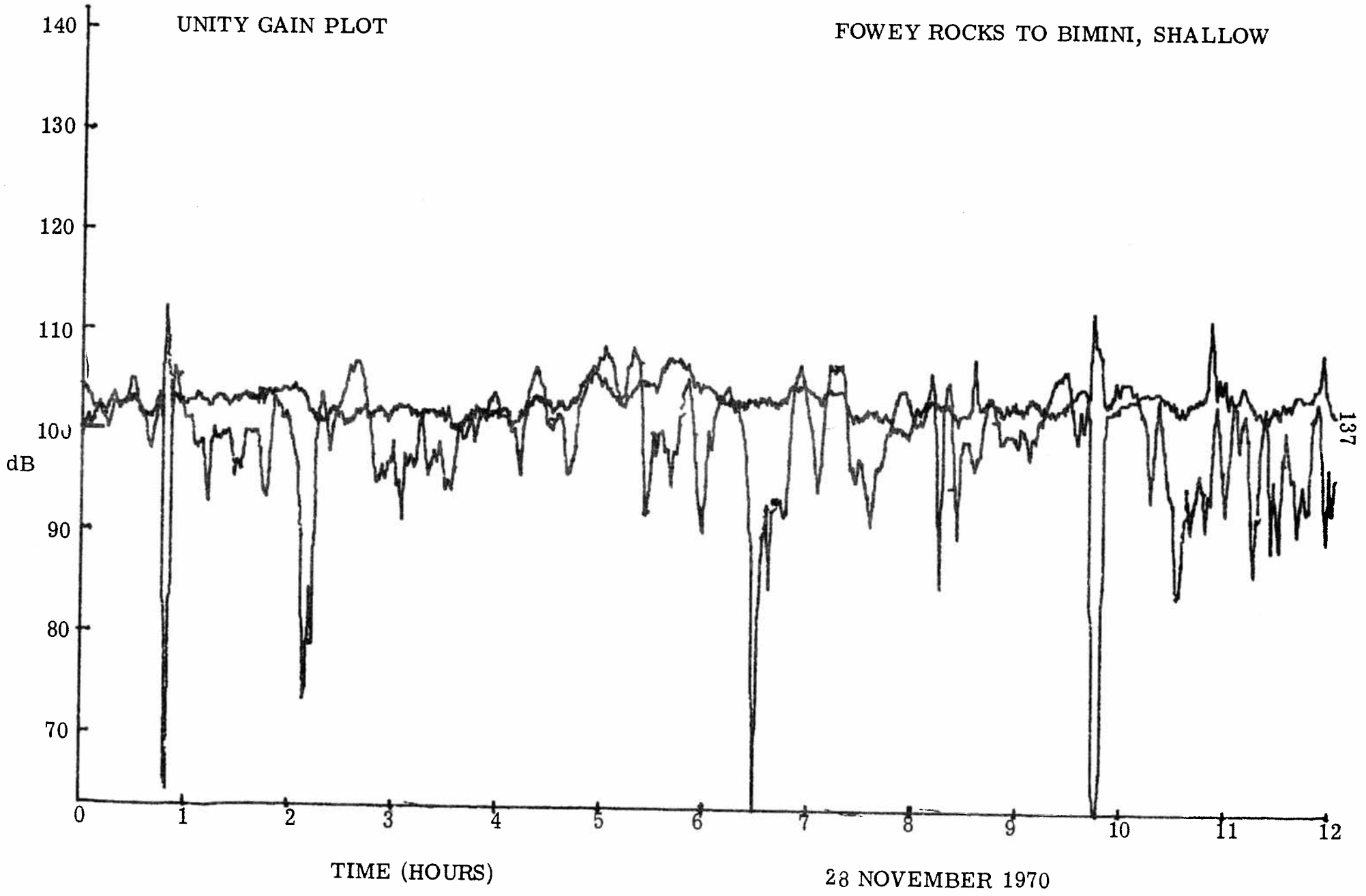
UNITY GAIN PLOT
FOWEY ROCKS TO BIMINI, SHALLOW
140
130
120
110
100
90
80
70
dB
137
0
1
2
3
4
5
6
7
8
9
10
11
12
TIME (HOURS)
28 NOVEMBER 1970

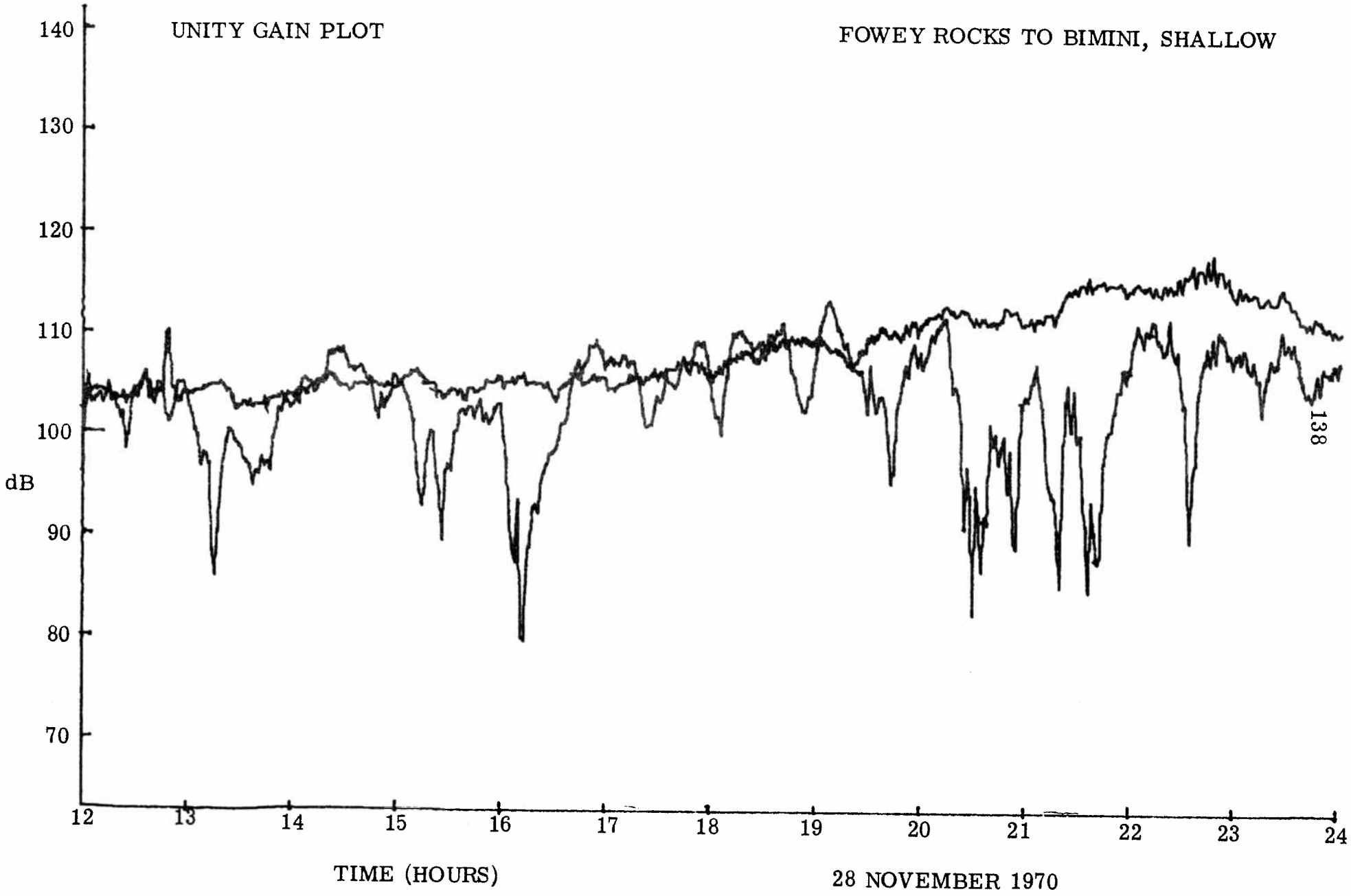
UNITY GAIN PLOT
FOWEY ROCKS TO BIMINI, SHALLOW
140
130
120
110
100
90
80
70
dB
138
12
13
14
15
16
17
18
19
20
21
22
23
24
TIME (HOURS)
28 NOVEMBER 1970

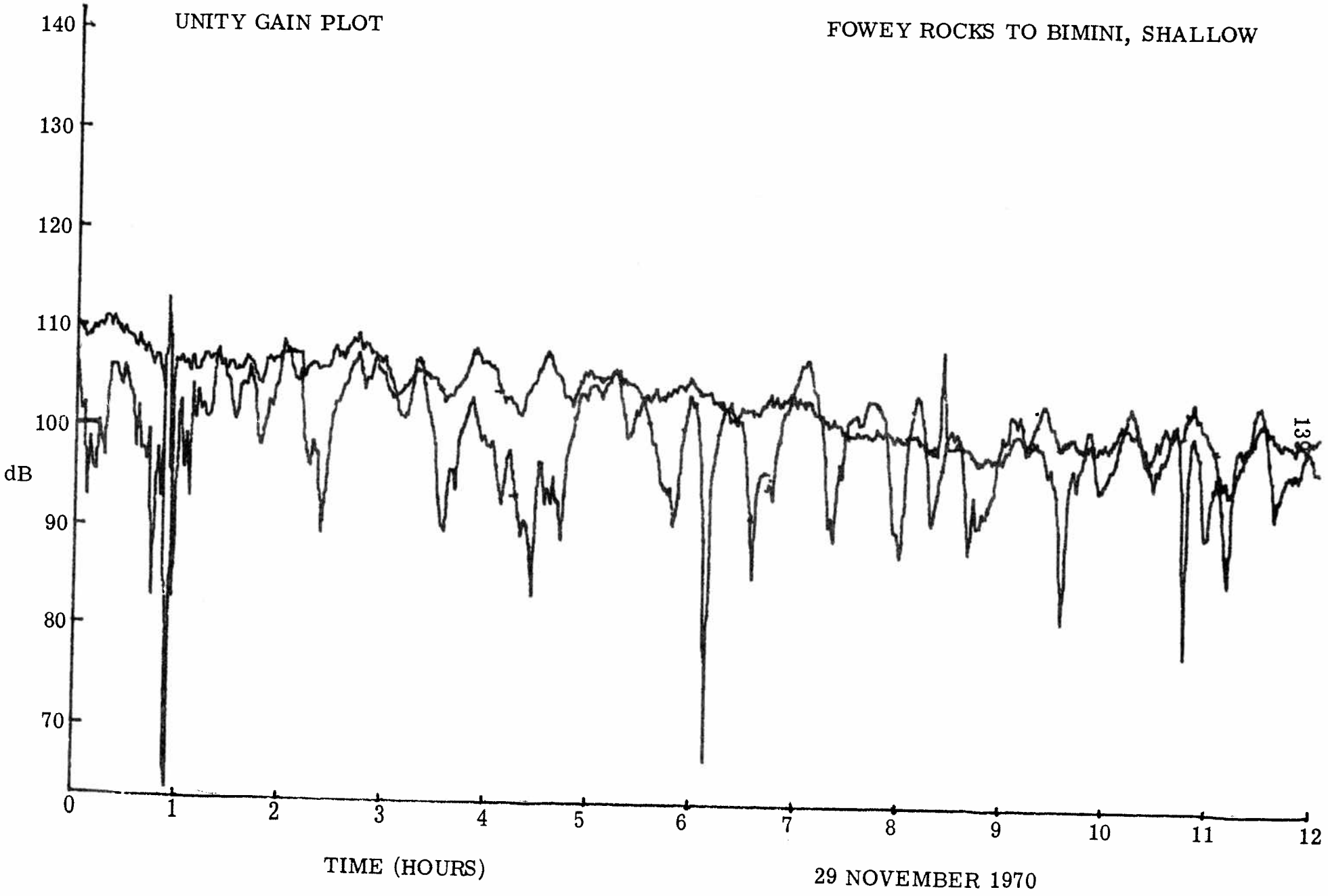
UNITY GAIN PLOT
FOWEY ROCKS TO BIMINI, SHALLOW
140
130
120
110
100
90
80
70
dB
0
1
2
3
4
5
6
7
8
9
10
11
12
TIME (HOURS)
29 NOVEMBER 1970
138

APPENDIX C

Appendix C contains the constant gain x bandwidth plots of the carrier, sideband, reverb and noise powers from the 7-mile data.

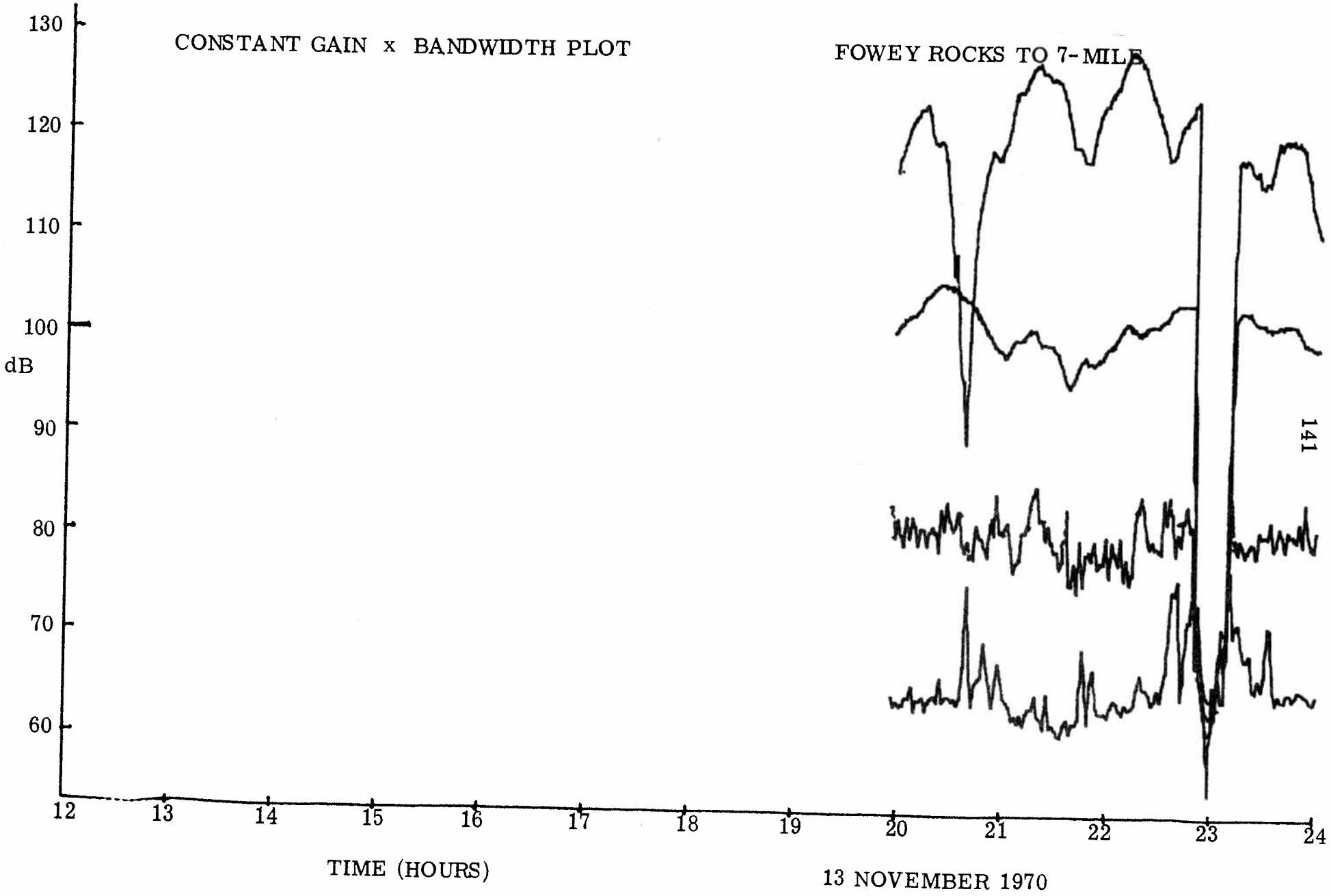
CONSTANT GAIN x BANDWIDTH PLOT
FOWEY ROCKS TO 7-MILE
130
120
110
100
dB
90
80
70
60
141
12
13
14
15
16
17
18
19
20
21
22
23
24
TIME (HOURS)
13 NOVEMBER 1970

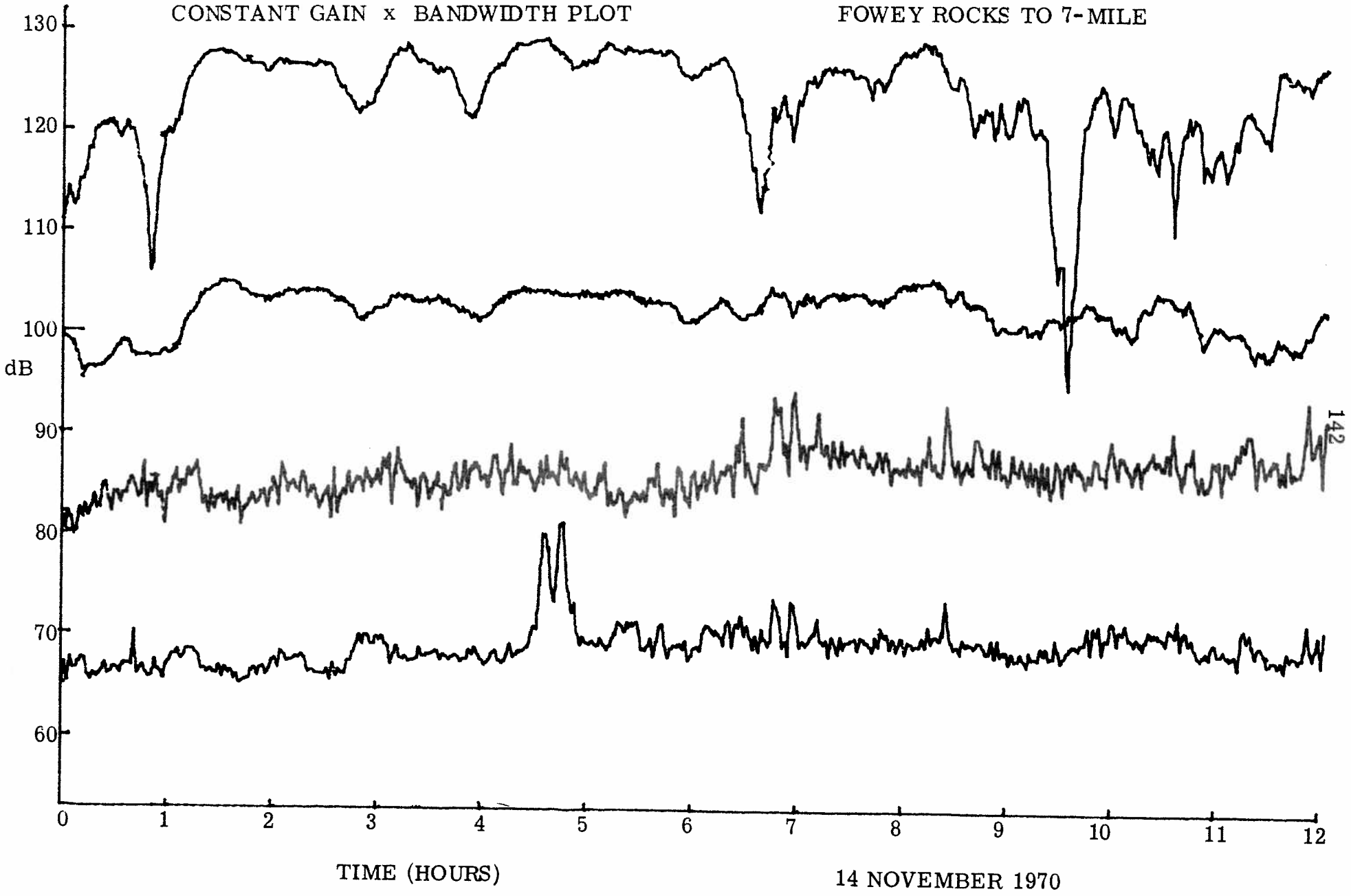
CONSTANT GAIN x BANDWIDTH PLOT
FOWEY ROCKS TO 7-MILE
130
120
110
100
dB
90
80
70
60
142
0
1
2
3
4
5
6
7
8
9
10
11
12
TIME (HOURS)
14 NOVEMBER 1970

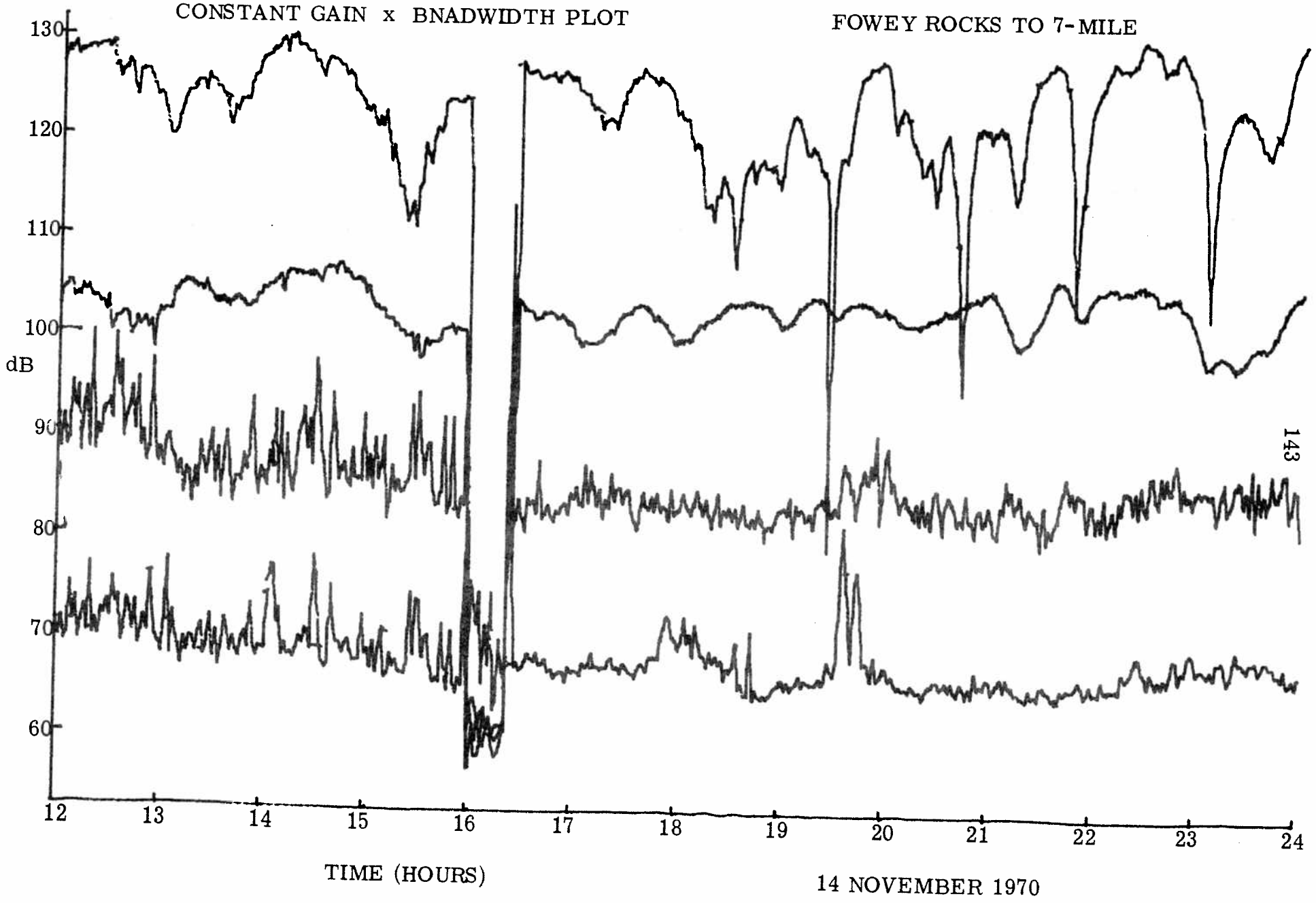
CONSTANT GAIN x BNADWIDTH PLOT
FOWEY ROCKS TO 7-MILE
130
120
110
100
dB
90
80
70
60
12
13
14
15
16
17
18
19
20
21
22
23
24
TIME (HOURS)
14 NOVEMBER 1970
143

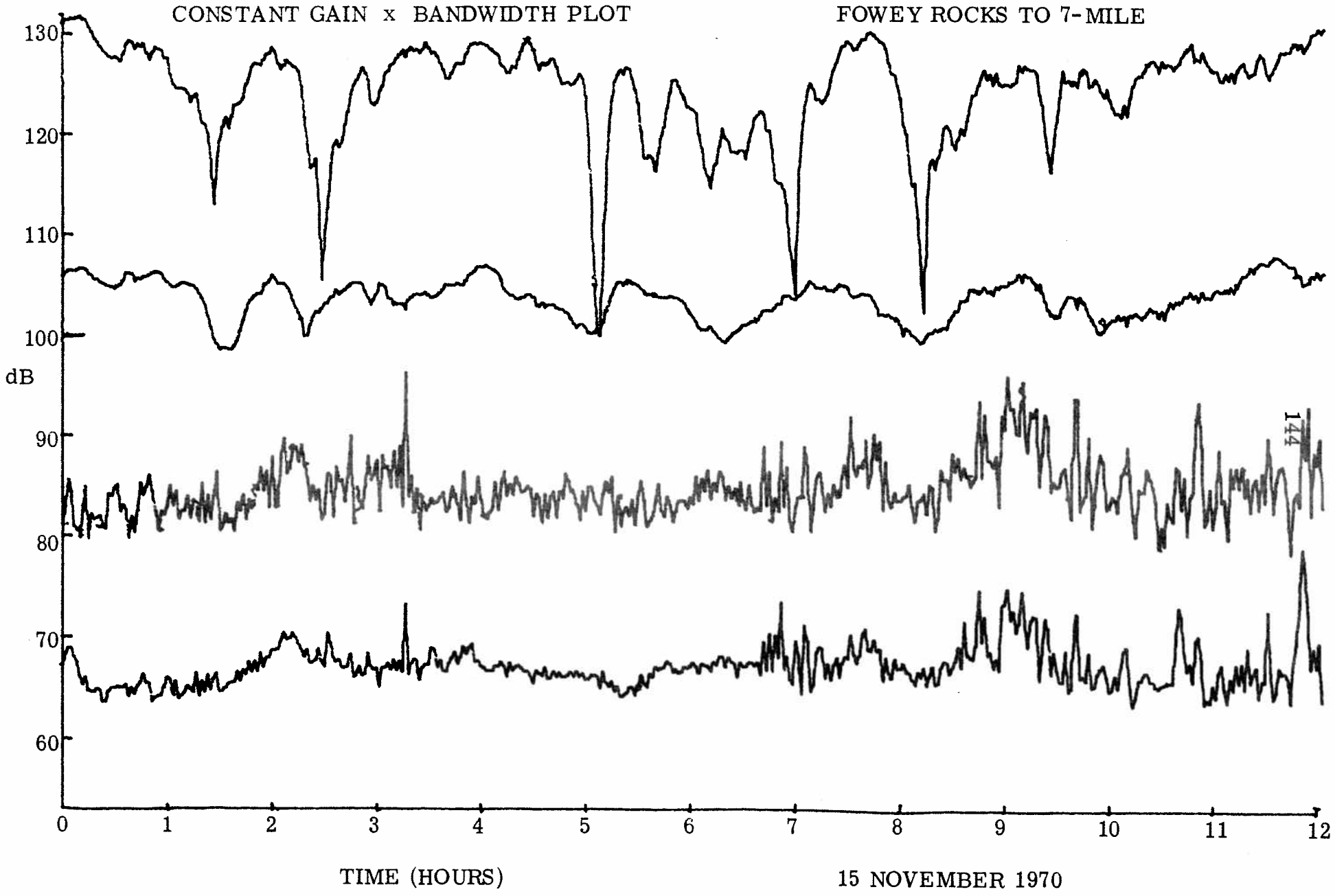
CONSTANT GAIN x BANDWIDTH PLOT
FOWEY ROCKS TO 7-MILE
130
120
110
100
dB
90
80
70
60
144
0
1
2
3
4
5
6
7
8
9
10
11
12
TIME (HOURS)
15 NOVEMBER 1970

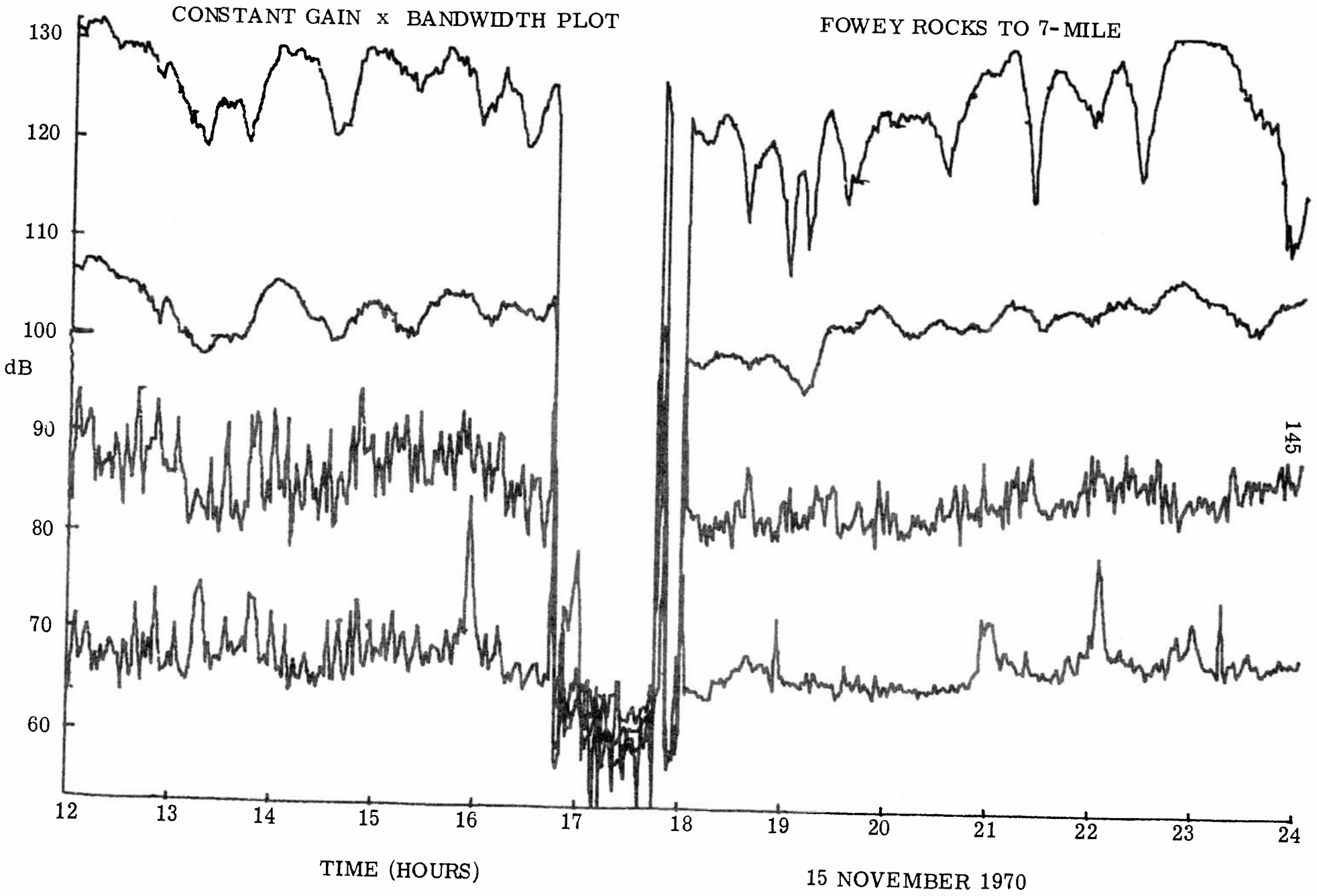
CONSTANT GAIN x BANDWIDTH PLOT
FOWEY ROCKS TO 7-MILE
130
120
110
100
dB
90
80
70
60
145
12
13
14
15
16
17
18
19
20
21
22
23
24
TIME (HOURS)
15 NOVEMBER 1970

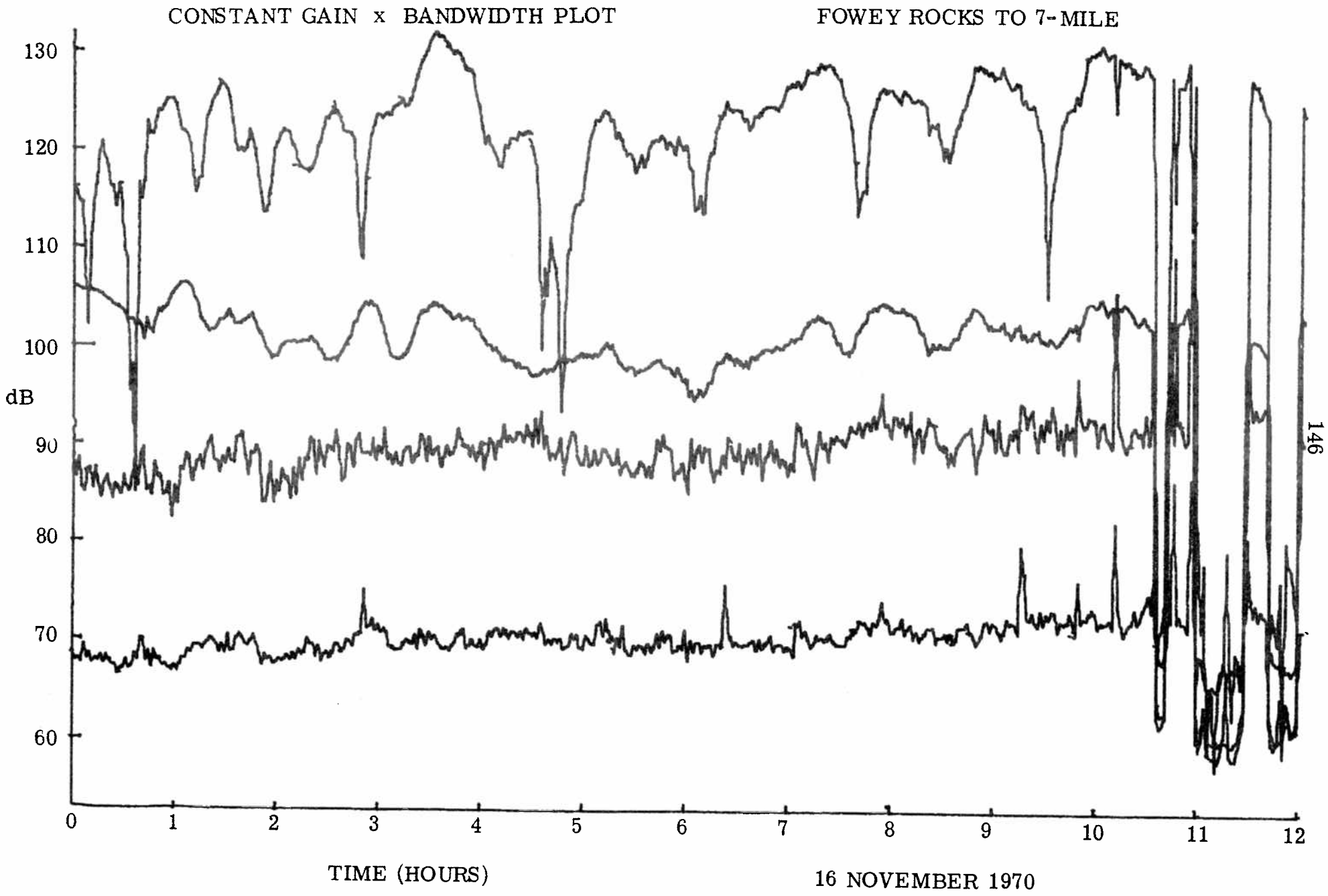
CONSTANT GAIN x BANDWIDTH PLOT
FOWEY ROCKS TO 7-MILE
130
120
110
100
dB
90
80
70
60
0
1
2
3
4
5
6
7
8
9
10
11
12
TIME (HOURS)
16 NOVEMBER 1970
146

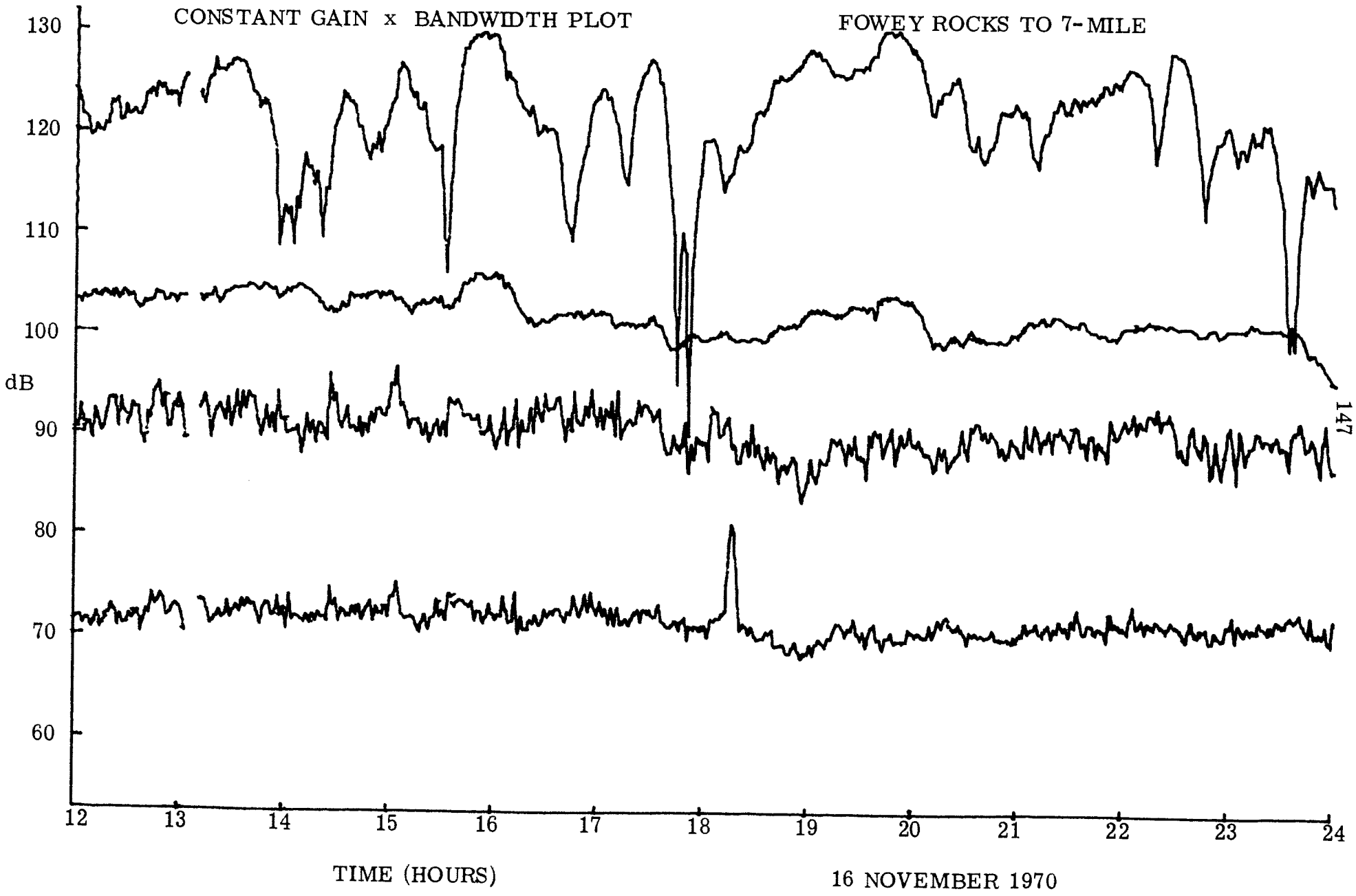
CONSTANT GAIN x BANDWIDTH PLOT
FOWEY ROCKS TO 7-MILE
130
120
110
100
dB
90
80
70
60
147
12
13
14
15
16
17
18
19
20
21
22
23
24
TIME (HOURS)
16 NOVEMBER 1970

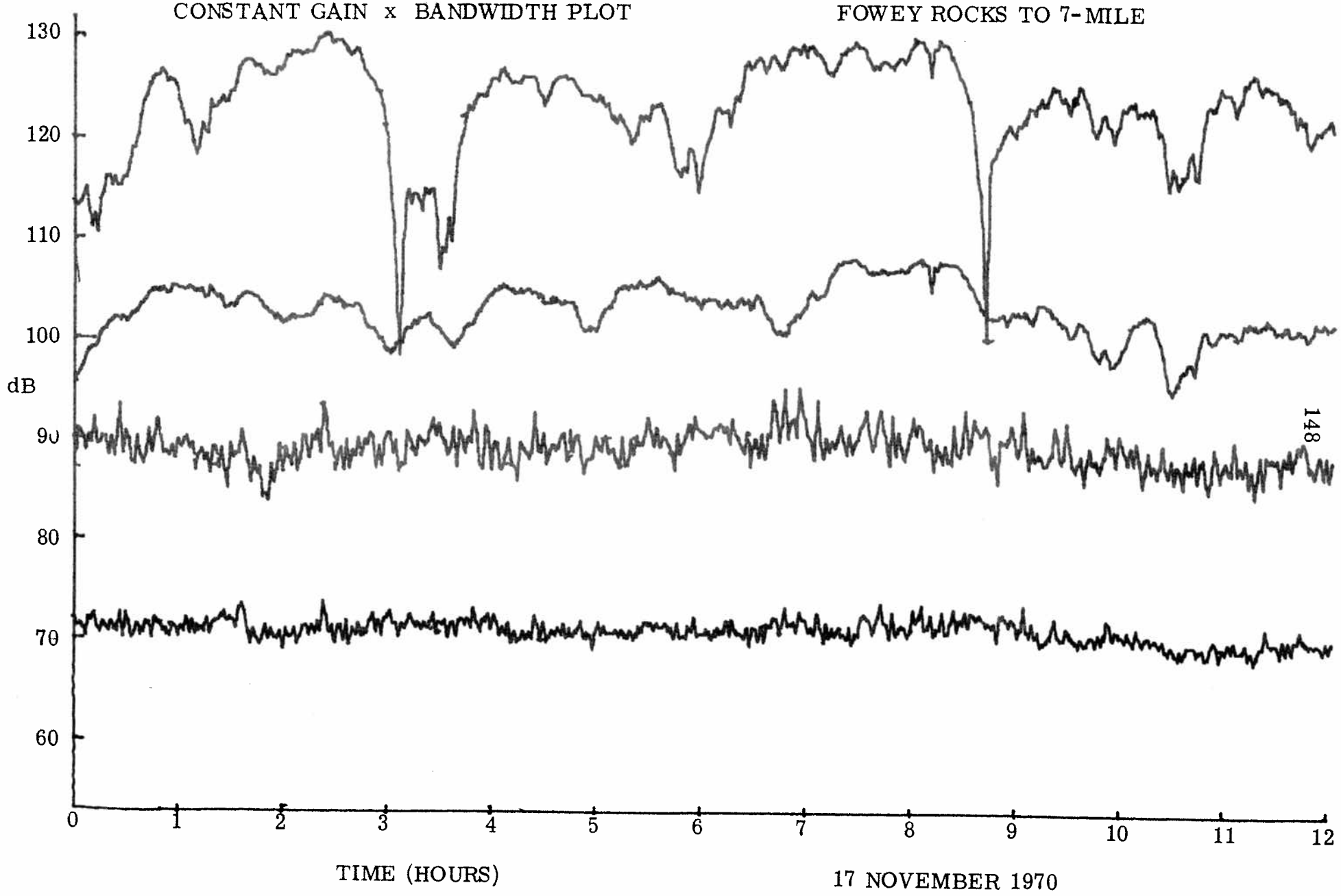
CONSTANT GAIN x BANDWIDTH PLOT
FOWEY ROCKS TO 7-MILE
130
120
110
100
dB
90
80
70
60
148
0
1
2
3
4
5
6
7
8
9
10
11
12
TIME (HOURS)
17 NOVEMBER 1970

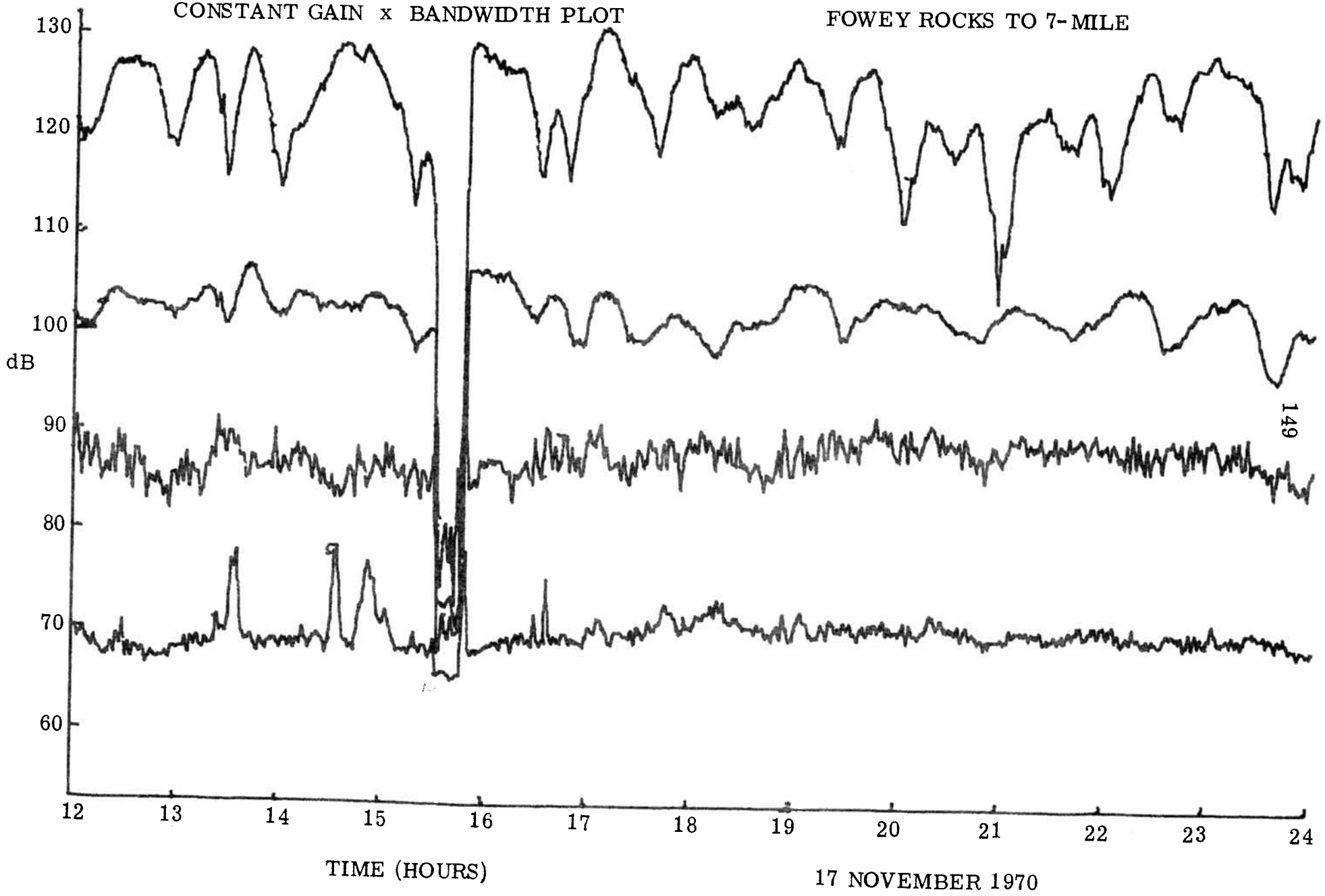
CONSTANT GAIN x BANDWIDTH PLOT
FOWEY ROCKS TO 7-MILE
130
120
110
100
dB
90
80
70
60
149
12
13
14
15
16
17
18
19
20
21
22
23
24
TIME (HOURS)
17 NOVEMBER 1970

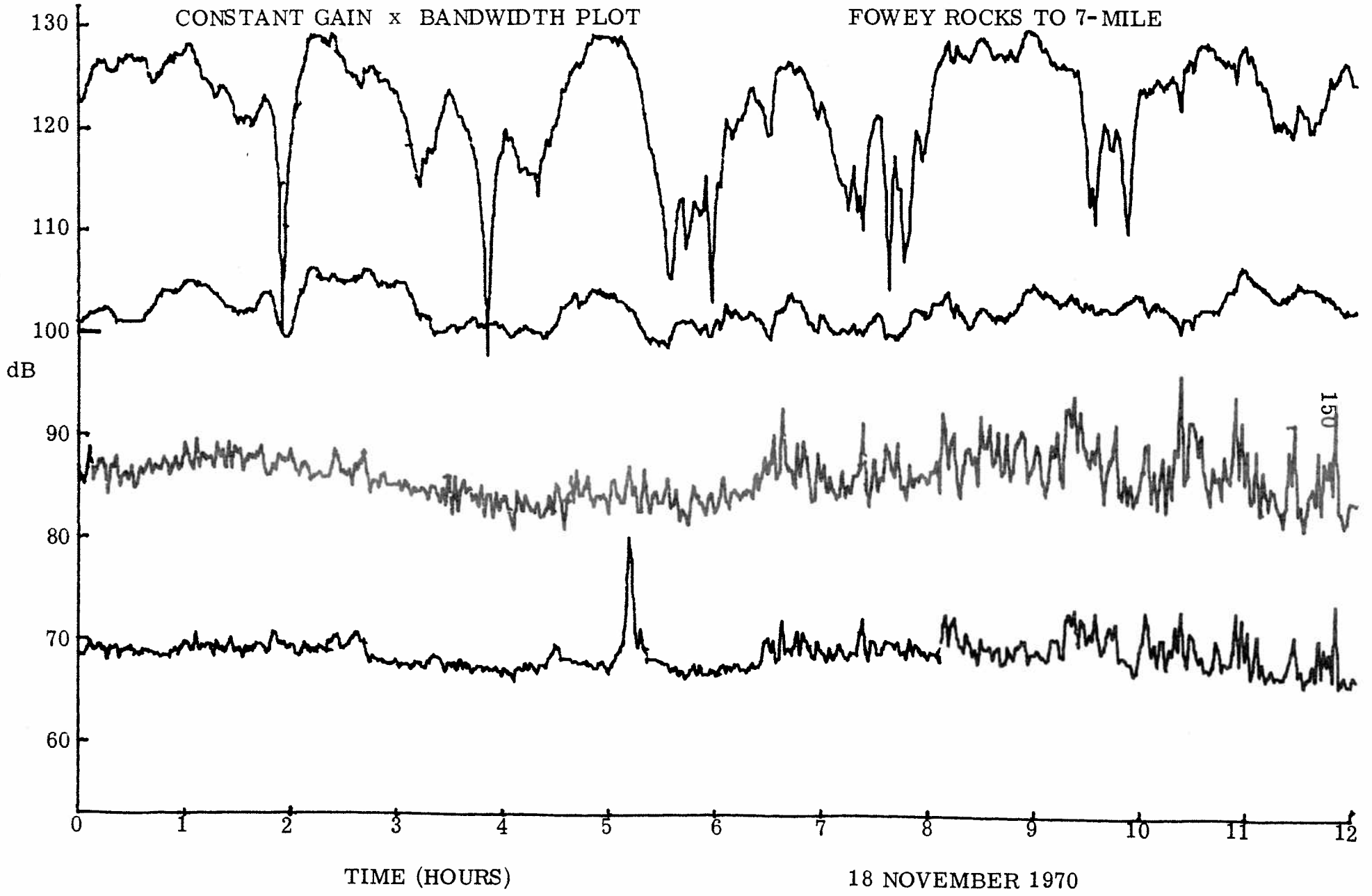
CONSTANT GAIN x BANDWIDTH PLOT
FOWEY ROCKS TO 7-MILE
130
120
110
100
dB
90
80
70
60
150
0
1
2
3
4
5
6
7
8
9
10
11
12
TIME (HOURS)
18 NOVEMBER 1970

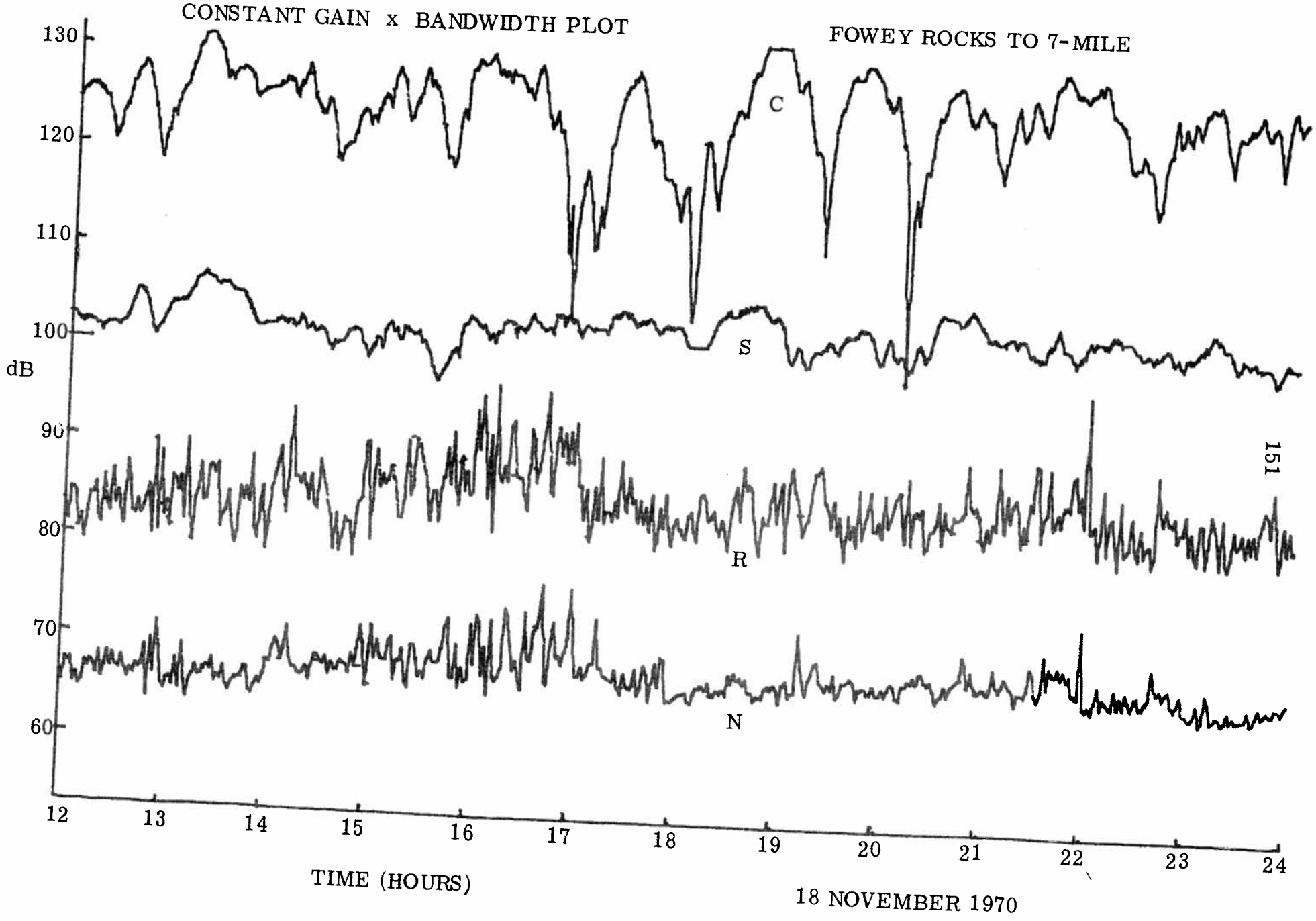
CONSTANT GAIN x BANDWIDTH PLOT
FOWEY ROCKS TO 7-MILE
130
120
110
100
dB
90
80
70
60
C
S
R
N
151
12
13
14
15
16
17
18
19
20
21
22
23
24
TIME (HOURS)
18 NOVEMBER 1970

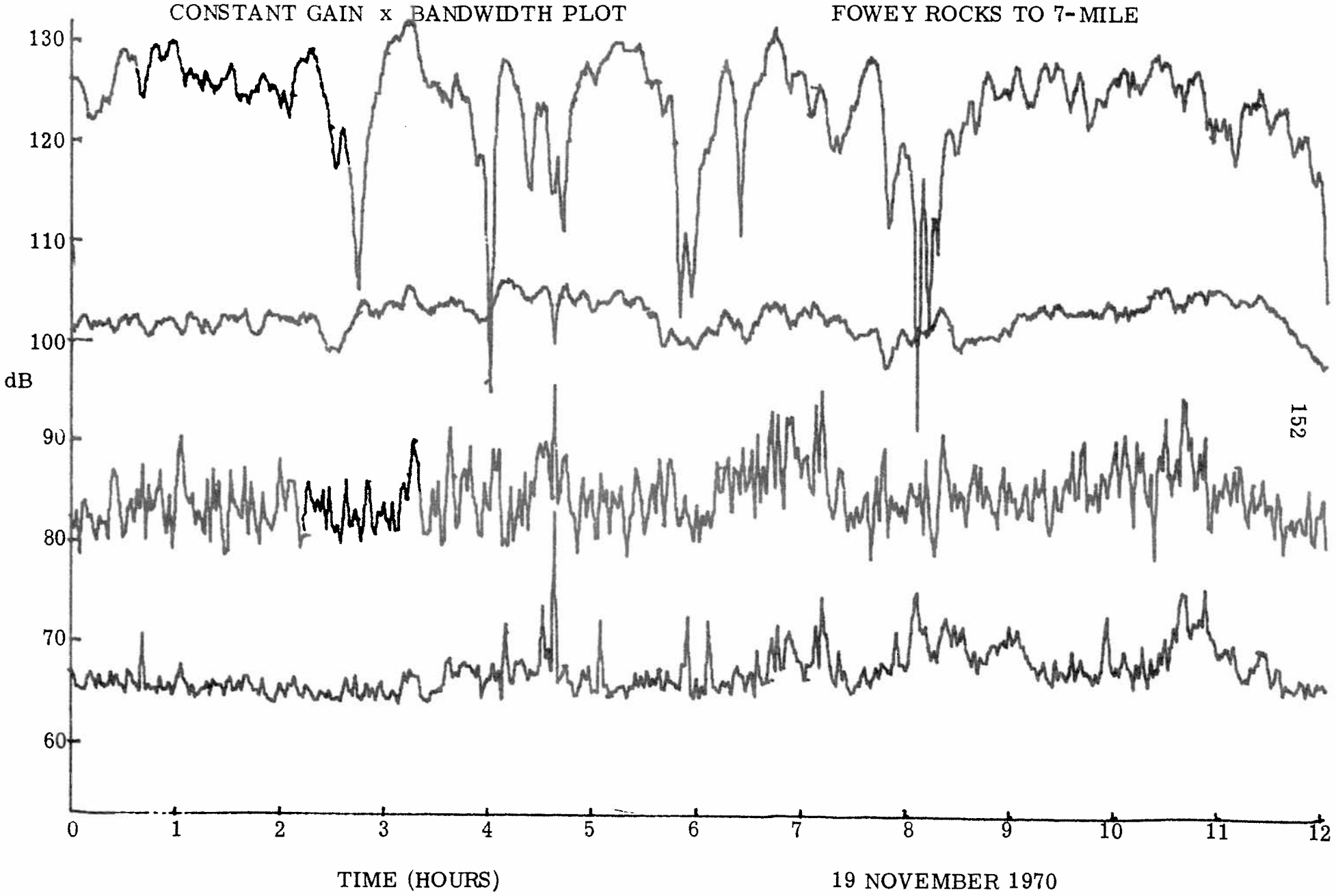
CONSTANT GAIN x BANDWIDTH PLOT
FOWEY ROCKS TO 7-MILE
130
120
110
100
dB
90
80
70
60
0
1
2
3
4
5
6
7
8
9
10
11
12
TIME (HOURS)
19 NOVEMBER 1970
152

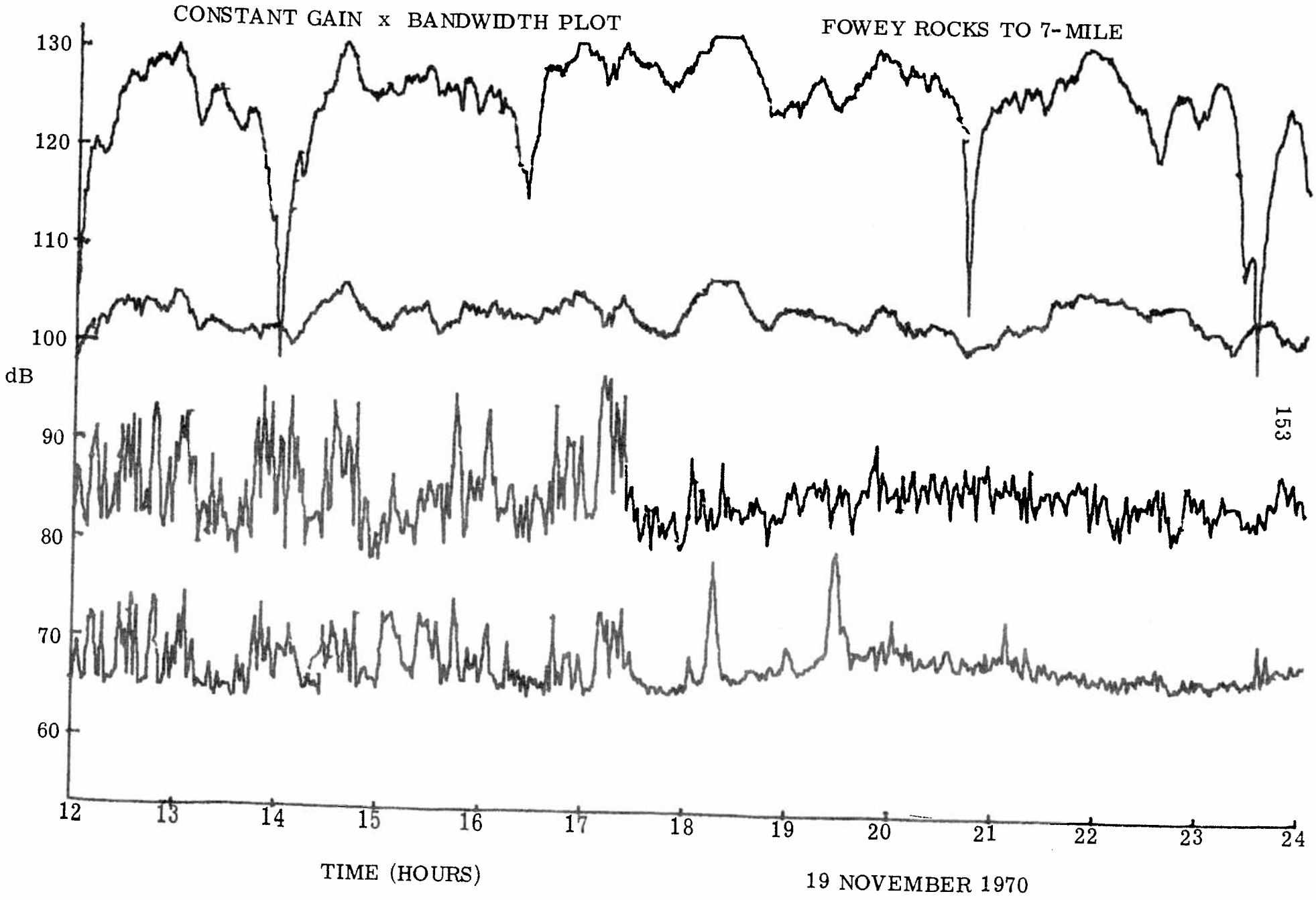
CONSTANT GAIN x BANDWIDTH PLOT
FOWEY ROCKS TO 7-MILE
130
120
110
100
dB
90
80
70
60
153
12
13
14
15
16
17
18
19
20
21
22
23
24
TIME (HOURS)
19 NOVEMBER 1970

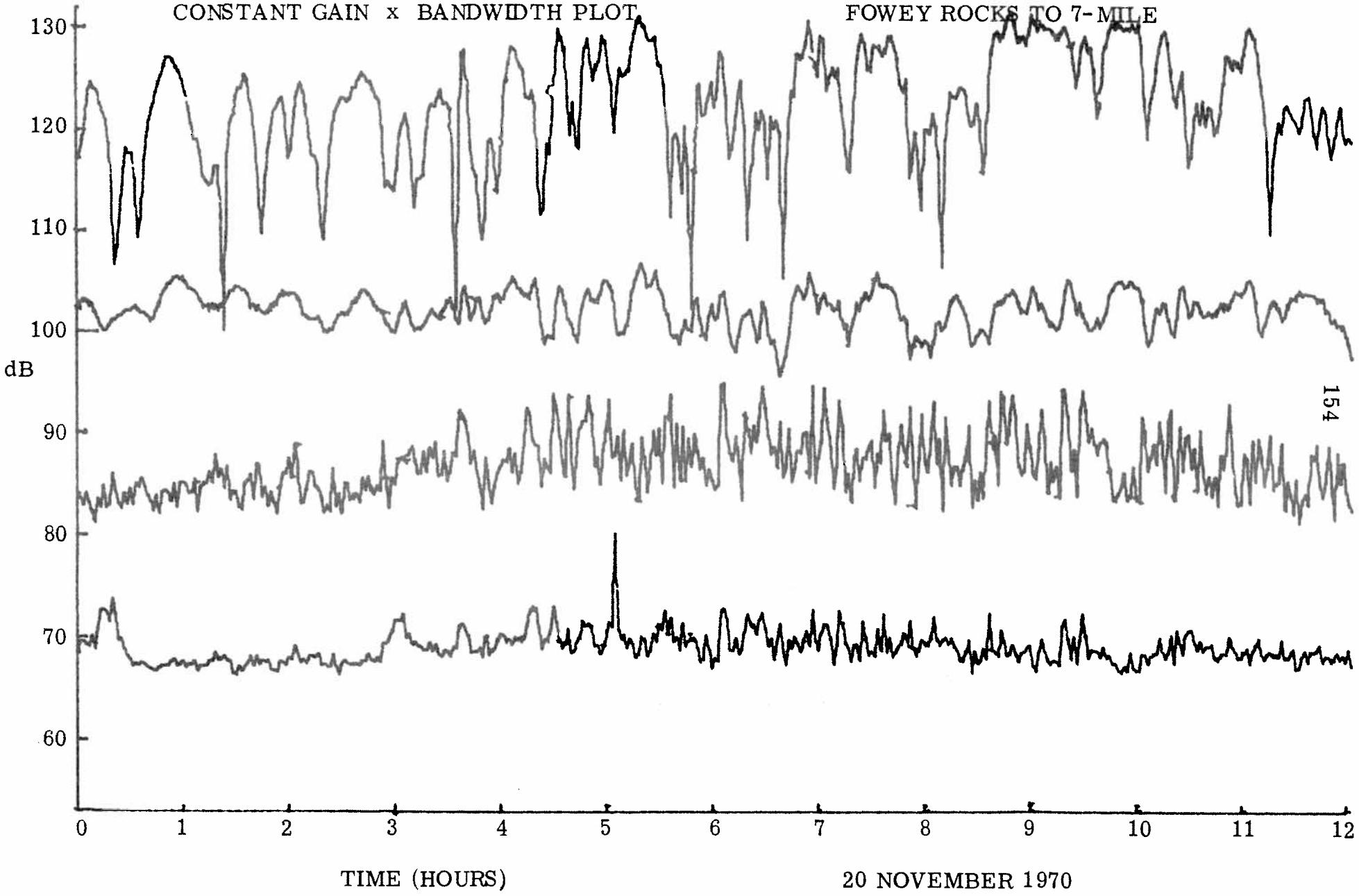
CONSTANT GAIN x BANDWIDTH PLOT
FOWEY ROCKS TO 7-MILE
130
120
110
100
dB
90
80
70
60
154
0
1
2
3
4
5
6
7
8
9
10
11
12
TIME (HOURS)
20 NOVEMBER 1970

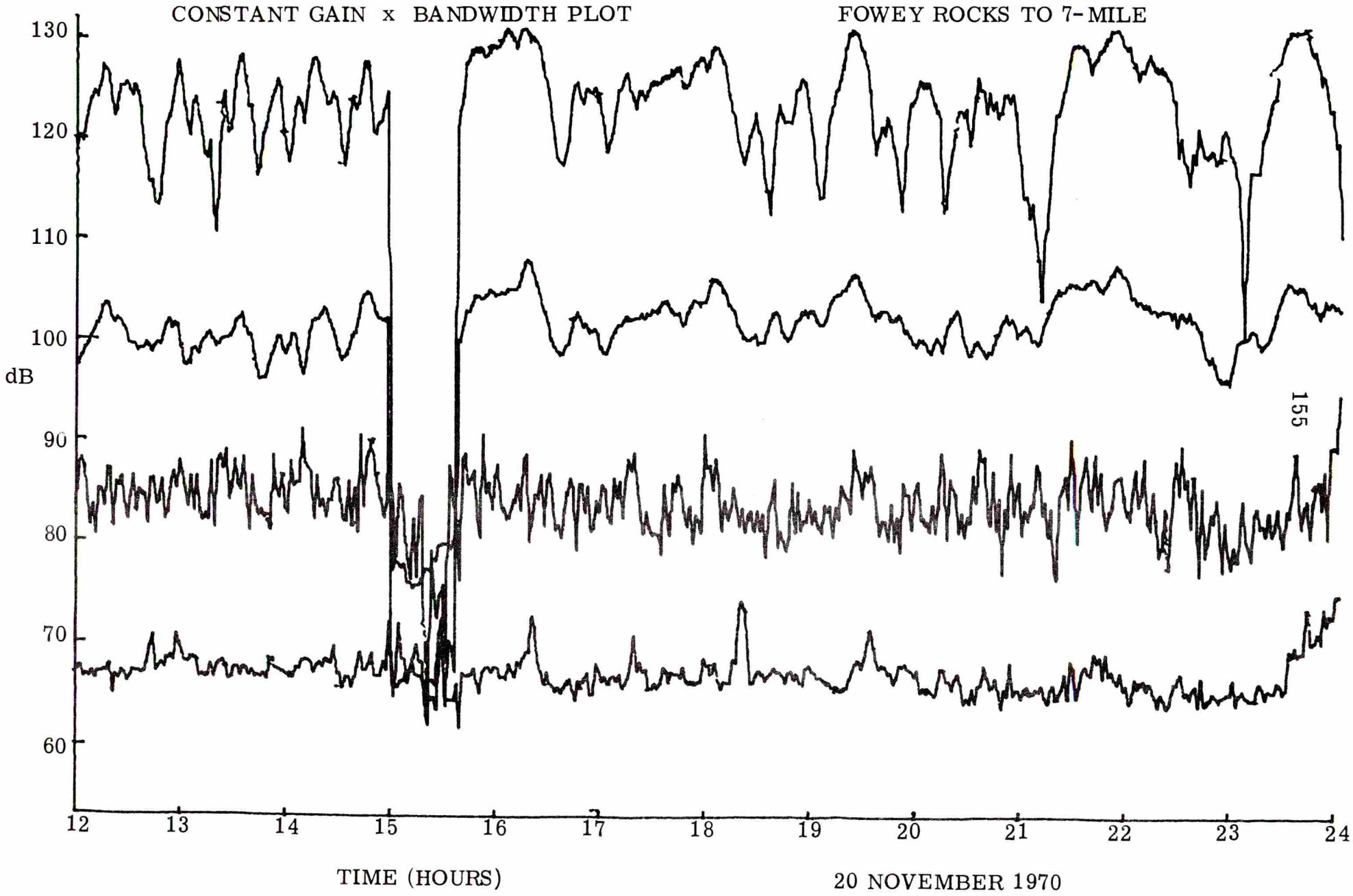
CONSTANT GAIN x BANDWIDTH PLOT
FOWEY ROCKS TO 7-MILE
130
120
110
100
dB
90
80
70
60
155
12
13
14
15
16
17
18
19
20
21
22
23
24
TIME (HOURS)
20 NOVEMBER 1970

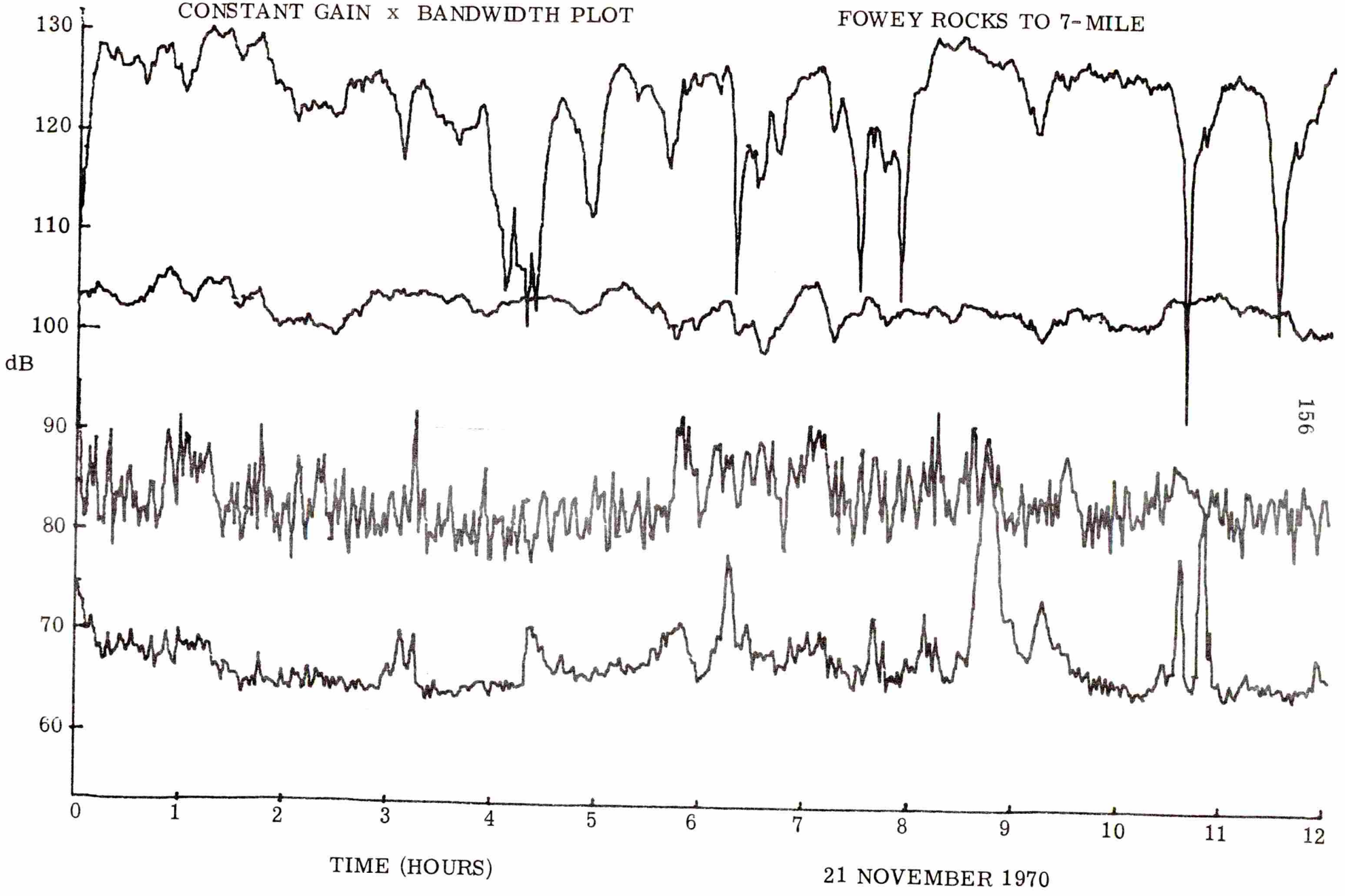
CONSTANT GAIN x BANDWIDTH PLOT
FOWEY ROCKS TO 7-MILE
130
120
110
100
dB
90
80
70
60
156
0
1
2
3
4
5
6
7
8
9
10
11
12
TIME (HOURS)
21 NOVEMBER 1970

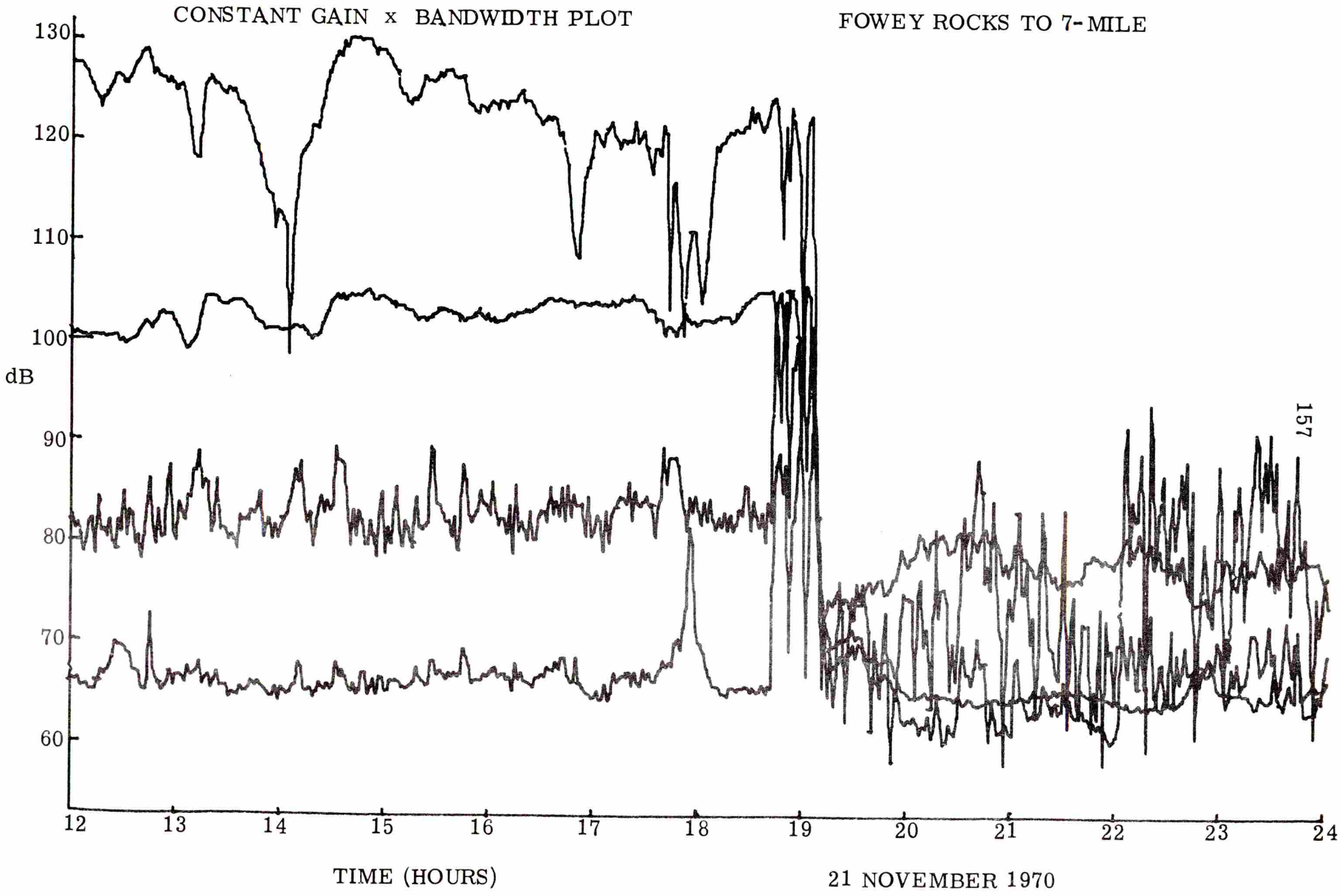
CONSTANT GAIN x BANDWIDTH PLOT
FOWEY ROCKS TO 7-MILE
130
120
110
100
dB
90
80
70
60
157
12
13
14
15
16
17
18
19
20
21
22
23
24
TIME (HOURS)
21 NOVEMBER 1970

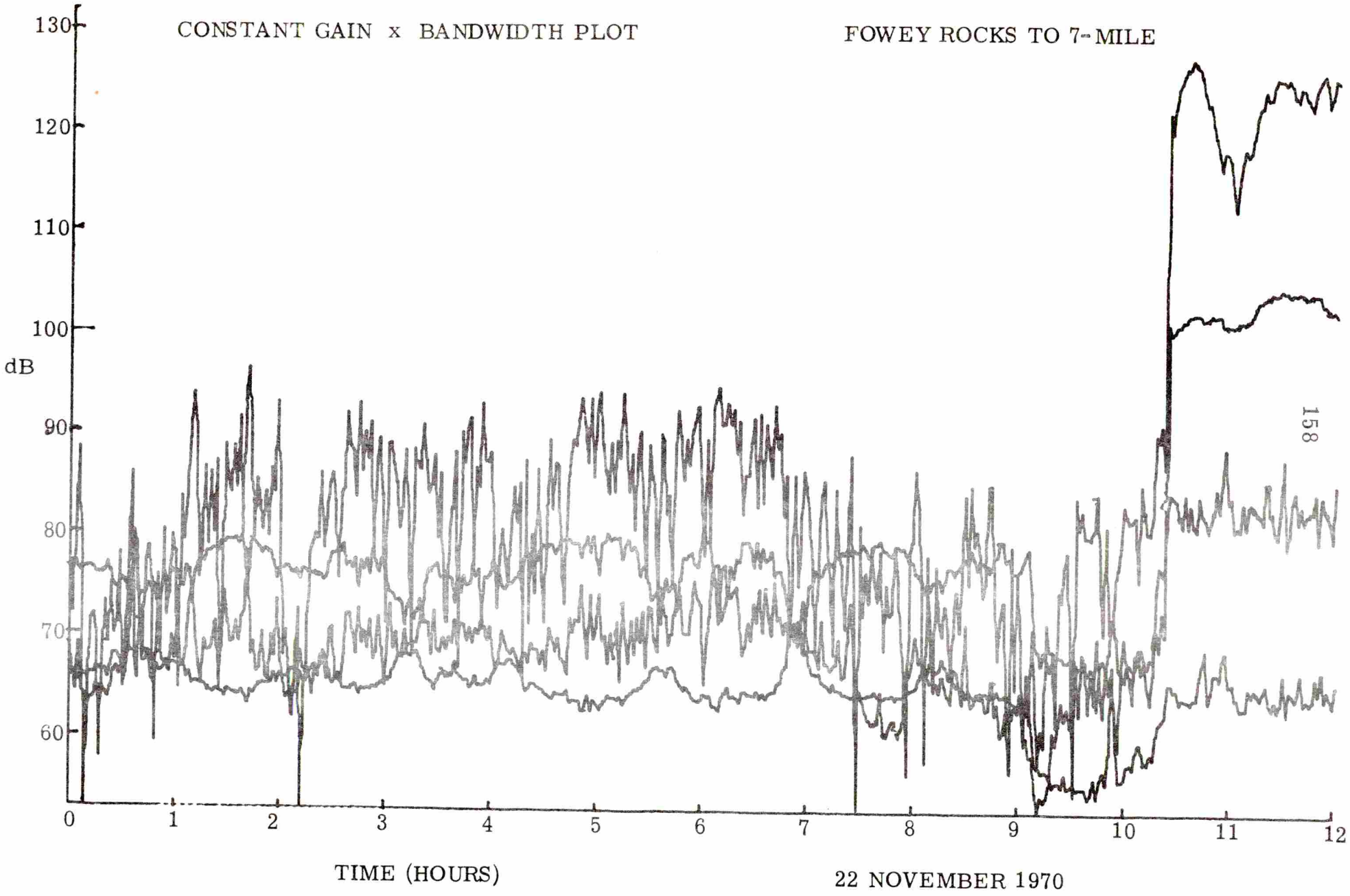
CONSTANT GAIN x BANDWIDTH PLOT
FOWEY ROCKS TO 7-MILE
130
120
110
100
dB
90
80
70
60
158
0
1
2
3
4
5
6
7
8
9
10
11
12
TIME (HOURS)
22 NOVEMBER 1970

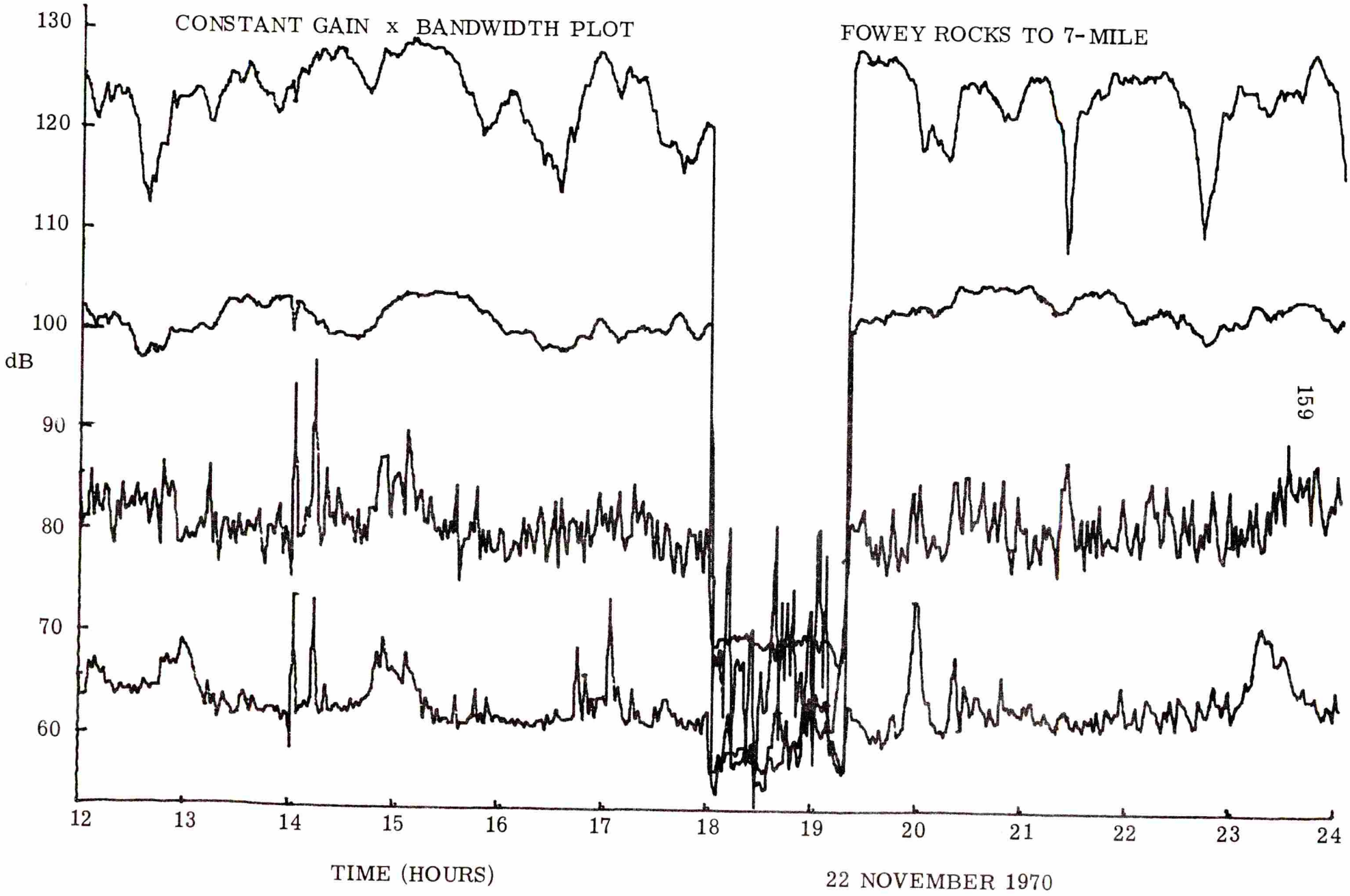
CONSTANT GAIN x BANDWIDTH PLOT
FOWEY ROCKS TO 7-MILE
130
120
110
100
dB
90
80
70
60
159
12
13
14
15
16
17
18
19
20
21
22
23
24
TIME (HOURS)
22 NOVEMBER 1970

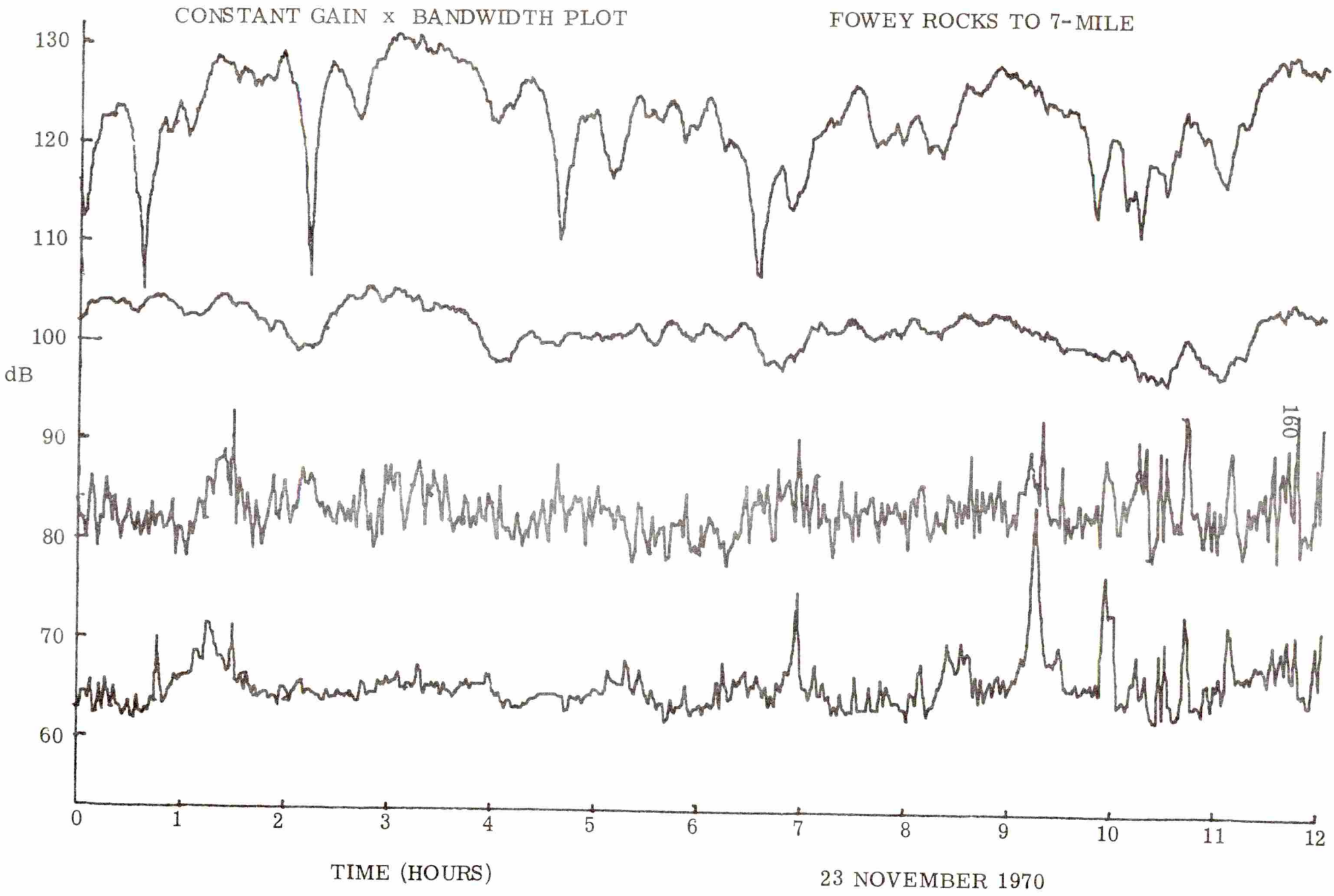
CONSTANT GAIN x BANDWIDTH PLOT
FOWEY ROCKS TO 7-MILE
130
120
110
100
dB
90
80
70
60
160
0
1
2
3
4
5
6
7
8
9
10
11
12
TIME (HOURS)
23 NOVEMBER 1970

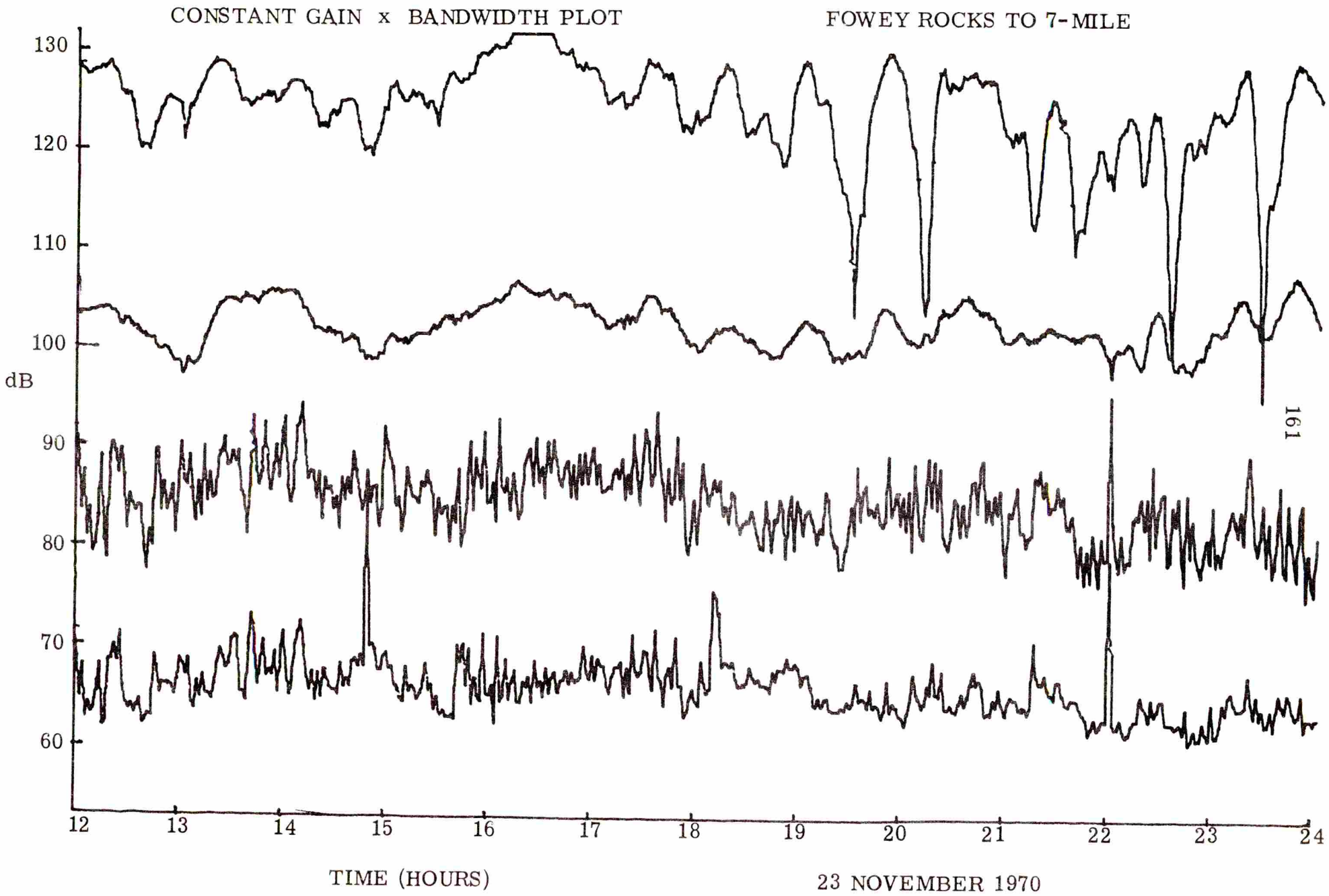
CONSTANT GAIN x BANDWIDTH PLOT
FOWEY ROCKS TO 7-MILE
130
120
110
100
dB
90
80
70
60
161
12
13
14
15
16
17
18
19
20
21
22
23
24
TIME (HOURS)
23 NOVEMBER 1970

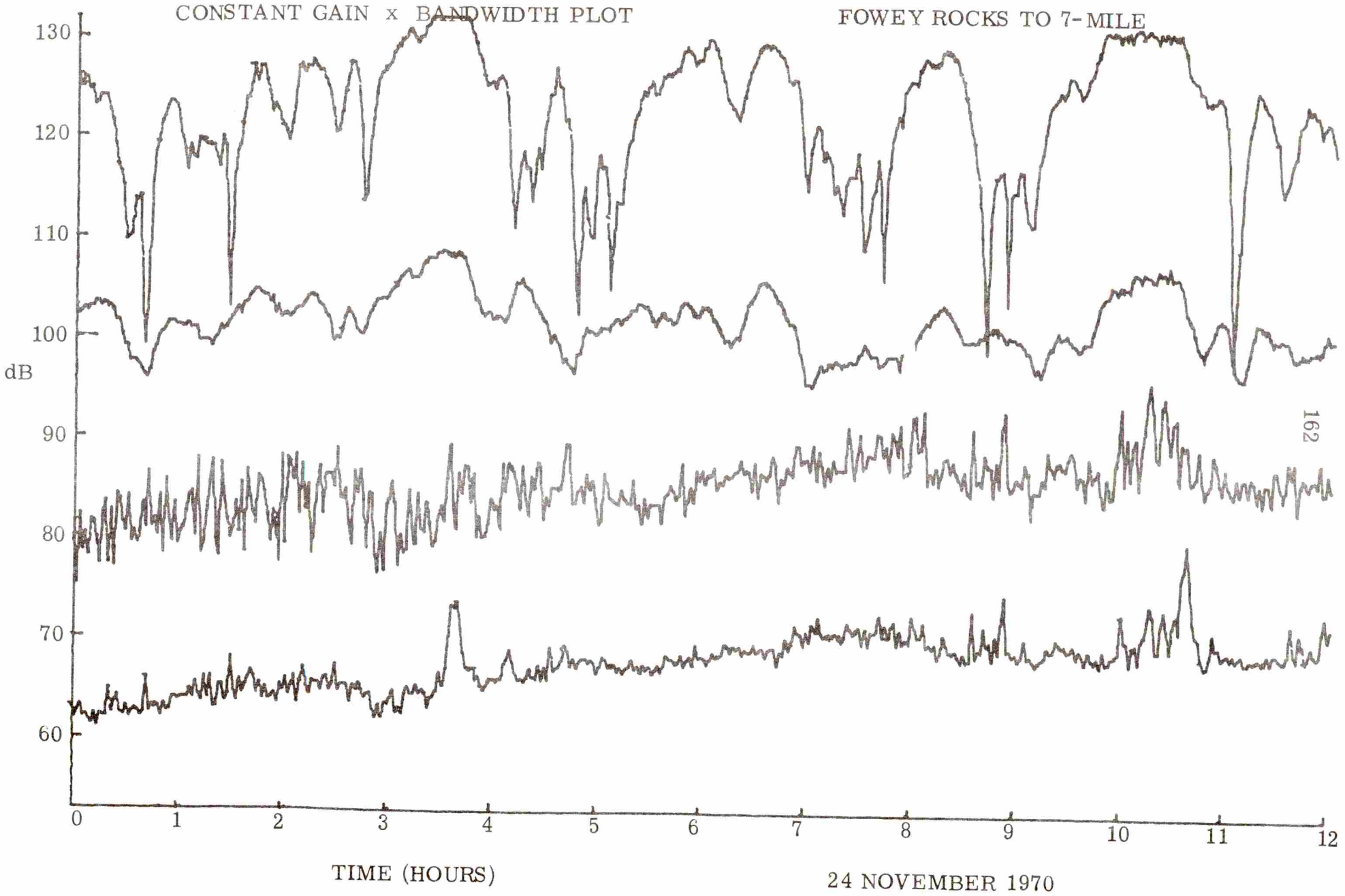
CONSTANT GAIN x BANDWIDTH PLOT
FOWEY ROCKS TO 7-MILE
130
120
110
100
dB
90
80
70
60
162
0
1
2
3
4
5
6
7
8
9
10
11
12
TIME (HOURS)
24 NOVEMBER 1970

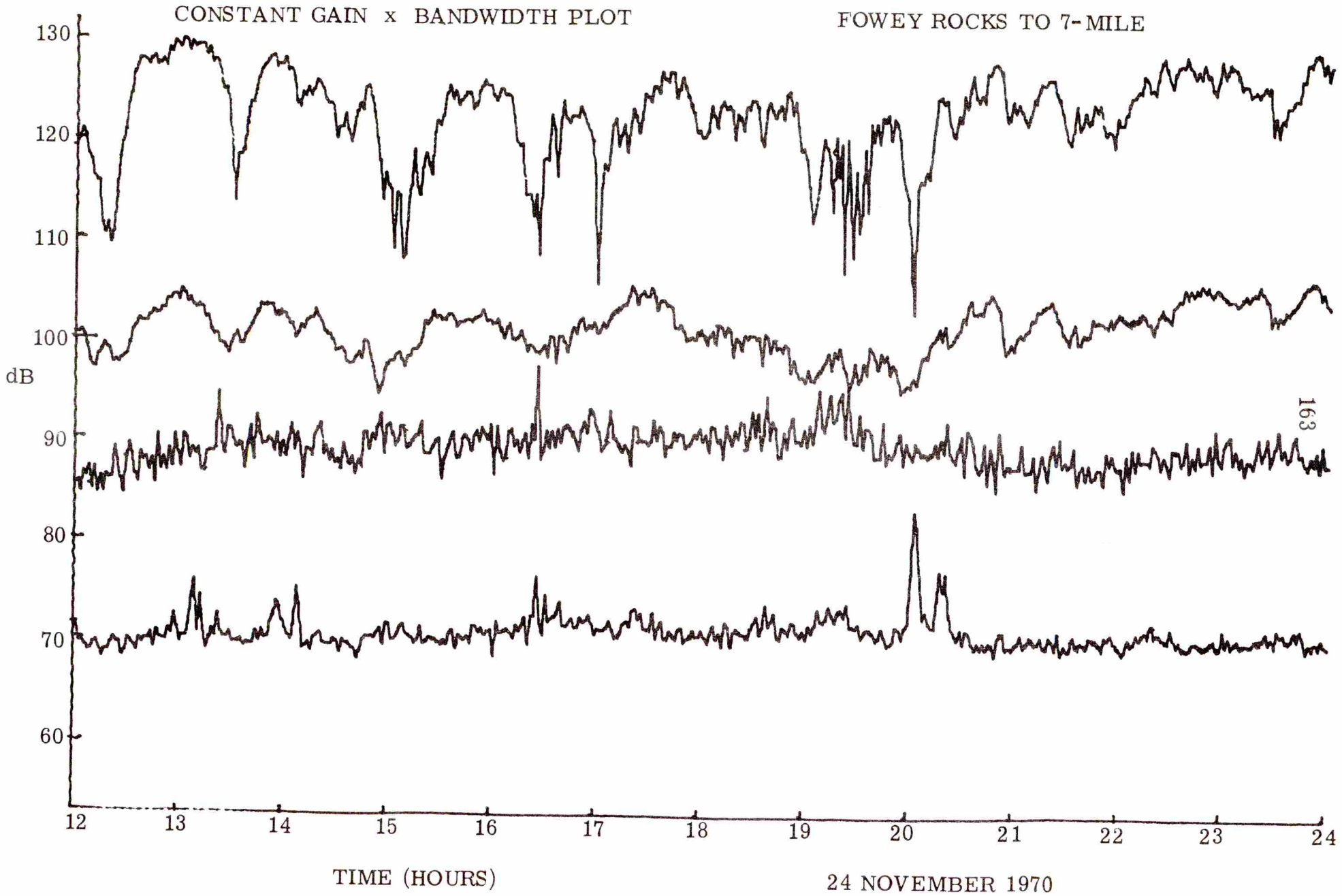
CONSTANT GAIN x BANDWIDTH PLOT
FOWEY ROCKS TO 7-MILE
130
120
110
100
dB
90
80
70
60
12
13
14
15
16
17
18
19
20
21
22
23
24
TIME (HOURS)
24 NOVEMBER 1970
163

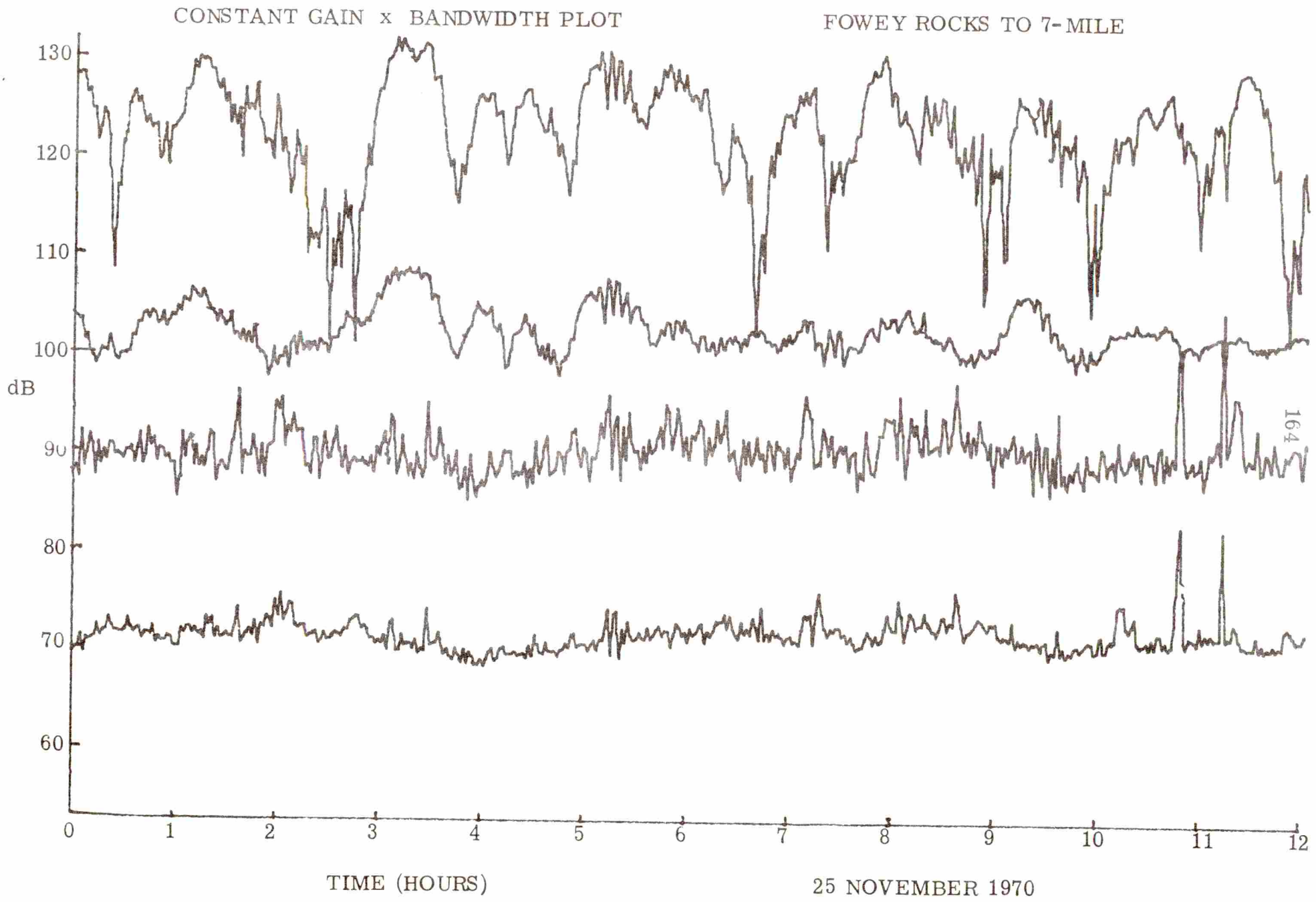
CONSTANT GAIN x BANDWIDTH PLOT
FOWEY ROCKS TO 7-MILE
130
120
110
100
dB
90
80
70
60
164
0
1
2
3
4
5
6
7
8
9
10
11
12
TIME (HOURS)
25 NOVEMBER 1970

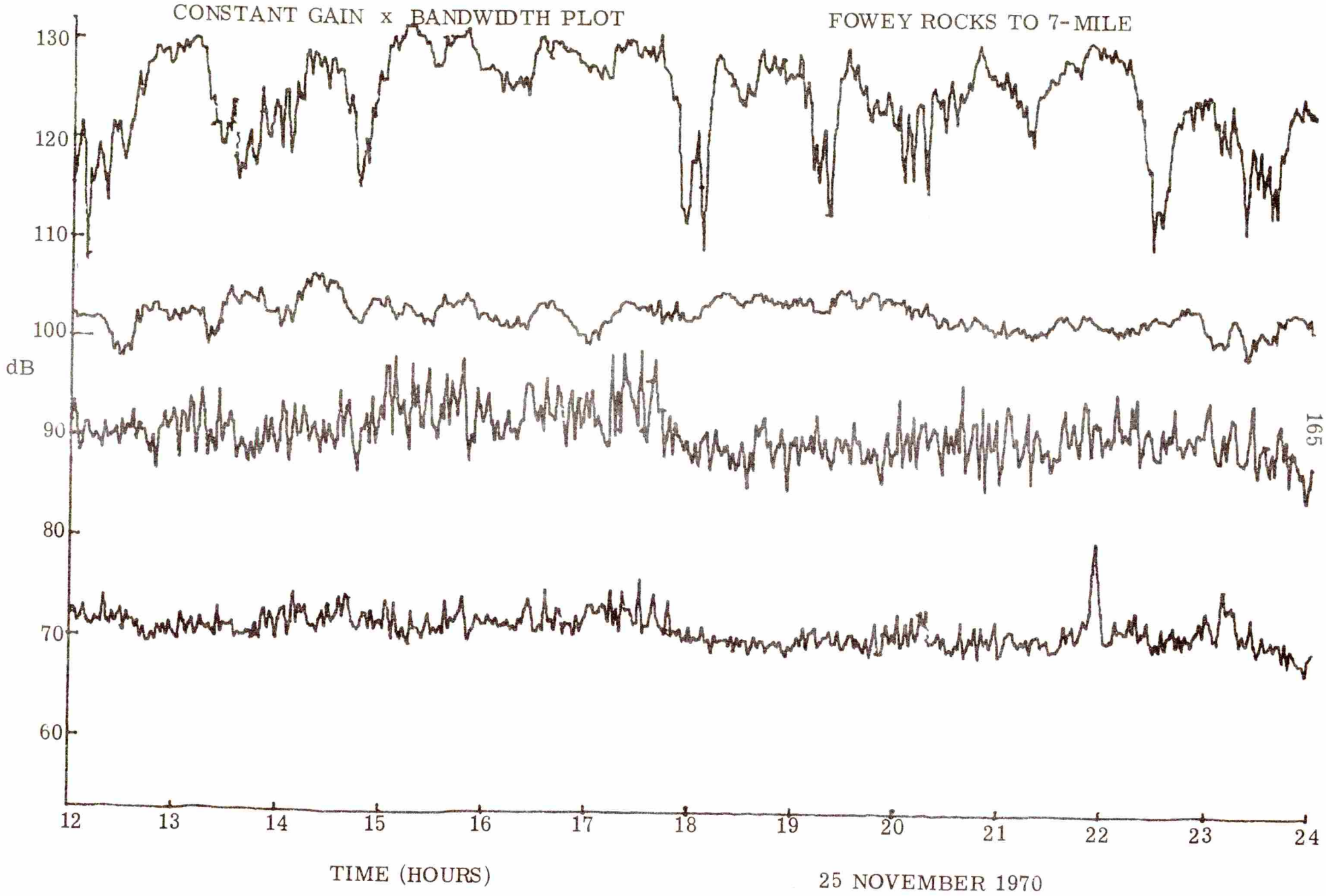
CONSTANT GAIN x BANDWIDTH PLOT
FOWEY ROCKS TO 7-MILE
130
120
110
100
dB
90
80
70
60
165
12
13
14
15
16
17
18
19
20
21
22
23
24
TIME (HOURS)
25 NOVEMBER 1970

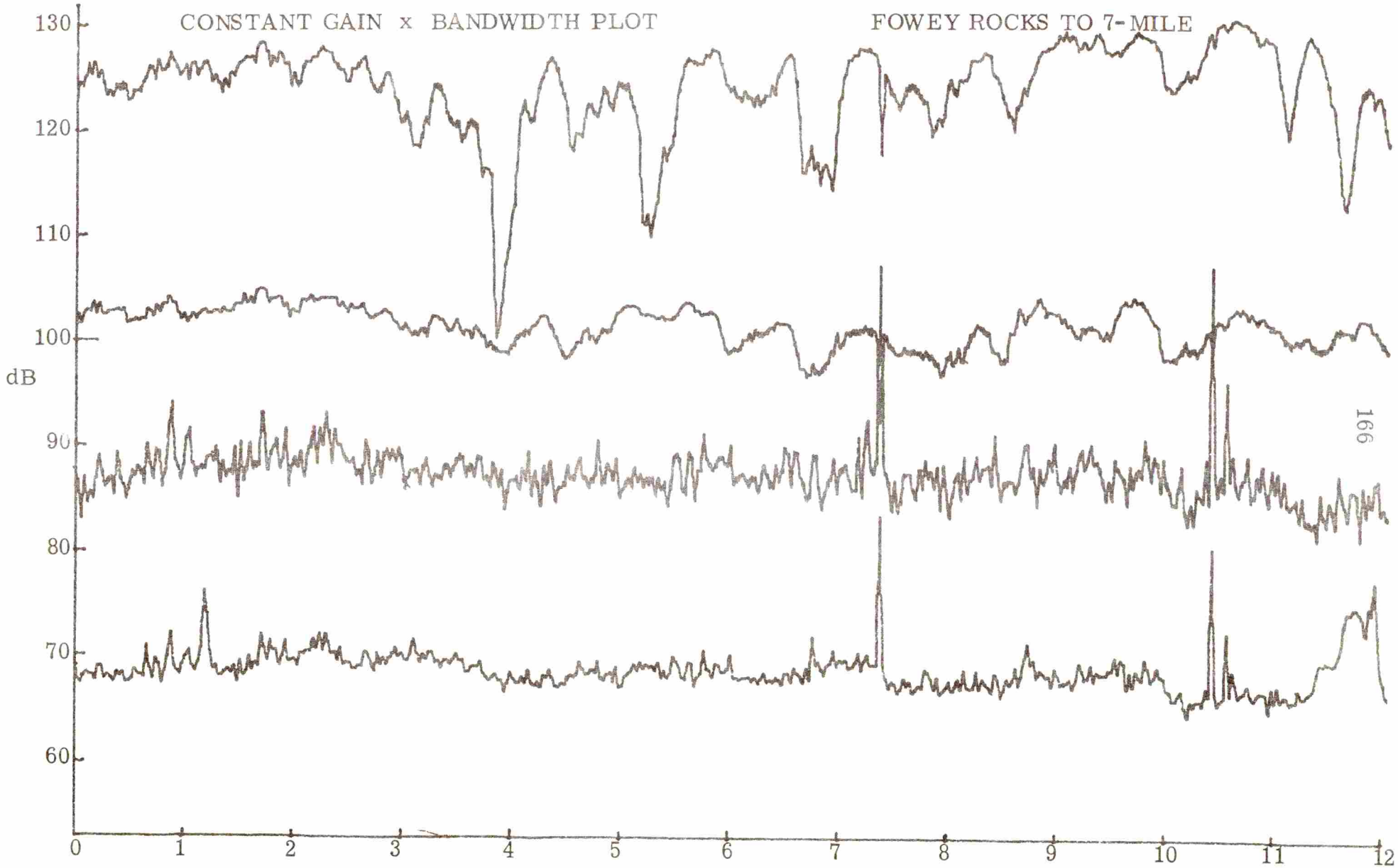
CONSTANT GAIN x BANDWIDTH PLOT
FOWEY ROCKS TO 7-MILE
130
120
110
100
90
80
70
60
dB
166
0
1
2
3
4
5
6
7
8
9
10
11
12
TIME (HOURS)
26 NOVEMBER 1970

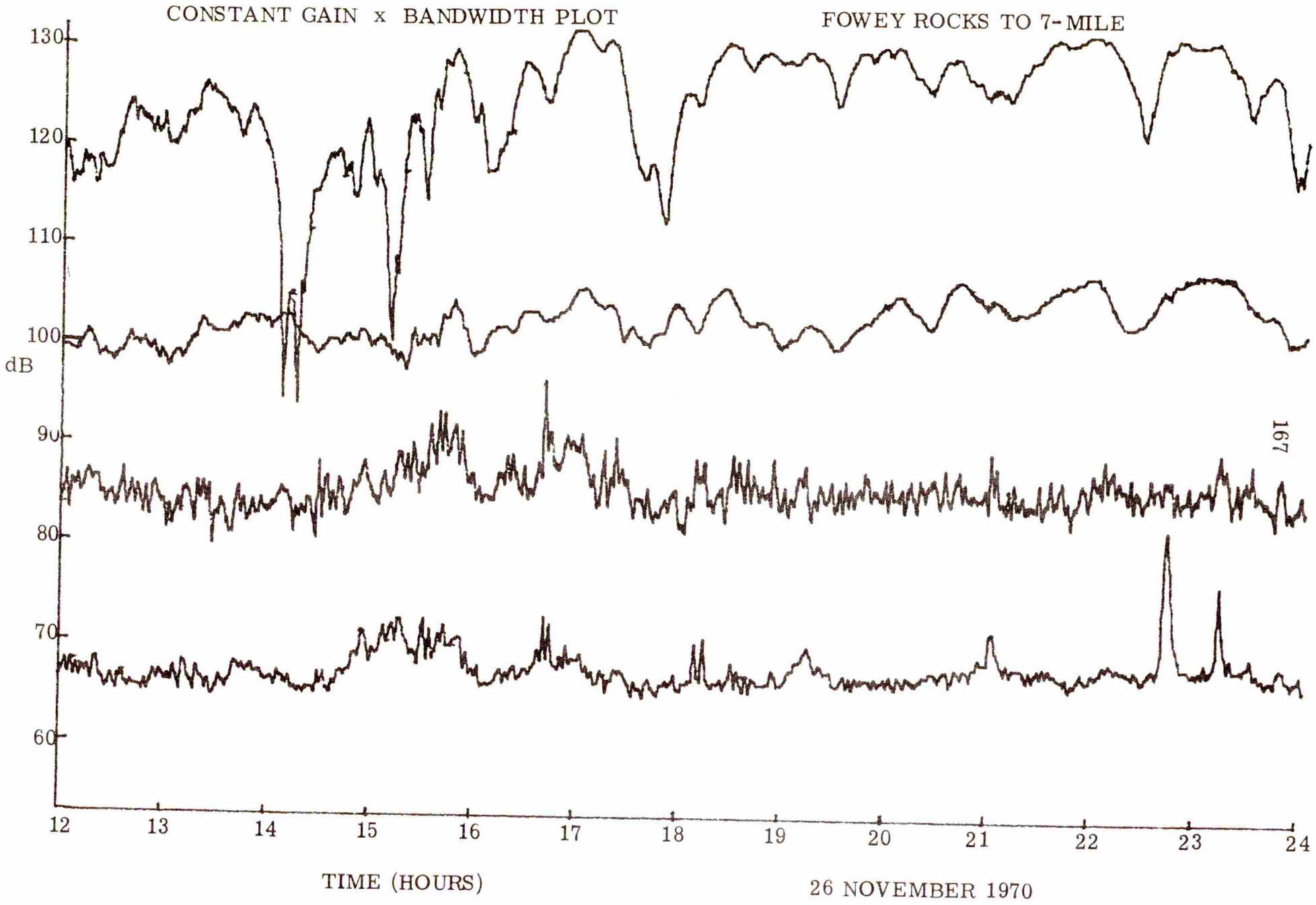
CONSTANT GAIN x BANDWIDTH PLOT
FOWEY ROCKS TO 7-MILE
130
120
110
100
dB
90
80
70
60
12
13
14
15
16
17
18
19
20
21
22
23
24
TIME (HOURS)
26 NOVEMBER 1970
167

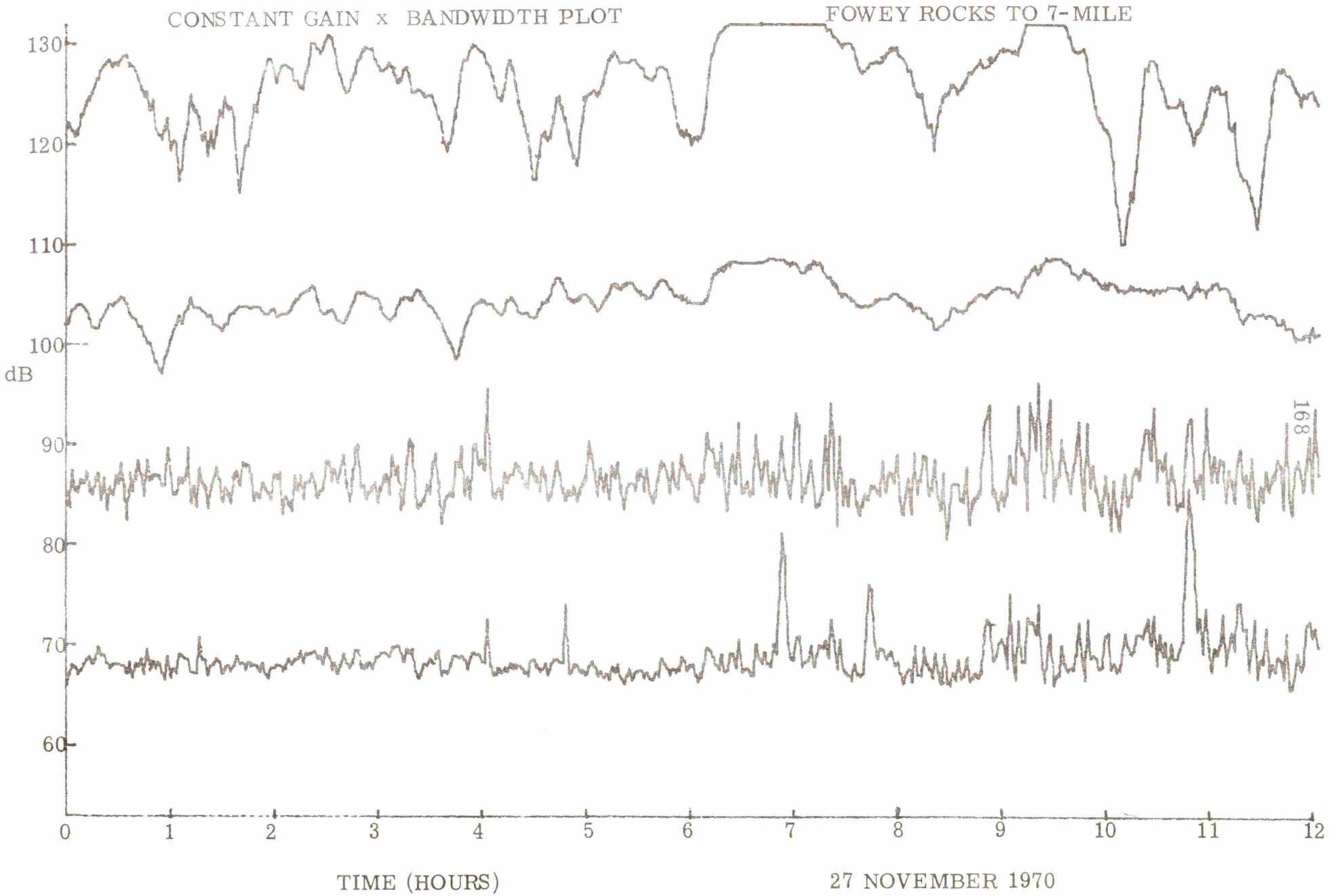
CONSTANT GAIN x BANDWIDTH PLOT
FOWEY ROCKS TO 7-MILE
130
120
110
100
dB
90
80
70
60
168
0
1
2
3
4
5
6
7
8
9
10
11
12
TIME (HOURS)
27 NOVEMBER 1970

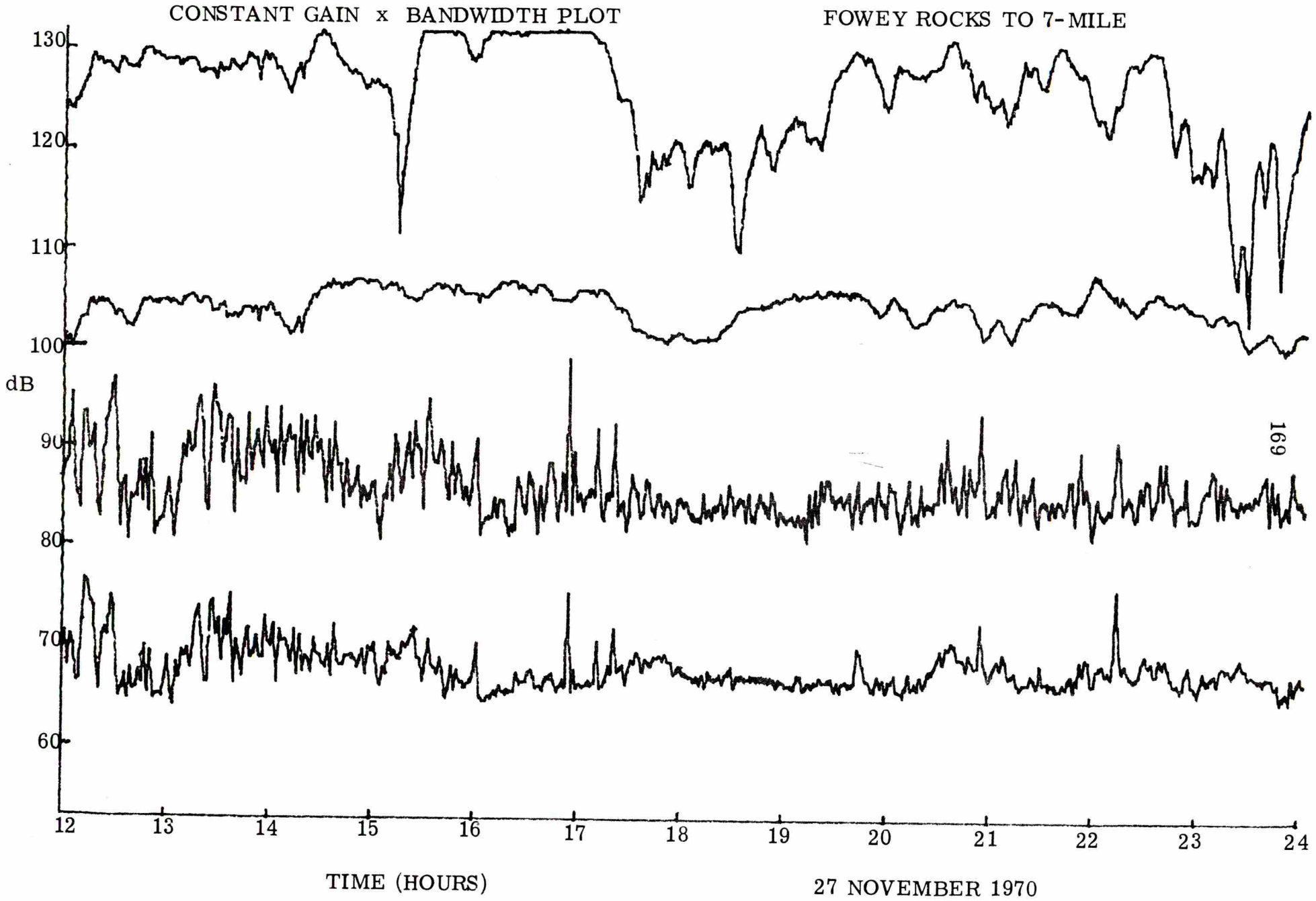
CONSTANT GAIN x BANDWIDTH PLOT
FOWEY ROCKS TO 7-MILE
130
120
110
100
dB
90
80
70
60
169
12
13
14
15
16
17
18
19
20
21
22
23
24
TIME (HOURS)
27 NOVEMBER 1970

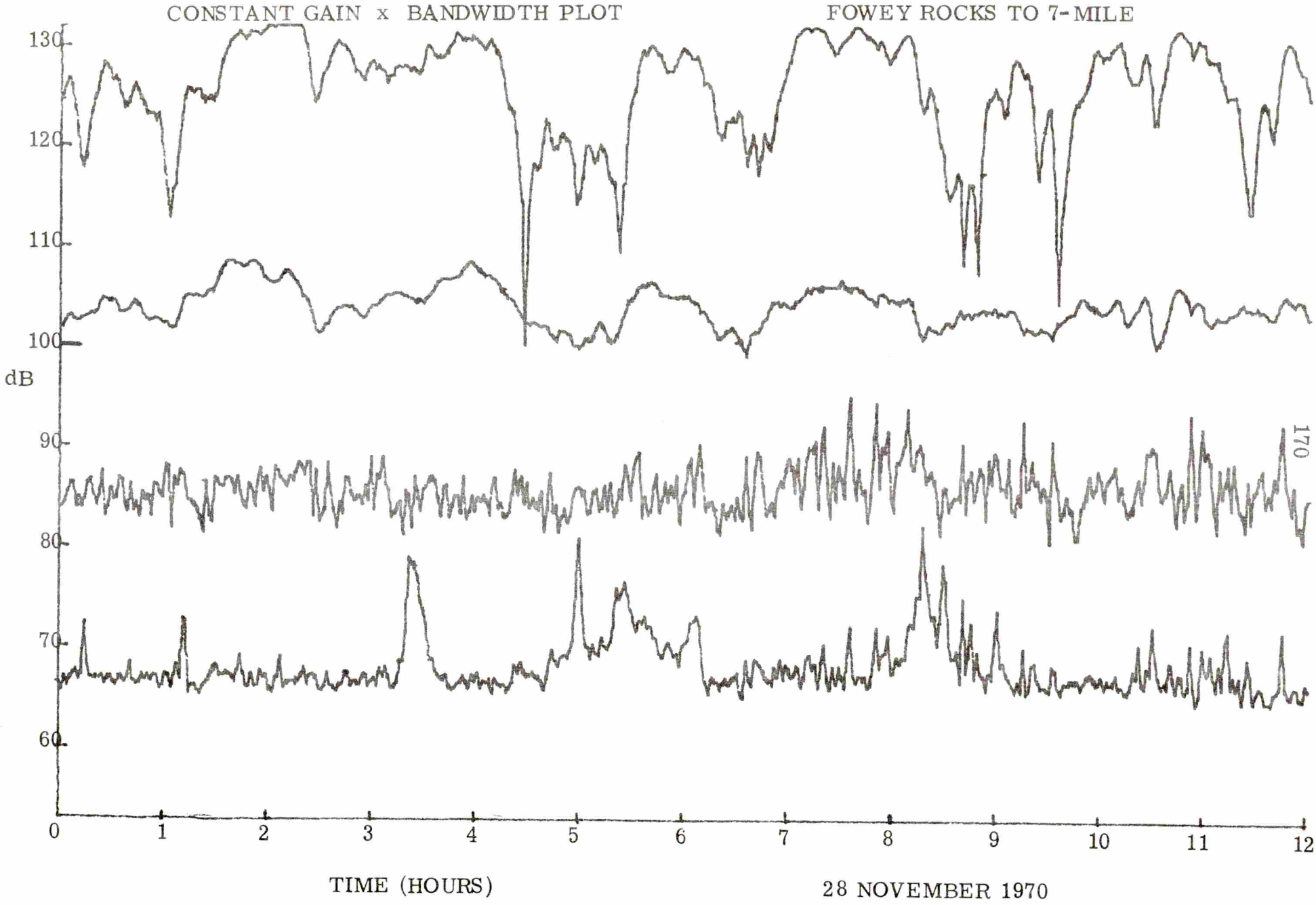
CONSTANT GAIN x BANDWIDTH PLOT
FOWEY ROCKS TO 7-MILE
130
120
110
100
dB
90
80
70
60
170
0
1
2
3
4
5
6
7
8
9
10
11
12
TIME (HOURS)
28 NOVEMBER 1970

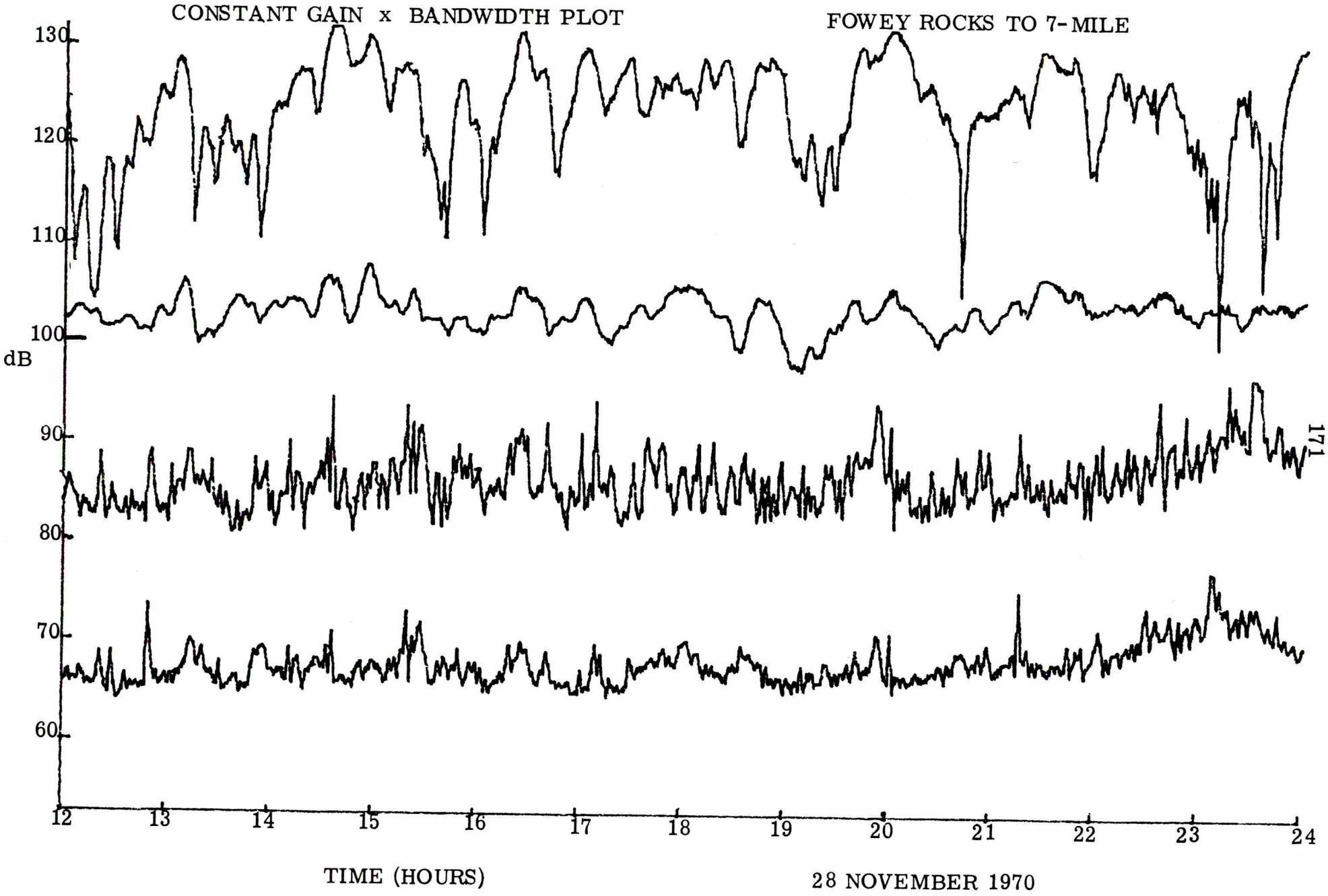
CONSTANT GAIN x BANDWIDTH PLOT
FOWEY ROCKS TO 7-MILE
130
120
110
100
dB
90
80
70
60
171
12
13
14
15
16
17
18
19
20
21
22
23
24
TIME (HOURS)
28 NOVEMBER 1970

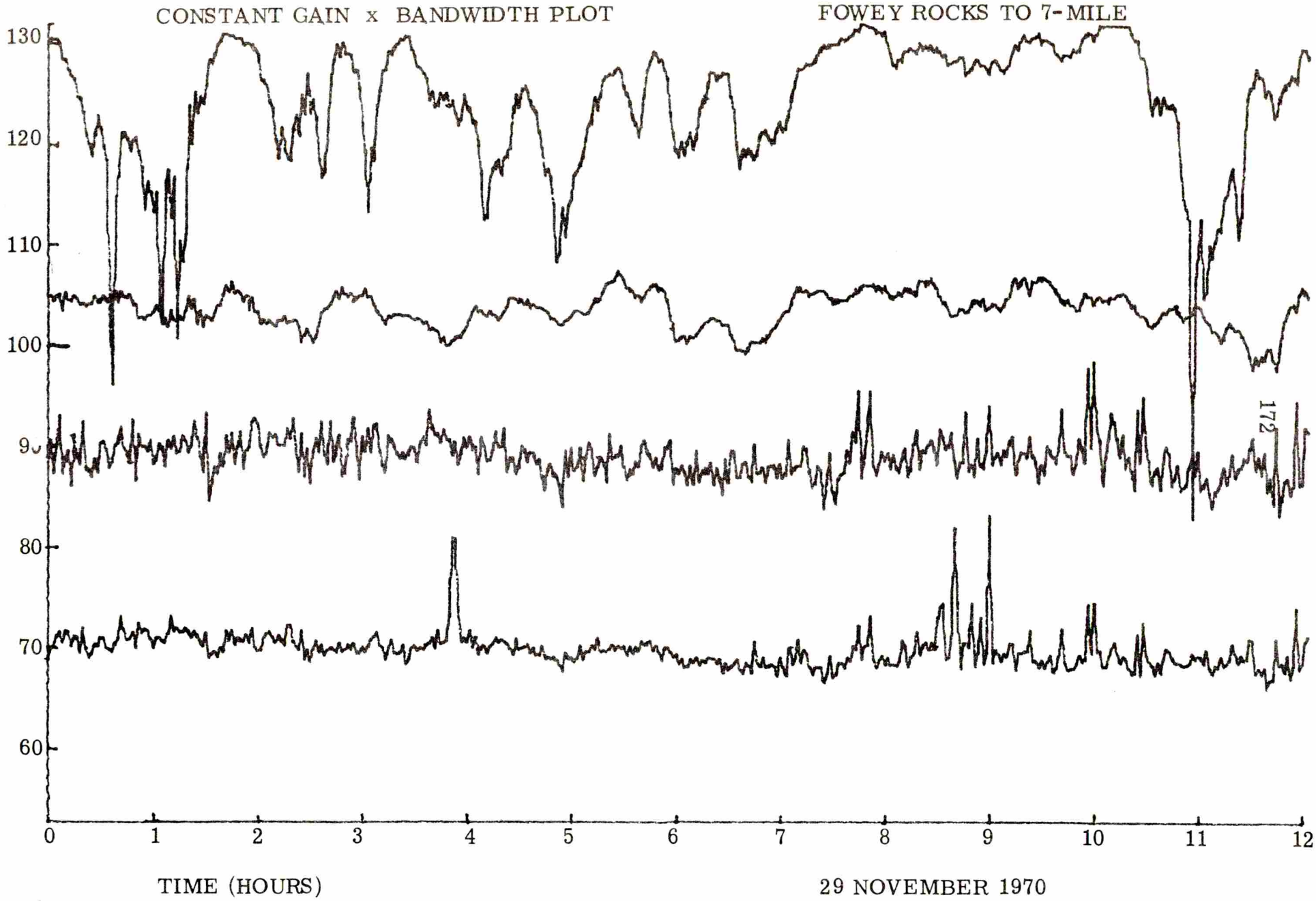
CONSTANT GAIN x BANDWIDTH PLOT
FOWEY ROCKS TO 7-MILE
130
120
110
100
90
80
70
60
172
0
1
2
3
4
5
6
7
8
9
10
11
12
TIME (HOURS)
29 NOVEMBER 1970

APPENDIX D

Appendix D contains the unity gain plots of the carrier and sideband powers from the 7-mile data.

UNITY GAIN PLOT

FOWEY ROCKS TO 7-MILE

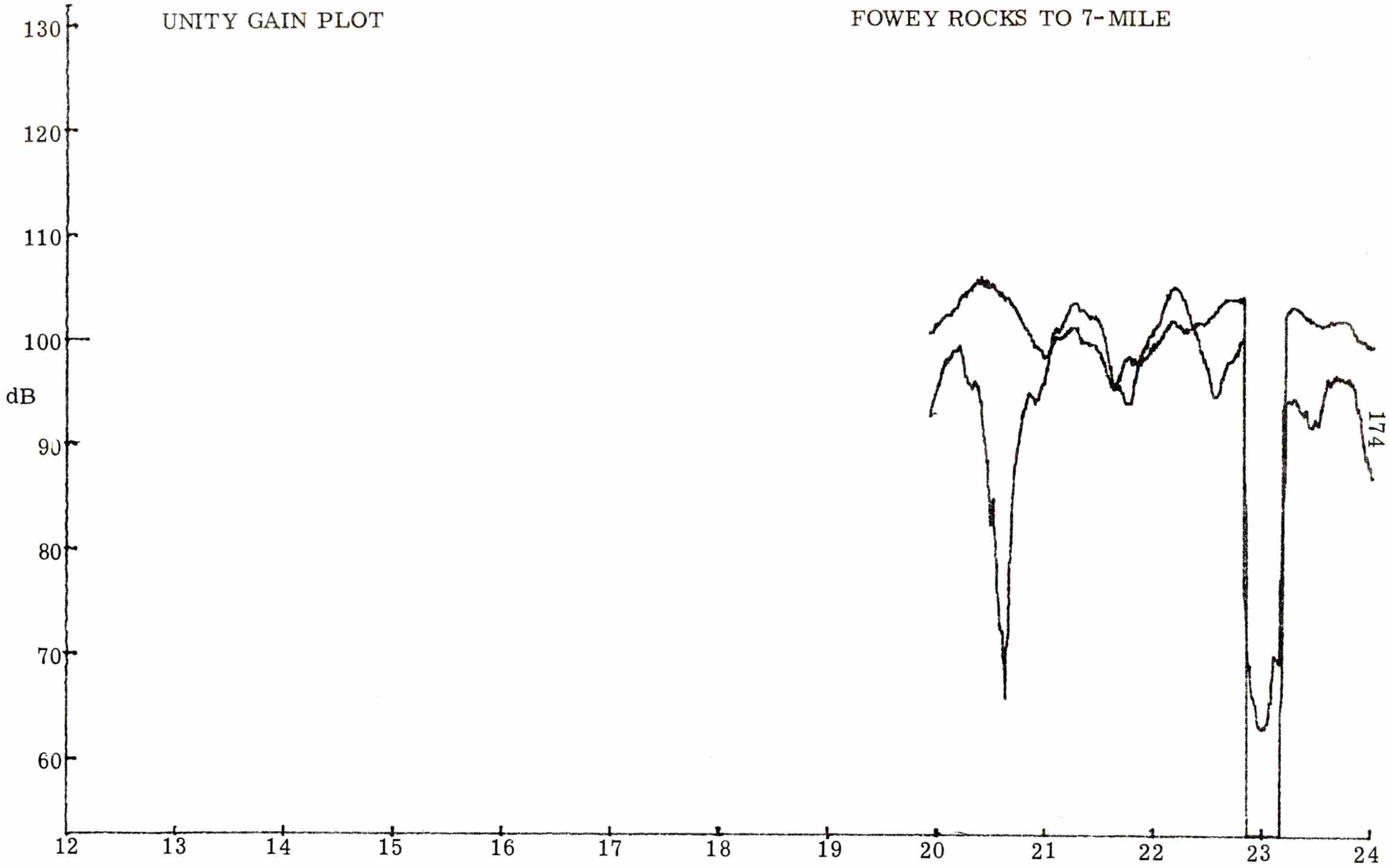

TIME (HOURS)

13 NOVEMBER 1970

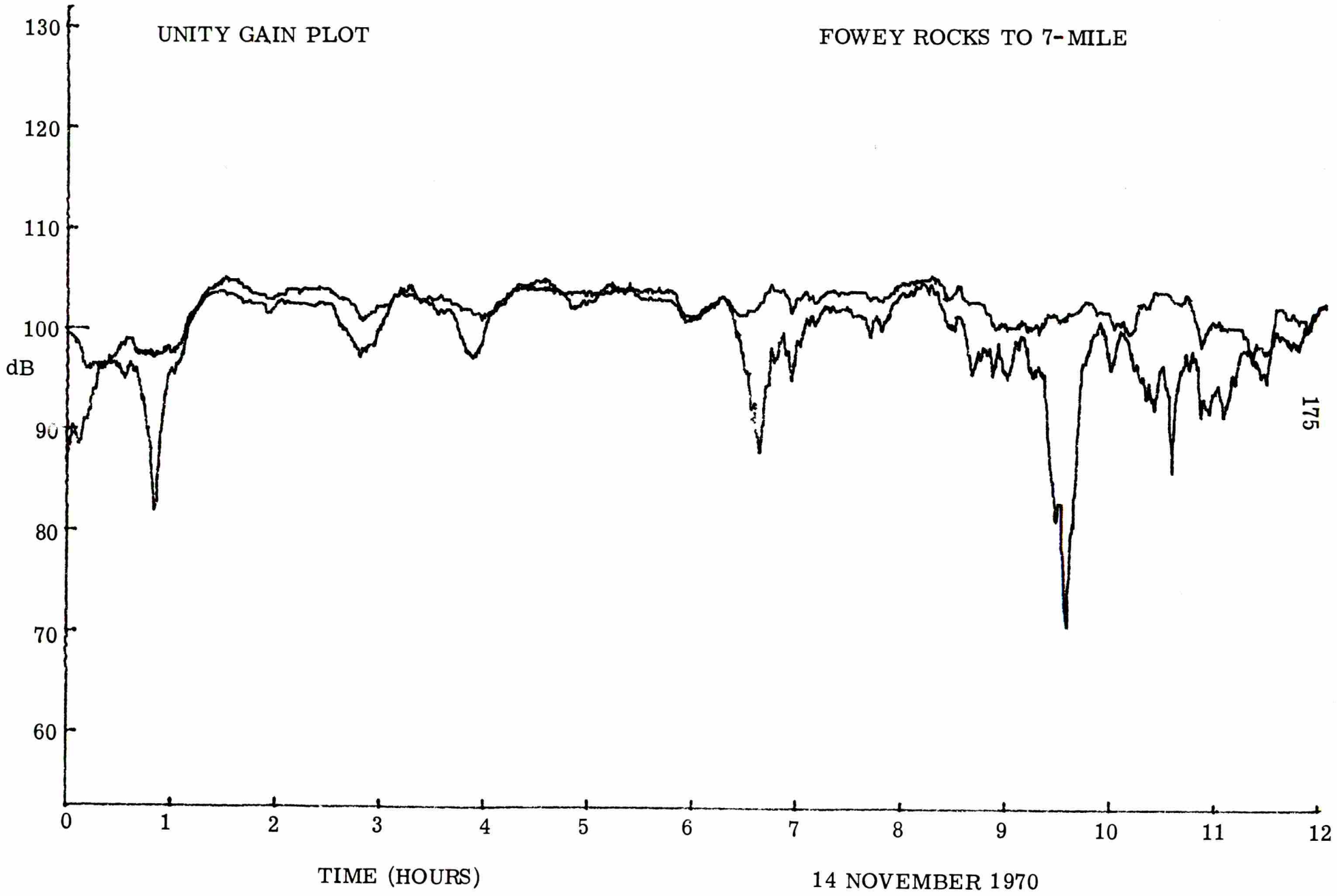
UNITY GAIN PLOT
FOWEY ROCKS TO 7-MILE
130
120
110
100
dB
90
80
70
60
0
1
2
3
4
5
6
7
8
9
10
11
12
TIME (HOURS)
14 NOVEMBER 1970
175

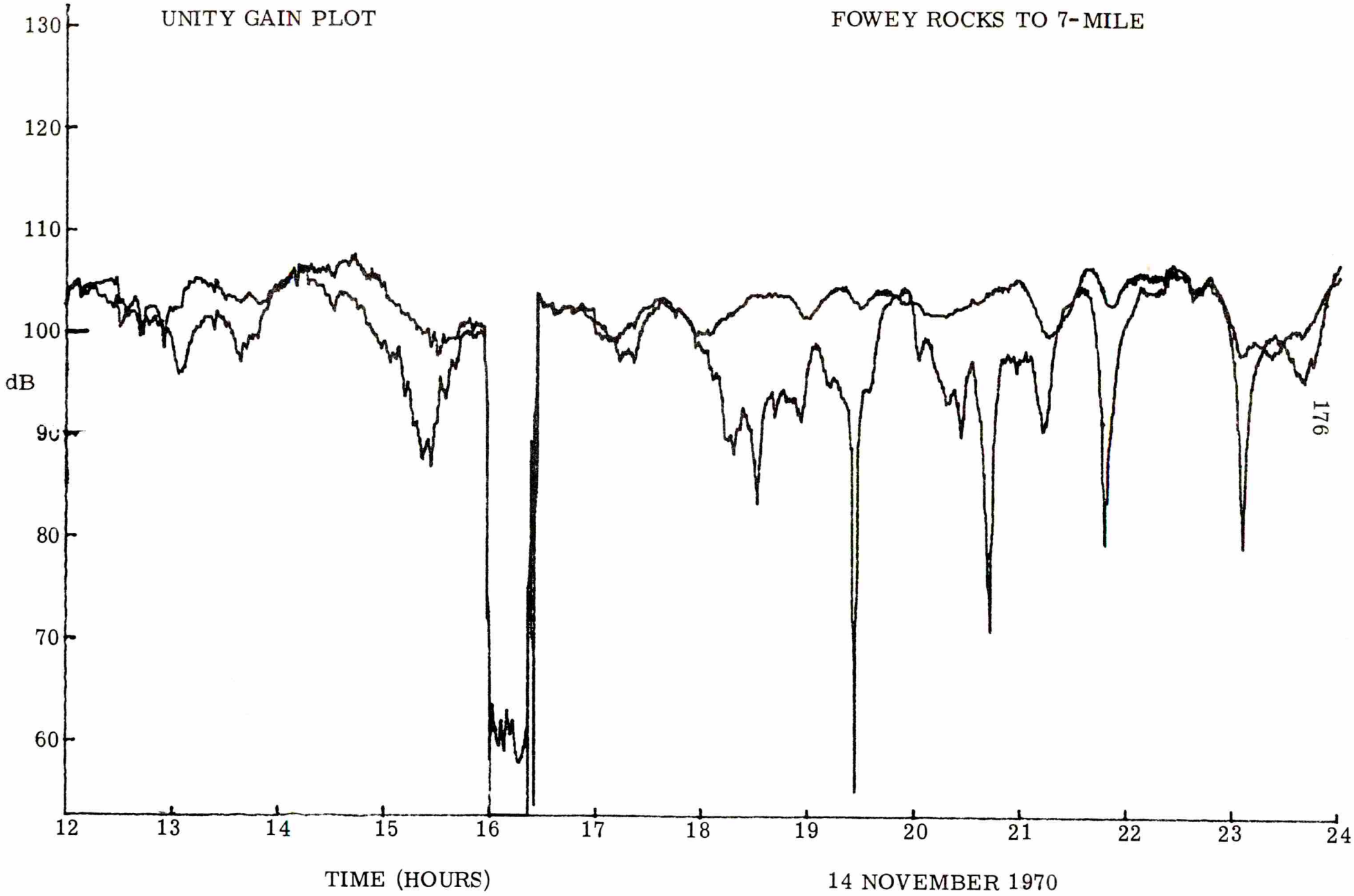
UNITY GAIN PLOT
FOWEY ROCKS TO 7-MILE
130
120
110
100
dB
90
80
70
60
12
13
14
15
16
17
18
19
20
21
22
23
24
176
TIME (HOURS)
14 NOVEMBER 1970

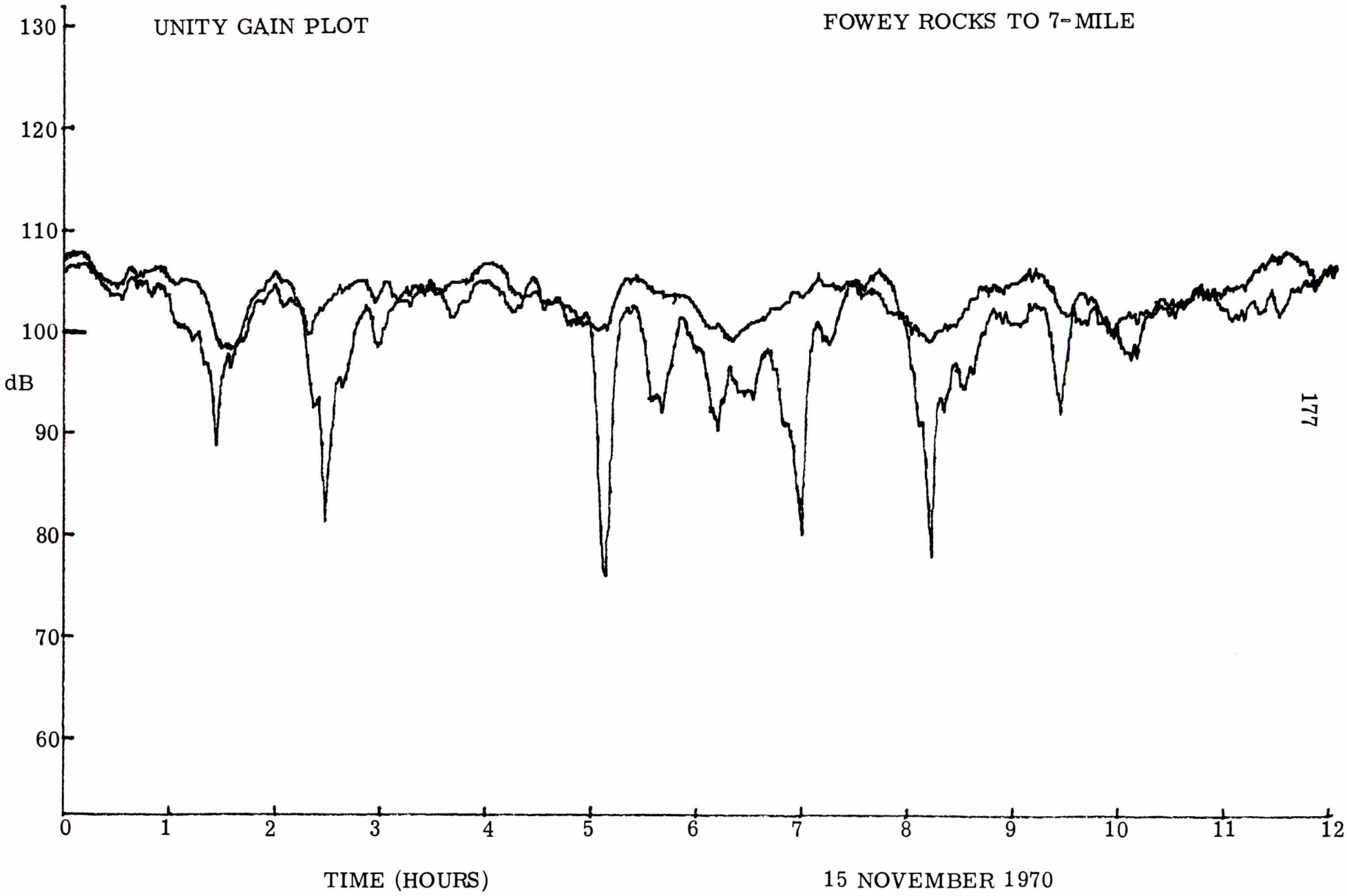
UNITY GAIN PLOT
FOWEY ROCKS TO 7-MILE
130
120
110
100
dB
90
80
70
60
0
1
2
3
4
5
6
7
8
9
10
11
12
TIME (HOURS)
15 NOVEMBER 1970
177

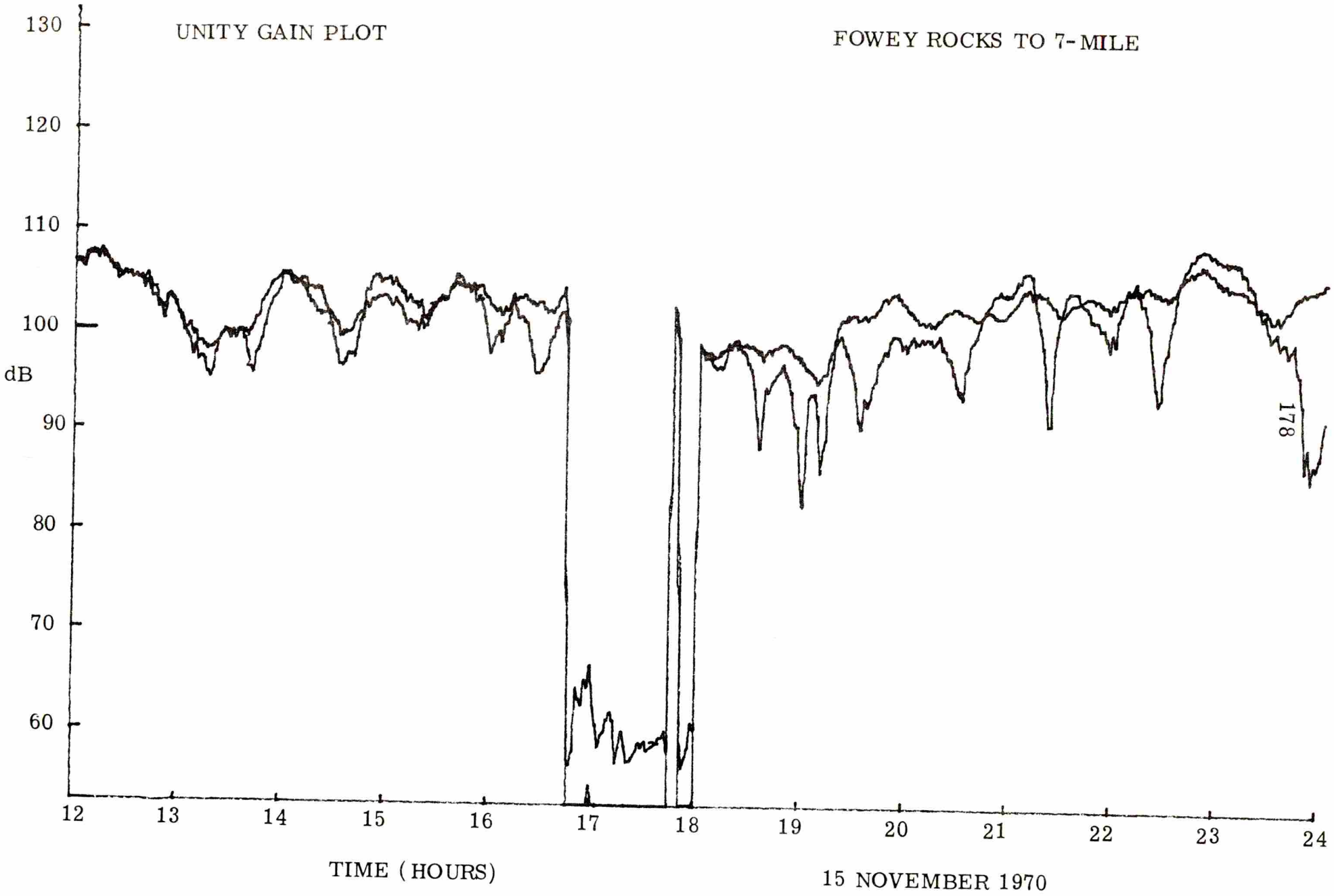
UNITY GAIN PLOT
FOWEY ROCKS TO 7-MILE
130
120
110
100
dB
90
80
70
60
178
12
13
14
15
16
17
18
19
20
21
22
23
24
TIME (HOURS)
15 NOVEMBER 1970

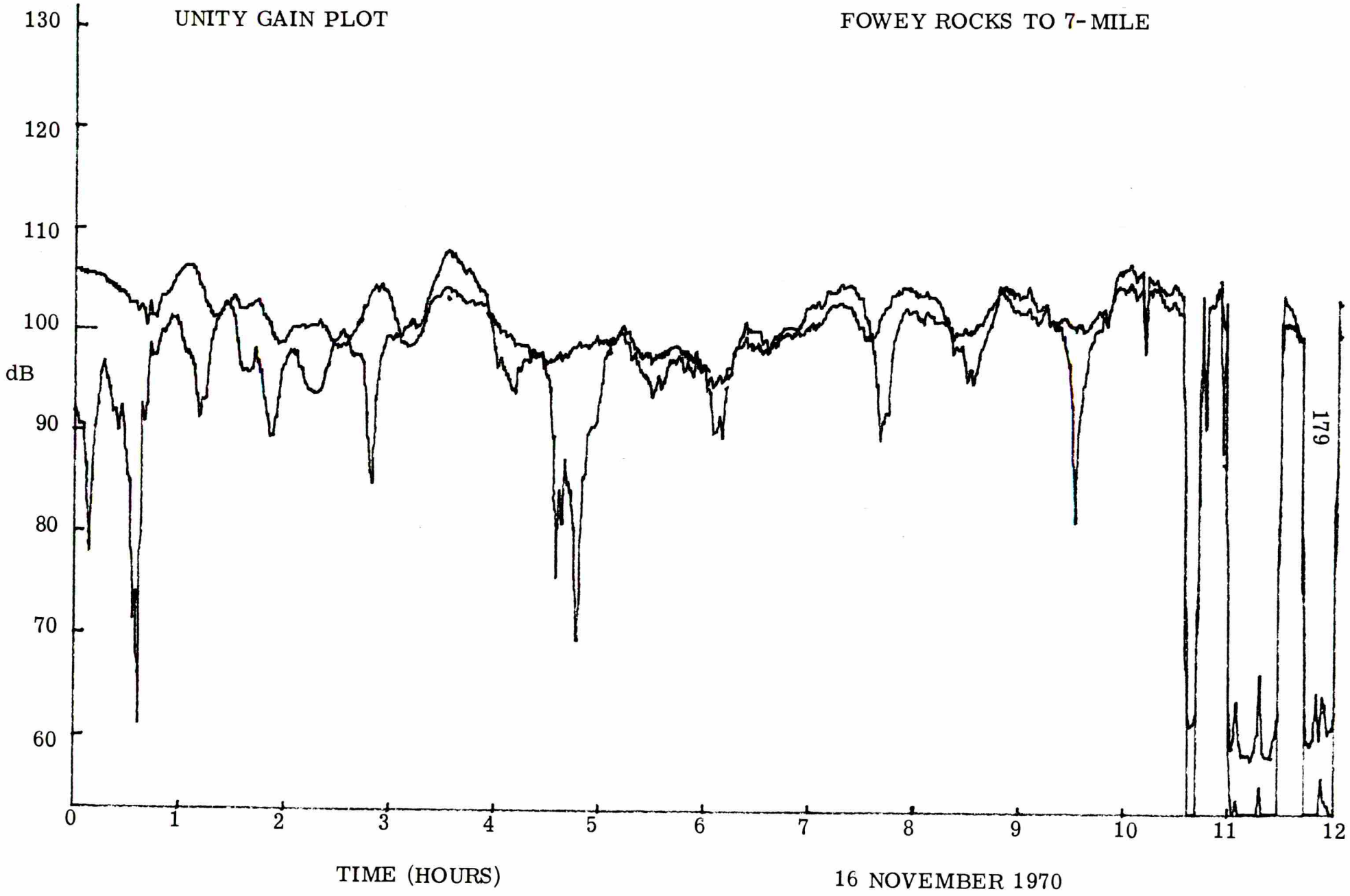
UNITY GAIN PLOT
FOWEY ROCKS TO 7-MILE
130
120
110
100
dB
90
80
70
60
0
1
2
3
4
5
6
7
8
9
10
11
12
TIME (HOURS)
16 NOVEMBER 1970
179

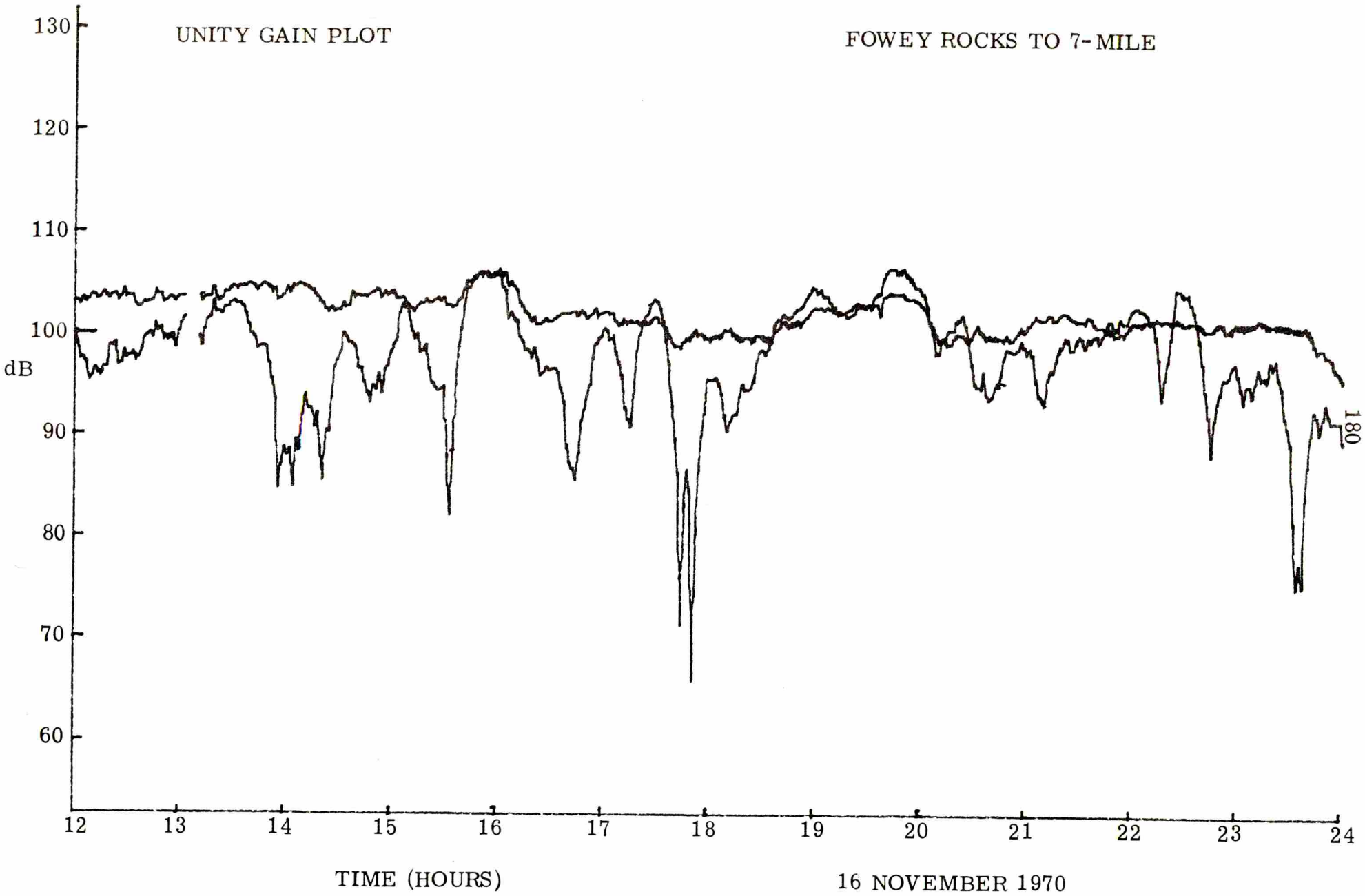
UNITY GAIN PLOT
FOWEY ROCKS TO 7-MILE
130
120
110
100
dB
90
80
70
60
180
12
13
14
15
16
17
18
19
20
21
22
23
24
TIME (HOURS)
16 NOVEMBER 1970

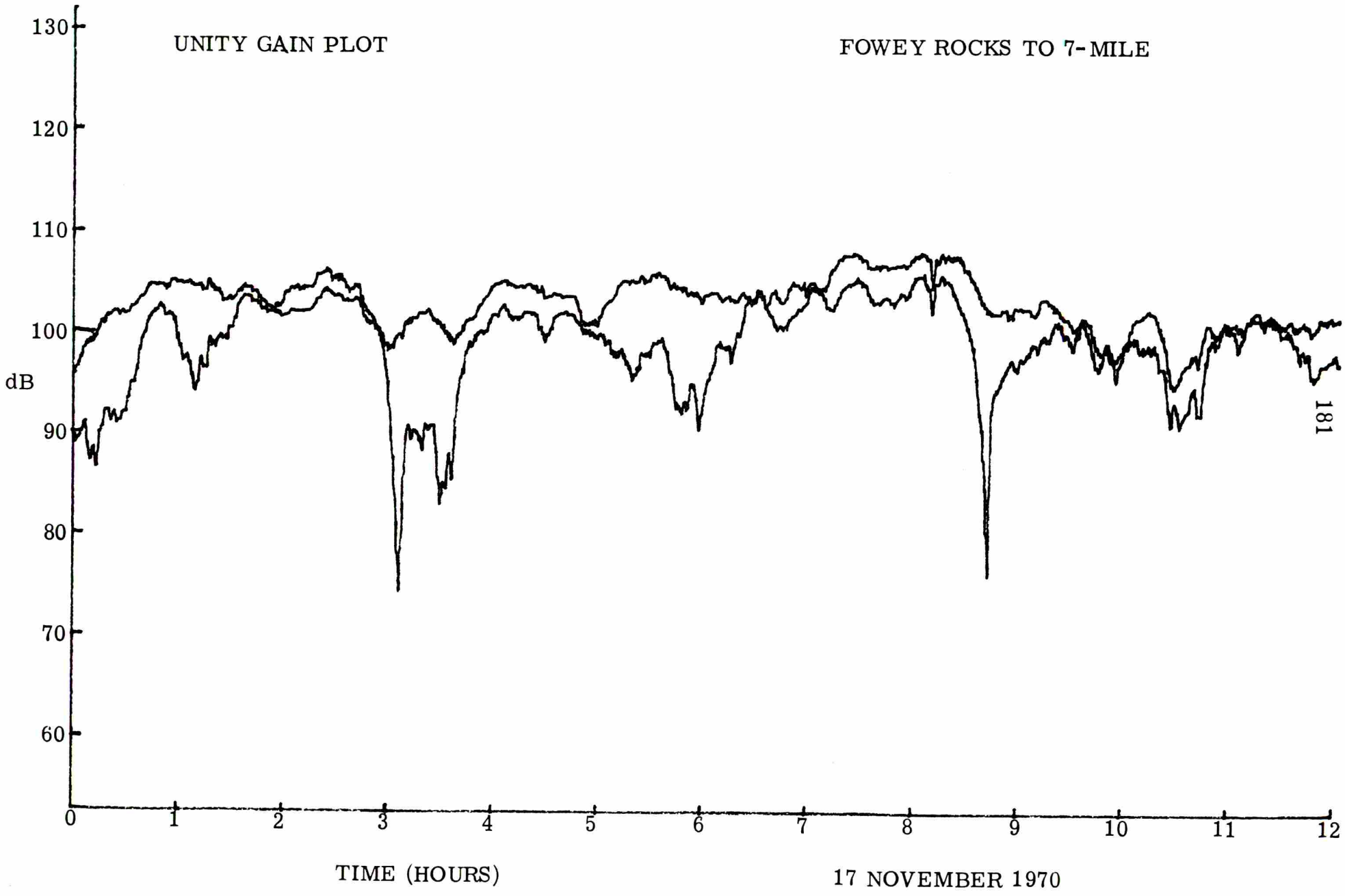
UNITY GAIN PLOT
FOWEY ROCKS TO 7-MILE
130
120
110
100
dB
90
80
70
60
181
0
1
2
3
4
5
6
7
8
9
10
11
12
TIME (HOURS)
17 NOVEMBER 1970

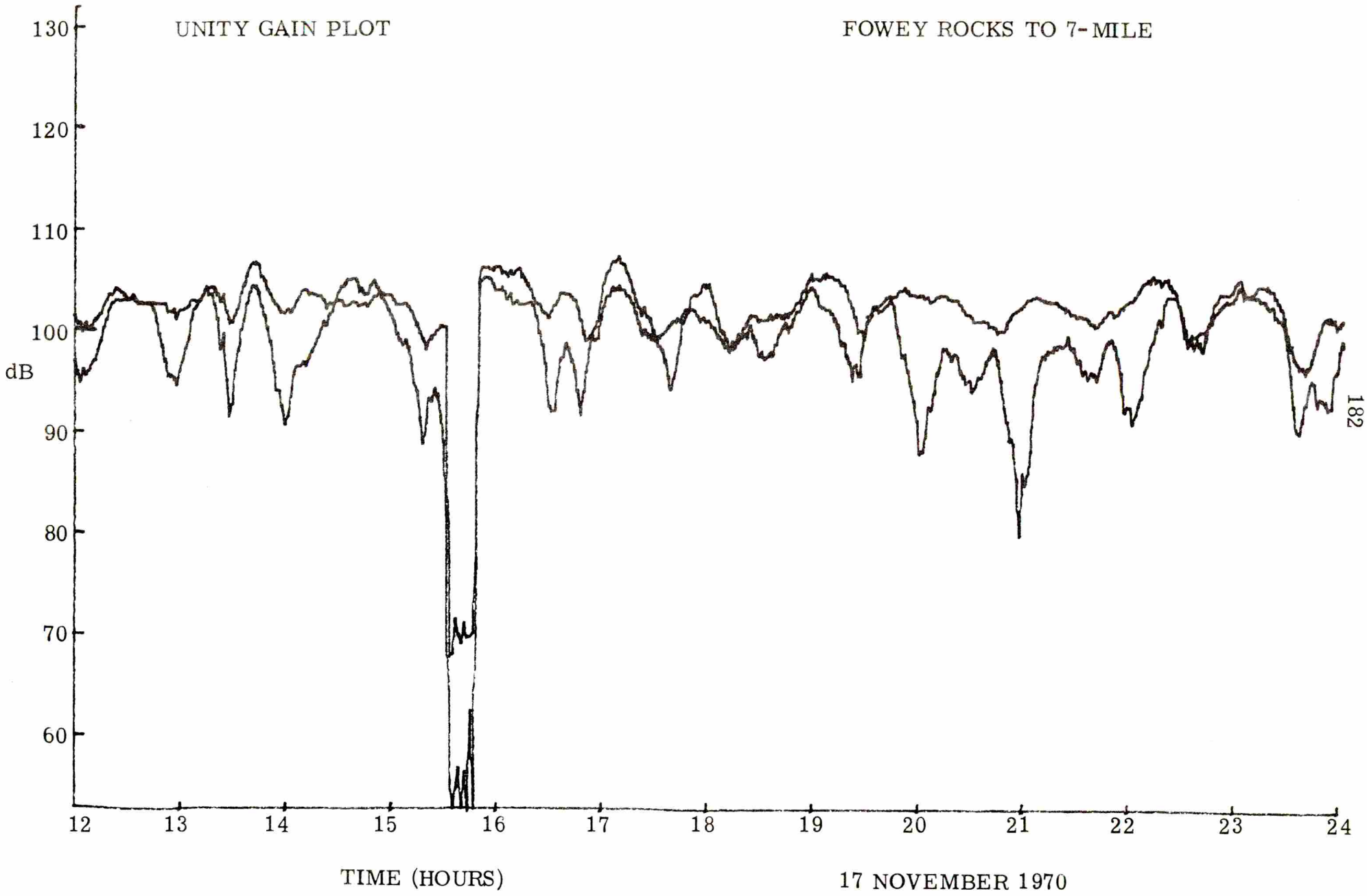
UNITY GAIN PLOT
FOWEY ROCKS TO 7-MILE
130
120
110
100
90
80
70
60
dB
182
12
13
14
15
16
17
18
19
20
21
22
23
24
TIME (HOURS)
17 NOVEMBER 1970

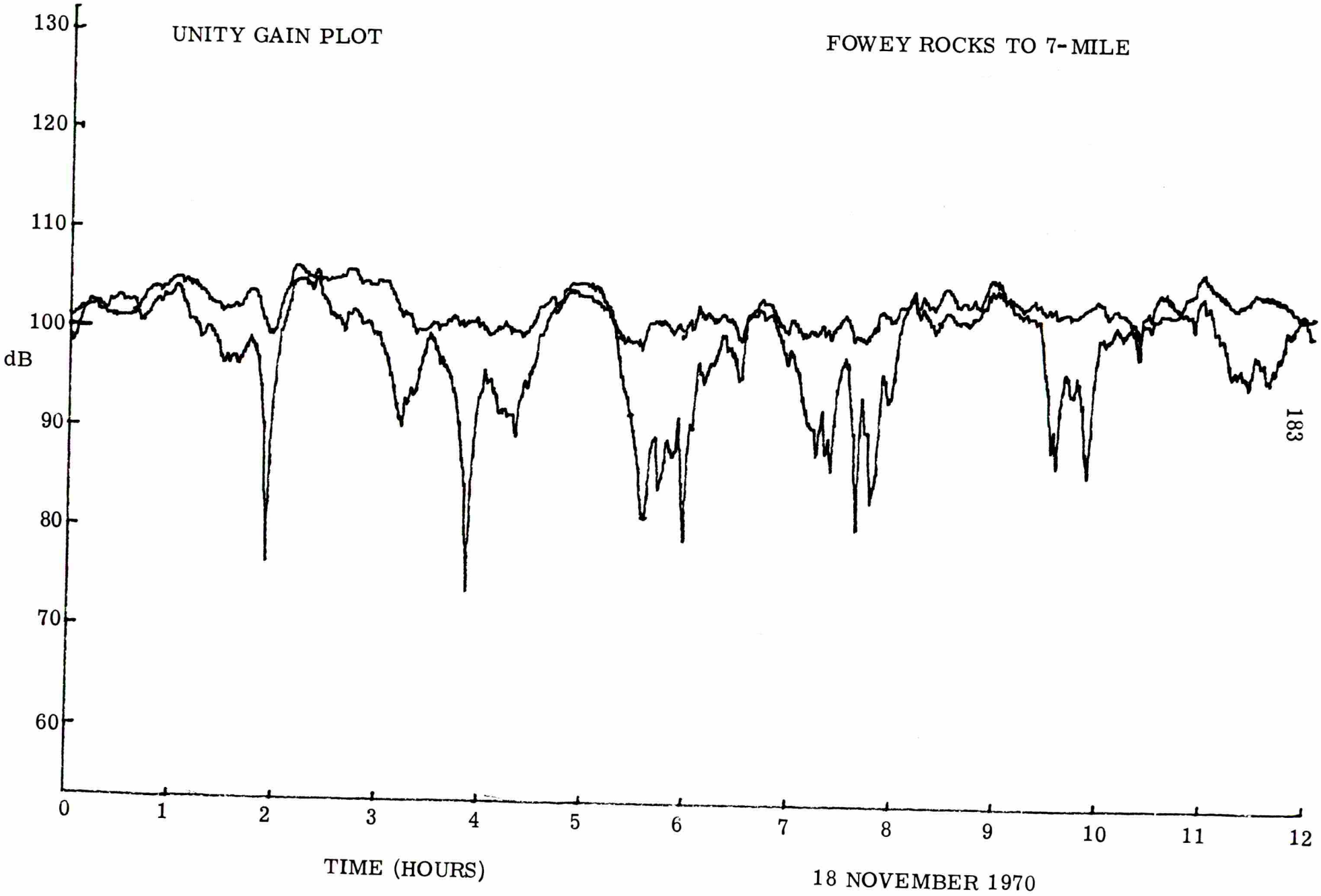
UNITY GAIN PLOT
FOWEY ROCKS TO 7-MILE
130
120
110
100
90
80
70
60
dB
0
1
2
3
4
5
6
7
8
9
10
11
12
TIME (HOURS)
18 NOVEMBER 1970
183

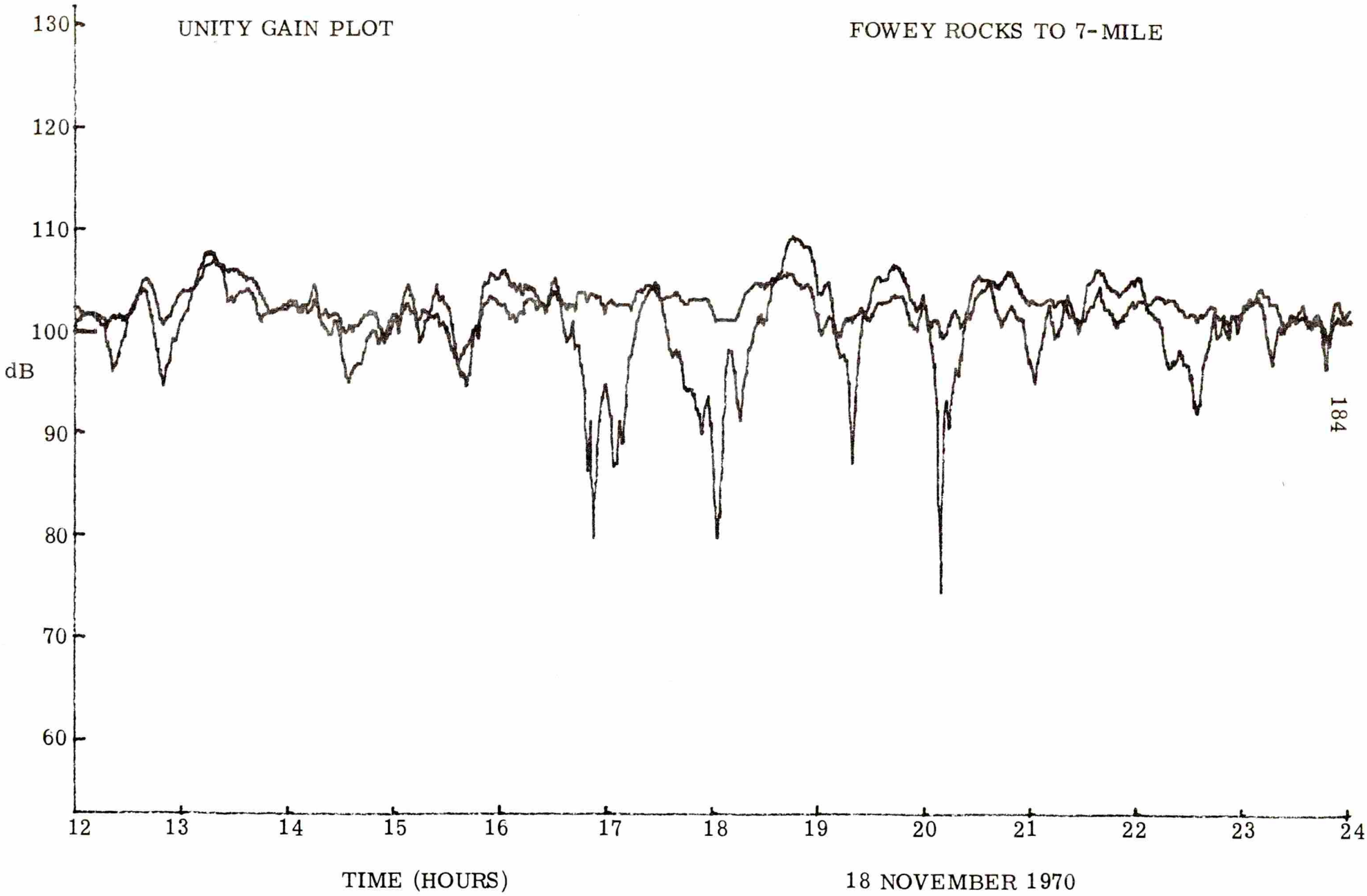
UNITY GAIN PLOT
FOWEY ROCKS TO 7-MILE
130
120
110
100
dB
90
80
70
60
184
12
13
14
15
16
17
18
19
20
21
22
23
24
TIME (HOURS)
18 NOVEMBER 1970

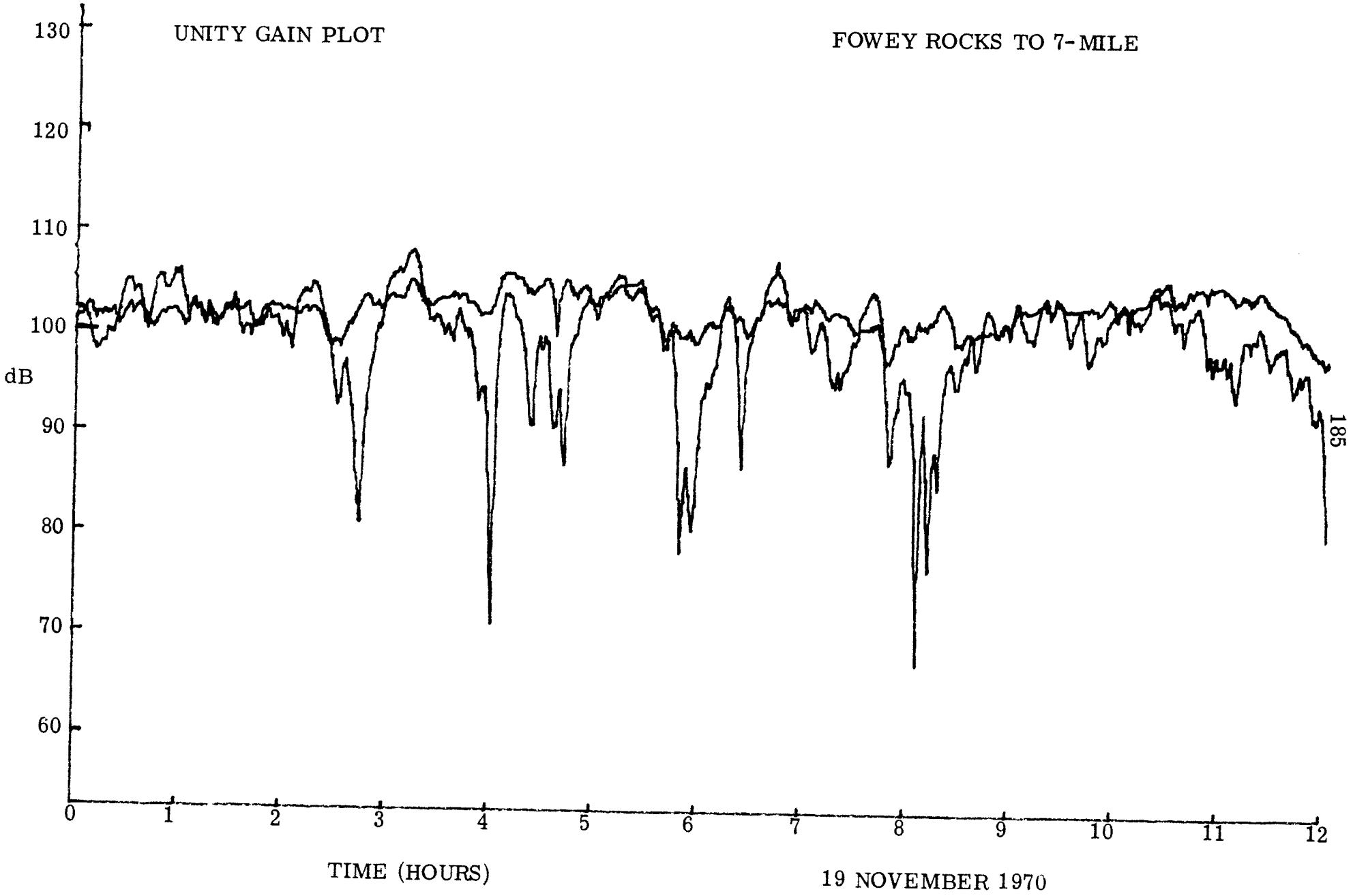
UNITY GAIN PLOT
FOWEY ROCKS TO 7-MILE
130
120
110
100
dB
90
80
70
60
185
0
1
2
3
4
5
6
7
8
9
10
11
12
TIME (HOURS)
19 NOVEMBER 1970

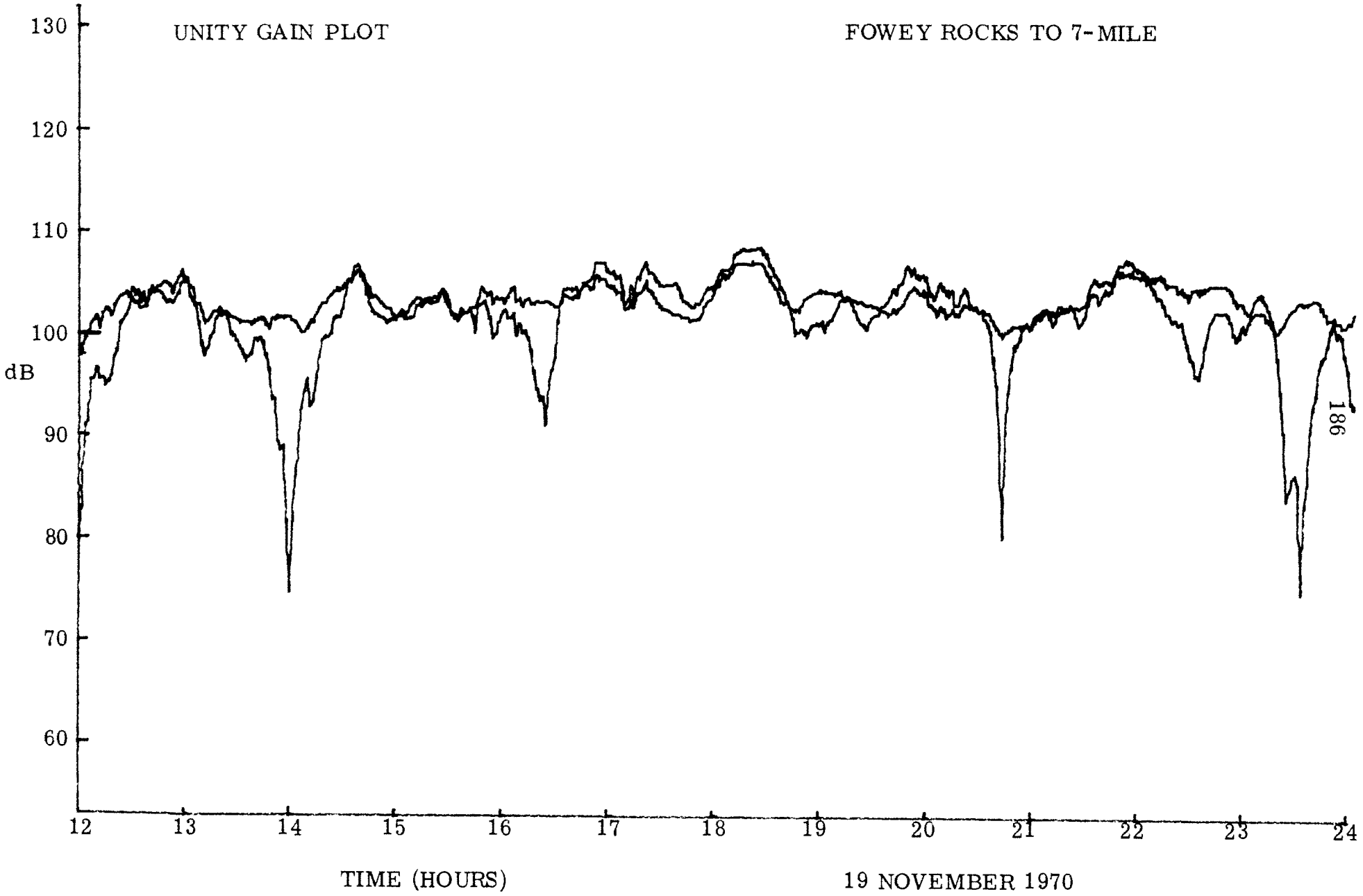
UNITY GAIN PLOT
FOWEY ROCKS TO 7-MILE
130
120
110
100
90
80
70
60
dB
186
12
13
14
15
16
17
18
19
20
21
22
23
24
TIME (HOURS)
19 NOVEMBER 1970

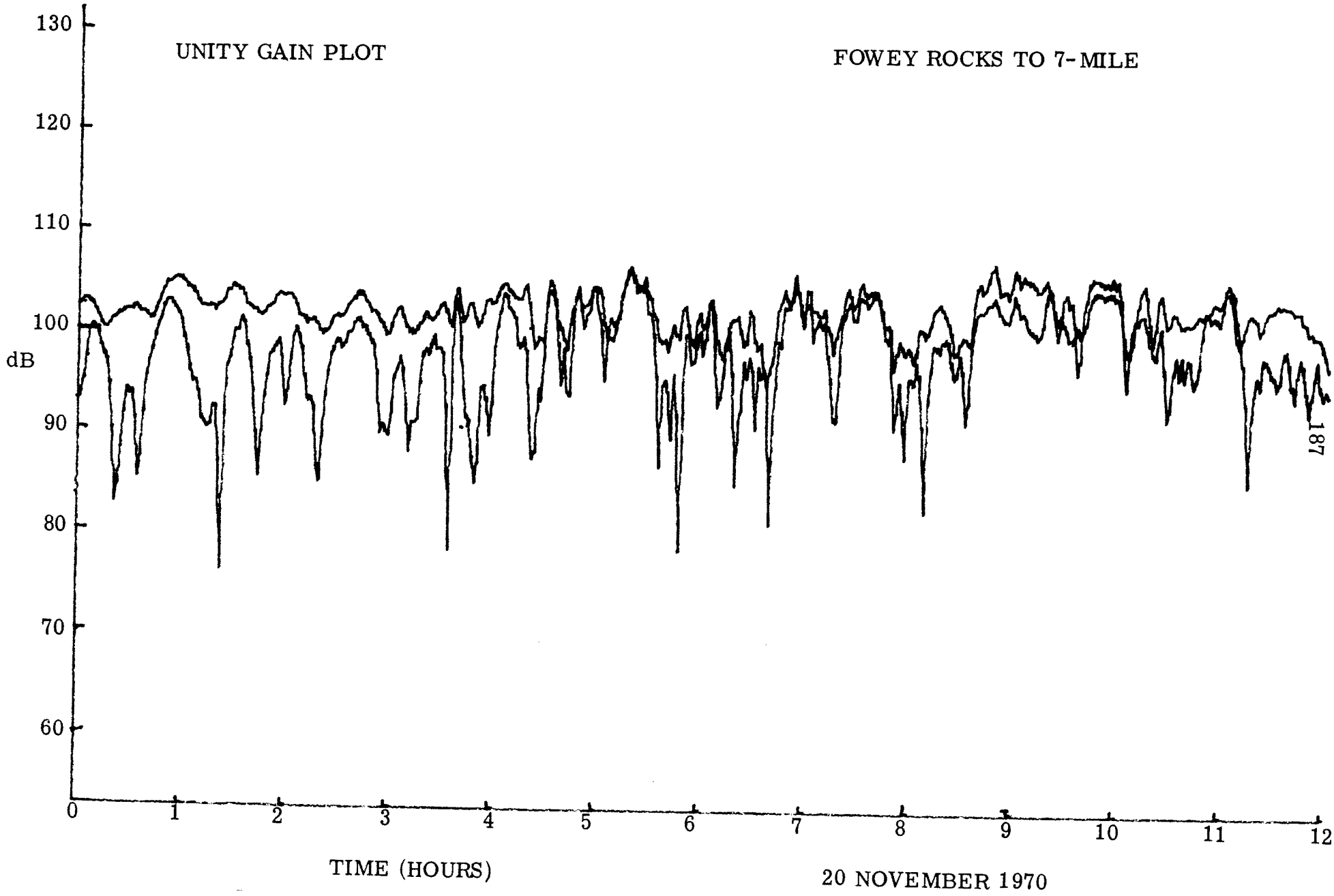
UNITY GAIN PLOT
FOWEY ROCKS TO 7-MILE
130
120
110
100
90
80
70
60
dB
187
0
1
2
3
4
5
6
7
8
9
10
11
12
TIME (HOURS)
20 NOVEMBER 1970

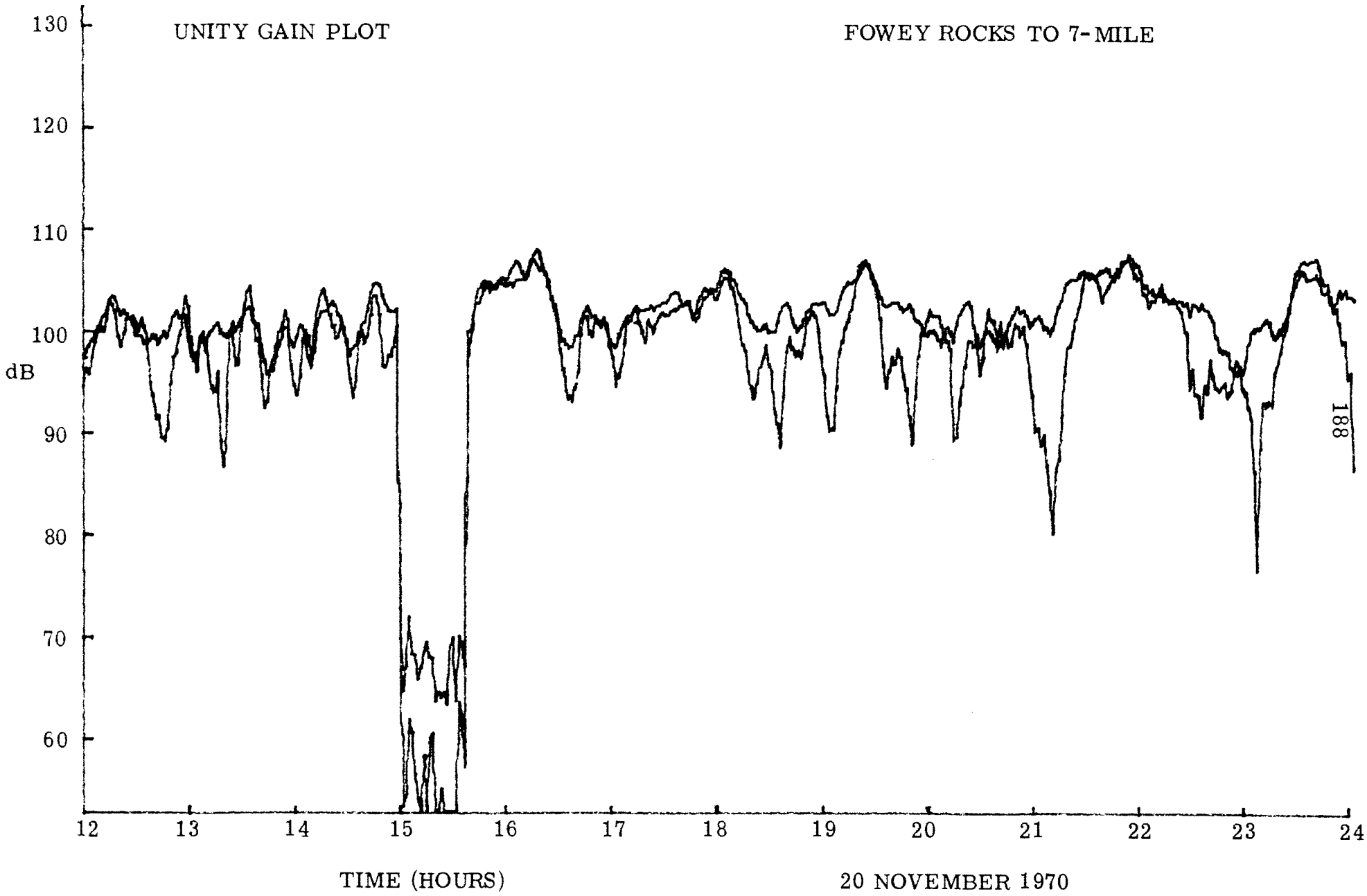
UNITY GAIN PLOT
FOWEY ROCKS TO 7-MILE
130
120
110
100
dB
90
80
70
60
188
12
13
14
15
16
17
18
19
20
21
22
23
24
TIME (HOURS)
20 NOVEMBER 1970

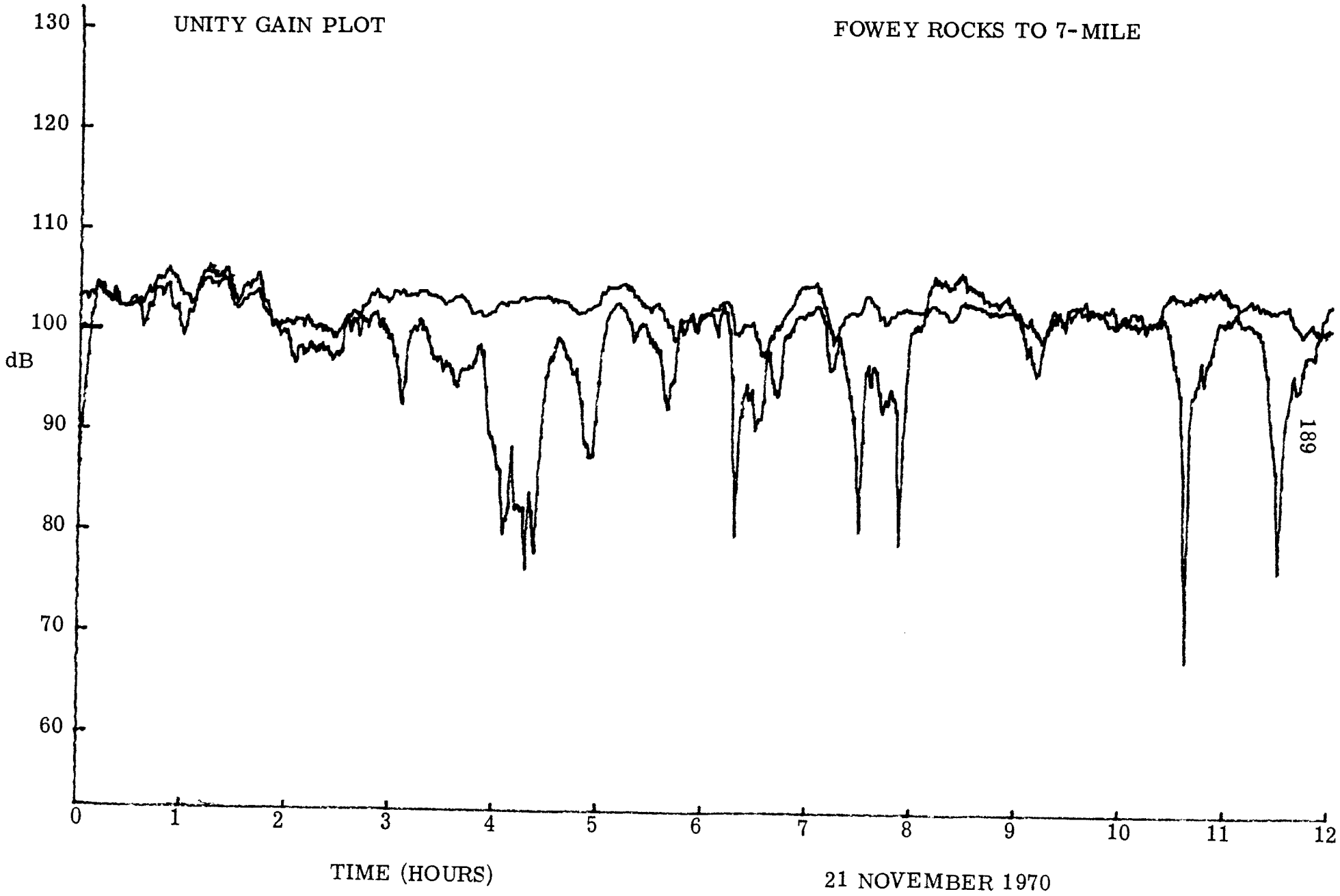
UNITY GAIN PLOT
FOWEY ROCKS TO 7-MILE
130
120
110
100
dB
90
80
70
60
189
0
1
2
3
4
5
6
7
8
9
10
11
12
TIME (HOURS)
21 NOVEMBER 1970

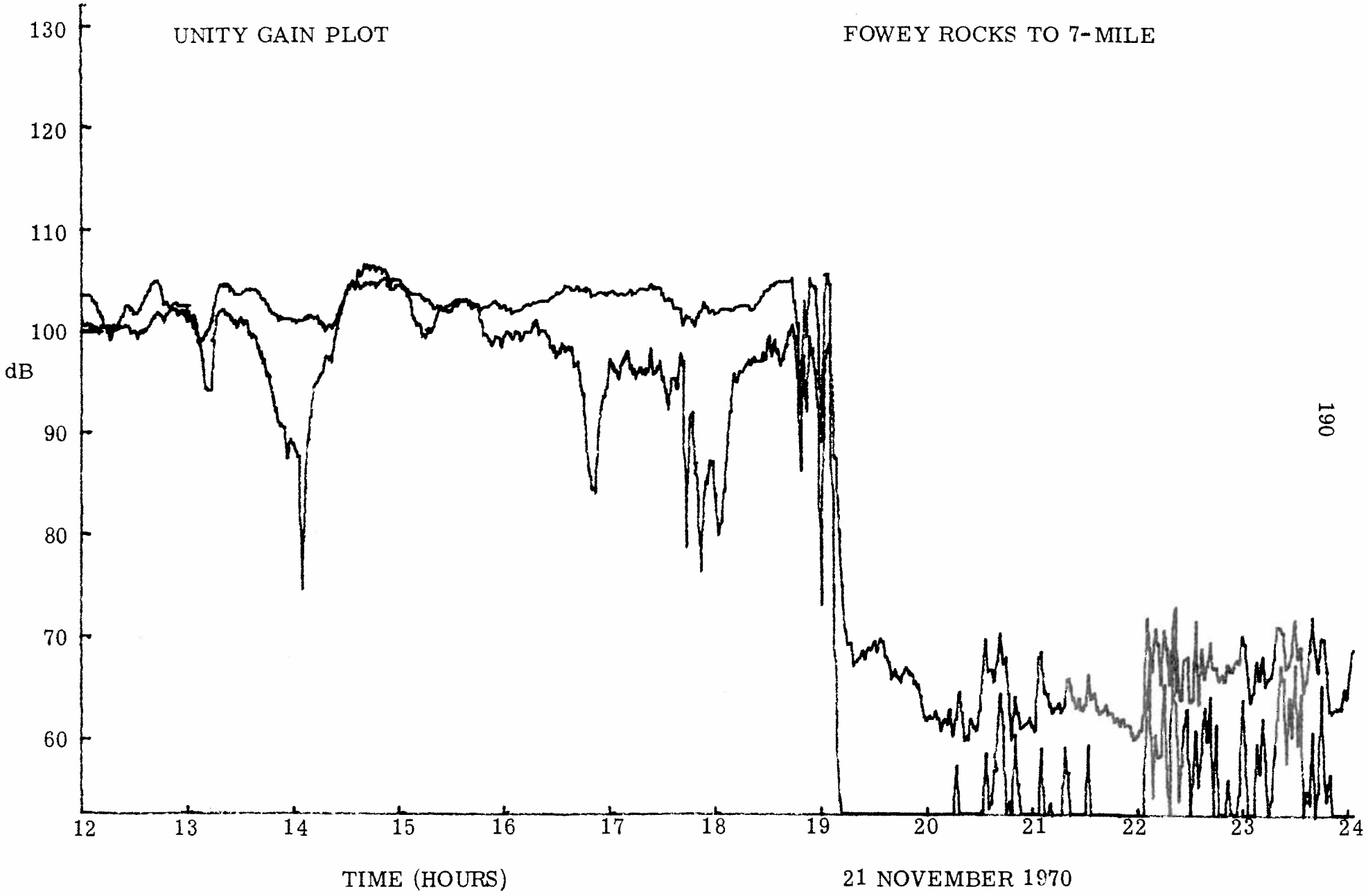
UNITY GAIN PLOT
FOWEY ROCKS TO 7-MILE
130
120
110
100
dB
90
80
70
60
12
13
14
15
16
17
18
19
20
21
22
23
24
TIME (HOURS)
21 NOVEMBER 1970
190

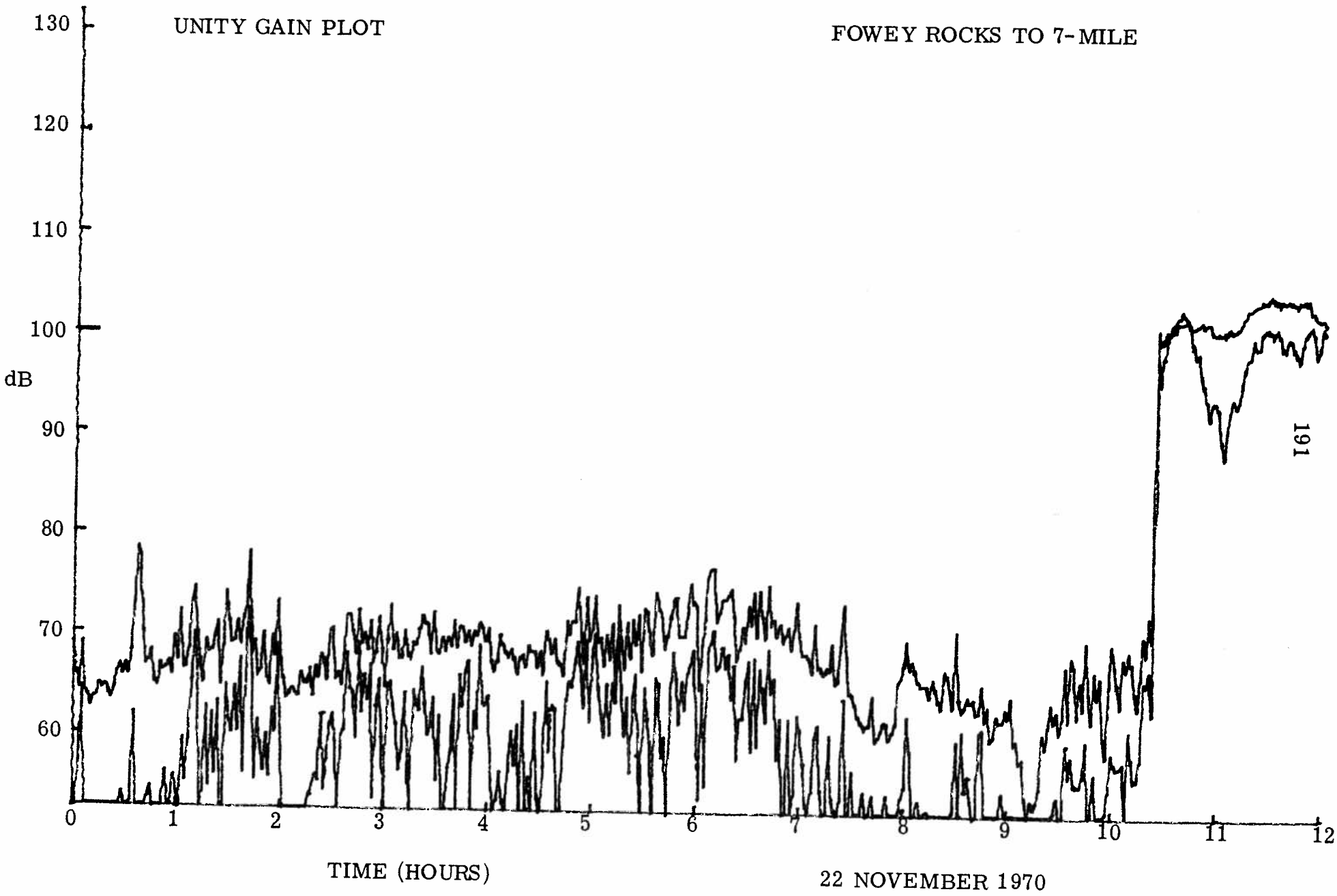
UNITY GAIN PLOT
FOWEY ROCKS TO 7-MILE
130
120
110
100
dB
90
80
70
60
0
1
2
3
4
5
6
7
8
9
10
11
12
TIME (HOURS)
22 NOVEMBER 1970
191

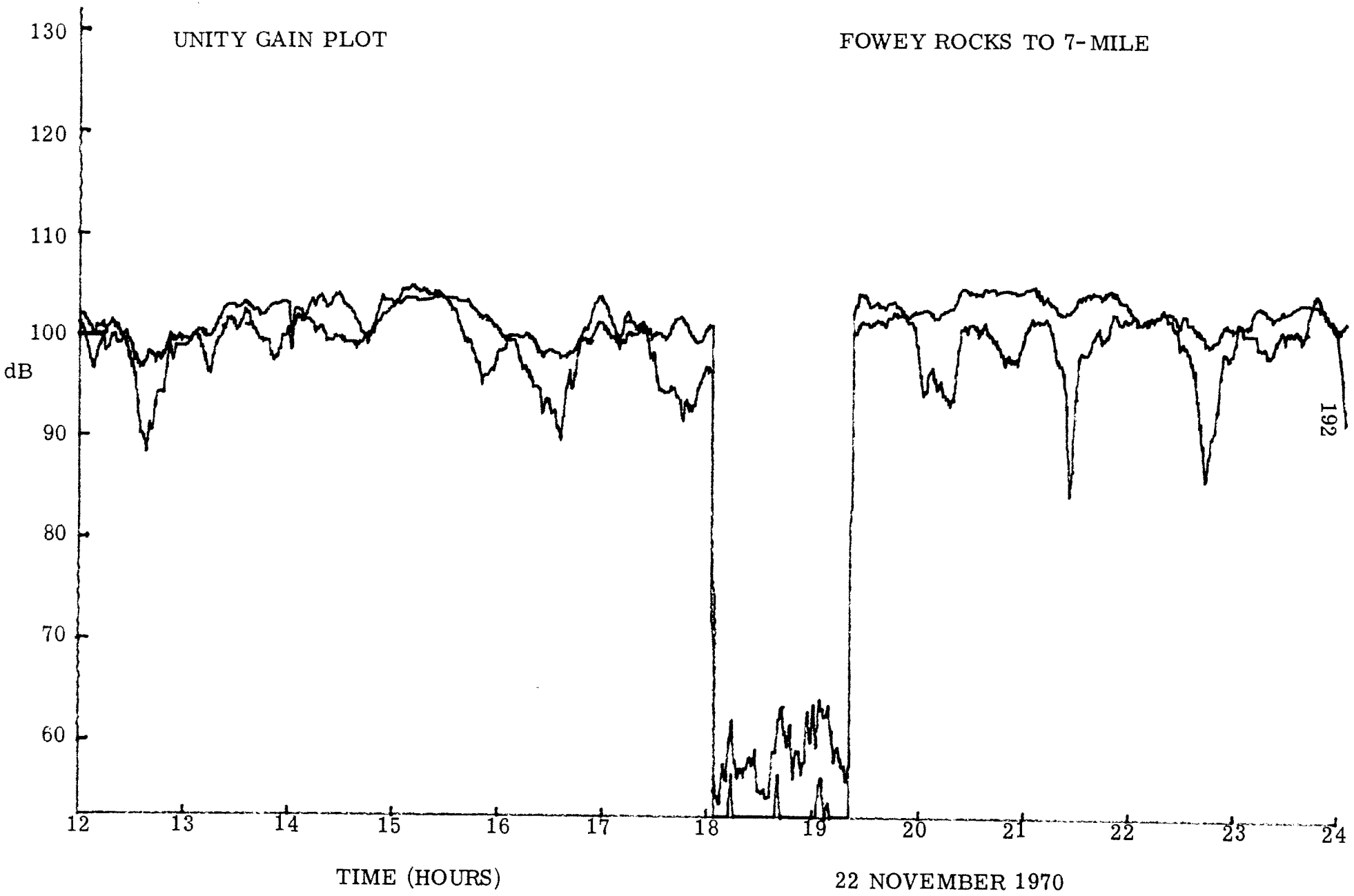
UNITY GAIN PLOT
FOWEY ROCKS TO 7-MILE
130
120
110
100
90
80
70
60
dB
192
12
13
14
15
16
17
18
19
20
21
22
23
24
TIME (HOURS)
22 NOVEMBER 1970

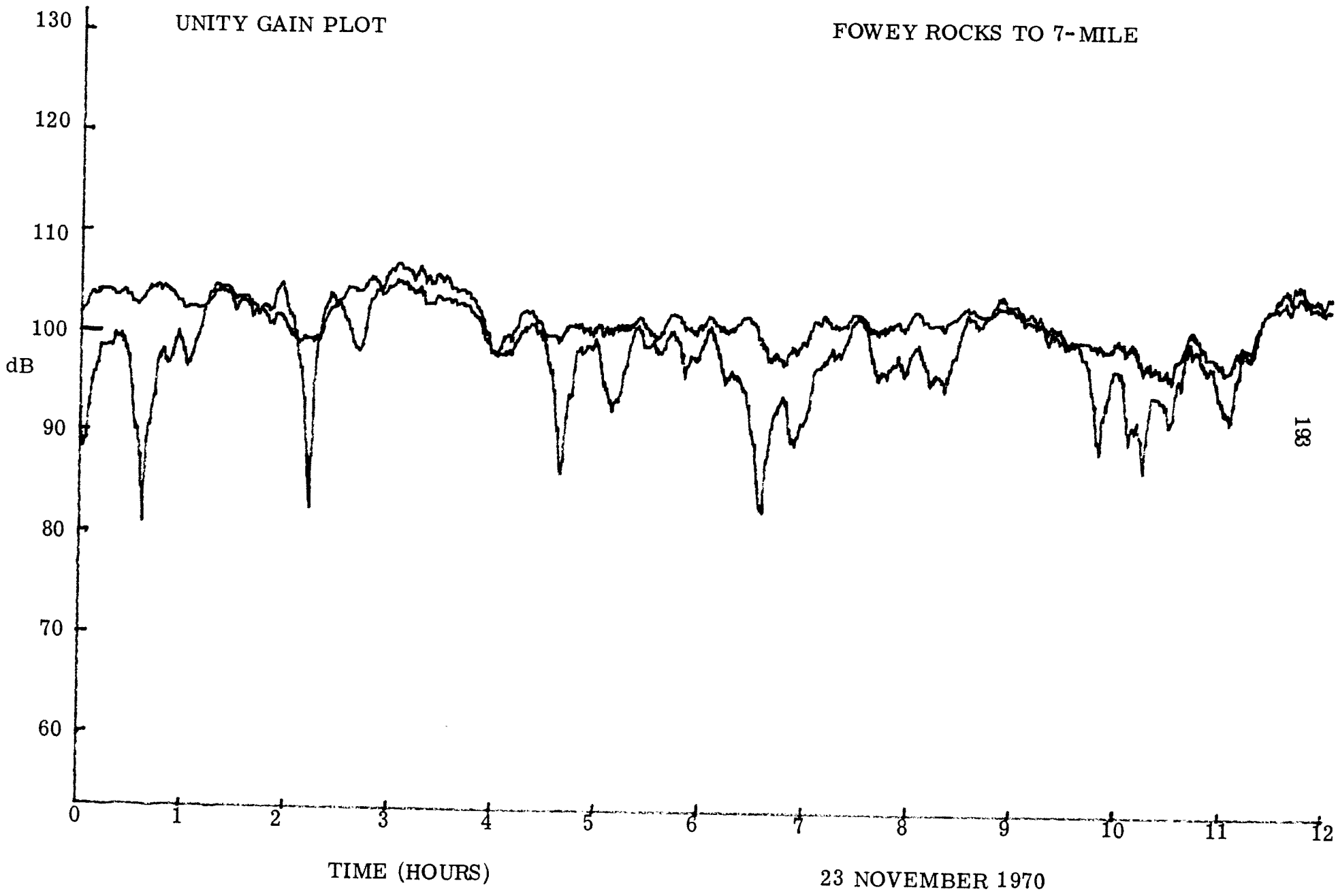
UNITY GAIN PLOT
FOWEY ROCKS TO 7-MILE
130
120
110
100
90
80
70
60
dB
0
1
2
3
4
5
6
7
8
9
10
11
12
TIME (HOURS)
23 NOVEMBER 1970
183

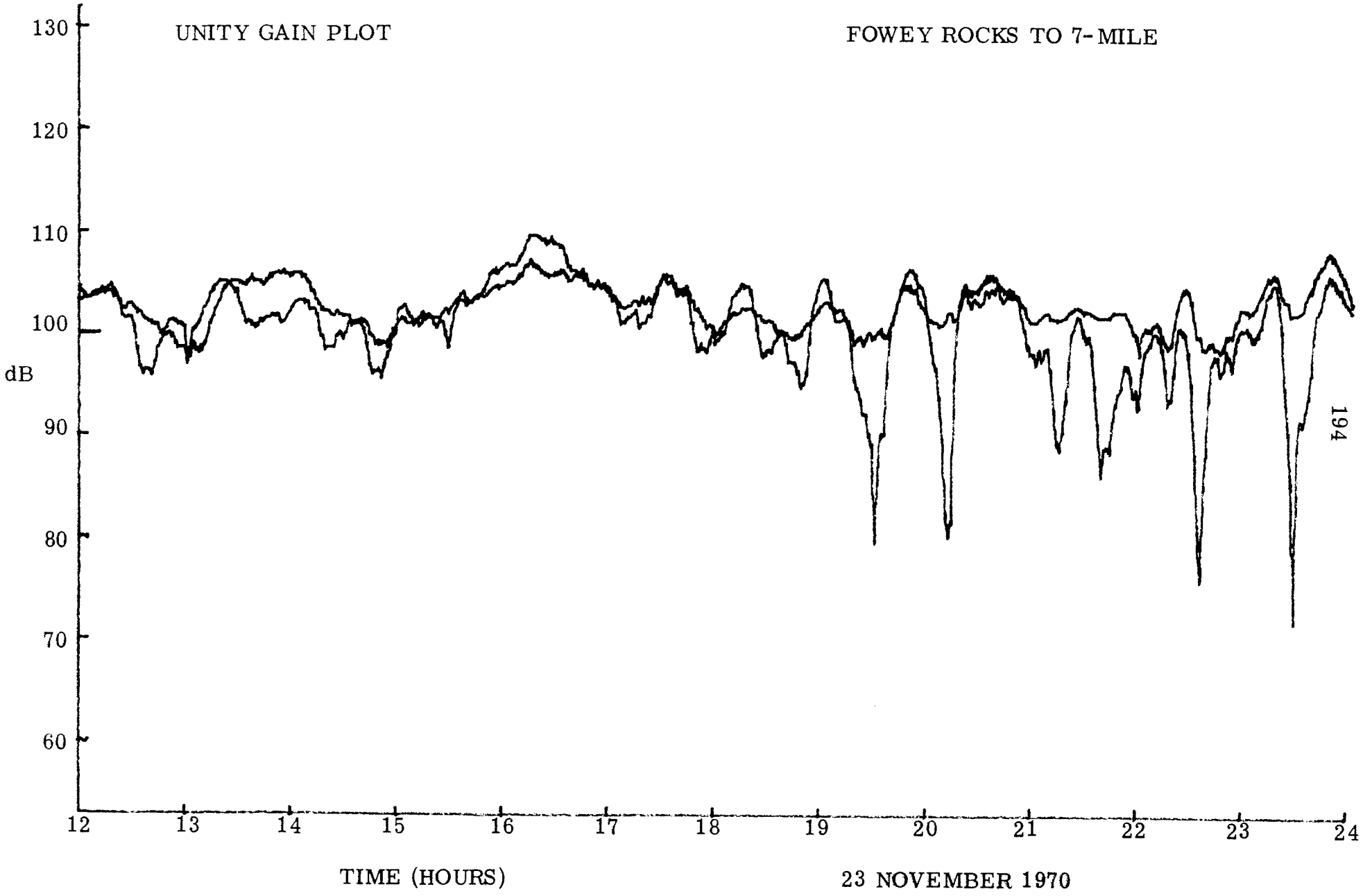
UNITY GAIN PLOT
FOWEY ROCKS TO 7-MILE
130
120
110
100
dB
90
80
70
60
194
12
13
14
15
16
17
18
19
20
21
22
23
24
TIME (HOURS)
23 NOVEMBER 1970

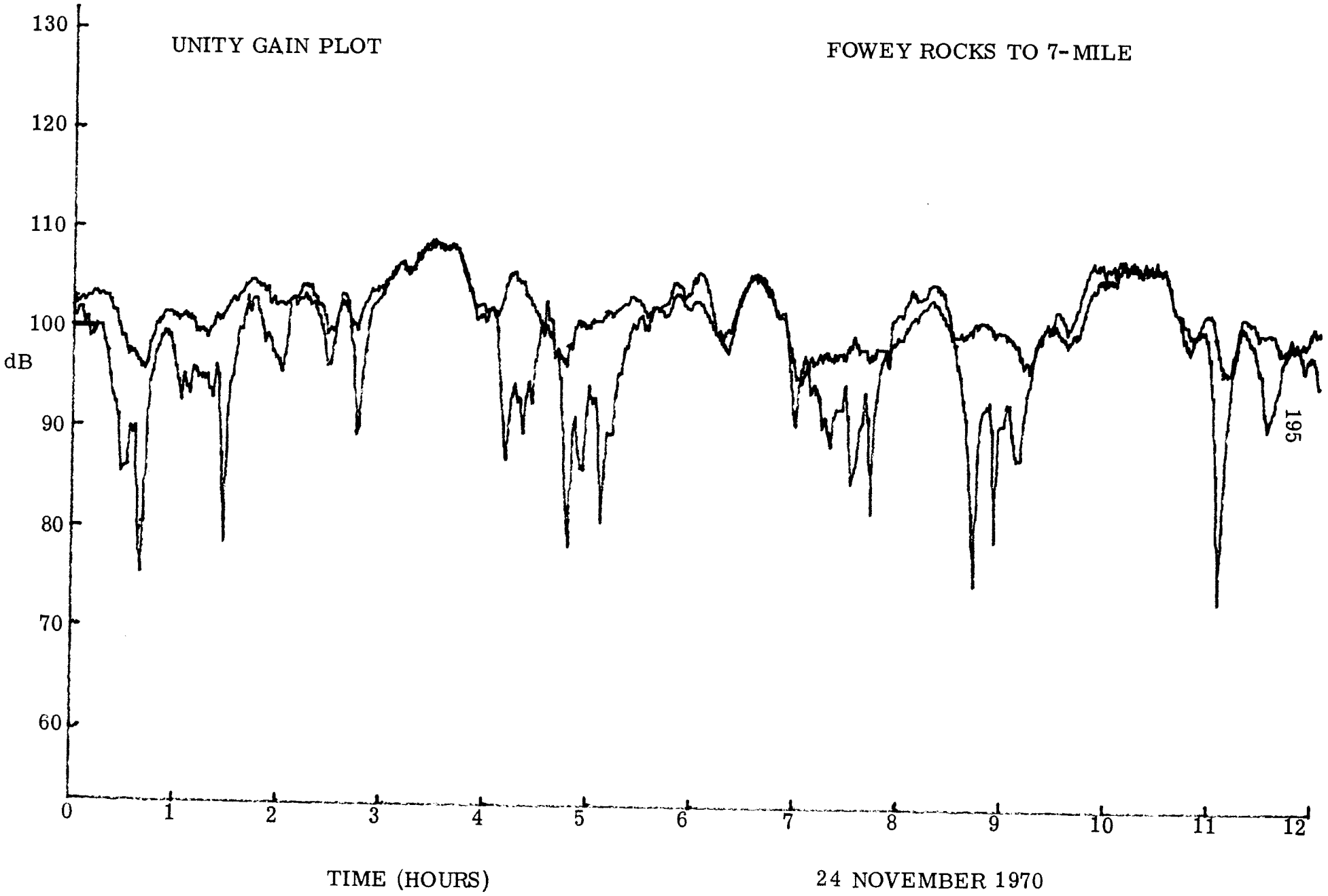
UNITY GAIN PLOT
FOWEY ROCKS TO 7-MILE
130
120
110
100
dB
90
80
70
60
195
0
1
2
3
4
5
6
7
8
9
10
11
12
TIME (HOURS)
24 NOVEMBER 1970

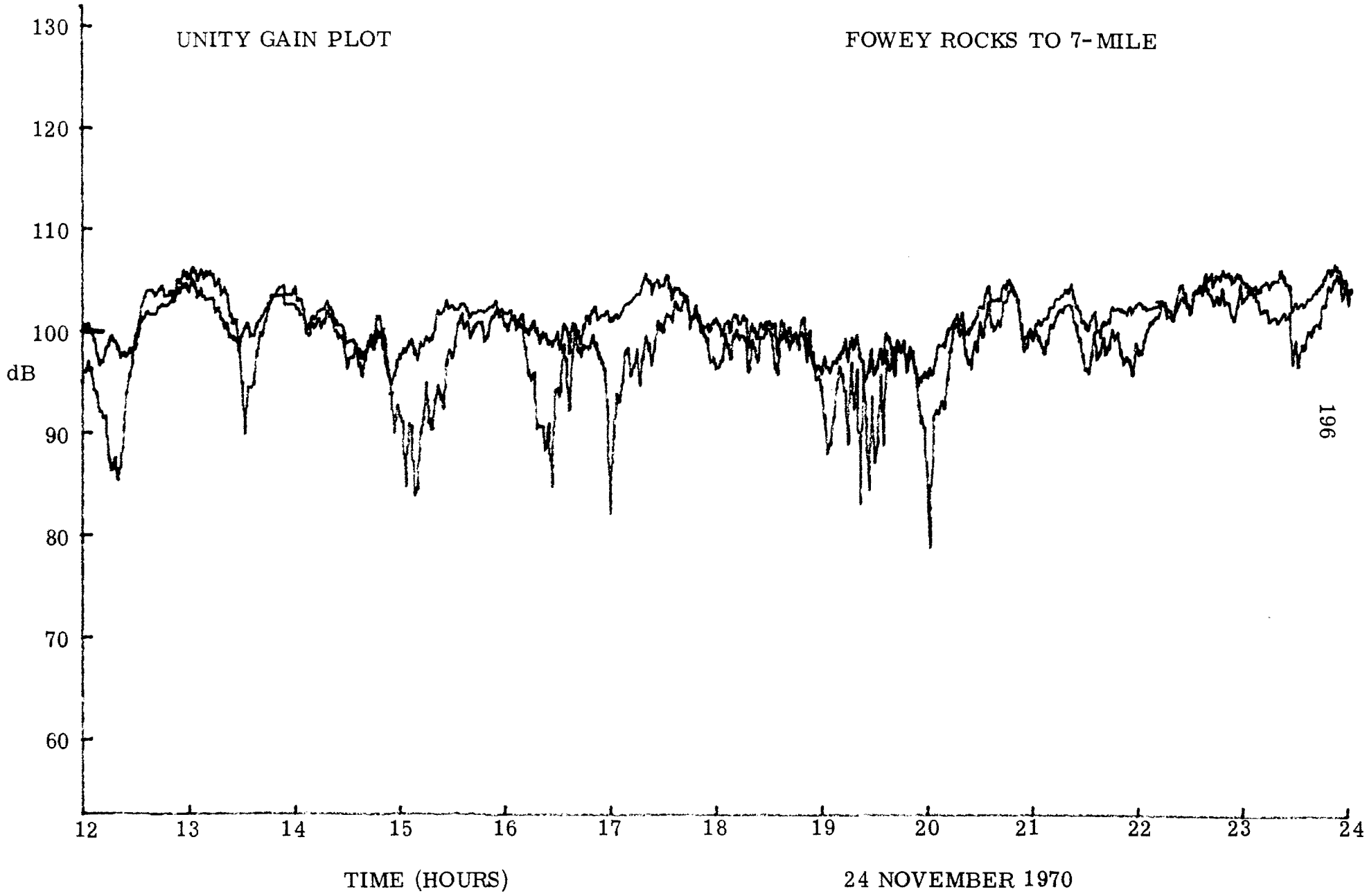
UNITY GAIN PLOT
FOWEY ROCKS TO 7-MILE
130
120
110
100
90
80
70
60
dB
196
12
13
14
15
16
17
18
19
20
21
22
23
24
TIME (HOURS)
24 NOVEMBER 1970

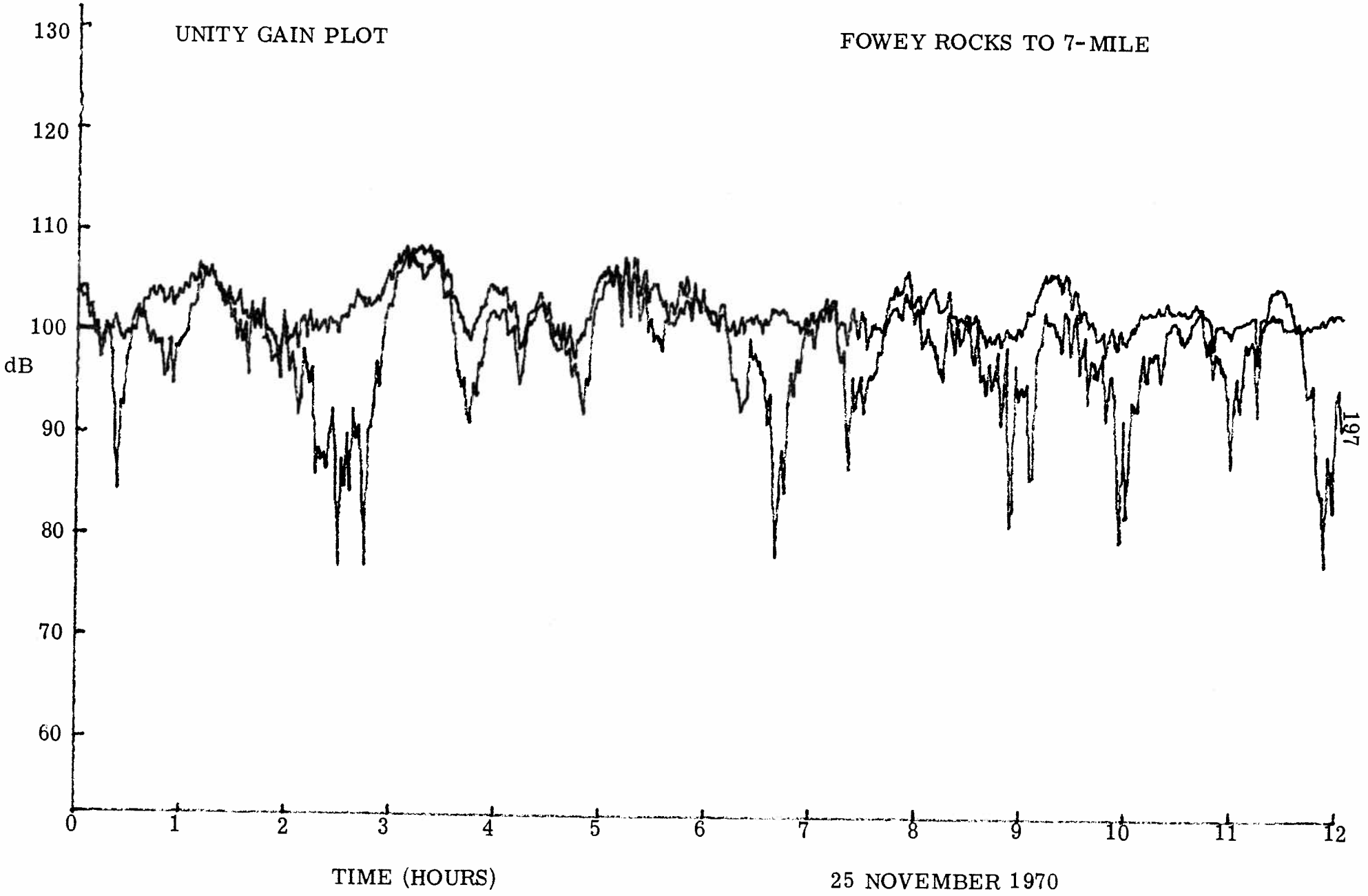
UNITY GAIN PLOT
FOWEY ROCKS TO 7-MILE
130
120
110
100
90
80
70
60
dB
0
1
2
3
4
5
6
7
8
9
10
11
12
TIME (HOURS)
25 NOVEMBER 1970
197

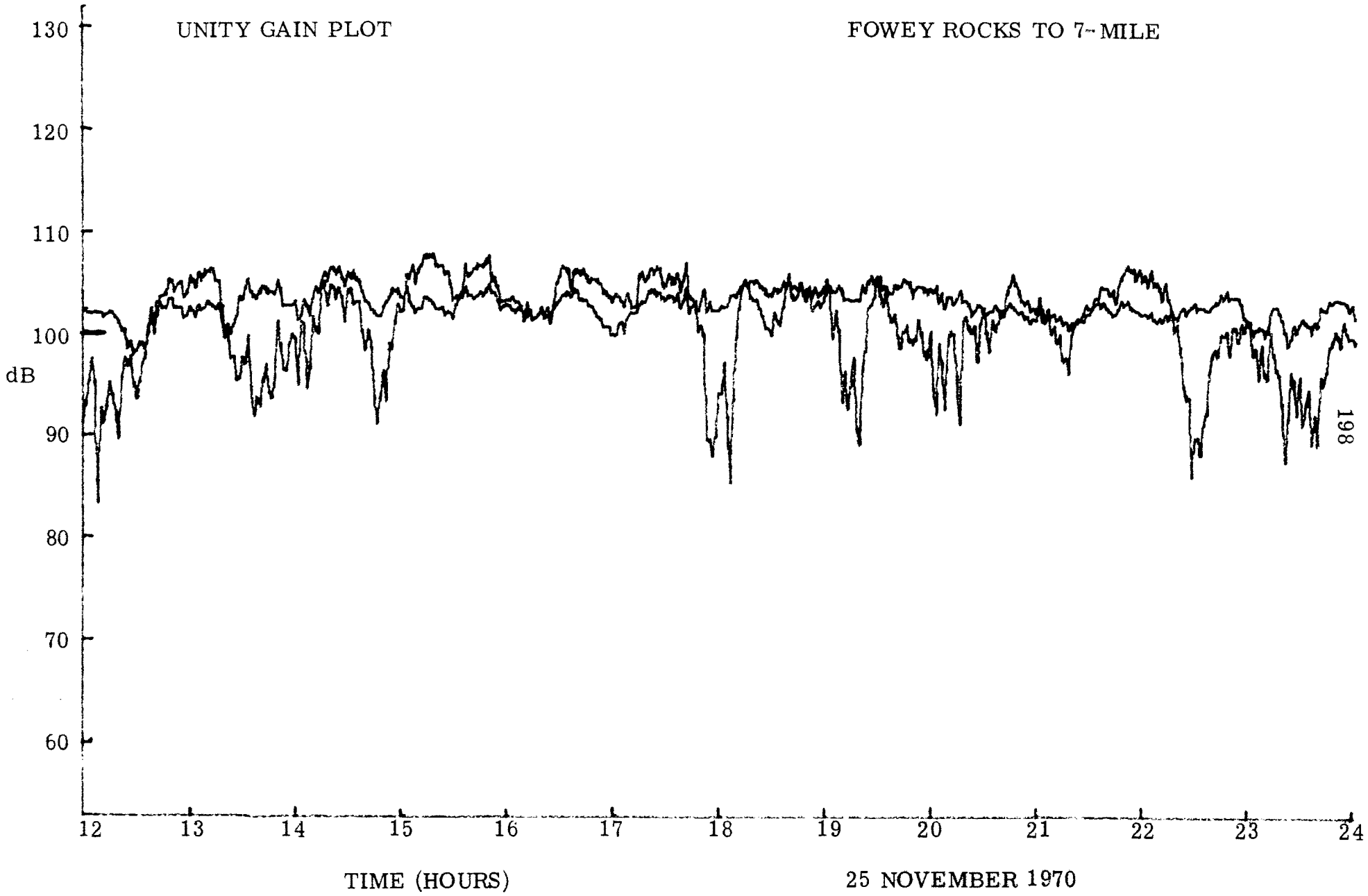
UNITY GAIN PLOT
FOWEY ROCKS TO 7-MILE
130
120
110
100
dB
90
80
70
60
198
12
13
14
15
16
17
18
19
20
21
22
23
24
TIME (HOURS)
25 NOVEMBER 1970

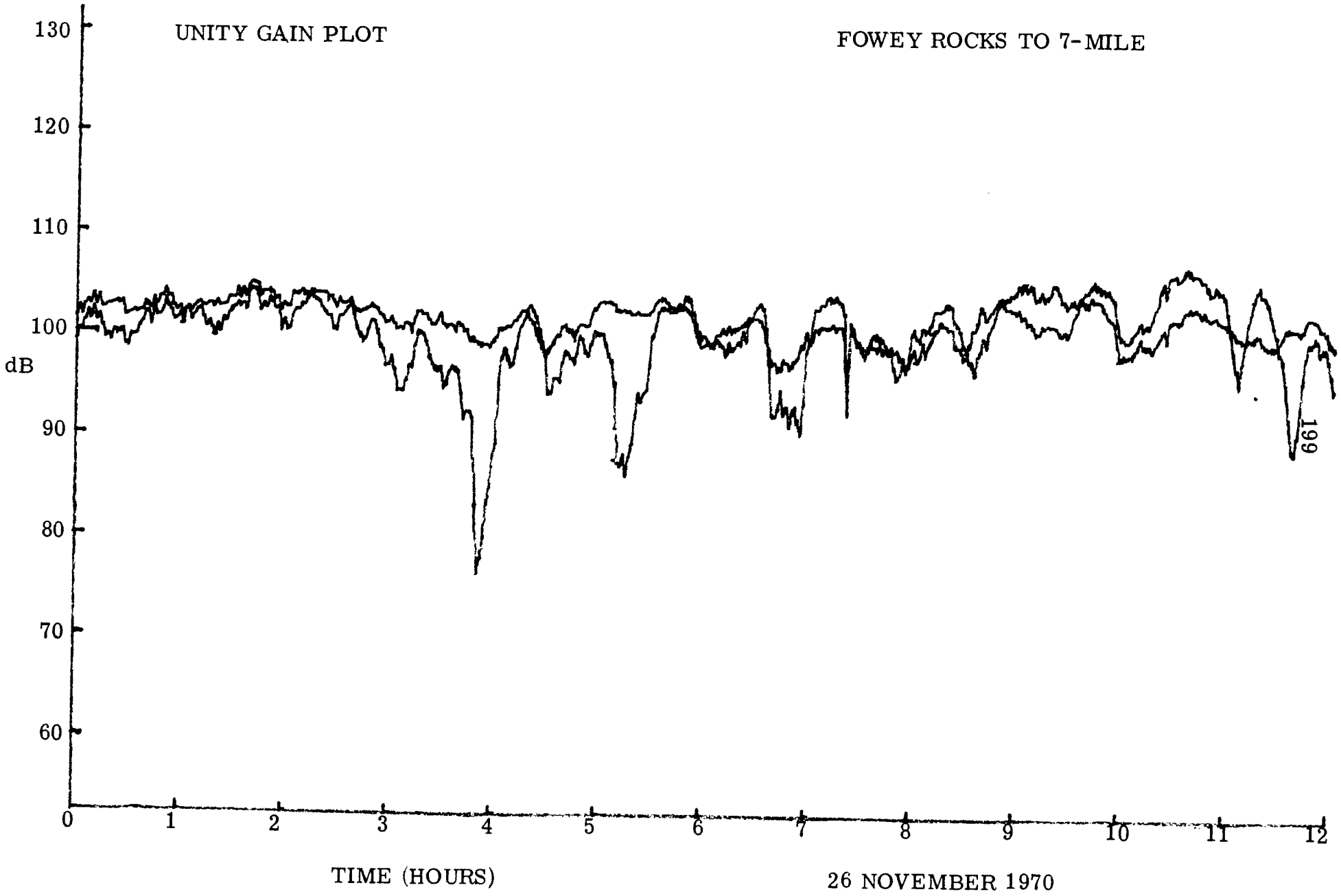
UNITY GAIN PLOT
FOWEY ROCKS TO 7-MILE
130
120
110
100
dB
90
80
70
60
199
0
1
2
3
4
5
6
7
8
9
10
11
12
TIME (HOURS)
26 NOVEMBER 1970

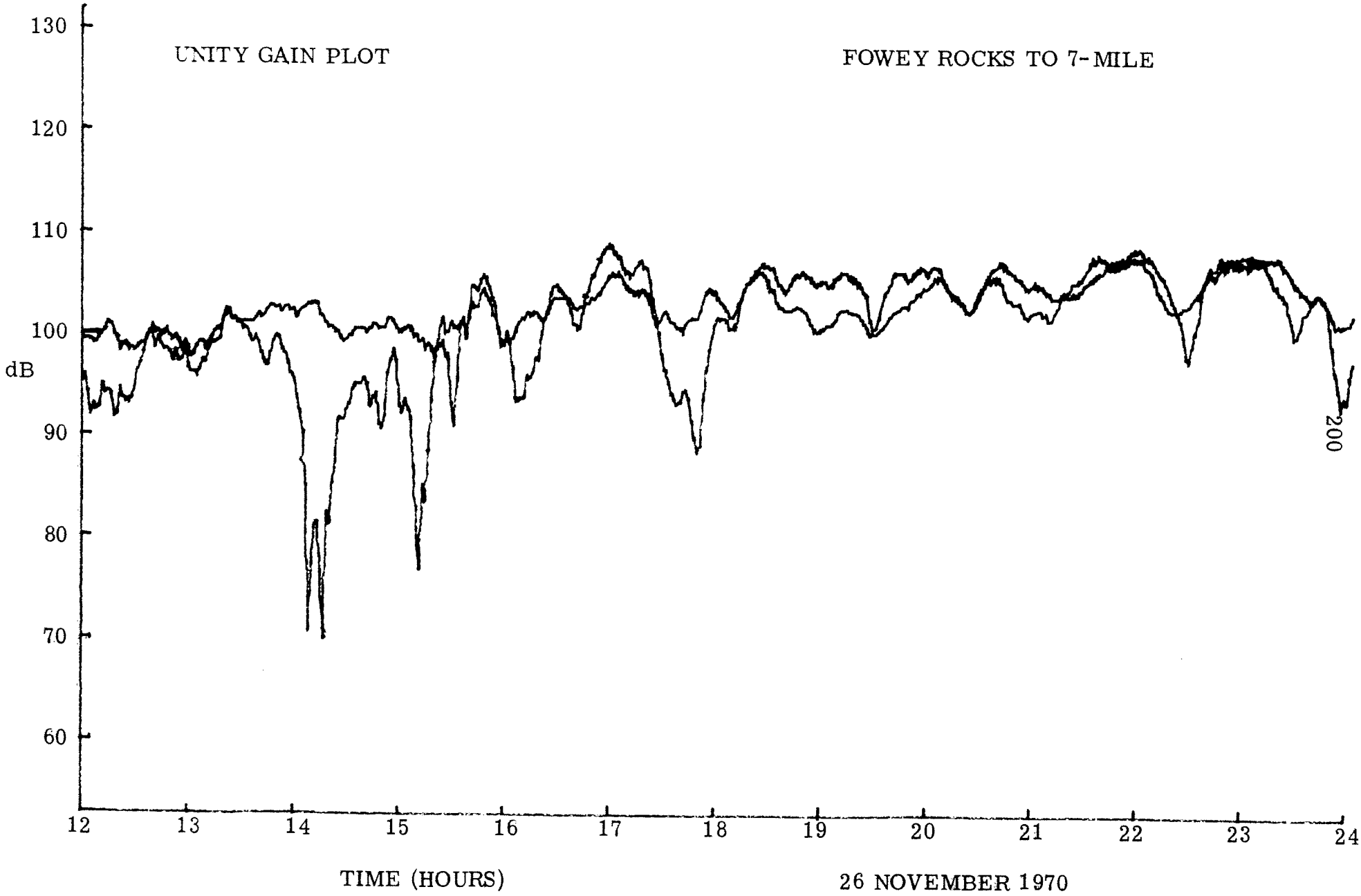
UNITY GAIN PLOT
FOWEY ROCKS TO 7-MILE
130
120
110
100
dB
90
80
70
60
200
12
13
14
15
16
17
18
19
20
21
22
23
24
TIME (HOURS)
26 NOVEMBER 1970

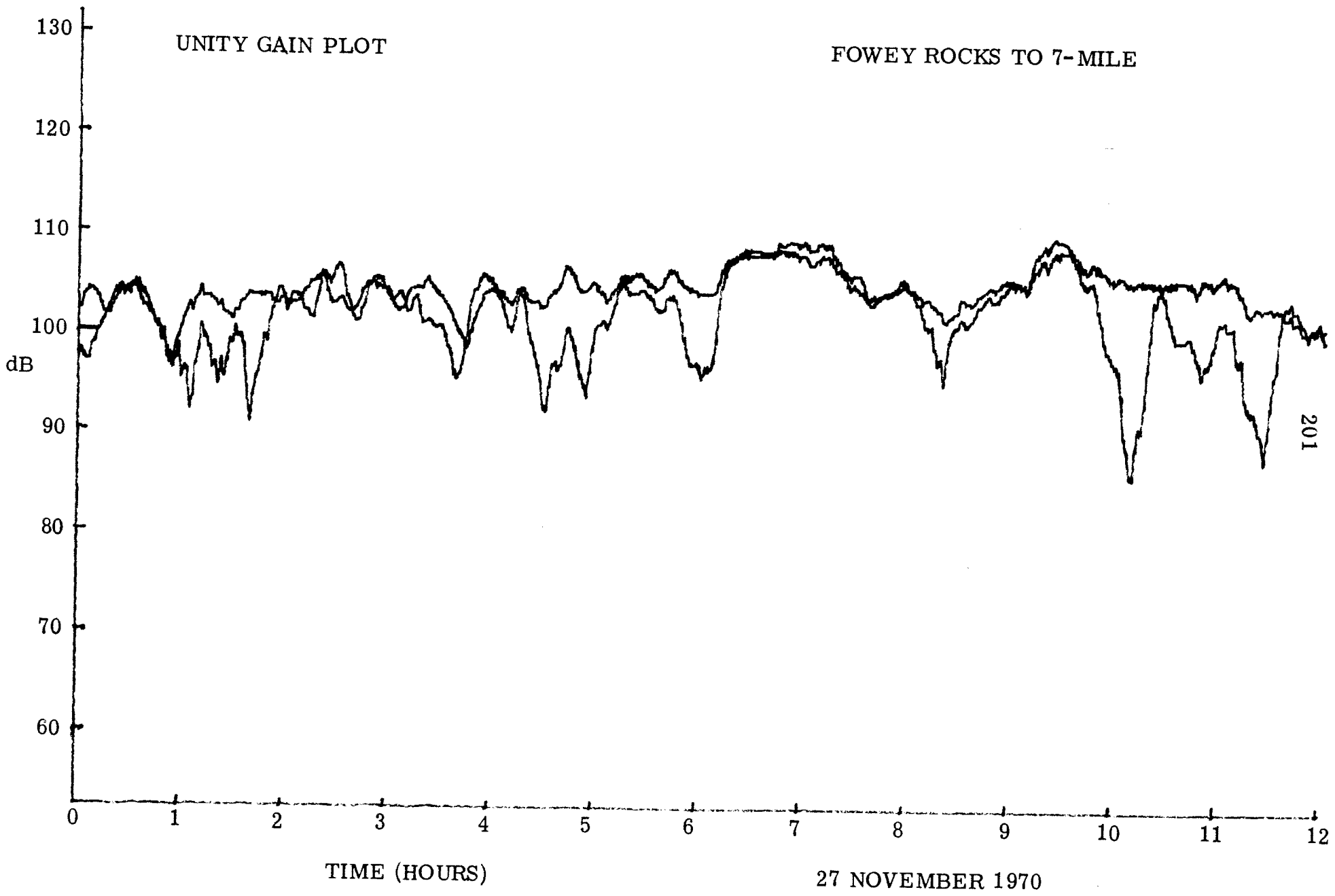
UNITY GAIN PLOT
FOWEY ROCKS TO 7-MILE
130
120
110
100
dB
90
80
70
60
201
0
1
2
3
4
5
6
7
8
9
10
11
12
TIME (HOURS)
27 NOVEMBER 1970

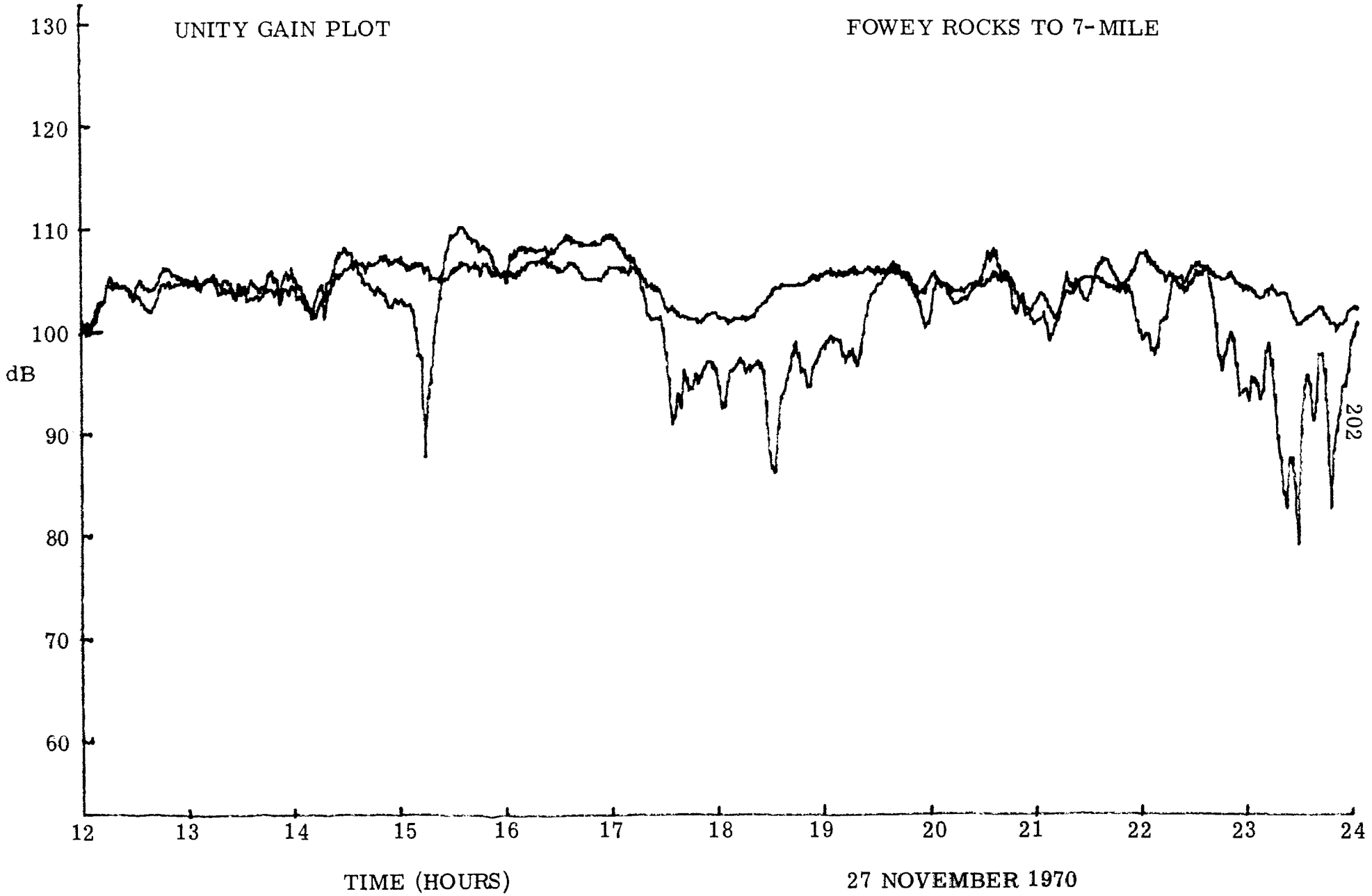
UNITY GAIN PLOT
FOWEY ROCKS TO 7-MILE
130
120
110
100
dB
90
80
70
60
202
12
13
14
15
16
17
18
19
20
21
22
23
24
TIME (HOURS)
27 NOVEMBER 1970

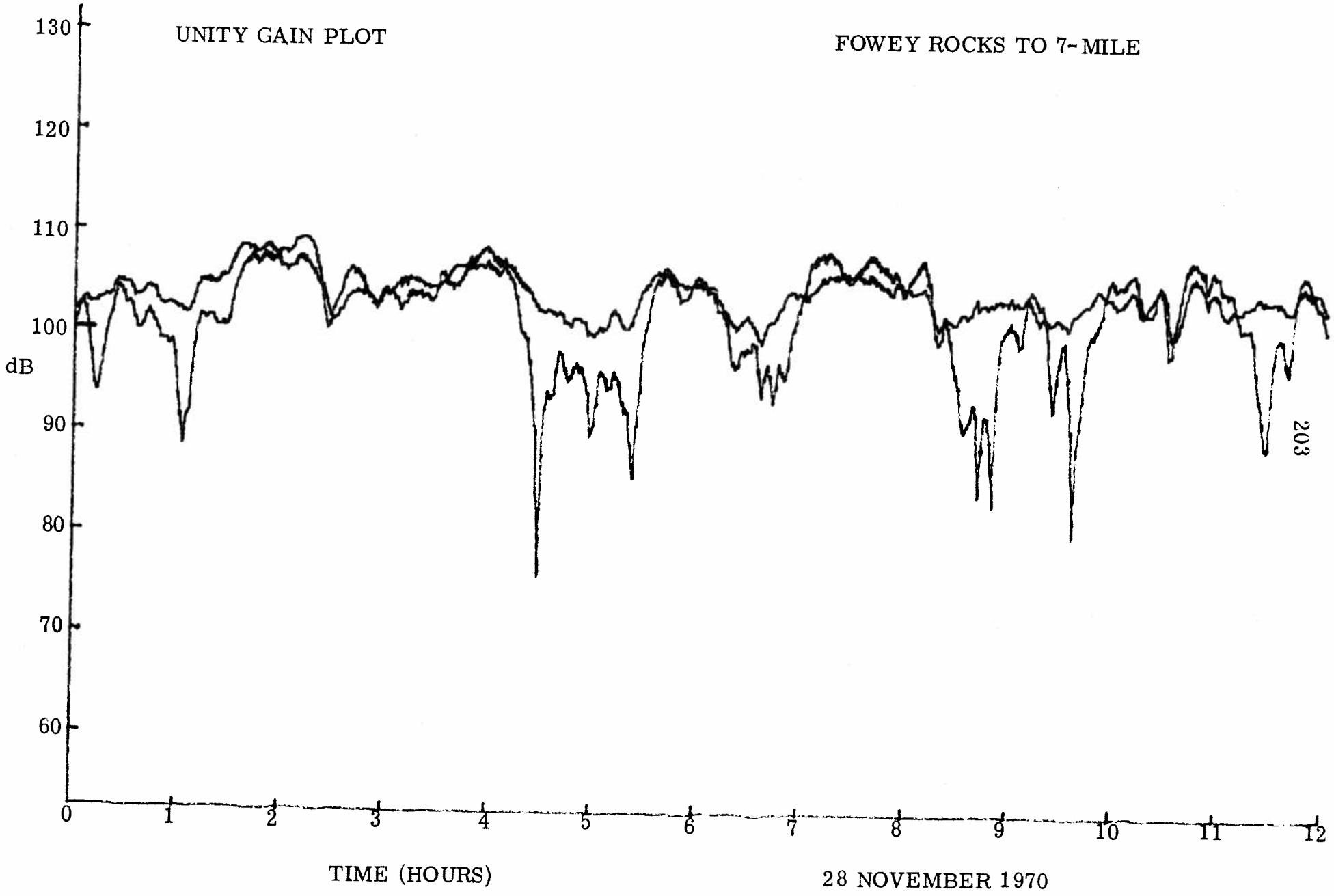
UNITY GAIN PLOT
FOWEY ROCKS TO 7-MILE
130
120
110
100
dB
90
80
70
60
0
1
2
3
4
5
6
7
8
9
10
11
12
TIME (HOURS)
28 NOVEMBER 1970
203

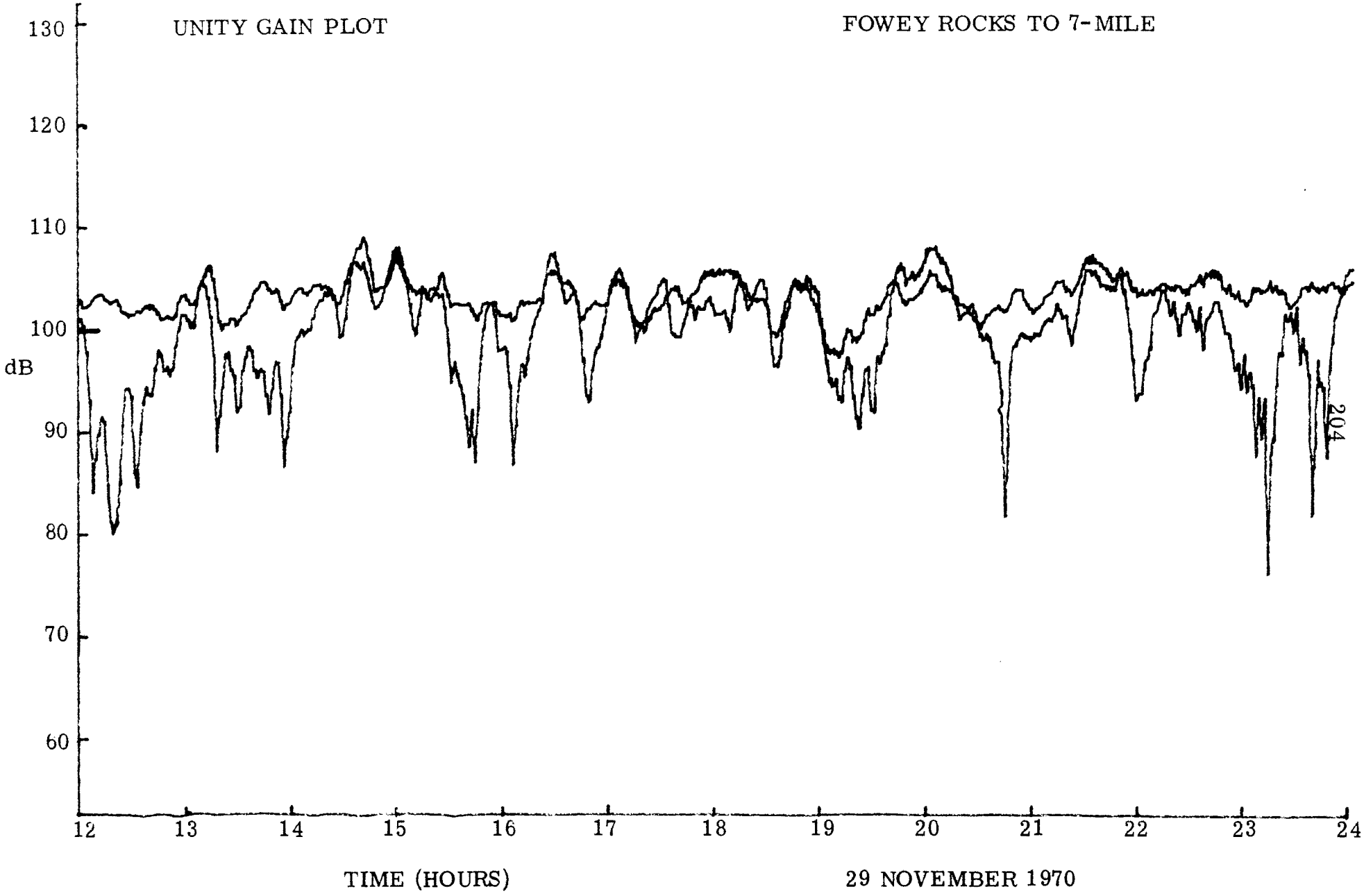
UNITY GAIN PLOT
FOWEY ROCKS TO 7-MILE
130
120
110
100
90
80
70
60
dB
2704
12
13
14
15
16
17
18
19
20
21
22
23
24
TIME (HOURS)
29 NOVEMBER 1970

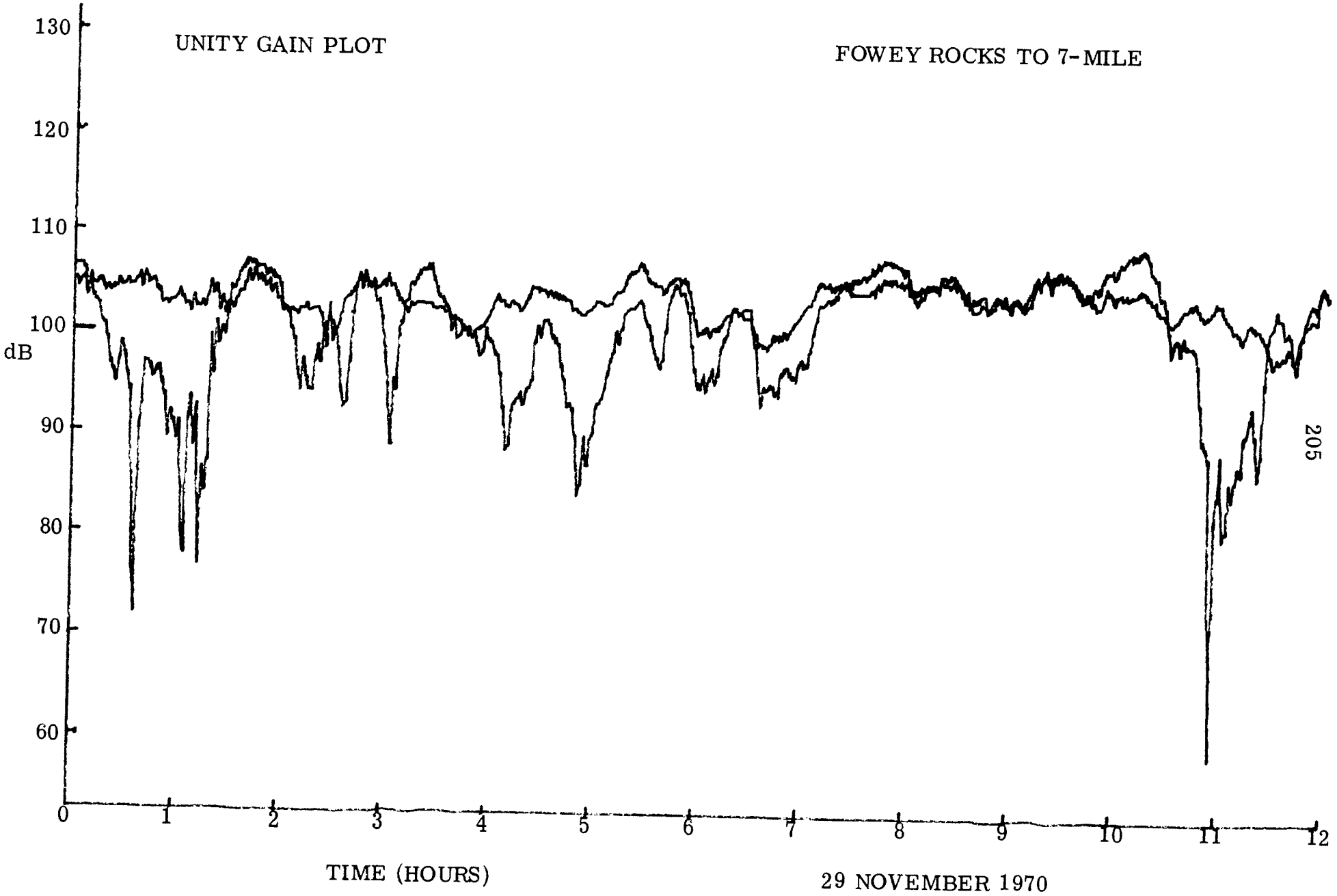
UNITY GAIN PLOT
FOWEY ROCKS TO 7-MILE
130
120
110
100
90
80
70
60
dB
0
1
2
3
4
5
6
7
8
9
10
11
12
TIME (HOURS)
29 NOVEMBER 1970
205

DISTRIBUTION LIST

	No. of Copies
Office of Naval Research (Code 468) (Code 102-OS) (Code 480) Navy Department Washington, D. C. 20360	1 1 1
Director, Naval Research Laboratory Technical Information Division Washington, D. C. 20390	6
Director Office of Naval Research Branch Office 1030 East Green Street Pasadena, California 91101	1
Office of Naval Research San Francisco Area Office 1076 Mission Street San Francisco, California 94103	1
Director Office of Naval Research Branch Office 495 Summer Street Boston, Massachusetts 02210	1
Office of Naval Research New York Area Office 207 West 24th Street New York, New York 10011	1
Director Office of Naval Research Branch Office 536 S. Clark Street Chicago, Illinois 60605	1
Director Naval Research Laboratory Attn: Library, Code 2029 (ONRL) Washington, D. C. 20390	8

DISTRIBUTION LIST (Cont.)

	No. of Copies
Commander Naval Ordnance Laboratory Acoustics Division White Oak, Silver Spring, Maryland 20907 Attn: Dr. Zaka Slawsky	1
Commanding Officer Naval Ship Research & Development Center Annapolis, Maryland 21401	1
Commander Naval Undersea Research & Development Center San Diego, California 92132 Attn: Dr. Dan Andrews Mr. Henry Aurand	2
Chief Scientist Navy Underwater Sound Reference Division P. O. Box 8337 Orlando, Florida 32800	1
Commanding Officer and Director Navy Underwater Systems Center Fort Trumbull New London, Connecticut 06321	1
Commander Naval Air Development Center Johnsville, Warminster, Pennsylvania 18974	1
Commanding Officer and Director Naval Ship Research and Development Center Washington, D. C. 20007	1
Superintendent Naval Postgraduate School Monterey, California 93940	1
Commanding Officer & Director Naval Ship Research & Development Center* Panama City, Florida 32402	1

*Formerly Mine Defense Lab.

DISTRIBUTION LIST (Cont.)

	No. of Copies
Naval Underwater Weapons Research & Engineering Station Newport, Rhode Island 02840	1
Superintendent Naval Academy Annapolis, Maryland 21401	1
Scientific and Technical Information Center 4301 Suitland Road Washington, D. C. 20390 Attn: Dr. T. Williams Mr. E. Bissett	2
Commander Naval Ordnance Systems Command Code ORD-03C Navy Department Washington, D. C. 20360	1
Commander Naval Ship Systems Command Code SHIPS 037 Navy Department Washington, D. C. 20360	1
Commander Naval Ship Systems Command Code SHIPS 00V1 Washington, D. C. 20360 Attn: CDR Bruce Gilchrist Mr. Carey D. Smith	2
Commander Naval Undersea Research & Development Center 3202 E. Foothill Boulevard Pasadena, California 91107	1
Commanding Officer Fleet Numerical Weather Facility Monterey, California 93940	1

DISTRIBUTION LIST (Cont.)

	No. of Copies
Defense Documentation Center Comeron Station Alexandria, Virginia 22314	20
Dr. James Probus Office of the Assistant Secretary of the Navy (R&D) Room 4E741, The Pentagon Washington, D. C. 20350	1
Mr. Allan D. Simon Office of the Secretary of Defense DDR&E Room 3E1040, The Pentagon Washington, D. C. 20301	1
CAPT J. Kelly Naval Electronics Systems Command Code EPO-3 Washington, D. C. 20360	1
Chief of Naval Operations Room 5B718, The Pentagon Washington, D. C. 20350 Attn: Mr. Benjamin Rosenberg	1
Chief of Naval Operations Rm 4C559, The Pentagon Washington, D. C. 20350 Attn: CDR J. M. Van Metre	1
Chief of Naval Operations 801 No. Randolph St. Arlington, Virginia 22203	1
Dr. Melvin J. Jacobson Rensselaer Polytechnic Institute Troy, New York 12181	1
Dr. Charles Stutt General Electric Co. P. O. Box 1088 Schenectady, New York 12301	1

DISTRIBUTION LIST (Cont.)

	No. of Copies
Dr. Alan Winder EDO Corporation College Point, New York 11356	1
Dr. T. G. Birdsall Cooley Electronics Lab. University of Michigan Ann Arbor, Michigan 48105	1
Dr. John Steinberg University of Miami Institute of Marine & Atmospheric Sciences Miami, Florida 33149	1
Mr. Robert Cunningham Bendix Corporation 11600 Sherman Way North Hollywood, California 91606	1
Dr. H. S. Hayre University of Houston Cullen Boulevard Houston, Texas 77004	1
Dr. Robert R. Brockhurst Woods Hole Oceanographic Institute Woods Hole, Massachusetts 02543	1
Dr. Stephen Wolff Johns Hopkins University Baltimore, Maryland 21218	1
Dr. M. A. Basin Litton Industries 8000 Woodley Avenue Van Nuys, California 91409	1
Dr. Albert Nuttall Navy Underwater Systems Center Fort Trumbull New London, Connecticut 06320	1

DISTRIBUTION LIST (Cont.)

	No. of Copies
Dr. Philip Stocklin Raytheon Company P. O. Box 360 Newport, Rhode Island 02841	1
Dr. H. W. Marsh Navy Underwater Systems Center Fort Trumbull New London, Connecticut 06320	1
Dr. David Middleton 35 Concord Ave., Apt. #1 Cambridge, Massachusetts 02138	1
Mr. Richard Vesper Perkin-Elmer Corporation Electro-Optical Division Norwalk, Connecticut 06852	1
Dr. Donald W. Tufts University of Rhode Island Kingston, Rhode Island 02881	1
Dr. Loren W. Nolte Dept. of Electrical Engineering Duke University Durham, North Carolina 27706	1
Dr. Thomas W. Ellis Texas Instruments, Inc. 13500 North Central Expressway Dallas, Texas 75231	1
Mr. Robert Swarts Honeywell, Inc. Marine Systems Center 5303 Shilshole Ave., N.W. Seattle, Washington, 98107	1
Mr. Charles Loda Institute for Defense Analyses 400 Army-Navy Drive Arlington, Virginia 22202	1

DISTRIBUTION LIST (Cont.)

	No. of Copies
Mr. Beaumont Buck General Motors Corporation Defense Research Division 6767 Holister Ave. Goleta, California 93017	1
Dr. M. Weinstein Underwater Systems, Inc. 8121 Georgia Avenue Silver Spring, Maryland 20910	1
Dr. Harold Saxton 1601 Research Blvd. TRACOR, Inc. Rockville, Maryland 20850	1
Dr. Thomas G. Kincaid General Electric Company P. O. Box 1088 Schenectady, New York 12305	1
Applied Research Laboratories The University of Texas at Austin Austin, Texas 78712 Attn: Dr. Loyd Hampton Dr. Charles Wood	3
Dr. Paul McElroy Woods Hole Oceanographic Institution Woods Hole, Massachusetts 02543	1
Dr. John Bouyoucos General Dynamics/ Electronics 1400 N. Goodman Street, P. O. Box 226 Rochester, New York 14603	1
Hydrospace Research Corporation 5541 Nicholson Lane Rockville, Maryland 20852 Attn: CDR Craig Olson	1
Cooley Electronics Laboratory University of Michigan Ann Arbor, Michigan 48105	25